Methods in Molecular Biology 1221

Springer Protocols

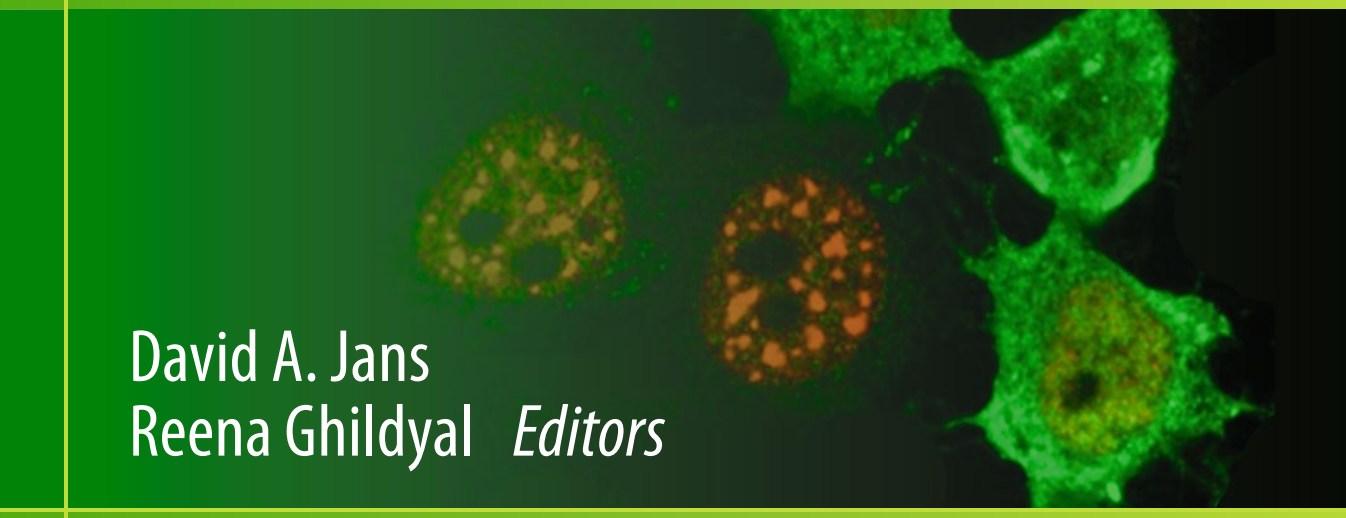

David A. Jans
Reena Ghildyal *Editors*

# Rhinoviruses

## Methods and Protocols

Humana Press

# METHODS IN MOLECULAR BIOLOGY

*Series Editor*
**John M. Walker**
**School of Life Sciences**
**University of Hertfordshire**
**Hatfield, Hertfordshire, AL10 9AB, UK**

For further volumes:
http://www.springer.com/series/7651

# Rhinoviruses

## Methods and Protocols

Edited by

**David A. Jans**

*Monash University, Melbourne, VIC, Australia*

**Reena Ghildyal**

*University of Canberra, Canberra, ACT, Australia*

Humana Press

*Editors*
David A. Jans
Monash University
Melbourne, VIC, Australia

Reena Ghildyal
University of Canberra
Canberra, ACT, Australia

ISSN 1064-3745 ISSN 1940-6029 (electronic)
ISBN 978-1-4939-1570-5 ISBN 978-1-4939-1571-2 (eBook)
DOI 10.1007/978-1-4939-1571-2
Springer New York Heidelberg Dordrecht London

Library of Congress Control Number: 2014948262


*Cover image*: Infection with rhinovirus leads to reduced localisation of Sam68 in nuclear bodies. HeLa cells infected with human rhinovirus 16 were fixed and probed for viral 3C proteinase (green) and cellular RNA-binding protein Sam68 (red), followed by confocal laser scanning microscopy.

Printed on acid-free paper

Humana Press is a brand of Springer
Springer is part of Springer Science+Business Media (www.springer.com)

# Preface

Human rhinoviruses (HRV) are the major cause of common colds as well as being recognized more recently as the major viral cause of asthma and chronic obstructive pulmonary disease (COPD) exacerbations. The advent of molecular diagnostic techniques and confirmation of HRV as the main cause of asthma exacerbations has led to a heightened interest in HRV biology, with a significant increase in our understanding of mechanisms of pathogenesis. Seminal discoveries of the past decade include the demonstration that HRV infection is not limited to the epithelium, but can infect subepithelial layers of the airway wall, the discovery of a third HRV genotype that with special properties in terms of disease severity, and the description of disrupted nuclear transport in HRV infected cells through action of the HRV proteases on the host cell nuclear pore. New and improved molecular, cellular, protocols developed specifically to studying HRV have played a key role in enabling all of these discoveries. Important technical advances include the development of a validated mouse model for HRV infection, the establishment of HRV infection in primary airway cells, the generation of a reverse genetics system for HRV, and application of spectroscopic and microscopic analysis to understanding HRV biology. Given the increasing global incidence of asthma, the importance of HRV in asthma and COPD exacerbations, together with the rapid advancements in methodology, this is a more than opportune time to bring together current state-of-the-art methodologies to study HRV biology.

HRV are the viruses most commonly isolated from persons experiencing mild upper respiratory illnesses (common colds). Although infections are chiefly limited to the upper respiratory tract, HRV may also cause otitis media and sinusitis. Importantly, HRVs may also exacerbate asthma, COPD, cystic fibrosis, chronic bronchitis, and serious lower respiratory tract illness in infants, elderly persons, and immunocompromised persons. Although infections occur all year round, the incidence is highest in the fall and the spring. 70–80 % of persons exposed to the virus have symptomatic disease, which in most cases is mild and self-limited.

Isolation of HRV was first accomplished by Pelon et al. and Price using Rhesus monkey kidney tissue cultures and nasopharyngeal washings from persons with colds. In 1960, Tyrrell and Parsons at Salisbury, isolated strain HGP by reducing the incubation temperature of cultures to 33 °C, lowering the pH of tissue culture media to around 7.0, and gently rotating cultures during incubation. A profusion of HRV serotypes was subsequently detected when the sensitive strains of human embryonic fibroblast cell cultures described by Hayflick and Moorehead and the conditions described by the Salisbury group were used routinely. The name “rhinovirus” was originally suggested by Andrews, and a description of the group was proposed by Tyrrell and Chanock in 1963. In 1967, a collaborative program assigned numbers 1A through 55 to the known HRV types. In 1971, a second phase added types 56 through 89, and a third phase increased the number to 100.

These multiple serotypes have also been grouped on the basis of cellular receptor specificity (major, utilizing intercellular adhesion molecule 1 (ICAM-1) and minor, low-density lipoprotein receptor (LDLR) groups) and sensitivity to antiviral capsid-binding compounds (A and B groups). Full-length and partial (mainly VP4/VP2 and VP1 coding regions) genome sequencing of prototype strains and clinical isolates has revealed two major HRV

genotypes or clades. This phylogenetic classification correlated better with antiviral drug sensitivity than with the receptor grouping, and suggested a fundamental division of HRVs into two species, HRV-A and HRV-B. The development of highly sensitive molecular techniques for detecting HRV genome in a variety of clinical specimens led to discovery of novel rhinoviruses designated HRV-C (aka HRV-A2 or HRV-X), that were subsequently shown to meet the species sequence demarcation criteria (less than 70 % amino acid identity in the P1, 2C and 3CD regions) in the genus Enterovirus (Chapter 1).

Clinical, diagnostic laboratories by and large utilize PCR- and sequencing-based techniques for isolating, identifying and genotyping HRV from clinical samples (Chapters 2–4). Virus culture has been the "gold standard" for laboratory diagnosis of respiratory virus infections and viruses are routinely propagated in susceptible cell lines for use in research laboratories where large quantities of high-titer virus suspensions are needed for investigations (Chapter 5). Additionally, cell culture-based assays are still required to determine concentrations of infectious virus and are used routinely in research laboratories (Chapter 7). However, current assays do not allow infectivity measurements of the HRV-C group, isolates of which do not grow in standard cell culture (e.g. HeLa or embryonic lung fibroblasts). This feature has most likely prevented their discovery until recent molecular diagnostic approaches that do not require virus isolation or passaging. Sequencing of the complete reference set of HRV-A and HRV-B at the full-genome level and comparative analysis with available complete genomes of HRV-Cs has confirmed clustering of all strains into three phylogenetically distinct groups. Recent advances in tissue culture, wherein the structure of the airway wall is able to be replicated in culture systems using primary human tissue have allowed the culture of HRV-C which should lead to future advances in our understanding of the pathology of this group of HRVs (Chapter 6).

The huge advancements in technical applications of biophysics and improvements in high-end imaging techniques have also had implications for HRV research among other infectious diseases. These high-resolution techniques have allowed scientists to dissect individual events in the attachment, infection, replication, assembly, and release of HRV, with resultant increases in our understanding of the intracellular mechanisms of this important virus (Chapters 8 and 9). HRV encoded proteases, like those of their picornavirus counterparts, play crucial roles in virus replication through their cleavage of the HRV polyprotein; inactivation of either protease results in inability to rescue infectious virus. The role of HRV proteases as mediators of virus pathogenesis has been known for some time; however recent increases in the known cellular targets has highlighted the fact that our knowledge of cellular targets of HRV proteases is still incomplete (Chapter 10). The importance of proteases as anti-HRV targets is shown by the effectiveness of the Pfizer antiviral Rupintrivir (a 3C protease inhibitor) in experimental HRV infections. In vitro functional assays are important to understand protein functions and one such assay is described in Chapter 11 to enable in depth study of cellular targets of HRV proteases.

A great advance in HRV research has been the availability of reverse genetics systems for specific minor and major group HRV (Chapter 12). These systems have facilitated the study of individual viral proteins in the context of the infected cell, allowing specific mutations to be inserted in the full length genome (Chapter 13). Although HRV infectious clones have only recently started to be used widely, they provide an invaluable tool to study HRV biology and will be crucial in any future drug or vaccine strategies.

The study of the host response to HRV was stalled for many years due to the lack of a suitable animal model; all *in vivo* investigations thus had to rely on examination of human clinical samples, which limited the investigation of HRV in the context of asthma.

The development of both minor group (wild type Balb/c) and major group (transgenic Balb/c) mouse infection models has opened up the field for *in vivo* studies and has already resulted in several publications on the host immune response to HRV infection (Chapter 14). This advance in HRV research has been supported by the development of techniques for HRV culture in suspension, which, aligned with classical purification techniques based on sucrose gradients has resulted in suspensions of high concentration of virus required for animal studies. Importantly, high-titer virus and validated mouse models will help to clarify the roles of specific host response pathways in HRV-induced asthma and COPD exacerbations in the future.

In short, HRV research has come a very long way from the virus's initial identification as the causative agent for common colds, with numerous molecular, cellular and in vivo tools now available, as this volume highlights. The approaches described have led to increased understanding of the clinical disease caused by HRV, including functions of its individual proteins and its replication. Much still remains to be investigated, however, as exemplified by the recent discovery of an important group of HRV that is now known to cause severe disease. Future research in the HRV area, driven by technical advances such as those showcased here, should ultimately enable the development of therapeutic approaches to combat HRV, and most importantly, its pathogenic effects in asthma exacerbation.

***Melbourne, VIC, Australia*** ***David A. Jans***
***Canberra, ACT, Australia*** ***Reena Ghildyal***

# Contents

*Preface* . . . . . *v*
*Contributors* . . . . . *xi*

1 Classification and Evolution of Human Rhinoviruses . . . . . 1
***Ann C. Palmenberg and James E. Gern***

2 Nested-RT-PCR and Multiplex RT-PCR for Diagnosis of Rhinovirus Infection in Clinical Samples . . . . . 11
***Xuelian Yu and Reena Ghildyal***

3 Molecular Identification and Quantification of Human Rhinoviruses in Respiratory Samples . . . . . 25
***Wai-Ming Lee, Kris Grindle, Rose Vrtis, Tressa Pappas, Fue Vang, Iris Lee, and James E. Gern***

4 Molecular Genotyping of Human Rhinovirus by Using PCR and Sanger Sequencing . . . . . 39
***Wei Wang, Jing He, Yi Liu, Lei Xu, Wencai Guan, and Yunwen Hu***

5 Growth of Human Rhinovirus in H1-HeLa Cell Suspension Culture and Purification of Virions . . . . . 49
***Wai-Ming Lee, Yin Chen, Wensheng Wang, and Anne Mosser***

6 Propagation of Rhinovirus-C Strains in Human Airway Epithelial Cells Differentiated at Air-Liquid Interface . . . . . 63
***Shamaila Ashraf, Rebecca Brockman-Schneider, and James E. Gern***

7 Infectivity Assays of Human Rhinovirus-A and -B Serotypes . . . . . 71
***Wai-Ming Lee, Yin Chen, Wensheng Wang, and Anne Mosser***

8 Application of FCS in Studies of Rhinovirus Receptor Binding and Uncoating . . . . . 83
***Shushan Harutyunyan, Arthur Sedivy, Gottfried Köhler, Heinrich Kowalski, and Dieter Blaas***

9 Capillary Electrophoresis, Gas-Phase Electrophoretic Mobility Molecular Analysis, and Electron Microscopy: Effective Tools for Quality Assessment and Basic Rhinovirus Research. . . . . 101
***Victor U. Weiss, Xavier Subirats, Mohit Kumar, Shushan Harutyunyan, Irene Gösler, Heinrich Kowalski, and Dieter Blaas***

10 Proteases of Human Rhinovirus: Role in Infection . . . . . 129
***Lora M. Jensen, Erin J. Walker, David A. Jans, and Reena Ghildyal***

11 A Protocol to Express and Isolate HRV16 3C Protease for Use in Protease Assays . . . . . 143
***Lora M. Jensen, Erin J. Walker, and Reena Ghildyal***

12 Reverse Genetics System for Studying Human Rhinovirus Infections . . . . . 149
***Wai-Ming Lee, Wensheng Wang, Yury A. Bochkov, and Iris Lee***

13 Reverse Genetic Engineering of the Human Rhinovirus Serotype 16 Genome to Introduce an Antibody-Detectable Tag . . . . . 171
***Erin J. Walker, Lora M. Jensen, and Reena Ghildyal***

14 Mouse Models of Rhinovirus Infection and Airways Disease . . . . . 181
***Nathan W. Bartlett, Aran Singanayagam, and Sebastian L. Johnston***

*Index* . . . . . *189*

# Contributors


Shamaila Ashraf • *Department of Pediatrics, School of Medicine and Public Health, University of Wisconsin, Madison, WI, USA*

Nathan W. Bartlett • *Airway Disease Infection Section, National Heart and Lung Institute, Imperial College London, London, UK*

Dieter Blaas • *Max F. Perutz Laboratories, Department of Medical Biochemistry, Medical University of Vienna, Vienna, Austria*

Yury A. Bochkov • *Department of Pediatrics, School of Medicine and Public Health, University of Wisconsin, Madison, WI, USA*

Rebecca Brockman-Schneider • *Department of Medicine, School of Medicine and Public Health, University of Wisconsin, Madison, WI, USA*

Yin Chen • *Department of Pharmacology and Toxicology, School of Pharmacy, University of Arizona, Tucson, AZ, USA*

James E. Gern • *Department of Pediatrics and Medicine, University of Wisconsin School of Medicine and Public Health, Madison, WI, USA*

Reena Ghildyal • *Centre for Research in Therapeutic Solutions, Faculty of Education, Science, Technology and Mathematics, University of Canberra, Bruce, ACT, Australia*

Irene Gösler • *Max F. Perutz Laboratories, Department of Medical Biochemistry, Medical University of Vienna, Vienna, Austria*

Kris Grindle • *Department of Pediatrics, School of Medicine and Public Health, University of Wisconsin, Madison, WI, USA*

Wencai Guan • *Pathogen Diagnosis and Biosafety Department, Shanghai Public Health Clinical Center, Fudan University, Shanghai, PR China*

Shushan Harutyunyan • *Max F. Perutz Laboratories, Department of Medical Biochemistry, Medical University of Vienna, Vienna, Austria*

Jing He • *Pathogen Diagnosis and Biosafety Department, Shanghai Public Health Clinical Center, Fudan University, Shanghai, PR China*

Yunwen Hu • *Pathogen Diagnosis and Biosafety Department, Shanghai Public Health Clinical Center, Fudan University, Shanghai, PR China*

David A. Jans • *Department of Biochemistry and Molecular Biology, Faculty of Health, Nursing and Medical Sciences, Monash University, Clayton, VIC, Australia*

Lora M. Jensen • *Centre for Research in Therapeutic Solutions, Faculty of Education, Science, Technology and Mathematics, University of Canberra, Canberra, ACT, Australia*

Sebastian L. Johnston • *Airway Disease Infection Section, National Heart and Lung Institute Imperial College London, London, UK*

Gottfried Köhler • *Max F. Perutz Laboratories, Department of Structural Biology, University of Vienna, Vienna, Austria*

Heinrich Kowalski • *Max F. Perutz Laboratories, Department of Medical Biochemistry, Medical University of Vienna, Vienna, Austria*

Mohit Kumar • *Max F. Perutz Laboratories, Department of Medical Biochemistry, Medical University of Vienna, Vienna, Austria*

Wai-Ming Lee • *Biological Mimetics, Inc., Frederick, MD, USA*

Iris Lee • *Department of Pediatrics, School of Medicine and Public Health, University of Wisconsin, Madison, WI, USA*
Yi Liu • *Pathogen Diagnosis and Biosafety Department, Shanghai Public Health Clinical Center, Fudan University, Shanghai, PR China*
Anne Mosser • *Department of Medicine, University of Wisconsin, Madison, WI, USA*
Ann C. Palmenberg • *Institute for Molecular Virology, University of Wisconsin-Madison, Madison, WI, USA*
Tressa Pappas • *Department of Pediatrics, School of Medicine and Public Health, University of Wisconsin, Madison, WI, USA*
Arthur Sedivy • *Max F. Perutz Laboratories, Department of Structural Biology, University of Vienna, Vienna, Austria*
Aran Singanayagam • *Airway Disease Infection Section, National Heart and Lung Institute Imperial College London, London, UK*
Xavier Subirats • *Department of Analytical Chemistry, University of Barcelona, Barcelona, Spain*
Fue Vang • *Department of Pediatrics, School of Medicine and Public Health, University of Wisconsin, Madison, WI, USA*
Rose Vrtis • *Department of Pediatrics, School of Medicine and Public Health, University of Wisconsin, Madison, WI, USA*
Erin J. Walker • *Faculty of Education, Science, Technology and Mathematics, Centre for Research in Therapeutic Solutions, University of Canberra, Bruce, ACT, Australia*
Wensheng Wang • *Global Biological Development, Bayer Healthcare, Berkeley, CA, USA*
Wei Wang • *Pathogen Diagnosis and Biosafety Department, Shanghai Public Health Clinical Center, Fudan University, Shanghai, PR China*
Victor U. Weiss • *Institute of Chemical Technologies and Analytics, Vienna University of Technology, Vienna, Austria*
Lei Xu • *Pathogen Diagnosis and Biosafety department, Shanghai Public Health Clinical Center, Fudan University, Shanghai, PR China*
Xuelian Yu • *Microbiology Branch, Xinjiang Medical University, Urumqi, People's Republic of China; Microbiology Branch, Shanghai Municipal Center for Disease Control and Prevention, Shanghai, People's Republic of China*

# Chapter 1

# Classification and Evolution of Human Rhinoviruses

**Ann C. Palmenberg and James E. Gern**

## Abstract

The historical classification of human rhinoviruses (RV) by serotyping has been replaced by a logical system of comparative sequencing. Given that strains must diverge within their capsid sequenced by a reasonable degree (>12–13 % pairwise base identities) before becoming immunologically distinct, the new nomenclature system makes allowances for the addition of new, future types, without compromising historical designations. Currently, three species, the RV-A, RV-B, and RV-C, are recognized. Of these, the RV-C, discovered in 2006, are the most unusual in terms of capsid structure, receptor use, and association with severe disease in children.

**Key words** Rhinovirus, Evolution, Virus taxonomy, Immunology, Drug resistance

## 1 Historical RV Classification

The human rhinoviruses currently comprise the RV-A, RV-B, and RV-C species of the *Enterovirus* genus in the *Picornaviridae* family. This classification status was not always the case. For the RV-A and RV-B, several historic clinical panels archived by the American Type Culture Collection were originally combined and indexed into 100 RV types after assessment of antigenic cross-reactivity or serotyping in rabbits. From these data, and from physical characteristics of the virions (e.g., pH lability), it was obvious that the full list of composite isolates easily subdivided into two related species, the *HRV-A* and *HRV-B*. For many years, these units were assigned to their own genus (*human rhinoviruses or HRV*) because the disease presentations (common cold) were observably different from other classical enteroviruses, like poliovirus, coxsackie virus, or ECHO (enteric cytopathic human orphan) viruses. Moreover, they were also different from all other original picornavirus genera, the *Aphthoviruses*, *Cardioviruses*, and *Hepatoviruses*. Before 1985, most virus taxonomy systems were weighted heavily towards phenotypic parameters (i.e., virion stability properties or disease etiologies)

David A. Jans and Reena Ghildyal (eds.), *Rhinoviruses: Methods and Protocols*, Methods in Molecular Biology, vol. 1221, DOI 10.1007/978-1-4939-1571-2_1, 


**Fig. 1** Genome map of a typical RV shows the protein names and their involvement in capsid formation or replication processes

as it was commonly argued (at that time) that medical-based classification made it easier to teach in clinical settings.

In 1984–1985, the first HRV (B14) was sequenced in its entirety in parallel with the virion crystal structure determination [1, 2]. Surprisingly, the B14 genome organization, including the full array of functional genes (Fig. 1), proved nearly identical to that of poliovirus 1, one of the earliest determined picornavirus sequences [3, 4]. Indeed, as more genome sequences followed, the pattern became evermore apparent. The HRV-A and HRV-B, while distinct in their own groupings, were enterovirus-like in all measures of genome comparisons and probably should be considered as species within that genus. The Picornavirus Study Group Subcommittee (SG) eventually made this recommendation to the International Committee on the Taxonomy of Viruses (ICTV), where it was subsequently adopted [5]. The thorough, deep sequence-based classification precedent established by this decision has helped shape taxonomy protocols for all virus families. As part of the *HRV-Enterovirus* reassignments, the term "Human" was dropped from the species names and 99 of the original types became simply known as "Rhinoviruses," or "RV," retaining the RV-A and RV-B species letter designations of the previous system. Within this reclassification context, and after further evaluation of genetic, immunogenic, and receptor use (decay-accelerating factor as a receptor) properties, RV-A87 was reassigned to the *Enterovirus D* species (EV-D68) [6].

## 2 Current Classification

New RV isolates are now rarely tested for immunogenicity. The current classification scheme is based on overt similarities in genome organization, capsid properties, and primary sequence conservation [7]. Strains are assigned to the RV-A or RV-B if they share greater than 70 % amino acid identity in the P1, 2C, and 3CD regions with other members. Within the respective species, isolates are subdivided into numeric genotypes that respect the historic naming system, but now rely almost entirely on sequence comparisons of the VP1 protein or VP4/VP2. The preferred nomenclature [8] designates the species letter

(A, B, or C), and type number (e.g., A16). Strain designations are unique to each Genbank accession number and rarely indicated unless required for clarity.

Assignment of a new strain to a known genotype generally requires >86–87 % aligned nucleic acid identity in either or both of the key capsid regions. Type assignments are considered tentative until at least the full VP1 sequence is completed and verified [8]. Full-genome sequencing revealed that some historic types were really more closely related than this (e.g., A54 and A98, or A29 and A44), and others such as A8 and A45, defining "clade D," were in fact so different from all other RV-A; they perhaps warrant eventual designation as another species [9]. Part of the ongoing mission of the Picornavirus Special Group (SG) is to continually sort out such discontinuities and attempt to provide a common code for new isolates and types as they are discovered. For example, in the past few years, six new types have been added to the RV-A (A101–A106) and five new types have been added to the RV-B (B100–B104). Isolates for A8 and A95 have been merged into a single type (A8), as have A54/A98 (to A54), and A29/A44 (to A29). Other types were split (e.g., B52 into B52 plus B104), or their isolates rearranged (e.g., A36 and A89). All these changes now more accurately reflect strain/type commonalities required by the overlying classification scheme.

An excellent recent review on this topic by McIntyre et al. summarizes the current state of the field [8]. Recent taxonomy proposals approved, or under consideration by the Picornavirus SG or by the ICTV, can be publically reviewed at http://www.ictvonline.org/virusTaxonomy.asp. Presently, the RV-A have 77 recognized types and the RV-B have 30 types. Type RV-A1 is unique in that it has assigned isolates that are sufficiently different as to warrant special distinction, as A1A and A1B subtypes. If these units are counted separately, it brings the RV-A to 78 types. Because of the recently recommended mergers among several closely related types, a few of the historic type numbers have been dropped from the current system and are no longer used (A44, A87, A95, A98). If a researcher should discover an isolate sufficiently different to warrant consideration as a new type, they should consult the website curated by the Picornavirus SG (http://www.picornaviridae.com). Via links on this site, comparative sequences can be submitted (preferably for the full capsid, but for the full VP1 gene at a minimum) for SG consideration. New type numbers are awarded sequentially. New species designations (*see* below for RV-C) require full ICTV approval.

## 3 Receptor and Drug Groups

The classic panel of 99 original RV-A and RV-B are the canonical agents of the "common cold." Many are well studied at the structural and clinical levels. All these isolates use either ICAM-1

(89 "major" types) or LDLR (10 "minor" types) as their cellular receptors. The molecular nuances of these interactions have been described by many co-crystallization and EM studies. The set of full-genome sequences, including at least one representative of each historic type, was completed in 2009 [10]. From this work, it became clear that the RV-A + B included in the major and minor groups conserve particular surface footprints that explain how and why these isolates use their respective receptors to interact with cells [11].

This same virus panel has been subjected to extensive characterizations according to composite strain sensitivities to a slate of potential therapeutics targeting their capsids [8]. The basic strategy is aimed at inhibiting the virus before infection by intercalating drugs into the unique surface "pockets" characteristic of all enterovirus virions. The type-specific sensitivities were found to subdivide, roughly along species lines, into two experimental groups [12]. The structures of 28 virus-drug complexes have been determined to atomic resolution. The Group-1 viruses (all RV-B plus A8, A13, A32, A43, A45, and A54) have long, narrow pockets interior to their VP1 proteins, which accommodate matching long-chain hydrophobic drugs. The Group-2 viruses (all other RV-A) have shorter, wider VP1 hydrophobic pockets, and therefore accept an alternate cohort of drugs. These points are important to any discussion of rhinovirus classification because there is frequent semantic confusion when dividing the historic strains into their species (RV-A or RV-B), or their receptor units (major or minor) or their drug Groups (1 or 2). It should be remembered that each term designates separate, non-overlapping properties. None of the most recently added RV types (i.e., A101–106 or B100–104) have ever been directly tested for receptor binding or drug sensitivity. Their respective activities, based on sequence comparison alone, *predict* them to be "major" in terms of receptor, but divided between Groups 1–2 (along species lines) for drug reactivity.

## 4 Rhinovirus C

In 2006 the discovery of a new RV species surprised the molecular and clinical communities [13]. The RV-C are clearly rhinoviruses, but unlike RV-A + B, they are not readily propagated in typical cell culture systems, including WI-38, WisL, BEAS-2B, A549, and HeLa lines [11]. These isolates are not "new" in terms of evolution, but rather they were physically undetected by all typical characterization methods that required cultured virus growth, such as plaque assays [11]. The current 51 recognized RV-C types (as binned by sequence analysis) were instead identified by PCR while fishing through patient samples for other RV. As with the RV-A + B, each RV-C type includes those isolates whose VP1 sequences

exceed 87 % pairwise identity at the nucleotide level [8, 14]. The RV-C have special clinical relevance since it is now recognized that these strains are associated with up to half of infections in young children [11]. They grow readily in both the lower and upper airways and tolerate higher growth temperatures in culture [15]. Moreover, the RV-C use cell receptors that are not common to the RV-A + B [11]. Unfortunately, these receptors are apparently lost whenever primary tissue snippets are transitioned to undifferentiated monolayers. RV-C can be grown in mucosal organ cultures, but this technique requires the availability of primary human donor samples [11]. Parallel work with differentiated sinus or bronchial epithelial cells at air-liquid interface (ALI) is promising [15, 16], but neither technique has yet produced enough virus for extensive biological studies. Instead, RV-C information relies heavily on comparative sequence analysis to maximize data from limited experimental samples.

To this end, a great many RV-C capsid fragments have been sequenced, and for about 32 types there are (nearly) full-length genome data [17]. Common to all known isolates in this species are unusually large relative deletions (indels) in the VP1 capsid protein. The fundamental VP1 protein cores superimpose among all RV, but the loops that connect the internal β-strands of the RV-C VP1 are shorter by ~22 amino acids relative to the RV-A, and ~28 amino acids relative to the RV-B. The composite structural loops containing these elements supply virtually all of the mass to the fivefold virion plateau. Therefore, the physical RV-C capsid structures are predicted to be very different from the RV-A + B over at least 1/3 of the virion surface [17]. The changes profoundly affect the receptor-binding platform, (predicted) type immunogenicity, and capsid-drug reactivity [17, 18].

## 5 Physical Characteristics

By way of review, all RV have genome organizations and (general) capsid structures similar to those of other *Enteroviruses* (Fig. 1). But unlike isolates in the other species of this genus, which remain viable at pH 3.0, RV particles (RV-A + B + C) are unstable below pH 5–6. The icosametric capsid (~30 nm diameter) has 60 copies each of proteins VP1, VP2, VP3, and VP4, named in order of descending electrophoretic mobility. The protein shell surrounds a densely packed, single-stranded, positive-sense, RNA genome of 7079 (RV-C1) to 7233 (RV-B92) bases, a count which does not include the variable length 3′ poly(A) tail. Like poliovirus, the surfaces of RV-A + B + C capsids are dominated by the three largest proteins. VP4 is internal to the structure, centered near the fivefold axis. Around the exterior fivefold plateau, a symmetrical "canyon" provides receptor-binding sites and immunogenic surfaces.

All RV-A + B are major (ICAM-1) or minor (LDLR) with regard to their receptor preference [19], but the cellular receptors used by the RV-C are certain to be different [11] and are currently unidentified. Bioinformatics predicts that the RV-C deletions in the VP1 regions will produce species-specific topologies for the canyon region and the fivefold plateau and the (common?) RV-C receptor is sure to be compatible with these dramatic changes.

The RV genomes are messenger sense, encoding the polyprotein reading frame (ORF) and multiple important RNA structural motifs. Adjacent to the 5′ cloverleaf, a regulatory feature for translation and replication, each RV encodes a strain-specific pyrimidine-rich tract that may be involved in suppressing innate immunity triggers [10]. The type-1 IRES is 3′ to this tract and includes a variable-length stem structure pairing the ORF start site (AUG) with an upstream AUG. Unlike poliovirus, intervening sequences between these AUGs are probably not scanned by initiating ribosomes [20]. The picornavirus VPg uridylylation reaction, required for RNA synthesis, is templated by a special structure called the *cre* (*cis*-acting replication element) whose location varies in every species of picornavirus. For the RV-A, the *cre* is in the 2A gene [21]. For the RV-B, the *cre* is in the 2C gene [21]. The RV-C *cre* has been proposed as one of the two sites in the 1B gene [10, 21, 22]. Neither has been confirmed experimentally. The short, 3′ untranslated sequences (UTR) are highly variable. Invariably, they configure as an inclusive stem motif displaying at least one bogus termination codon in the terminal loop. This codon may be in-frame or out-of-frame with the authentic ORF stop site, and has been proposed to play a role in the recruitment of translation termination factors [10].

## 6 Genetic Relationships

As might be expected from the original RV typing system, a large degree of sequence diversity among the RV manifests as amino acid changes in capsid surface regions mapped as neutralizing immunogenic epitopes (Nims). The high frequency of mutational fixation in these Nims, particularly for VP1, is one of the key reasons for the plethora of recognized RV genotypes. Although it is possible to measure and define comparative relationships among any set of extant isolates, it is virtually impossible to retrace the exact lineages that gave rise to them. "Evolutionary" trees created from VP1 data are quite different from those using VP2/4, 3D, 3C, the IRES, or other regions of the genome [10]. In part this is because nonstructural genes (except for 2A) fix mutations at more variable rates. But recombination (*see* below) is also frequent within and between strains from different RV species. Few if any of even the most characteristic lineages are known to breed true. At best a representative phylogram (Fig. 2) can illustrate some measure of relationships among the major clades and highlight

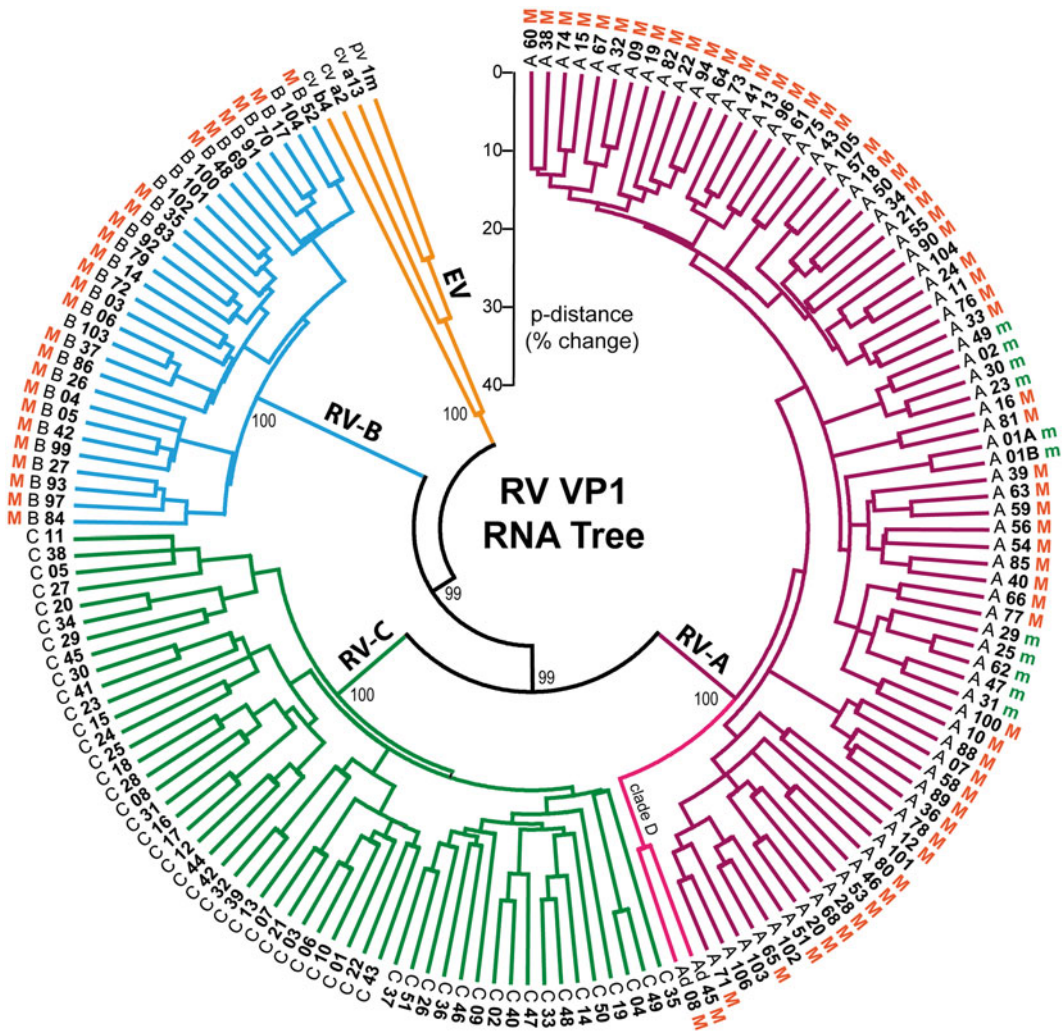


**Fig. 2** Circle phylogram of relationships for currently recognized genotypes [8] of RV-A, RV-B, and RV-C. The tree was calculated with neighbor-joining methods from aligned, VP1 RNA sequences, and rooted with data from four enteroviruses (EV) of the EV-A, EV-B, and EV-C species, similar to ref. 10. The Major ("M," ICAM-1) and minor ("m," LDLR) receptor groups are indicated if determined experimentally. The RV-C receptor is unknown. Bootstrap values (percent of 200 replicates) are indicated at key nodes

those genotypes that are most similar to each other. When parsing new clinical isolates into their appropriate types, it is always important to remember that the larger the sequence that is compared, the more accurate the putative classification. Deep sequence alignments [8] covering ~1,000 VP1 datasets are especially valuable when discriminating, say, A25/A62, B52/B104, or other very similar types. As is characteristic of most such trees, no matter how they are calculated, this current depiction places the RV-A and RV-C more closely together on the tree than either is to the RV-B. Moreover, within the RV-A, a distinctive "clade D" (A8/A45) always branches off on its own from the other genotypes [10, 23].

At present, there are too few isolates within this clade to change the classification (RV-D?), but as the taxonomy system continues to evolve, that idea remains a possibility.

## 7 Recombination

In addition to the multitude of available VP1 sequences, completion of the full cohort of RV-A+B genome sequences [10] identified extensive evidence for historic recombination which, de facto, created several of the existing genotype clades (Fig. 3). A18, A34, A54,

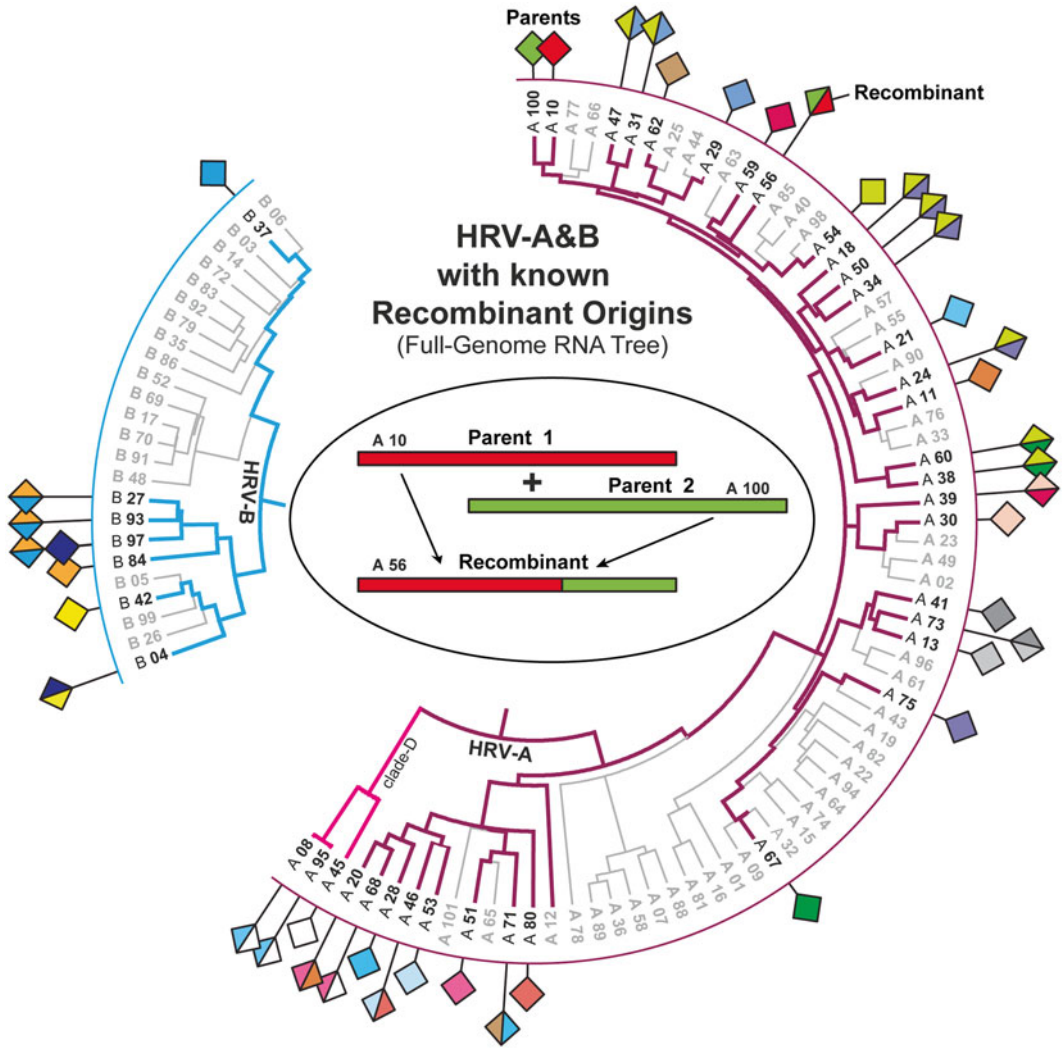


**Fig. 3** Recombinant origins for many RV-A&B were uncovered by full-genome sequencing [10]. Parents (*solid boxes*) or progeny (*two-color boxes*) are founders of many extant clades. This illustration is modified from "Field's Virology" (2013), Ch 18, "Rhinoviruses," Wolters Kluwer, publishers

and A24 are independent derivatives of events between A54 and A75, for example. A54 is also a parent of A38 and A60. Similarly, B27, B93, and B97 have common parents in B37 and B42. Some of these viruses are promiscuous (!) and evidently, simultaneous infections must be a common event. Surprisingly though, none of these known recombinants have exchanged capsid regions. The most common trades include the 5′ UTR, primarily upstream of the IRES, or less frequently, fragments from P2–P3 regions. More recent, deep RV data from multiple field isolates has confirmed this idea, and now show clearly that the RV-A and RV-C frequently recombine between themselves, and when they do, they usually exchange not the expected capsid Nims, but 5′ UTR regions, and (often) their respective 2A protease genes [24, 25]. Comparative 2A work is under way to document why these particular recombinants are apparently favored. Possibly, divergent protease specificities may help these viruses regulate the overall cell response to infection.

## Acknowledgements

This work was supported by NIH grant U19 AI104317. The authors thank Wolters Kluwer, publishers of Field's Virology (2013), for permission to include certain text and figures from Ch 18, "Rhinoviruses" by the same authors.

### References

1. Stanway G, Hughes PJ, Mountford R et al (1984) The complete nucleotide sequence of a common cold virus: human rhinovirus 14. Nucleic Acids Res 12:7859–7875
2. Erickson JW, Frankenberger EA, Rossmann MG et al (1983) Crystallization of a common cold virus, human rhinovirus 14: isomorphism with poliovirus crystals. Proc Natl Acad Sci U S A 80:931–934
3. Kitamura N, Semler BL, Rothberg PG et al (1981) Primary structure, gene organization and polypeptide expression of poliovirus RNA. Nature 291:547–553
4. Racaniello VR, Baltimore D (1981) Molecular cloning of poliovirus cDNA and determination of the complete nucleotide sequence of the viral genome. Proc Natl Acad Sci U S A 78: 4887–4891
5. Carstens EB, Ball LA (2009) Ratification vote on taxonomic proposals to the International Committee on Taxonomy of Viruses (2008). Arch Virol 154:1181–1188
6. Savolainen C, Blomqvist S, Mulders MN et al (2002) Genetic clustering of all 102 human rhinovirus prototype strains: serotype 87 is close to human enterovirus 70. J Gen Virol 83:333–340
7. Palmenberg AC, Rathe J, Liggett S (2010) Analysis of the complete genome sequences of human rhinovirus. J Allergy Clin Immunol 125:1190–1199
8. McIntyre CL, Knowles NJ, Simmonds P (2013) Proposals for the classification of human rhinovirus species A, B and C into genotypically assigned types. J Gen Virol 94: 1791–1806
9. Rathe JA, Liu X, Tallon LJ et al (2010) Full-genome sequence and analysis of a novel human rhinovirus strain within a divergent HRV-A clade. Arch Virol 155:83–87
10. Palmenberg AC, Spiro D, Kuzmickas R et al (2009) Sequencing and analysis of all known human rhinovirus genomes reveals structure and evolution. Science 324:55–59
11. Bochkov YA, Palmenberg AC, Lee W-M et al (2011) Molecular modeling, organ culture and reverse genetics for a newly identified human rhinovirus C. Nat Med 17:627–632

12. Andries K, Dewindt B, Snoeks J et al (1990) Two groups of rhinoviruses revealed by a panel of antiviral compounds present sequence divergence and differential pathogenicity. J Virol 64:1117–1123
13. Dominguez SR, Briese T, Palacios G et al (2008) Multiplex MassTag PCR for respiratory pathogens in pediatric nasopharyngeal washes by conventional diagnostic testing shows a high prevalence of viruses belonging to a newly recognized rhinovirus clade. J Clin Virol 43: 219–222
14. Simmonds P, McIntyre C, Savolainen-Kopra C et al (2010) Proposals for the classification of human rhinovirus species C into genotypically assigned types. J Gen Virol 91:2409–2419
15. Ashraf S, Brockman-Schneider R, Bochkov YA et al (2013) Biological characteristics and propagation of human rhinovirus-C in differentiated sinus epithelial cells. Virology 436:143–149
16. Hao W, Bernard K, Patel N et al (2012) Infection and propagation of human rhinovirus C in human airway epithelial cells. J Virol 86:24–32
17. Basta HA, Sgro J-Y, Palmenberg AC (2013) Modeling of the human rhinovirus C capsid suggests a novel topology with insights on receptor preference and immunogenicity. Virology 448:176–184
18. Basta HA, Ashraf S, Bochkov YA et al (2013) Modeling of the human rhinovirus C capsid and antiviral drug resistance. Virology 448:82–90
19. Vlasak M, Roivainen M, Reithmayer M et al (2005) The minor receptor group of human rhinovirus (HRV) includes HRV23 and HRV25, but the presence of a lysine in the VP1 H1 loop is not sufficient for receptor binding. J Virol 79:7389–7395
20. Jackson RJ (1996) Initiation site selection mechanisms. In: Hershey JWB, Mathews MB, Sonenberg N (eds) Translational control. Cold Spring Harbor Laboratory Press, New York, NY, pp 71–112
21. Steil BP, Barton DJ (2009) Cis-active RNA elements (CREs) and picornavirus RNA replication. Virus Res 139:240–252
22. Cordey S, Gerlach D, Junier T et al (2008) The cis-acting replication elements define human enterovirus and rhinovirus species. RNA 14: 1568–1578
23. Ledford RM, Patel NR, Demenczuk TM et al (2004) VP1 sequencing of all human rhinovirus serotypes: insights into genus phylogeny and susceptibility to antiviral capsid-binding compounds. J Virol 78:3663–3674
24. Huang T, Wang W, Bessaud M et al (2009) Evidence of recombination and genetic diversity in human rhinoviruses in children with acute respiratory infection. PLoS One 4:e6355
25. McIntyre CL, McWilliam Leitch EC, Savolainen-Kopra C et al (2010) Analysis of genetic diversity and sites of recombination in human rhinovirus species C. J Virol 84:10297–10310

# Chapter 2

# Nested-RT-PCR and Multiplex RT-PCR for Diagnosis of Rhinovirus Infection in Clinical Samples

**Xuelian Yu and Reena Ghildyal**

## Abstract

Human rhinoviruses (HRVs) are positive-stranded RNA viruses belonging to the *Enterovirus* genus in the family of *Picornaviridae*. Identification of the specific strain in HRV disease has been difficult because the traditional serological method is insensitive, labor intensive, and cumbersome. With the fast progress in molecular biological technique, more sensitive and faster molecular methods have been developed, such as polymerase chain reaction (PCR), reverse transcriptase (RT)-PCR, and real-time RT-PCR. To improve the technique for defining the links between illnesses and specific strains of HRV, we developed RT-PCR specific for HRV as routine base. A multiplex RT-PCR that simultaneously identifies 12 respiratory viruses including HRV is also routinely used in our lab. Here we have described the specific steps of methods for identification of HRV from clinical samples, such as sample preparation, isolation of total RNA, nested-RT-PCR for HRV, Seeplex® RV15 ACE Detection method, gel electrophoresis, how to use the QIAxcel® capillary electrophoresis system, and results interpretation.

**Key words** Human rhinovirus, Nucleic acid isolation, Polymerase chain reaction (PCR), Reverse transcription (RT)-PCR, Nest-PCR, Multiplex PCR

## 1 Introduction

Human rhinoviruses (HRVs), members within genus *Enterovirus* in the family *Picornaviridae*, have a positive-strand RNA genome of 7,200 nucleotides covalently linked at the 5′ end to the viral protein 3B (VPg) and is translated cap-independently by internal ribosomal entry into a polyprotein (VP4-VP2-VP3-VP1-2A-2B-2C-3A-3B-3C-3D), which yields the 11 proteins through various independently functioning intermediates, upon cleavage by viral proteases [1]. HRVs were originally classified into two species, A and B, and approximately 100 serotypes [2–4]. Advances in molecular methods led to the characterization of the third HRV group, a genetically heterogeneous third species, HRV species C(HRV-C) [5, 6]. Identification of the specific strain in HRV disease has been difficult because the traditional serological method is insensitive,

David A. Jans and Reena Ghildyal (eds.), *Rhinoviruses: Methods and Protocols*, Methods in Molecular Biology, vol. 1221, DOI 10.1007/978-1-4939-1571-2_2, 

labor intensive, and cumbersome [7], which requires the isolation of HRV in susceptible cell cultures and neutralization tests against all 101 serotype-specific antisera [3].

To improve the technique for defining the links between illnesses and specific strains of HRV, more sensitive and faster molecular methods have been developed. PCR, RT-PCR, and real-time RT-PCR represent the latest diagnostic methods that provide robust, reproducible results.

We present here an RT-PCR for identification of HRVs and a multiplex RT-PCR that simultaneously identifies 12 respiratory viruses; these assays are routinely used in our laboratory for diagnosis of HRV infection in clinical samples and have been optimized to enable simultaneous handling of large numbers of samples.

## 2 Materials

### 2.1 Sample Preparation

1. Sterile collection tubes with nasopharyngeal aspirates.
2. Flocked tipped swabs with nasal secretions.
3. Sterile saline (0.9 % solution of sodium chloride).
4. Microcentrifuge.
5. Eagle's Minimum Essential Medium (E-MEM) OR Virus Transport Medium (VTM) (*see* **Note 1**).

### 2.2 Isolation of Total RNA

1. Viral RNA isolation kit.
2. Ethanol (96–100 %).
3. Microcentrifuge tubes (1.5 ml).
4. Sterile, RNase-free pipette tips with aerosol barrier
5. Microcentrifuge (with rotor for 2-ml tubes).

### 2.3 RT-PCR

1. Ethanol (96–100 %).
2. Reverse Transcriptase Kit (e.g., SuperScriptTM III, Invitrogen).
3. DNA Polymerase PCR Kit (e.g., GoTaq Green Master Mix, Promega or MangoTaq, Bioline).
4. Seeplex® RV15 ACE Detection Kit (Seegene).
5. Primers (Table 1).
6. RNase-free tips (10, 100, and 1,000 μl).
7. 96-Well plates for PCR with membranes for sealing.
8. GeneAmp PCR system 9700 (Applied Biosystems, *see* **Note 3**).

### 2.4 Gel Electrophoresis

1. Agarose.
2. DNA gel-loading dye.
3. DNA molecular weight marker.
4. Ethidium bromide.

**Table 1**
**Primers for HRV nested-PCR**

| Primer name | Primer sequence (5′–3′) | Target gene | Amplicon length |
|---|---|---|---|
| First run PCR | | | |
| RV-F1 | CTCCGGCCCCTGAATRYGGCTAA | | |
| RV-R1 | TCIGGIARYTTCCASYACCAICC | | |
| Second run PCR | | | |
| RV-F2 | ACCRASTACTTTGGGTRWCCGTG | 5′ NCR-VP4/VP2 | 110 bp |
| RV-R2 | CTGTGTTGAWACYTGAGCICCCA | | |

Bases are shown in single-letter symbols; *A* Adenine, *C* Cytosine, *T* Thymine, *G* Guanine, *W* A/T, *S* C/G, *R* A/G, *Y* C/T, *I* Inosine

5. Electrophoretic buffers.
6. Electrophoresis apparatus.
7. UV transilluminator.
8. QIAxcel® capillary electrophoresis system.

## 3 Methods

### *3.1 Sample preparation (See Notes 4–6)*

1. All samples are collected in sterile tubes in the clinic and sent to microbiology laboratory for testing within 3 h of collection. Samples should be stored at 4 °C at this time (*see* **Note 4**).

   For respiratory virus diagnostics two kinds of samples are collected, nasopharyngeal aspirates (NPA) and nasal swabs. NPAs require specialist equipment that must be handled by trained personnel; this procedure should be performed according to local safety and clinical guidelines. Nasal swabs are collected by inserting flocked tipped swabs into nostrils and must be performed by trained personnel only and according to local safety and clinical guidelines. Swabs must be inserted into tubes with VTM immediately after collection.

2. 1.5 ml sterile saline is added into each tube of NPA; tubes are centrifuged at 14,000 rpm (20,000 × *g*) for 2 min; the supernatant is removed and pellet is resuspended in 200 μl of E-MEM, aliquoted, and kept at −70 °C.

   Nasal swabs are squeezed ten times against the tube walls in VTM and removed; tubes are centrifuged at 3,000 rpm (200 × *g*) for 2 min; the supernatant is aliquoted and kept at −70 °C.

### *3.2 Isolation of Total RNA*

The protocol presented here is based on the QIAamp viral RNA isolation kit; any kit for isolation of total RNA from cell-free body fluids may be used in its stead (*see* **Notes 2** and 7).

1. Equilibrate samples and Buffer AVE to room temperature (15–25 °C).

2. Check that Buffer AW1, Buffer AW2, and Carrier RNA have been prepared according to the manufacturer's instructions. Redissolve any precipitates in Buffer AVL/Carrier RNA by heating, if necessary, and cool to room temperature before use. All centrifugation steps are carried out at room temperature.
3. Pipette 560 µl of prepared Buffer AVL containing Carrier RNA into a 1.5-ml microcentrifuge tube. Add 140 µl treated NPAs/nasal swab solution to the Buffer AVL/Carrier RNA in the microcentrifuge tube. Mix by pulse-vortexing for 15 s. Incubate at room temperature for 10 min.
4. Briefly centrifuge the 1.5-ml microcentrifuge tube to remove drops from the inside of the lid.
5. Add 560 µl of ethanol (96–100 %) to the sample, and mix by pulse-vortexing for 15 s. After mixing, briefly centrifuge the 1.5-ml microcentrifuge tube to remove drops from inside the lid.
6. Carefully apply 630 µl of the solution from **step 5** to the QIAamp spin column (in a 2-ml collection tube) without wetting the rim. Close the cap, and centrifuge at 6,000×*g* (8,000 rpm) for 1 min. Discard the filtrate.
7. Carefully open the QIAamp spin column, and repeat **step 6**.
8. Carefully open the QIAamp spin column, and add 500 µl of Buffer AW1. Close the cap, and centrifuge at 6,000×*g* (8,000 rpm) for 1 min. Place the QIAamp spin column in a clean 2-ml collection tube, and discard the tube containing the filtrate.
9. Carefully open the QIAamp spin column, and add 500 µl of Buffer AW2. Close the cap and centrifuge at full speed (14,000 rpm; 20,000×*g*) for 3 min. Continue directly with **step 10**, or to eliminate any chance of possible Buffer AW2 carryover, perform **step 9(a)**, and then continue with **step 10**.
   (a) (Optional): Place the QIAamp spin column in a new 2-ml collection tube (not provided), and discard the old collection tube with the filtrate. Centrifuge at full speed for 1 min.
10. Place the QIAamp spin column in a clean 1.5-ml microcentrifuge tube. Discard the old collection tube containing the filtrate. Carefully open the QIAamp spin column and add 60 µl of Buffer AVE equilibrated to room temperature. Close the cap, and incubate at room temperature for 1 min. Centrifuge at 6,000×*g* (8,000 rpm) for 1 min. Viral RNA is stable for up to 1 year when stored at −20 °C or −70 °C.

## 3.3 RT-PCR

### 3.3.1 First-Strand cDNA Synthesis

We routinely perform reverse transcription using random hexamers and SuperScriptTM III Reverse Transcriptase Kit on GeneAmp PCR system 9700 according to the manufacturer's recommendations. Any other reverse transcriptase system can be

used, keeping in mind that some optimization may be required for optimal results (*see* **Note 9**).

1. Briefly centrifuge each reagent provided in the kit.
2. Prepare pre-mix 1 in a sterile, nuclease-free microcentrifuge tube as below, mix by brief vortex, and centrifuge briefly:

| **Pre-mix 1 (for one reaction)** | |
|---|---|
| 5 μg Total RNA | 5 μl |
| 50 ng/μl random primer | 1 μl |
| 10 mM dNTP mix | 1 μl |
| DNase- and RNase-free water | 3 μl |
| Total volume | 10 μl |

   Calculate the required total amount of each reagent based on the number of reactions (samples + controls).
3. Label a 96-well plate, as the cDNA plate. Pipette 10 μl of pre-mix into each well of the cDNA plate; cover with the sealing membrane and briefly centrifuge the plate.
4. Place the cDNA plate into GeneAmp PCR system 9700, and incubate at 65 °C for 5 min. Take the cDNA plate out and put it on the ice. Centrifuge briefly before removing the membrane seal.
5. Take another sterile, nuclease-free 1.5 ml microcentrifuge tube labeled as pre-mix 2. Add the following reagents (shown for one reaction); mix by quick vortex, and centrifuge briefly.

| **Pre-mix 2 (for one reaction):** | |
|---|---|
| 10× RT buffer | 2 μl |
| 25 mM $MgCl_2$ | 4 μl |
| 0.1 M DTT | 2 μl |
| RNase OUT(40 U/μl) | 1 μl |
| SuperScript III RT(200 U/μl) | 1 μl |
| Total volume of pre-mix 2 | 10 μl |

   Calculate the required amount of each reagent based on the number of reactions (samples + controls).
6. Pipet 10 μl of pre-mix 2 into each well of the cDNA plate; cover it with the sealing membrane carefully and briefly centrifuge the plate.

7. Place the cDNA plate into GeneAmp PCR system 9700, run the following cycling parameter: one cycle of (25 °C, 10 min); followed by one cycle of 50 °C, 50 min; then one cycle of (85 °C, 5 min) to stop the reaction. Take the plate out and put it on the ice. Centrifuge briefly before removing the sealing membrane.
8. Pipet 1 μl of RNase H into each well of the cDNA plate; cover carefully with membrane seal and centrifuge briefly.
9. Place the cDNA plate into GeneAmp PCR system 9700, and run one cycle of (37 °C, 20 min).
10. The first-strand cDNA is synthesized and can serve as the template in the nested-PCR or the multiplex PCR or stored at −20 °C for future use.

### 3.3.2 Nested-PCR

This procedure consists of two PCR cycles, the first run PCR using the cDNA as template and the second run PCR using the amplimers from the first run PCR as template.

1. First Run PCR
   1. Prepare pre-mix 1 in the reagent preparation room (*see* **Note 8**). Completely thaw and thoroughly vortex the buffer prior to use; then briefly centrifuge each reagent.
   2. In a sterile, nuclease-free microcentrifuge tube combine the following components to prepare the pre-mix 1 (shown for one reaction); mix by quick vortex and centrifuge briefly.

| **Pre-mix 1 (for one reaction)** | |
|---|---|
| Nuclease-free water | 8.25 μl |
| 5× colorless GoTaq flexi buffer | 5 μl |
| $Mgcl_2$ solution, 25 mM | 2 μl |
| PCR nucleotide mix, 10 mM each | 0.5 μl |
| Primers | 1 μl |
| Go Taq DNA polymerase (5 u/μl) | 0.25 μl |
| Total volume of pre-mix 1 | 17 μl |

   Calculate the necessary amount of each reagent based on the number of reactions (samples + controls).
   3. Label a 96-well plate as the first run PCR plate. Pipet 17 μl of pre-mix 1 into each well of the first run PCR plate; Transfer the first run PCR plate from the reagent preparation room to the template preparation room. Open the cDNA plate and pipet 3 μl of cDNA template from the cDNA plate into each corresponding well of the first run PCR plate.

4. Cover the 96-well plates with the membrane for PCR plate carefully; briefly centrifuge the plate.
5. Place the first run PCR plate into the GeneAmp PCR system 9700 in the nucleic acid amplification room, and run the following cycling parameter:

| | |
|---|---|
| 94 °C 30 s | |
| 55 °C 1 min | 45 cycles |
| 72 °C 1 min | |
| 72 °C 10 min | |

2. Second run PCR.
   1. Prepare pre-mix 2 in the reagent preparation room. Completely thaw and thoroughly vortex the buffer prior to use; then briefly centrifuge each reagent.
   2. In a sterile, nuclease-free microcentrifuge tube combine the following components to prepare the pre-mix 2 (shown for one reaction); mix by quick vortex and centrifuge briefly.

| **Pre-mix 2 (for one reaction)** | |
|---|---|
| Nuclease-free water | 10.25 μl |
| 5× colorless GoTaq flexi buffer | 5 μl |
| $Mgcl_2$ solution, 25 mM | 2 μl |
| PCR nucleotide mix, 10 mM each | 0.5 μl |
| Primers | 1 μl |
| Go Taq DNA polymerase(5u/μl) | 0.25 μl |
| Total volume of pre-mix 2 | 19 μl |

   Calculate the necessary amount of each reagent based on the number of reactions (samples + controls).
   3. Label another 96-well plate as the second run PCR plate. Pipet 19 μl of pre-mix 2 into each well of the second run PCR plate.
   4. Transfer the second run PCR plate from the reagent preparation room to the template preparation room. Open the first run PCR plate and pipet 1 μl of DNA template from the first run PCR plate into each corresponding well of the second run PCR plate.
   5. Cover the second run PCR plate with the membrane for PCR plate carefully; briefly centrifuge the plate.

6. Place the second run PCR plate into the GeneAmp PCR system 9700 in the nucleic acid amplification room, and run the following cycling parameter:

| | |
|---|---|
| 94 °C 30 s | |
| 55 °C 1 min | 35 cycles |
| 72 °C 1 min | |
| 72 °C 10 min | |

7. After analysis of the PCR products by electrophoresis, irradiate the PCR products with UV light (365 nm) for 20 min to prevent carryover contamination.

### 3.3.3 Multiplex PCR for 15 Respiratory Viruses

We usually use the Seeplex RV15 ACE Detection Kit to simultaneously detect 15 common respiratory viruses. The Seeplex kit is very widely used in clinical microbiology laboratories around the world. The viruses included influenza (Flu) A/B, respiratory syncytial viruses (RSV) A/B, human metapneumovirus (hMPV), human parainfluenza viruses (PIV) 1/2/3/4, human adenovirus (AdV), human rhinovirus (HRV), human coronavirus 229E/NL63 and OC43/HKU1, human bocavirus (HBoV) and human enterovirus.

1. Prepare master mix in the reagent preparation room. Completely thaw and thoroughly vortex the buffer prior to use, and then briefly centrifuge each reagent.
2. Add the following reagents (shown for one reaction) to a sterile, nuclease-free microcentrifuge tube, mix by quick vortex, and centrifuge briefly:

| | |
|---|---|
| 5× RV 15 ACE PM | 4 μl |
| 2× Multiple master mix | 2 μl |
| 8-MOP solution | 3 μl |
| Water | 8 μl |
| Total volume of master mix | 17 μl |

   Calculate the necessary amount of each reagent based on the number of reactions (samples + controls).
3. Label a 96-well plate as the RV15 PCR plate. Aliquot 17 μl of master mix into each well the RV15 PCR plate.
4. Transfer the RV15 PCR plate from the Reagent preparation room to the template preparation room. Pipet 3 μl of cDNA template from the cDNA plate into each corresponding well of the RV 15 PCR plate. Use 3 μl of ACE NC for the negative control PCR. Use 3 μl of ACE PC for the positive control PCR.


**Fig. 1** Gel image of rhinovirus nested-RT-PCR products. The nasopharyngeal aspirate (NPA) samples (S) 1, 3, 5, 9, 10, 21, and 32 were collected from seven children with lower respiratory tract infection. Respiratory epithelial cells were collected from NPAs and processed for RNA isolation followed by nested-RT-PCR as described in Subheadings 2 and 3. PCR products were separated on 2 % agarose gel electrophoresis and visualized by ethidium bromide staining; the relevant DNA marker is indicated

5. Cover the RV 15 PCR plate with sealing membrane and briefly centrifuge the plate.
6. Place the RV 15 PCR plate into the preheated 94 °C GeneAmp PCR system 9700 in the nucleic acid amplification room, and immediately run the PCR reaction using the following program:

| | |
|---|---|
| 94 °C 0.5 min | |
| 60 °C 1.5 min | 40 cycles |
| 72 °C 1.5 min | |
| 72 °C 10 min | |

*3.3.4 Analysis of PCR Products*

PCR products may be analyzed by agarose gel electrophoresis or by capillary electrophoresis. Figure 1 depicts a typical pattern obtained by gel electrophoresis, while Fig. 2 depicts a typical pattern obtained by capillary electrophoresis.

1. Separate the PCR products from the second run PCR by 2 % agarose gel electrophoresis and visualize by UV transillumination (*see* Chapter 3 for detailed method).
   (a) For reactions containing the 5× Green GoTaq™ Reaction Buffer, load samples onto the gel directly after amplification.
   (b) For reactions not containing any indicator dyes, add gel-loading dye (e.g., bromophenol blue) before loading on the gel.
   (c) Please *see* Fig. 1 for a picture of a sample gel of nested-PCR products from nasal swabs collected from children with suspected lower respiratory tract infection.
   (d) There are single bright bands at the 110 bp size location of the positive control (PC), lanes labeled S5, S10, S21, and S32, but no bands around the same location in the negative control (NC), S1, S3, and S9 lanes.

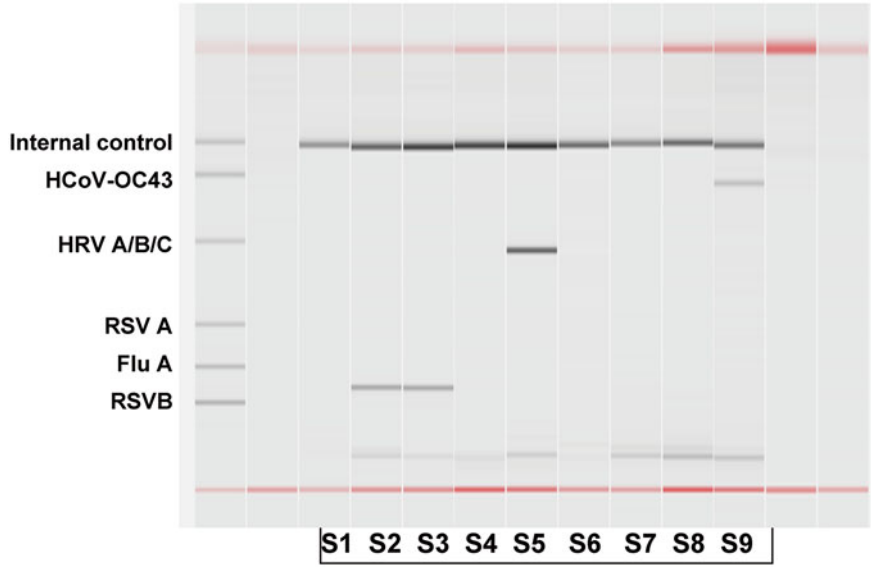


**Fig. 2** Image of Seeplex RV 15 Multiplex products using QIAxcel capillary electrophoresis. NPA samples (S) 1–9 were collected from nine children with lower respiratory tract infection. NPA samples were processed for cell isolation, RNA extraction, and reverse transcription as in Fig. 1. Seeplex RV 15 Multiplex PCR was performed as described in the text and PCR products separated by the QIAxcel® Novel 12-channel capillary electrophoresis system. The reference table for RV15 ACE Detection (B set) marker is indicated

2. Capillary electrophoresis using QIAxcel system (*see* **Note 10**). The 96-well plates can be run directly in the QIAxcel® capillary electrophoresis system. Separation is performed in a capillary of a precast gel cartridge. Each sample is automatically loaded (according to voltage and time parameters) into an individual capillary and voltage is applied. As the molecules migrate through the capillary, they pass a detector that measures the fluorescent signal. A photomultiplier detector converts the emission signal into electronic data, which are then transferred to the computer for further processing using BioCalculator software. After processing, the data are displayed as an electropherogram and a gel image.
   (a) The 0.2-ml 12-tube strips containing QX Alignment Marker and QX Intensity Calibration Marker (if required) should fit loosely in the MARKER1 and MARKER2 position.
   (b) QX Alignment Markers should be replaced every 15–20 runs or as needed.
   (c) When not in use, the 12-tube strip containing QX Alignment Marker should be stored at −20 °C. It should be equilibrated to operating temperature (20–25 °C) and centrifuged briefly before use.

(d) If the QIAxcel gel cartridge is being used for the first time, intensity calibration should be performed (*see* **Note 11**).

(e) Preparation of the gel cartridge:
Add 10 ml QX Wash Buffer to both reservoirs of the QX Cartridge Stand (provided with the QIAxcel instrument) and cover with 3 ml mineral oil (supplied).
Remove the QIAxcel gel cartridge from its packaging and carefully wipe off any soft gel debris from the capillary tips using a soft tissue.
Remove the purge cap seal from the back of the QIAxcel gel cartridge and place it in the QX Cartridge Stand.
Incubate new cartridges in the QX Cartridge Stand for 20 min prior to use.

(f) Preparing the buffer tray:
Allow all reagents to equilibrate to room temperature (15–25 °C) before use.
Wash the buffer tray with hot water and rinse thoroughly with deionized water.
Fill the WP and WI positions of the buffer tray with 8 ml QX Wash Buffer.
Fill the BUF position of the buffer tray with 18 ml QX Separation Buffer.
Carefully add mineral oil to all three positions to prevent evaporation: add 2 ml mineral oil to positions WP and WI and 4 ml mineral oil to position BUF. All three positions should be covered with mineral oil.
Insert the buffer tray into the buffer tray holder so that the slots for the 12-tube strips face the front of the instrument.

(g) Preparing QX Alignment Markers:
Load 15 µl QX Alignment Marker into each well of a QX 0.2 ml 12-tube strip.
Add one drop of mineral oil to each well, and insert the strip into the MARKER1 position of the buffer tray. Important: The 12-tube strip should fit loosely in the MARKER1 position on the buffer tray.

(h) Installing a QIAxcel gel cartridge and smart key:
Remove the QIAxcel gel cartridge from the QX Cartridge Stand; open the cartridge door and insert the QIAxcel gel cartridge into the QIAxcel system. The cartridge description label should face the front and the purge hole should face the back of the system.
Insert the smart key into the smart key socket. The smart key can be inserted in either direction.
Close the cartridge door. The cartridge ID, number of runs remaining, and cartridge type will be displayed

automatically in the "Instrument Control" window once the smart key is latched. The system will not recognize the cartridge and will not operate if the smart key is not inserted.

Add the DNA size marker (supplied with the kit) into the black well (*see* **Note 12**).

Load the 96-well plate containing the samples. The minimum sample volume required for analysis is 10 μl. Less than 0.1 μl of the sample will be loaded onto the QIAxcel gel cartridge for analysis. The remaining DNA can be kept for reanalysis or downstream processing.

Results for nine nasal swab samples assayed by the Seeplex RV15 multiplex PCR products are shown in Fig. 2. According to the reference table provided by the manufacturer, samples 2 and 3 are probably positive for influenza A (a second specific PCR and/or sequencing of the PCR product needs to be performed to confirm), sample 5 is positive for HRV, and sample 9 is positive for CoV-OC43. The size of samples 2 and 3 is equal to influenza A, the size of sample 5 is equal to human rhinovirus A/B/C, and the size of sample 9 is equal to human coronavirus OC43. Samples 4, 6, 7, and 8 are negative for all the respiratory viruses detected by Seeplex assay.

## 4 Notes

1. E-MEM or VTM can be used to collect samples for virus testing. If desired, commercial VTM preparations can be used.
2. The protocol described here has been optimized for the Roche MagnaPure LC 2.0 system; however, any comparable system for isolation of total RNA from clinical samples may be used, but may require modification of the protocol to optimize results.
3. Any PCR equipment that is able to handle multiple samples in a 96-well format will be suitable.
4. The clinical samples collected from patients with lower respiratory tract infection should be kept in 4 °C refrigerator and sent to microbiological laboratory within 8 h post-collection; If samples cannot be sent to laboratory within 8 h post-collection, they should be frozen at −70 °C.
5. Appropriate personal protective equipment (laboratory coat, mask, gloves) should be worn at all times when handling human specimens.
6. All clinical samples collected from patients with lower respiratory tract infection should be handled in a biological safety cabinet.

7. When the number of samples to be analyzed is less than 10, it is quicker and more convenient to isolate the total RNA from samples manually by using the QIAamp® Viral RNA Mini Kit. When the number of samples is more than 10, it is laborious and time consuming to isolate the total RNA from samples manually and an automated system, e.g., the Roche MagnaPure LC 2.0, may be used.
8. Prepare the PCR pre-mix only in the pre-mix preparation room. Assay the first-strand cDNA synthesis and perform template DNA/RNA or cDNA pipetting in the template room. Do not apply the first-strand cDNA synthesis in the pre-mix preparation room to avoid contamination of the following PCR test. Ensure that the plates are covered and sealed with a membrane before they are transfered to PCR machine in the PCR amplification room.
9. The 8-channel micropipette is preferred when using 96-well plates. It is less laborious and more accurate to aliquot reagent and pipet template DNA/RNA or cDNA into each well. Using multichannel micropipette also helps to reduce the contamination during PCR assay process.
10. The QIAxcel system offers a number of advantages over traditional slab-gel electrophoresis, including higher detection sensitivity, less sample wastage (minimal sample input volumes), fast analysis of up to 96 samples, and automated loading and analysis, making it the preferred method for analysis of DNA products when large numbers of samples are processed.
11. This step is not necessary if the QIAxcel gel cartridge has already been calibrated, unless it is being used on a different QIAxcel instrument or a different computer is used to operate the instrument. If a different computer is used, the calibration log file must be transferred from the computer used to operate the instrument to the new computer so that it is not necessary to run the calibration again.
12. Once created, a single DNA reference marker table can be used for the entire life of the cartridge. However, variations in separation temperature of the cartridge and buffer can introduce variations in DNA size determination. For optimal results, we recommend creating a new DNA reference marker table every 8 runs or after each 96-well plate.

## Acknowledgements

This work was supported by the Public Health Academic Leader Project (grant number GWDTR201201) from Shanghai Municipal Health Bureau.

## References

1. Rueckert RR (1996) Picornavirus structure and multiplication in Virology. In: Fields BN, Knipe DM, Howley PM (eds) Virology. Raven Press Ltd., New York, NY, p 609–654
2. Pelon W, Mogabgab WJ, Phillips IA, Pierce WE (1957) A cytopathogenic agent isolated from naval recruits with mild respiratory illnesses. Proc Soc Exp Biol Med 94:262–267
3. Hamparian VV, Colonno RJ, Cooney MK, Dick EC, Gwaltney JM Jr, Hughes JH, Jordan WS Jr, Kapikian AZ, Mogabgab WJ, Monto A et al (1987) A Collaborative report: Rhinoviruses–extension of the numbering system from 89 to 100. Virology 159:191–192
4. Kapikian AZ, Conant RM, Hamparian VV, Chanock RM, Dick EC (1971) A collaborative report: Rhinoviruses–extension of the numbering system. Virology 43:524–526
5. Lamson D, Renwick N, Kapoor V, Liu Z, Palacios G, Ju J, Dean A, St George K, Briese T, Lipkin WI (2006) MassTag polymerase-chain-reaction detection of respiratory pathogens, including a new rhinovirus genotype, that caused influenza-like illness in New York State during 2004–2005. J Infect Dis 194: 1398–1402
6. McErlean P, Shackelton LA, Lambert SB, Nissen MD, Sloots TP, Mackay IM (2007) Characterisation of a newly identified human rhinovirus, HRV-QPM, discovered in infants with bronchiolitis. J Clin Virol 39:67–75
7. Oberste MS, Nix WA, Maher K, Pallansch MA (2003) Improved molecular identification of enteroviruses by RT-PCR and amplicon sequencing. J Clin Virol 26:375–377

# Chapter 3

# Molecular Identification and Quantification of Human Rhinoviruses in Respiratory Samples

**Wai-Ming Lee, Kris Grindle, Rose Vrtis, Tressa Pappas, Fue Vang, Iris Lee, and James E. Gern**

## Abstract

PCR-based molecular assays have become standard diagnostic procedures for the identification and quantification of human rhinoviruses (HRVs) and other respiratory pathogens in most, if not all, clinical microbiology laboratories. Molecular assays are significantly more sensitive than traditional culture-based and serological methods. This advantage has led to the recognition that HRV infections are common causes for not only upper airway symptoms but also more severe lower respiratory illnesses. In addition, molecular assays improve turnaround time, can be performed by technicians with ordinary skills, and can easily be automated. This chapter describes two highly sensitive and specific PCR-based methods for identifying and quantifying HRVs. The first is a two-step PCR method for the detection and typing of HRV. The second is a pan-HRV real-time quantitative (q) PCR method for measuring viral loads in respiratory samples.

**Key words** Molecular typing, HRV type, Species, Real-time quantitative PCR, Viral load

## 1 Introduction

Human rhinoviruses (HRVs) are the most prevalent human viruses infecting billions of people annually [1–3], and HRVs have long been recognized as the cause of >50 % of all acute upper respiratory illnesses (common colds), the most frequent human illnesses [1, 2]. The recent advent of PCR-based molecular assays has demonstrated that HRV infections are also common causes of more severe lower respiratory illnesses, particularly in at-risk populations such as infants, the elderly, the immunocompromised, and those with underlying respiratory disorders (asthma, chronic obstructive respiratory disease [COPD], and cystic fibrosis) [4–9]. Interestingly, one-third of HRV infections are asymptomatic [10–12]. Therefore, understanding the roles of viral, host, and environmental determinants in HRV illness severity may lead to measures for preventing and curing HRV illnesses.

David A. Jans and Reena Ghildyal (eds.), *Rhinoviruses: Methods and Protocols*, Methods in Molecular Biology, vol. 1221, DOI 10.1007/978-1-4939-1571-2_3, 

HRV is composed of a large group of small positive-stranded RNA viruses with diverse capsid sequences. They belong to the picornavirus family and are close cousins of polioviruses. HRV has about 150 distinct types or members. They are divided into three species: A (75 types), B (25 types), and C (about 50 types) according to serological and genome sequence variations [2, 12–18]. The 100 HRV-A and -B types were identified and assigned as serotypes between 1956 and 1987 with traditional culture-based, biochemical and serological methods [10, 19, 20]. Each serotype was defined by 20-fold or greater differences in antiserum neutralization titers during reciprocal cross-neutralization tests against the other 99 serotypes [3, 20]. The 50 HRV-C types were identified only recently with modern PCR and sequencing techniques as they do not grow in traditional cell culture systems (12, 21–25; *see* Chapter 1 in this volume).

The traditional culture method for HRV detection, identification, and quantification is laborious, time consuming, and cumbersome [20, 26, 27]. More importantly, it is insensitive because traditional cell cultures do not support the growth of HRV-C types, which amount to about one-third of all HRVs, and many field strains of HRV-A and -B serotypes do not induce clear cytopathic effects (CPE) due to poor growth in culture. Typically, infectious virus can be detected from only about 20 % of respiratory samples that have tested positive for HRV by PCR [11, 28].

The allergy and asthma research group of the University of Wisconsin—Madison (UW) is one of the leading teams in the world conducting large-scale epidemiological studies to elucidate the roles of viral, host, and environmental determinants in the severity of HRV illness [29, 30]. In order to generate unbiased data sets, the UW team developed a series of highly sensitive and specific molecular assays for the comprehensive identification of HRVs and other respiratory viruses in respiratory specimens [12, 22, 28, 31, 32], including a two-step PCR method for the detection and typing of HRV and a pan-HRV real-time quantitative (q) PCR method for measuring the viral loads of HRV in respiratory specimens. This chapter describes these two methods in detail.

Briefly, the two-step PCR method is composed of a first step "touchdown" PCR for highly specific amplification of the target sequence of HRV [33, 34] followed by conventional PCR for efficient production of sufficient amount of target DNA for sequencing and other analyses. Two assays for two different genome regions of HRV have been developed with this PCR method. The 5′ NCR assay amplifies a 390 nt fragment of the 5′ noncoding region (NCR) and the VP4-2 assay amplifies a 640 nt fragment of the capsid protein genes VP4-VP2. The 5′ NCR and VP4-2 assays detect as few as 10 copies and 50 copies of cDNA per reaction, respectively.

The resulting PCR fragments can be sequenced directly to provide 300 nt 5′ NCR or 420 nt VP4-VP2 sequences for typing. The 5′ NCR assay is very sensitive for HRV identification. In a recent community study by the UW team [12], 1,445 nasal samples from 209 children were analyzed and the 5′ NCR assay detected HRV in 60.7 and 35.1 % of samples from sick and healthy children, respectively. Typing was successful in 98.7 % of the HRV-positive samples. The VP4-2 assay is about 80 % as sensitive as the 5′ NCR assay, and is useful for confirming the typing results of the 5′ NCR assay.

The UW team has developed a database of 5′ NCR sequences of 152 HRV types [12] for convenient type assignment, after sequencing >3,000 HRV-positive clinical samples with no new types was detected in the last 500 samples. These sequences have been submitted to GenBank. Their accession numbers are EU126663-EU126789, FJ968439-FJ968447, and JX041186-JX041202. The 152 types include the 100 classical HRV-A and -B serotypes (denoted R) and 52 new types (denoted W) [12]. The 52 new types include 46 HRV-C and 6 HRV-A types [12].

The pan-HRV qPCR method was originally developed based on the conserved sequences at the 5′ NCR of the 100 classical HRV-A and -B serotypes of ATCC [32, 35]. However, it is also applicable to the new HRV-C types with one or two nucleotide modifications in the forward PCR primer because the target sequences are also conserved in HRV-Cs. Of the 100 classical serotypes, 91 have complete sequence identity with the two qPCR primers and the probe, and the remaining 9 serotypes have only a single mismatch. Experimental test results showed that the assay can accurately quantify 96 serotypes, and only a one-base modification in the forward PCR primer is required for quantifying the remaining 4 serotypes: HRV-18, -33, -70, and -72. In our assays, purified HRV16 virions with known concentrations are used as a calibration standard. The serially diluted HRV16 standards are extracted, reverse-transcribed, and quantified in parallel with the respiratory samples. A typical standard curve has a six-log linear range (from $1 \times 10^4$ to $1 \times 10^9$ virions) and an efficiency of 1.9–2.1.

Like other PCR-based assays, our molecular assays are very susceptible to contamination due to their great sensitivity. Therefore, it is important to be vigilant to avoid contamination. A good molecular assay laboratory necessitates an optimal lab space arrangement with technicians that practice proper techniques and carefully adhere to lab procedures. Please *see* ref. 36 for how to set up a contamination-free clean molecular assay laboratory. In addition, a comprehensive set of negative controls should always be performed in parallel with the samples.

## 2 Materials

### 2.1 Total RNA Extraction

1. Eppendorf thermomixer.
2. Sterile disposables:
   (a) 1.5-mL DNA LoBind (LB) eppi tube (Eppendorf).
   (b) 100- to 1,000-µl barrier pipette tips.
   (c) 20- to 200-µl barrier pipette tips.
   (d) 0.1- to 10-µl barrier pipette tips.
   (e) 50-ml capped tubes.
   (f) 14-ml polypropylene tubes.
3. Reagents for RNA work:
   (a) Trizol LS.
   (b) Chloroform.
   (c) 2-Propanol.
   (d) Ethanol—absolute.
   (e) Glycoblue, 15 µg/µl (Invitrogen AM9515).
   (f) DNase/RNase-free distilled water.
4. Carrier mixture for 30 samples (*see* **Note 1**):
   To 1,140 µl 5× NA extraction buffer, add 60 µl of glycoblue (15 µg/µl).
5. Distilled water.
6. 5× NA extraction buffer:
   To 220 ml distilled water, add the following ingredients, and filter sterilize:
   (a) 125 ml 2 M Tris, pH 7.5.
   (b) 150 ml 5 M NaCl.
   (c) 5 ml 0.5 M EDTA.

### 2.2 cDNA Synthesis

1. Sterile disposables:
   (a) *See* Subheading 2.1 above.
   (b) 0.2-ml thin-wall polypropylene eight-tube strips for PCR.
   (c) Domed eight-cap strips for 0.2-ml PCR tubes.
   (d) 0.5-ml DNA LoBind (LB) eppi tube (Eppendorf 022431005).
2. Reagents for cDNA synthesis (*see* **Note 2**):
   (a) AMV-RT, 10 U/µl and 5× reaction buffer.
   (b) Random hexa-primers.
   (c) RNasin, 40 U/µl.
   (d) 10 mM dNTP.

### 2.3 Molecular Typing

1. PCR machine.
2. PCR primers for 5′ NCR assay (*see* **Note 3**):
   (a) Forward primer mix BF1 is a mixture of 25 μM of primers B1, B2, and B3:
      - B1: CAAGCACTTCTGTTTCCCC.
      - B2: CAAGCACTTCTGTTACCCC.
      - B3: CAAGCACTTCTGTCTCCCC.

   (b) Reverse primer FR2: ACGGACACCCAAAGTAG.
3. PCR primers for VP4-2 assay:
   (a) Forward primer VP4-F1: CTCCGGCCCCTGAATRYGG CTAA.
   (b) Reverse primer VP4-R1: TCIGGIARYTTCCASYACC AICC.
4. Sterile disposables: *See* Subheading 3.2 above.
5. Platinum PCR SuperMix HF (Invitrogen) (*see* **Note 4**).
6. DNase/RNase-free distilled water.
7. Reagents for agarose gel analysis of the PCR product:
   (a) 10× TBE.
   (b) Agarose.
   (c) 10× BlueJuice gel loading buffer (Invitrogen 10816-015).
   (d) 1 kb DNA ladder.

### 2.4 Pan-HRV qPCR

1. qPCR primers:
   (a) Forward primer D110: CTAGCCTGCGTGG, 200 μM in water.
   (b) Reverse primer RVQ1: AAACACGGACACCCAAAGT AGT, 200 μM in water.
   (c) Probe RVQ2: 6FAM-TCCTCCGGCCCCTGA-MGB-NFQ, 100 μM in water.
2. 5× primer mixture:
   To 950 μl DNase/RNase-free water, add the following ingredients:
   (a) 22.5 μl D110 (4.5 μM).
   (b) 22.5 μl RVQ1 (4.5 μM).
   (c) 5 μl RVQ2 (0.5 μM).
3. 2× TaqMan Universal PCR Master mix (Applied Biosystems 4364338).
4. 2× SsoFast Probes Supermix (Bio-Rad, 172-5231).
5. Microseal B film.
6. 96-well PCR plate-Hard-Shell.
7. DNase/RNase-free distilled water.

## 3 Methods

### 3.1 Total RNA Extraction

1. Add 40 μl carrier mixture and 0.75 ml Trizol LS to each 350 μl nasal wash sample in a 1.5-ml LB eppi tube (*see* **Note 5**).
2. Vortex the mixture in an Eppendorf thermomixer for 10 min (min) at room temperature (RT).
3. Microfuge for 3 s to remove sample solution from the cap, and then open the cap of each eppi tube carefully to avoid cross contamination.
4. Add 230 μl chloroform to each sample.
5. Vortex the mixture in a thermomixer for 5 min at RT.
6. Microfuge (5 min, RT) to separate the aqueous and organic phases (*see* **Note 6**).
7. Transfer ~700 μl of the upper aqueous solution from the extraction eppi tube into a new 1.5-ml LB eppi tube containing 600 μl isopropanol.
8. Mix well, and then incubate at RT for >1 h (hour) for RNA precipitation.
9. Microfuge (10 min, RT) to pellet the RNA precipitant.
10. Remove supernatant with a new P1000 tip for each sample.
11. Add 0.6 ml 75 % ethanol and then vortex vigorously for 15 s.
12. Microfuge for 2 min at RT and then remove supernatant with a new P1000 tip.
13. Repeat **steps 11** and **12** once.
14. Air-dry the RNA pellet.
15. Add 22 μl DNase/RNase-free water to each pellet and then vortex vigorously to dissolve the RNA.
16. Store the RNA at −80 °C until cDNA synthesis.

### 3.2 cDNA Synthesis

1. Prepare an RTase reaction mixture for one reaction with the following recipe:
   (a) 12.25 μl DNase/RNase-free water.
   (b) 10 μl 5× AMV-RTase buffer.
   (c) 5 μl 10 mM dNTP.
   (d) 1.25 μl random primers.
   (e) 0.75 μl RNasin.
   (f) 0.75 μl AMV-RTase.
2. Add 30 μl of RTase mixture and then 20 μl of RNA into each 0.2-ml PCR tube.
3. Run the following reverse transcriptase (RTase) program in a PCR machine:

(a) 25 °C for 5 min.

(b) 42 °C for 10 min.

(c) 50 °C for 20 min.

(d) 85 °C for 5 min.

4. Transfer the reaction mixture to 0.5-ml LB eppi tube and then store at –20 °C.

### 3.3 Molecular Typing

#### 3.3.1 Two-Step PCR Reaction

First Step PCR

1. Prepare a PCR mixture for one reaction with the following recipe:

   (a) 23 μl Platinum PCR SuperMix HF.

   (b) 0.5 μl forward primer (25 μM).

   (c) 0.5 μl reverse primer (25 μM).

   For 5′ NCR assay: forward primer is BF1 and reverse primer is FR2.
   For VP4-2 assay: forward primer is VP4-F1 and reverse primer is VP4-R1.

2. Add 24 μl of PCR mixture and then 2 μl of cDNA into each 0.2-ml PCR tube.

3. Start "touchdown" PCR program:
   The "touchdown" PCR program starts with a "hot start" of 2 min at 94 °C, followed by "annealing temperature step-down" cycles (the cycles are 94 °C for 20 s, 68 °C down to 52 °C (2 °C intervals)) for 30 s, and then 68 °C for 40 s. There are 3 cycles for each annealing temperature down to 54 °C followed by 12 cycles at 52 °C, and then a final 5 min at 68 °C.

4. Transfer the PCR product to 0.5-ml LB eppi tube and then store at –20 °C.

Second Step PCR

1. Prepare a PCR mixture for one reaction with the following recipe:

   (a) 45 μl Platinum PCR SuperMix.

   (b) 1 μl forward primer (25 μM).

   (c) 1 μl reverse primer (25 μM).

   For 5′ NCR assay: forward primer is BF1 and reverse primer is FR2.
   For VP4-2 assay: forward primer is VP4-F1 and reverse primer is VP4-R1.

2. Add 47 μl of PCR mixture and then 5 μl "touchdown" PCR product into each 0.2-ml PCR tube.

3. Run the following conventional PCR program.

   (a) 94 °C for 2 min.

   (b) 94 °C for 20 s.

   (c) 52 °C for 30 s.

   (d) 68 °C for 40 s (1 min for 1 kb fragment).

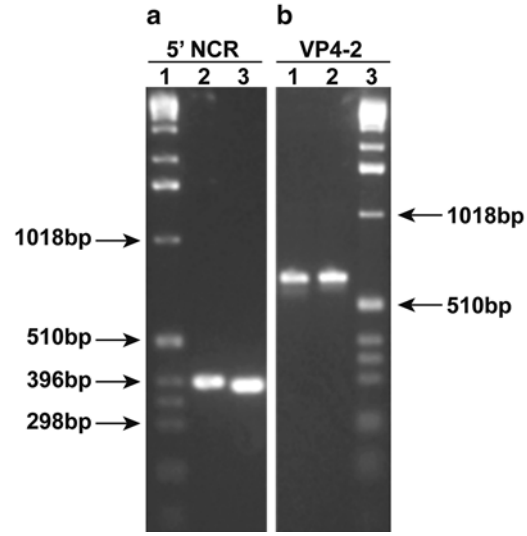


**Fig. 1** Typical agarose gel analysis results of the DNA products from the two-step PCR of the molecular typing assay. RNA extraction, cDNA synthesis, and two-step PCR were performed as described in Subheadings 3.1, 3.2, and 3.3.1. The PCR product (4 μl) of each sample was electrophoresed in a 1.2 % agarose gel and the gel was stained with EtBr (Subheading 3.3.2). Panel (**a**). The 5′ NCR assay gives a 400 bp band. *Lane 1* is the 1 kb DNA ladder marker (Invitrogen), *lanes 2* and *3* are two different nasal samples. Panel (**b**). The VP4-2 assay gives a 640 bp band. *Lanes 1* and *2* are two different nasal samples, and *lane 3* is the 1 kb DNA ladder marker (Invitrogen)

(e) Repeat steps (**b**)–(**d**) 27 times.

(f) 68 °C for 3 min.

(g) 4 °C forever.

4. Transfer the PCR product to a 0.5-ml LB eppi tube and then store at −20 °C.

### *3.3.2 Agarose Gel Analysis and Sequencing of the PCR Product*

1. Run 4 μl PCR product in a 1.2 % agarose gel and use ethidium bromide staining to estimate the amount of the target PCR fragment.
2. If the sample gives a visible 400 bp band (5′ NCR assay) or 640 bp band (VP4-2 assay), it can be used for sequencing directly (Fig. 1).
3. Prepare a sequencing premix with the following recipe for one reaction, and then send the sample to your favorite sequencing facility (*see* **Note 7**).

(a) 16 μl DNase/RNase-free water.

(b) 5 μl 2.5 μM sequencing primer (FR2 for 5′ NCR and VP4-F1 for VP4-2 assay).

(c) 4 μl PCR reaction product.

*3.3.3 Processing of Sequences from Sequencing Facility*

1. For the partial 5′ NCR:
   (a) Generate the "reverse complement" of the sequences from the sequencing facility since the FR2 primer produces a negative-sense sequence and the reference sequences are positive sense.
   (b) Remove the extra sequences upstream of CCCCGG and downstream of GGCTAA of each sequence to generate the approximately 300 nt sequence for alignment and phylogenetic tree analysis.
2. For the VP4-2 sequences:
   (a) Use the sequences from the sequencing facility directly for analysis since they are positive sense.
   (b) Remove the extra sequence upstream of the start codon of VP4 (ATGGG) and the sequence after nt# 420 of each sequence to generate a 420 nt sequence for alignment and phylogenetic tree analysis.

*3.3.4 Type Assignment by Alignment and Phylogenetic Tree Analysis of the 5′ NCR Sequences Using ClustalX Program [37]*

1. Prepare a sequence file (labeled XYZ) in FASTA format containing your new sequences and the 152 5′ NCR reference sequences.
2. Put the sequence file in a folder (labeled XYZ-Tree).
3. Launch the ClustalX program.
4. Open the sequence file by selecting "Load Sequences" under "File" menu, and then selecting the file XYZ in the folder XYZ-Tree.
5. Start the alignment by selecting "Do Complete Alignment" under "Alignment" menu with default options.
6. Construct the phylogenetic tree by selecting "Draw NJ Tree" under "Tree" menu with default options. A tree file called XYZ.ph will be generated after the computing is done.
7. Launch NJPLOT program (*see* **Note 8**) and then open file "XYZ.ph." This will generate a graphic file "XYZ.PICT" that contains a tree structure showing the phylogenetic relationship of your new sequences and the 152 reference sequences (*see* **Note 9**).
8. Assign the type/serotype with which the sequence clustered. Occasionally, you may have sequences of an enterovirus and, rarely, a brand new HRV type beyond the 52 new HRV types. *See* **Note 10** for dealing with these new sequences.

### 3.4 Pan-HRV qPCR

We have good results with two different commercially available qPCR mixes: TaqMan Universal PCR Master Mix of Applied Biosystems and SsoFAST Probes Supermix of Bio-Rad. Their reaction conditions are slightly different.

*3.4.1 Reaction Using TaqMan Universal PCR Master Mix*

1. Prepare reaction mixture with the following recipe for one reaction:
   (a) 7 μl DNase/RNase-free water.
   (b) 15 μl 2× TaqMan Universal PCR Master Mix.
   (c) 6 μl 5× primer mix.
2. Add 28 μl of reaction mixture into each well of the 96-well plate.
3. Add 2 μl cDNA into each well.
4. Load the plate into a qPCR machine and operate according to the manual.
5. Thermal cycling conditions:
   (a) 50 °C for 2 min.
   (b) 95 °C for 10 min.
   (c) Repeat steps (a) and (b) once.
   (d) 95 °C for 15 s.
   (e) 60 °C for 1 min.
   (f) Repeat **steps (d)** and **(e)** for 40 cycles.
6. The results are the number of copies of HRV genomic RNA per 350 μl of nasal wash sample if the standard curve is constructed with $10^4$, $10^5$, $10^6$, $10^7$, $10^8$, and $10^9$ copies of HRV16 virion RNA per reference sample in one eppi tube.

*3.4.2 Reaction Using Bio-Rad SsoFAST™ Probes Supermix*

1. Prepare reaction mixture with the following recipe for one reaction:
   (a) 4 μl DNase/RNase-free water.
   (b) 10 μl 2× SsoFast Probes Supermix.
   (c) 4 μl 5× primer mix.
2. Add 18 μl reaction mixture into each well of a 96-well plate.
3. Add 2 μl cDNA into each well.
4. Load the plate into a qPCR machine and operate according to the manual.
5. Thermal cycling condition:
   (a) 95 °C for 30 s (once) (*see* **Note 11**).
   (b) 95 °C for 5 s.
   (c) 60 °C for 30 s.
   (d) Repeat **steps (b)** and **(c)** for 40 cycles.
6. The results are the number of copies of HRV genomic RNA per 350 μl of nasal wash sample if the standard curve is constructed with $10^4$, $10^5$, $10^6$, $10^7$, $10^8$, and $10^9$ copies of HRV16 genomic RNA per reference sample in one eppi tube.

## 4 Notes

1. 5× NA extraction buffer is added to bring the concentration of NaCl to about 300 mM for nucleic acid precipitation. Glycoblue is used as a carrier to help the precipitation of RNA. Its blue color also helps to visualize the RNA pellets to avoid discarding the pellets by mistake. However, we have found that reverse transcriptase activity is inhibited by high concentration of glycoblue, so use glycoblue according to the recipe.
2. We also had good results with the High-Capacity cDNA Reverse Transcription kit with RNase inhibitor (Applied Biosystems 4374967).
3. Primers are typically ordered from Eurofins-MWG-Operon or Sigma-Proligo. The basic "desalt" grade is sufficient for both "touchdown" and conventional PCR.
4. It is important to use Platinum PCR SuperMix HF (Invitrogen 12532-016). We have tested a number of commercially available PCR mixes. Platinum PCR SuperMix HF consistently gives the highest amplification efficiency.
5. The optimal volume of nasal wash sample for this extraction procedure is 350 μl. It could be increased to a maximum of 400 μl. If the sample volume is <350 μl, add PBS to bring the volume to 350 μl. It is important to record the volume of each sample used for extraction. The number is needed for subsequent calculation of the amount of viral RNA in each original sample.
6. If your sample has a lot of cellular material, a significant amount of white precipitants will be formed and scattered in the lower part of the aqueous layer after the 5-min microcentrifugation. These white precipitants are composed of cellular DNA and protein and should not be transferred into the next eppi tube along with the RNA-containing aqueous layer. To better separate these white precipitants from the RNA solution, we incubate the eppi tubes at RT for 30 min after the 5-min microcentrifugation and then microfuge the eppi tubes again for another 5 min. This step removes the white precipitants from the lower part of the aqueous layer.
7. For most of the samples, 4 μl of the PCR product gives a visible DNA band in a standard agarose gel analysis, and is sufficient for preparing one sequencing reaction premix for the sequencing facility at the Biotech Center, UW—Madison. Different sequencing facilities may have different requirements. Please consult your sequencing facility for the instruction of making your sequencing reaction premixes.
8. NJPLOT program: http://pbil.univ-lyon1.fr/software/njplot.html.

9. Since the phylogenetic tree has >152 types (reference and unknown), its branches and labels are difficult to read because they are crowded in the "XYZ.PICT" file. To better visualize the tree, the "XYZ.PICT" file could be opened with Adobe Illustrator and then adjusted (e.g., decreasing the font size of the labels) to make the tree more legible.
10. An enterovirus sequence will appear as an outgroup branching from the HRV-B group. You can use the BLAST function of GenBank (http://blast.ncbi.nlm.nih.gov/Blast.cgi) to confirm that it is an enterovirus sequence.
    The sequence of a brand new HRV type will cluster with one of the reference sequences but with a long branch (distance) from that reference sequence. To determine if this is a new type, the pairwise nucleotide divergence (PND) between the two is needed. To obtain the PND, just include the "% identity matrix" option in "Output Format Options" under "Tree" menu of ClustalX. This will generate a file "XYZ.pim" that has the pairwise percent identity. PND equals to (100 % minus pairwise percent identity). Our current cutoff for a new type is ≥8 % PND from the nearest reference type [12].
11. Extend **step (a)** from 30 s to 2 min if a cloned target sequence in the form of double-stranded plasmid DNA is used as standard.

## References


1. Turner RB, Couch RB (2007) Rhinoviruses. In: Knipe DM, Howley PM (eds) Fields virology. Lippincott Williams and Wilkins, Philadelphia, PA, pp 895–909
2. Turner RB, Lee WM (2009) Rhinovirus. In: Richman DD, Whitley RJ, Hayden FG (eds) Clinical virology. ASM, Washington, DC, pp 1063–1082
3. Rueckert R (1996) Picornaviridae: the viruses and their replication. In: Fields BN, Knipe DM, Howley PM et al (eds) Fields virology, 3rd edn. Lippincott-Raven, Philadelphia, PA, pp 609–654
4. Busse WW, Lemanske RF Jr, Gern JE (2010) Role of viral respiratory infections in asthma and asthma exacerbations. Lancet 376:826–834
5. Gern JE (2010) The ABCs of rhinoviruses, wheezing, and asthma. J Virol 84:7418–7426
6. Ruuskanen O, Waris M, Ramilo O (2013) New aspects on human rhinovirus infections. Pediatr Infect Dis J 32:553–555
7. Jartti L, Langen H, Soderlund-Venermo M, Vuorinen T, Ruuskanen O, Jartti T (2011) New respiratory viruses and the elderly. Open Respir Med J 5:61–69
8. Kaiser L, Aubert JD, Pache JC, Deffernez C, Rochat T, Garbino J, Wunderli W, Meylan P, Yerly S, Perrin L et al (2006) Chronic rhinoviral infection in lung transplant recipients. Am J Respir Crit Care Med 174:1392–1399
9. Miller EK, Lu X, Erdman DD, Poehling KA, Zhu Y, Griffin MR, Hartert TV, Anderson LJ, Weinberg GA, Hall CB et al (2007) Rhinovirus-associated hospitalizations in young children. J Infect Dis 195:773–781
10. Peltola V, Waris M, Osterback R, Susi P, Ruuskanen O, Hyypia T (2008) Rhinovirus transmission within families with children: incidence of symptomatic and asymptomatic infections. J Infect Dis 197:382–389
11. Wright PF, Deatly AM, Karron RA, Belshe RB, Shi JR, Gruber WC, Zhu Y, Randolph VB (2007) Comparison of results of detection of rhinovirus by PCR and viral culture in human nasal wash specimens from subjects with and without clinical symptoms of respiratory illness. J Clin Microbiol 45:2126–2129

12. Lee WM, Lemanske RF Jr, Evans MD, Vang F, Pappas T, Gangnon R, Jackson DJ, Gern JE (2012) Human rhinovirus species and season of infection determine illness severity. Am J Respir Crit Care Med 186:886–891
13. Horsnell C, Gama RE, Hughes PJ, Stanway G (1995) Molecular relationships between 21 human rhinovirus serotypes. J Gen Virol 76(Pt 10):2549–2555
14. Kistler AL, Webster DR, Rouskin S, Magrini V, Credle JJ, Schnurr DP, Boushey HA, Mardis ER, Li H, DeRisi JL (2007) Genome-wide diversity and selective pressure in the human rhinovirus. Virol J 4:40
15. Ledford RM, Patel NR, Demenczuk TM, Watanyar A, Herbertz T, Collett MS, Pevear DC (2004) VP1 sequencing of all human rhinovirus serotypes: insights into genus phylogeny and susceptibility to antiviral capsid-binding compounds. J Virol 78:3663–3674
16. Palmenberg AC, Spiro D, Kuzmickas R, Wang S, Djikeng A, Rathe JA, Fraser-Liggett CM, Liggett SB (2009) Sequencing and analyses of all known human rhinovirus genomes reveal structure and evolution. Science 324:55–59
17. Savolainen C, Blomqvist S, Mulders MN, Hovi T (2002) Genetic clustering of all 102 human rhinovirus prototype strains: serotype 87 is close to human enterovirus 70. J Gen Virol 83:333–340
18. Tapparel C, Junier T, Gerlach D, Cordey S, Van Belle S, Perrin L, Zdobnov EM, Kaiser L (2007) New complete genome sequences of human rhinoviruses shed light on their phylogeny and genomic features. BMC Genomics 8:224
19. Price WH (1956) The isolation of a new virus associated with respiratory clinical disease in humans. Proc Natl Acad Sci USA 42:892–896
20. Hamparian VV, Colonno RJ, Cooney MK, Dick EC, Gwaltney JM Jr, Hughes JH, Jordan WS Jr, Kapikian AZ, Mogabgab WJ, Monto A et al (1987) A collaborative report: rhinoviruses–extension of the numbering system from 89 to 100. Virology 159:191–192
21. McErlean P, Shackelton LA, Lambert SB, Nissen MD, Sloots TP, Mackay IM (2007) Characterisation of a newly identified human rhinovirus, HRV-QPM, discovered in infants with bronchiolitis. J Clin Virol 39:67–75
22. Lee WM, Kiesner C, Pappas T, Lee I, Grindle K, Jartti T, Jakiela B, Lemanske RF Jr, Shult PA, Gern JE (2007) A diverse group of previously unrecognized human rhinoviruses are common causes of respiratory illnesses in infants. PLoS One 2:e966
23. Lau SK, Yip CC, Tsoi HW, Lee RA, So LY, Lau YL, Chan KH, Woo PC, Yuen KY (2007) Clinical features and complete genome characterization of a distinct human rhinovirus (HRV) genetic cluster, probably representing a previously undetected HRV species, HRV-C, associated with acute respiratory illness in children. J Clin Microbiol 45:3655–3664
24. Kistler A, Avila PC, Rouskin S, Wang D, Ward T, Yagi S, Schnurr D, Ganem D, Derisi JL, Boushey HA (2007) Pan-viral screening of respiratory tract infections in adults with and without asthma reveals unexpected human coronavirus and human rhinovirus diversity. J Infect Dis 196:817–825
25. Bochkov YA, Palmenberg AC, Lee WM, Rathe JA, Amineva SP, Sun X, Pasic TR, Jarjour NN, Liggett SB, Gern JE (2011) Molecular modeling, organ culture and reverse genetics for a newly identified human rhinovirus C. Nat Med 17:627–632
26. Conant RM, Hamparian VV (1968) Rhinoviruses: basis for a numbering system. II. Serologic characterization of prototype strains. J Immunol 100:114–119
27. Kapikian AZ, Conant RM, Hamparian VV et al (1967) Rhinoviruses: a numbering system. Nature 213:761–762
28. Lee WM, Grindle K, Pappas T, Marshall D, Moser M, Beaty E, Shult P, Prudent J, Gern J (2007) High-throughput, sensitive, and accurate multiplex PCR-microsphere flow cytometry system for large-scale comprehensive detection of respiratory viruses. J Clin Microbiol 45:2626–2634
29. Lemanske RF Jr (2002) The childhood origins of asthma (COAST) study. Pediatr Allergy Immunol 13(Suppl 15):38–43
30. Gern JE (2010) The urban environment and childhood asthma study. J Allergy Clin Immunol 125:545–549
31. Kloepfer KM, Olenec JP, Lee WM, Liu G, Vrtis RF, Roberg KA, Evans MD, Gangnon RE, Lemanske RF Jr, Gern JE (2012) Increased H1N1 infection rate in children with asthma. Am J Respir Crit Care Med 185:1275–1279
32. Denlinger LC, Sorkness RL, Lee WM, Evans MD, Wolff MJ, Mathur SK, Crisafi GM, Gaworski KL, Pappas TE, Vrtis RF et al (2011) Lower airway rhinovirus burden and the seasonal risk of asthma exacerbation. Am J Respir Crit Care Med 184:1007–1014
33. Ireland DC, Kent J, Nicholson KG (1993) Improved detection of rhinoviruses in nasal and throat swabs by seminested RT-PCR. J Med Virol 40:96–101
34. Don RH, Cox PT, Wainwright BJ, Baker K, Mattick JS (1991) 'Touchdown' PCR to circumvent spurious priming during gene amplification. Nucleic Acids Res 19:4008

35. Mathur SK, Fichtinger PS, Kelly JT, Lee WM, Gern JE, Jarjour NN (2013) Interaction between allergy and innate immunity: model for eosinophil regulation of epithelial cell interferon expression. Ann Allergy Asthma Immunol 111(25–31):e21
36. Mifflin TE (2003) Setting up a PCR laboratory. In: Dieffenbach GS, Dveksler GS (eds) PCR primer: a laboratory manual. Cold Spring Harbor Laboratory Press, Cold Spring Harbor, NY, pp 5–14
37. Chenna R, Sugawara H, Koike T, Lopez R, Gibson TJ, Higgins DG, Thompson JD (2003) Multiple sequence alignment with the Clustal series of programs. Nucleic Acids Res 31: 3497–3500

# Chapter 4

# Molecular Genotyping of Human Rhinovirus by Using PCR and Sanger Sequencing

**Wei Wang, Jing He, Yi Liu, Lei Xu, Wencai Guan, and Yunwen Hu**

## Abstract

Human rhinovirus (HRV) is the virus most often associated with acute upper respiratory tract infections. Advances in molecular detection have shown that HRV is also the major viral cause of asthma exacerbations. Genotypic assignment and identification of HRV types are of significant value in the investigation of type-associated differences in disease outcomes, transmission, and epidemiology. Here, we describe a genotyping process involving two separate RT-PCR assays, targeted to VP4/VP2 and 5′ UTR regions of HRV genome, respectively. Together with the reference sequences of each HRV species, the generated sequences are used to construct phylogenetic tree for genotyping.

**Key words** Human rhinovirus, Genotyping, VP4/VP2, 5′ UTR

## 1 Introduction

Human rhinovirus (HRV) is the virus most often associated with acute upper respiratory tract infections, usually causing a self-limiting illness that is clinically similar to other viral respiratory infections. Advances in molecular detection have shown that HRV is also the major viral cause of asthma exacerbations [1–4].

More than 100 serotypes of HRV have been described, grouped into three species based on their whole-genome sequencing, termed HRV-A, HRV-B, and HRV-C (Palmenberg and Gern, this volume). Genetic characterization of HRVs detected by molecular methods has revealed greater diversity than previously described; approximately one-third of HRV infections are now known to be caused by HRV-C, uncultureable in vitro, and therefore entirely missed by traditional virus isolation methods [5, 6]. HRVs within each species show remarkable genetic and, where determined, antigenic heterogeneity. HRV-A and HRV-B isolates were originally characterized serologically, with 75 and 25 serotypes, respectively, being classified

David A. Jans and Reena Ghildyal (eds.), *Rhinoviruses: Methods and Protocols*, Methods in Molecular Biology, vol. 1221, DOI 10.1007/978-1-4939-1571-2_4, 

by cross-neutralization assays by 1987. However, as well as being laborious, time consuming, and requiring extensive panels of antisera specific to each serotype, classification by neutralization cannot be used for HRV-C because of their refractoriness to cell culture.

The HRV genome is a single-chain positive-sense RNA, with a total length of about 7.2 kb containing the 5′ untranslated region (UTR), a single open reading frame (ORF), and the 3′ UTR with a poly A tail. The similarity in amino acid sequence among HRV-A, HRV-B, and HRV-C is less than 70 % and HRV genotypes can be identified by the sequence of VP4/VP2 and 5′ UTR regions of the viral genome [7].

Genotypic assignment and identification of HRV are of significant value in the investigation of type-associated differences in disease outcomes, transmission, and epidemiology.

## 2 Materials

Prepare all solutions using ultrapure water (prepared by purifying deionized water to attain a sensitivity of 18 MΩ cm at 25 °C).

### 2.1 RT-PCR

1. Takara One Step PrimeScript™ RT-PCR Kit (*see* **Note 1**).
2. TaKaRa Ex Taq® Kit.
3. dNTP mix, 10 mM, any supplier.
4. RNase-free water, any supplier.
5. Synthesized DNA primers targeting to 5′ UTR and VP4/VP2 regions (Table 1), any supplier.
6. PCR tubes 0.2 mL appropriate for the thermocycler, any supplier.
7. Eppendorf Mastercycler.

**Table 1**
**Primers used for HRV genotyping**

| Sequence 5′ → 3′ | Orientation[a] | Target | Position[b] | Product size | Reference |
|---|---|---|---|---|---|
| CCGGCCCCTGAATGYGGCTAA | OS | VP4/VP2 | 458 | 667 | [8] |
| ACATRTTYTSNCCAAANAYDCCCAT | OAS | | 1,125 | | |
| ACCRACTACTTTGGGTGTCCGTG | IS | | 547 | 540 | |
| TCWGGHARYTTCCAMCACCANCC | IAS | | 1,087 | | |
| CAAGCACTTCTGTYWCCCC | S | 5′ UTR | 179 | 372 | [9] |
| ACGGACACCCAAAGTAG | AS | | 551 | | |

[a] *OS* outer sense, *OAS* outer antisense, *IS* inner sense, *IAS* inner antisense, *S* sense, *AS* antisense
[b] The base positions of the primers were numbered according to the HRV-B serotype 14 genome (GenBank accession number NC_001490)

### 2.2 Agarose Gel Electrophoresis

1. Agarose powder (low melting point, analytical grade), any supplier.
2. DNA size marker, covering from 100 bp to 1 kb, any supplier (e.g., Takara DL2000).
3. 6× Loading buffer (30 mM EDTA, 36 % glycerol, 0.035 % xylene cyanol, 0.05 % bromophenol blue), any supplier.
4. 50× TAE buffer, PH 8.5: Weigh 242 g Tris base (MW = 121.1) and transfer to the glass beaker with stir bar to dissolve in about 600 mL of water. Add 37.2 g $Na_2EDTA \cdot 2H_2O$ and 57.1 mL glacial acetic acid. Mix and adjust pH with NaOH. Make final volume to 1 L with water. Store at room temperature.
5. 2 % agarose gel costaining ethidium bromide: Prepare 1× TAE buffer by adding 20 mL 50× TAE buffer to 980 mL water in cylinder. Weigh appropriate agarose powder and dissolve in 1× TAE buffer in a glass beaker by gently heating in a microwave oven to get 2 % agarose gel solution. Add ethidium bromide with a final concentration in 0.5 μg/mL into the solution. Cast the gel in a gel cassette with an appropriate size comb.

### 2.3 Purification of PCR Products by Gel Extraction

1. Qiagen MinElute Gel Extraction Kit (*see* **Note 1**).
2. Ethanol (96–100 %).
3. Sodium acetate 3 M, pH 5.0: Weigh 40.8 g NaAc · 3H2O and dissolve in 40 mL water. Mix and adjust pH with glacial acetic acid. Make final volume to 100 mL with water. Autoclave and then store at room temperature.
4. Isopropanol (100 %).
5. Microcentrifuge.
6. Water bath or dry heating block.

### 2.4 Phylogeny Analysis

1. Suitable software package to analyze data (e.g., MEGA v5).

## 3 Methods

The genotyping process includes two separate RT-PCR assays, targeted to VP4/VP2 and 5′ UTR regions, respectively, [8, 9]. The VP4/VP2 assay is composed of one-step RT-PCR reaction and a nested-PCR reaction. The 5′ UTR assay is a one-step RT-PCR reaction. The primers used are shown in Table 1. The amplification products are purified and sent for sequencing to a commercial sequencing service company. Together with the reference sequences of each HRV species, the generated sequences are used to construct phylogenetic tree for genotyping. For RNA extraction from clinical samples, please refer to Chapter 3 in this volume.

### 3.1 Genotyping PCR Based on VP4/VP2 Region

All reactions are set up on ice unless otherwise specified.

#### 3.1.1 One-Step RT-PCR

1. In the pre-PCR room (*see* **Note 2**), prepare the reaction mix in 25 μL reaction volume containing 12.5 μL 2× reaction buffer, 200 μM of each primer, 0.5 μL reverse transcriptase, and 0.5 μL Taq polymerase.
2. In the template room, add 2.5 μL of the extracted RNA into the reaction mix in each 0.2 mL PCR tube.
3. In the thermocycler room, place the PCR tubes in the thermocycler and start the program. The cycling conditions are 42 °C for 10 min, 94 °C for 2 min, 45 cycles at 94 °C for 15 s, 52 °C for 30 s, 72 °C for 30 s, and then 72 °C for 10 min.
4. Prepare 2 % agarose gel in the electrophoresis area, mix 10 μL PCR products with 2 μL 6× loading buffer, and then run the gel at 120 V for 30 min. The expected product size is 667 bp.

#### 3.1.2 Nested-PCR

1. In the pre-PCR room, prepare the reaction mix in 25 μL reaction volume containing 2.5 μL 10× reaction buffers, 800 nM dNTP, 200 μM of each primer, 1.5 mM MgCl, and 0.2 μL Taq polymerase.
2. In an additional template room or PCR cabinet, add 2.5 μL of the RT-PCR product into the reaction mix in each 0.2 mL PCR tube.
3. In the thermocycler room, place the PCR tubes in the thermocycler and start the program. The cycling conditions are 94 °C for 5 min, 25 cycles of 94 °C for 15 s, 50 °C for 30 s, 72 °C for 30 s, and then 72 °C for 10 min.
4. Prepare 2 % agarose gel in the electrophoresis area, mix 10 μL PCR products with 2 μL 6× loading buffer, and then run the gel at 120 V for 30 min. The expected product size is 540 bp (*see* Fig. 1).

### 3.2 Genotyping One-Step RT-PCR Based on 5′ UTR Region

1. In the pre-PCR room, prepare the reaction mix in 25 μL reaction volume containing 12.5 μL 2× reaction buffer, 600 μM of each primer, 0.5 μL reverse transcriptase, and 0.5 μL Taq polymerase.
2. In the template room, add 2.5 μL of the extracted RNA into the reaction mix in each 0.2 mL PCR tube.
3. In the thermocycler room, place the PCR tubes in the thermocycler and start the program. The cycling conditions are 42 °C for 20 min, 95 °C for 2 min, 40 cycles as 95 °C for 30 s, 52 °C for 30 s, 72 °C for 30 s, and then 72 °C for 10 min.
4. Prepare 2 % agarose gel in the electrophoresis area, mix 10 μL PCR products with 2 μL 6× loading buffer, and then run the gel at 120 V for 30 min. The expected product size is 372 bp (*see* Fig. 2).


**Fig. 1** Electrophoresis image of one-step RT-PCR targeting to 5′ UTR region of HRV. *Lanes 1–13* show the amplification results of 13 different clinical samples. *Lane N* presents the template of RNAs extracted from non-HRV-infected specimen. *Lane P* presents the template RNAs extracted from cultivated HRV strain. *B* blank, *M* DNA size maker from 100 to 2,000 bp

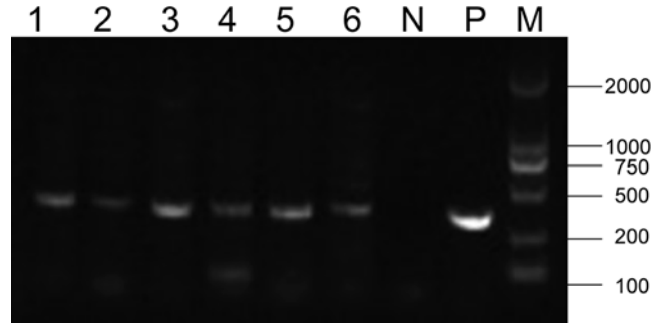


**Fig. 2** Electrophoresis image of nested-PCR targeting to VP4/VP2 region of HRV. *Lanes 1–6* show the amplification products of six different clinical samples. *Lane N* presents the template of RNAs extracted from non-HRV-infected specimen. *Lane P* presents the template RNAs extracted from cultivated HRV strain. *M* DNA size maker from 100 to 2,000 bp

### *3.3 Purification of Amplification Products by Using Gel Extraction*

1. Excise the DNA fragment from the agarose gel with a clean, sharp scalpel.
2. Weigh the gel slice in a colorless tube. Add three volumes of Buffer QG to one volume of gel (100 mg or approximately 100 μL).
3. Incubate at 50 °C for 10 min (or until the gel slice has completely dissolved).
4. After the gel slice has dissolved completely, check that the color of the mixture is yellow (similar to Buffer QG without dissolved agarose). If the color of the mixture is orange or violet, add 10 μL of 3 M sodium acetate, pH 5.0, and mix. The color of the mixture will turn to yellow.

5. Add one gel volume of isopropanol to the sample and mix by inverting the tube several times.
6. Place a MinElute column in a provided 2 mL collection tube in a suitable rack.
7. To bind DNA, apply the sample to the MinElute column, and centrifuge at 13,000 rpm for 1 min. Discard the flow-through and place the MinElute column back in the same collection tube.
8. Add 500 μL of Buffer QG to the spin column and centrifuge at 13,000 rpm for 1 min. Discard the flow-through and place the MinElute column back in the same collection tube.
9. To wash, add 750 μL of Buffer PE to the MinElute column and centrifuge at 13,000 rpm for 1 min. Discard the flow-through and centrifuge the MinElute column for an additional 1 min at 13,000 rpm.
10. Place the MinElute column into a clean 1.5 mL microcentrifuge tube.
11. To elute DNA, add 10 μL of Buffer EB (10 mM Tris–Cl, pH 8.5) or water to the center of the membrane, let the column stand for 1 min, and then centrifuge at 13,000 rpm for 1 min. Collect the flow-through which has the purified DNA.
12. Send the purified products with the PCR primers used for sequencing.

### 3.4 Phylogenetic Analysis

DNA sequences used for 5′ UTR region analysis are based on HRV-14 nt 179–551 and those used for VP4/VP2 gene analysis are based on HRV-14 nt 547–1,087.

1. Assemble the generated sequences by using suitable software (e.g., Vector NT or BioEdit) and format the sequences in Fasta file.
2. Download HRV reference genome sequences from GenBank in Fasta format. Extract the fragment sequences of the target regions from the whole-genome sequences by using suitable software (e.g., Vector NT or BioEdit).
3. Start software MEGA version 5.0 (*see* **Note 1**).
4. Choose alignment|new|DNA sequence, and then click edit|insert sequence from the files, including the reference sequences and the sequences to analyze.
5. Choose alignment|clustalW for multiple alignment analysis.
6. Choose phylogeny|construct NJ tree.
7. Choose nucleotide|p-distance option, and test|Interior Branch|1000 option, and then click computer to get the tree.

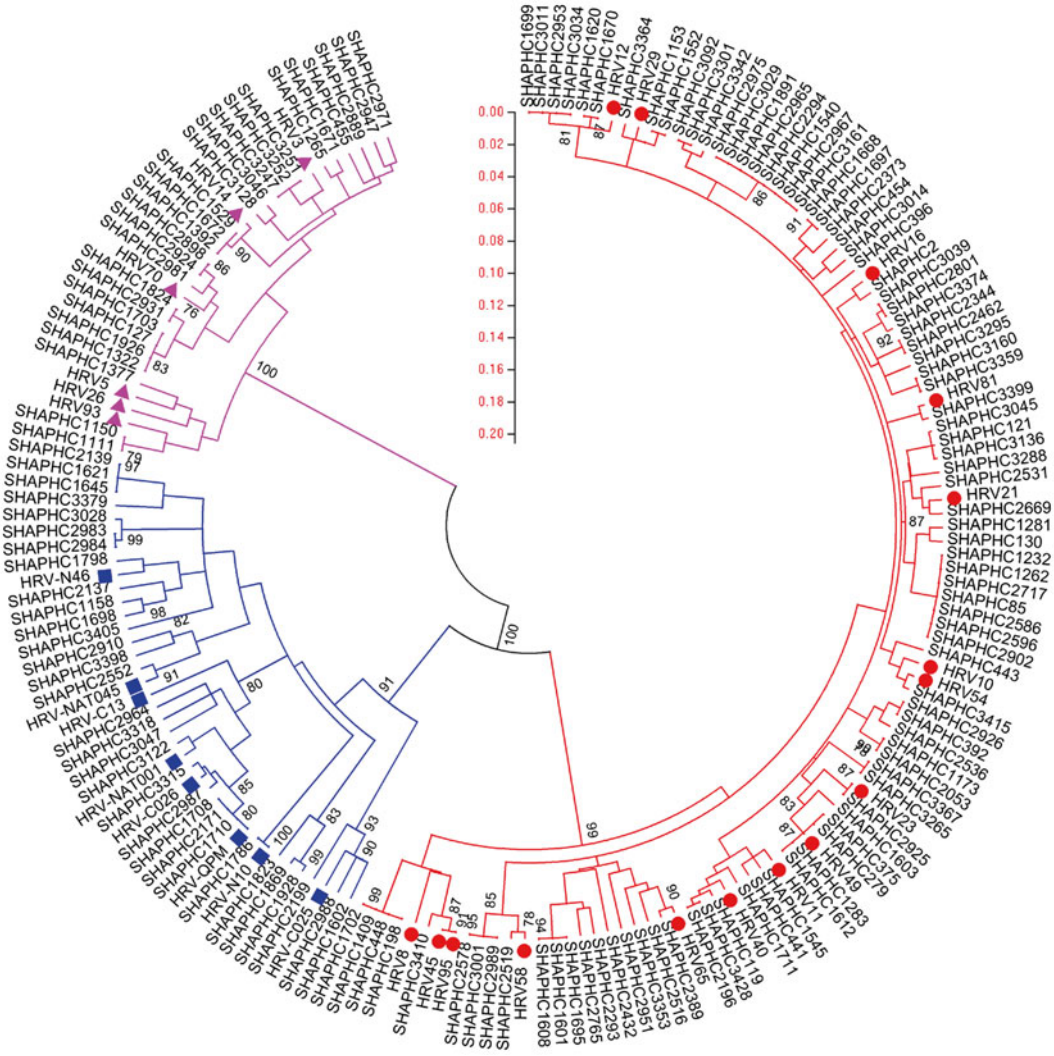


**Fig. 3** Phylogenetic analysis of 148 HRV strains based on the partial nucleotide sequences of VP4/VP2 (370 nt, position 626–996 numbered according to the HRV-A16 reference sequence, L24917). The phylogenetic tree was constructed using the neighbor-joining method and *p*-distance model with bootstrap replicated from 1,000 trees using Molecular Evolutionary Genetics Analysis version 5.0 (MEGA5); values of 75 % or greater are shown. Genetic distance (nucleotide substitutions per site) is represented by the scale bar. The clinical HRV strains in our study are named as SHAPHC followed by the laboratory number of specimen. For the reference strains, *red circles*, *magenta triangles*, and *blue squares* designate HRV-A, HRV-B, and HRV-C, respectively

8. Choose image|save as TIFF or pdf format.
9. Based on the clusters obtained in the phylogenetic tree, identify the genotype of each sequence. *See* Figs. 3 and 4 for an example of the kind of phylogenetic trees obtained.

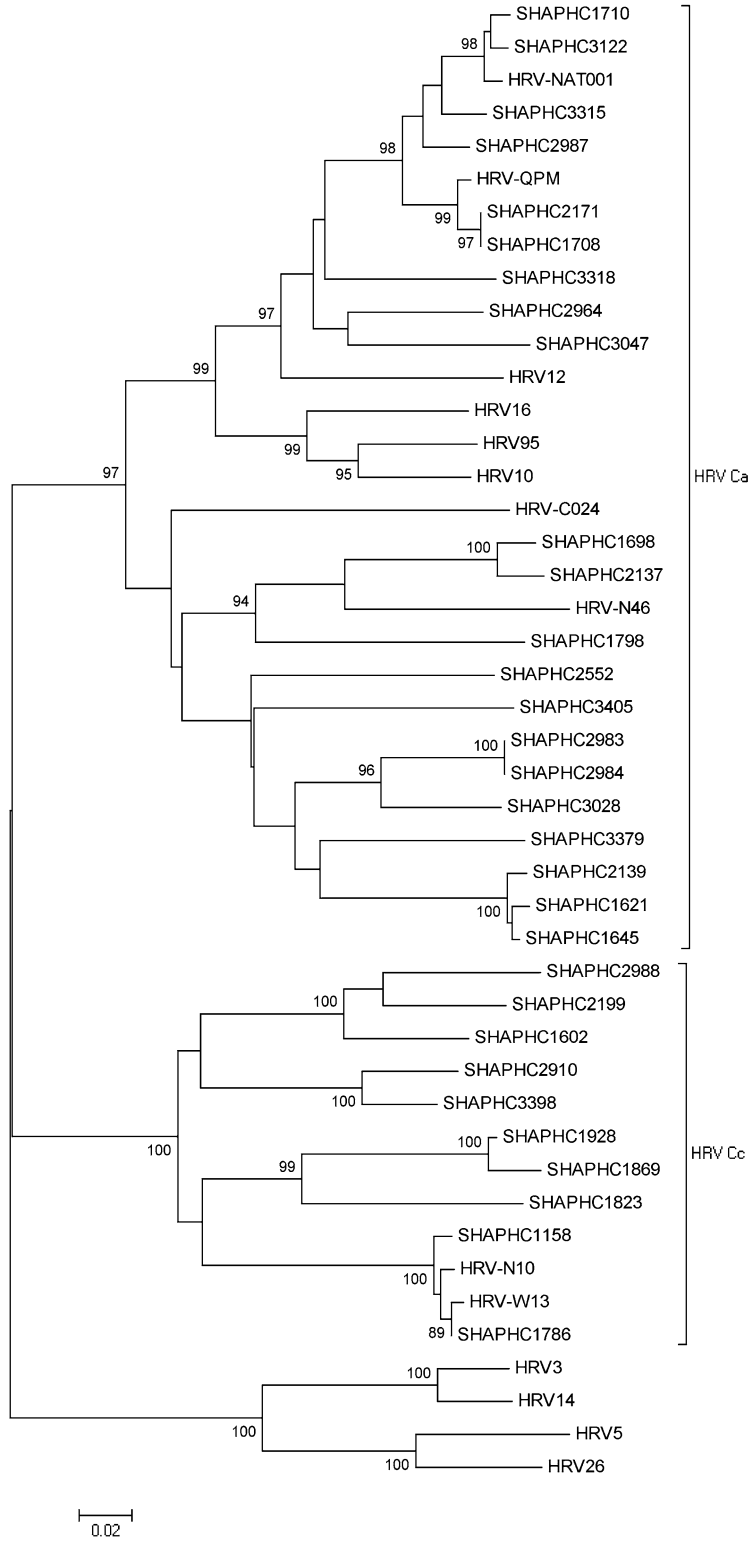


**Fig. 4** Phylogenetic analysis of 31 HRV-C-positive strains based on the partial nucleotide sequences of 5′ NCR (265 nt, position 172–436 numbered according to the HRV-A16 reference sequence, L24917). The phylogenetic tree was constructed using the neighbor-joining method and *p*-distance model with bootstrap replicated from 1,000 trees using Molecular Evolutionary Genetics Analysis version 5.0 (MEGA5); values of 75 % or greater are shown. Genetic distance (nucleotide substitutions per site) is represented by the scale bar

## 4 Notes

1. Although the protocol described here is for specific commercial kits, comparable kits from any commercial supplier may be used, keeping in mind that some optimization may be required.
2. The whole genotyping process should be performed in three separate rooms, respectively, for mix preparation, template RNA addition, and thermocycler running. Keep the electrophoresis area far from the PCR area.

### References


1. Gavala ML, Bertics PJ, Gern JE (2011) Rhinoviruses, allergic inflammation, and asthma. Immunol Rev 242(1):69–90, PMCID: 3119863
2. Mackay AJ, Hurst JR (2013) COPD exacerbations: causes, prevention, and treatment. Immunol Allergy Clin North Am 33(1):95–115
3. Mak RK, Tse LY, Lam WY, Wong GW, Chan PK, Leung TF (2011) Clinical spectrum of human rhinovirus infections in hospitalized Hong Kong children. Pediatr Infect Dis J 30(9):749–753
4. Ko FW, Ip M, Chan PK, Chan MC, To KW, Ng SS et al (2007) Viral etiology of acute exacerbations of COPD in Hong Kong. Chest 132(3):900–908
5. Lau SK, Yip CC, Tsoi HW, Lee RA, So LY, Lau YL et al (2007) Clinical features and complete genome characterization of a distinct human rhinovirus (HRV) genetic cluster, probably representing a previously undetected HRV species, HRV-C, associated with acute respiratory illness in children. J Clin Microbiol 45(11):3655–3664, PMCID: 2168475
6. McErlean P, Shackelton LA, Andrews E, Webster DR, Lambert SB, Nissen MD et al (2008) Distinguishing molecular features and clinical characteristics of a putative new rhinovirus species, human rhinovirus C (HRV C). PLoS One 3(4):e1847, PMCID: 2268738
7. Palmenberg AC, Spiro D, Kuzmickas R, Wang S, Djikeng A, Rathe JA et al (2009) Sequencing and analyses of all known human rhinovirus genomes reveal structure and evolution. Science 324(5923):55–59
8. Wisdom A, Leitch EC, Gaunt E, Harvala H, Simmonds P (2009) Screening respiratory samples for detection of human rhinoviruses (HRVs) and enteroviruses: comprehensive VP4-VP2 typing reveals high incidence and genetic diversity of HRV species C. J Clin Microbiol 47(12):3958–3967, PMCID: 2786677
9. Lee WM, Kiesner C, Pappas T, Lee I, Grindle K, Jartti T et al (2007) A diverse group of previously unrecognized human rhinoviruses are common causes of respiratory illnesses in infants. PLoS One 2(10):e966, PMCID: 1989136

# Chapter 5

# Growth of Human Rhinovirus in H1-HeLa Cell Suspension Culture and Purification of Virions

**Wai-Ming Lee, Yin Chen, Wensheng Wang, and Anne Mosser**

## Abstract

HeLa cell culture is the most widely used system for in vitro studies of the basic biology of human rhinovirus (HRV). It is also useful for making sufficient quantities of virus for experiments that require highly concentrated and purified virus. This chapter describes the protocols for producing a large amount of HeLa cells in suspension culture, using these cells to grow a large quantity of virus of HeLa-adapted HRV-A and -B serotypes, and making highly concentrated virus stock and highly purified virions. These purified HRV virions are free of cellular components and suitable for experiments that are sensitive to cellular contaminations.

**Key words** HeLa cells, Suspension culture, High-titer virus stock, Purified virions

## 1 Introduction

Human rhinovirus (HRV) is a large group of small RNA viruses that infect airway epithelial cells and are a major cause of respiratory illnesses [1–6]. HRV belongs to the picornavirus family and has about 150 distinct types or members. They are divided into three species: A (75 types), B (25 types), and C (about 50 types) according to serological and genome sequence variations [2, 5–13]. The 100 HRV-A and HRV-B types were isolated and assigned as serotypes between 1956 and 1987 by traditional cultural, biochemical, and serological methods [14–16]. They are small (15–30 nm) RNA viruses that are ether resistant but acid sensitive. They grow optimally at 32–35 °C. Each serotype was defined by 20-fold or greater differences in antiserum neutralization titers during reciprocal cross-neutralization tests against the other 99 serotypes [8, 16]. The prototype strains of these serotypes are available at ATCC. The 50 HRV-C types were identified recently with modern PCR and sequencing techniques [2, 17–20].

David A. Jans and Reena Ghildyal (eds.), *Rhinoviruses: Methods and Protocols*, Methods in Molecular Biology, vol. 1221, DOI 10.1007/978-1-4939-1571-2_5, 

Their sequences are more closely related to those of HRV-A and -B serotypes than to other GenBank sequences. HRV-C does not grow in traditional primary cell cultures and continuous cell lines. They were recently found to grow in differentiated airway epithelial cells in air-liquid interface culture or sinus organ culture (21–23; also *see* Ashraf et al., Chapter 6). Several additional HRV-A and HRV-B types have been identified by PCR and sequencing techniques [2]. However, they have not been characterized by traditional culture methods.

The HeLa cell was the first established continuous human cell line and it is the most widely used cell for studying human cellular and molecular biology [24, 25]. It has contributed to over 60,000 research papers so far [25]. Since it was developed in 1951, it has been distributed to many different laboratories around the world and evolved into many strains under different culture conditions. The HRV-sensitive HeLa cell strain (H1) was first developed as a monolayer culture in Dr. Vincent Hamparian's lab in the early 1960s [26–28] and subsequently adapted to growth in suspension in Dr. Roland Rueckert's lab in the late 1960s [29]. It has become the standard for propagating HRVs and studying HRV biology. HRV-A and -B serotypes typically need several passages to adapt to HeLa cells. Once adapted, they usually grow to reasonably high titers and form visible plaques in HeLa cell monolayer, thus making them suitable for molecular biology studies. Studies of HeLa-adapted serotypes 1A, 2, 3, 14, 16, and 39 have provided most of our current knowledge about HRV biology: receptor interaction, entry, uncoating, viral protein synthesis, viral RNA replication, host range determinants, capsid assembly, atomic structures, and antigenicity of the virions [8, 30–44].

The H1-HeLa cell has a number of features that make it a good system for HRV molecular biology studies. First, unlike primary airway epithelial cells, H1-HeLa cells produce a negligible amount of interferon to inhibit HRV infection and replication. Second, infected H1-HeLa cells yield five to ten times more progeny virus than any other cell types that are known to be permissive for HRV growth such as fetal lung fibroblast diploid cells (MRC-5 and WI-38) and epithelial cells. Third, H1-HeLa cells are highly susceptible to HRV infection due to the presence of a high density of viral receptors (both major and minor) on their surfaces. Typically, a moderate MOI of 10 PFU (plaque-forming unit) HRV per cell causes a simultaneous infection of >90 % of cells in an H1-HeLa culture. Fourth, H1-HeLa cells grow easily to a high density ($5 \times 10^5$ cells per ml) in a simple suspension culture in a 37 °C shaker, very much like a bacterial culture. Lastly, H1-HeLa cells from suspension culture readily form stainable monolayers on dishes that support the development of visible plaques from adapted HRV serotypes.

Currently, growing HRV in H1-HeLa suspension culture is the only practical way to make sufficient virus for virion purification and experiments that require highly concentrated virus.

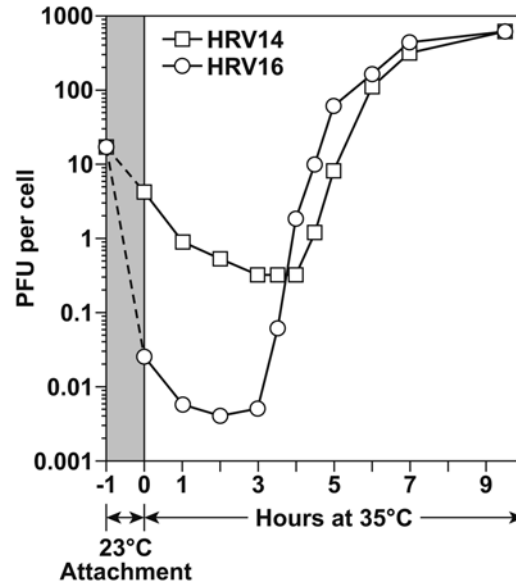


**Fig. 1** Single-step growth curves of HRV-14 and HRV-16 in H1-HeLa cell suspensions. Virus (15 PFU/cell) was attached to cells in PBSA1 at 23 °C for 1 h (*shaded zone*). After unattached viruses were removed by centrifugation and washing with PBSA1, virus-cell complexes were resuspended in warm (35 °C) growth medium to initiate virus growth (zero time). Infectivity (PFU/cell) was determined by plaque assay of supernatant fluids on H1-HeLa cell monolayers after freeze-thawing and clarifying samples of infected cells withdrawn at the indicated times. The infectivity at −1 h (*gray zone*) indicates the titer of input virus after diluting into PBSA1 before mixing with cells

Compared to closely related poliovirus I, HRVs have significantly lower progeny virus yields. The virion yield of the most productive HRV strain, the Hela-adapted HRV-14, is about 20–30 % of that of poliovirus I. Typically one liter of H1-HeLa cell suspension culture (in three 500-ml flasks) produces $5 \times 10^8$ cells. The cells can be easily concentrated 100-fold with a 5-min low-speed centrifugation into 10 ml for efficient HRV infection. The infected cells are then cultured in a very-high-density suspension ($5 \times 10^6$ cells per ml) for viral growth. Since HRVs are not lytic, >95 % of the progeny viruses remain inside the infected cells when the viral growth cycle is completed (about 8 h after infection, Fig. 1). Thus a 5-min low-speed centrifugation is sufficient to concentrate $1 \times 10^{11}$ PFU of virus into a small cell pellet. The viruses can then be released from the infected cells for making a high-titer stock by three freeze-thaw cycles or for virion purification by a simple NP-40 detergent lysis. The virions can be purified from the cellular components by a two-step centrifugation process (sucrose cushion and then gradient). Typically, $5 \times 10^8$ H1-HeLa cells yield about 200 μg of highly purified virions. In contrast, sixty 100-mm dishes would be needed to produce the same amount of virus if monolayer cultures

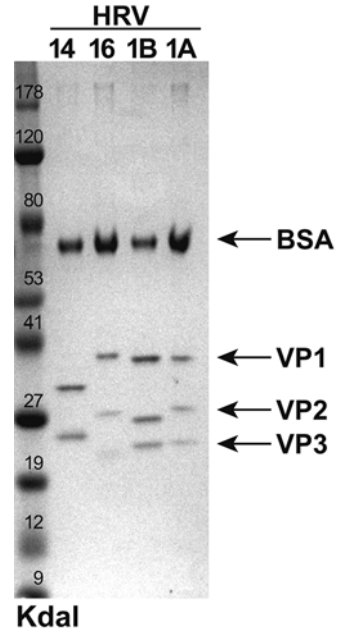


**Fig. 2** Purity of HRV-1A, 1B, 14, and 16 virion preparations after sucrose cushion and gradient purification. HeLa-adapted HRV lab strains were grown in H1-HeLa cell suspension cultures (Subheading 3.2.1). Virions were released from infected cells (Subheading 3.2.4) and then purified by centrifugation through a sucrose cushion and then a sucrose gradient (Subheadings 3.3.1 and 3.3.2). The sucrose gradient fractions containing the virions were isolated. The virion concentration was determined by $OD_{260}$ absorbance (Subheading 3.3.3). Two μg of virion from each serotype were analyzed using PAGE and Coomassie blue staining. Only viral capsid proteins and BSA (an ingredient of the sucrose gradient buffer) were detected. The VP2 and VP3 of HRV14 migrated at the same position [35]

are used. Obviously, handling 60 dishes would require much more work and time than working with three 500-ml flasks.

The purified HRV virions are ideal for experiments that require homogeneous virus free of cellular components, such as X-ray crystallographic determination of the structures of the HRV virion and its complexes with antibodies or receptors; in vitro studies of the interaction between HRV and human airway epithelial cells, PBMCs, macrophages, neutrophils, and dendritic cells; and studies of in vivo immune responses to HRV infection in a mouse model system and immunization of animals for making antibodies and hybridoma cells [31, 33–36, 40, 41, 45–50].

This chapter describes the protocols for producing a large amount of H1-HeLa cells in suspension culture, using these cells to grow a large quantity of virus of HRV-A and -B serotypes, making highly concentrated virus stock, purifying the HRV virions from cellular materials, and determining the concentration of the HRV virions. These protocols are routinely used to produce highly purified virions of HeLa-adapted HRV serotypes 1A, 1B, 2, 14, and 16 (Fig. 2) in our laboratory.

## 2 Materials

### 2.1 Suspension Culture of H1-HeLa Cells

1. H1-HeLa cells (ATCC CRL-1958) (*see* **Note 1**).
2. Incubator shaker (e.g., New Brunswick G24).
3. −80 °C freezer.
4. Liquid nitrogen tank.
5. A benchtop refrigerated centrifuge (e.g., Beckman Allegra).
6. Sterile disposables for tissue culture:
   (a) 500-ml disposable polycarbonate Erlenmeyer flask, Vent Cap (e.g., Corning 431145).
   (b) 250-ml disposable polycarbonate Erlenmeyer flask, Vent Cap (e.g., Corning 431144).
   (c) 250-ml sterile disposable centrifuge tubes.
   (d) 14-ml polypropylene tubes.
   (e) 15-ml blue cap tubes.
   (f) 50-ml Falcon blue cap tubes.
   (g) 10-ml sterile pipettes.
   (h) 5-ml sterile pipettes.
   (i) 1-ml sterile pipettes.
   (j) Aluminum foil.
   (k) 2-ml cryovials.
   (l) 1.5-ml microfuge tubes.
7. Medium B-NCS:
   To 500 ml sMEM (Invitrogen 11380037), add the following ingredients:
   (a) 5 ml nonessential amino acids (Invitrogen 1114050).
   (b) 5 ml L-glutamine (Invitrogen 2503081).
   (c) 5 ml penicillin, streptomycin (Invitrogen 15140163).
   (d) 5 ml pluronic F68 (Invitrogen 24040-32).
   (e) 50 ml newborn calf serum (Invitrogen 16010-159).
8. Medium B-NCS-DMSO (*see* **Note 2**):
   To 40 ml medium B-NCS, add 10 ml DMSO (dimethyl sulfoxide).
9. PBSI: PBS with calcium and magnesium.
10. PBSA1 (0.1 % BSA):
    To 500 ml PBSI, add 6.7 ml 7.5 % bovine albumin fraction V.
11. PBSA2 (0.01 % BSA):
    To 500 ml PBSI, add 0.67 ml 7.5 % bovine albumin fraction V.

### 2.2 Production of High-Titer HRV-Infected Cell Lysate

1. *See* Subheading 2.1 above for incubator shaker, sterile disposables, centrifuge, PBSI, PBSA1, and PBSA2.
2. Medium B-FBS:
   To 500 ml sMEM (Invitrogen 11380037), add the following ingredients:
   (a) 5 ml nonessential amino acids (Invitrogen 1114050).
   (b) 5 ml L-glutamine (Invitrogen 2503081).
   (c) 5 ml penicillin, streptomycin (Invitrogen 15140163).
   (d) 5 ml pluronic F68 (Invitrogen 24040-32).
   (e) 50 ml fetal bovine serum (Invitrogen 10437-028).
3. 1 M HEPES buffer, pH 7.2–7.5 (Invitrogen 15630-080).

### 2.3 Production of Highly Purified HRV Virions

1. High-speed centrifuge.
2. Ultracentrifuge (Beckman L90).
3. Gradient Master system (BioComp Instruments, www.biocompinstruments.com).
4. *See* Subheading 2.1 above for sterile disposables, PBSI, PBSA1, and PBSA2.
5. Filter units for sterilization:
   (a) 500-ml 0.20-μm filter unit.
   (b) 1,000-ml 0.20-μm filter unit
6. SW41 Ultra-Clear centrifuge tubes (Beckman 344059).
7. RNase A, dissolved in sterile TE to 10 μg/μl.
8. 10 % NP-40 (Nonidet P40) in deionized water.
9. 10 % *N*-lauroylsarcosine sodium salt in deionized water.
10. 2-Mercaptoethanol.
11. TE buffer:
    To 494 ml deionized water, add the following ingredients, and then filter-sterilize.
    (a) 5 ml 1 M Tris–HCl, pH 8.0.
    (b) 1 ml 0.5 M EDTA.
12. Buffer 4:
    To 390 ml deionized water, add the following ingredients, and then filter-sterilize.
    (a) 10 ml 1 M Tris acetate, pH 7.5.
    (b) 100 ml 5 M NaCl.
13. 30 % (w/v) sucrose cushion solution:
    Dissolve 180 g sucrose in buffer 4 to a final volume of 600 ml, and then filter-sterilize.
14. 7.5 % sucrose solution (w/w):

Dissolve 7.5 g sucrose in 92.5 ml PBSA2, and then filter-sterilize.

15. 45 % sucrose solution (w/w):

    Dissolve 45 g sucrose in 55 ml PBSA2, and then filter-sterilize.

## 3 Methods

### 3.1 Suspension Culture of H1-HeLa Cells

#### 3.1.1 Maintenance of a Suspension Cell Stock

1. Thaw a cryovial of cells ($1.5 \times 10^7$ cells) at room temperature (RT) (*see* **Note 3**).
2. Transfer the cells into a 15-ml blue-cap tube containing 8 ml of medium B-NCS, cap tightly, and then invert the tube several times to mix the contents.
3. Pellet cells ($500 \times g$, 4 °C, 5 min).
4. Discard supernatant and wash the cell pellet gently into a 250-ml Erlenmeyer flask/vent cap containing 150 ml medium B-NCS.
5. Cover the cap with a small piece of aluminum foil (*see* **Note 4**).
6. Incubate the flask in an incubator shaker (230 rpm, 37 °C) for 2–3 days.
7. Count the cells with a hemocytometer every day from day 2 (*see* **Note 5**).
8. When the cell count reaches 500 per μl, pass the cells by diluting them to 50 cells per μl with fresh medium B-NCS.

#### 3.1.2 Production of Large Quantity of Cells for Virus Production

When a large quantity of cells is needed for virus work, cells are grown in 500-ml Erlenmeyer flask/vent cap containing 350 ml medium B-NCS, modifying **step 4** of Subheading 3.1.1.

#### 3.1.3 Cryo-Preservation of H1-HeLa Cells

1. Grow 350 ml of H1-HeLa cell suspension culture to 400 cells per μl (*see* **Note 6**), a total of $1.4 \times 10^8$ cells.
2. Pellet cells ($500 \times g$, 4 °C, 5 min) in two 250-ml centrifuge bottles.
3. Resuspend and wash cells into a 50-ml blue-cap tube with 6 ml cold medium B-NCS.
4. Add 8 ml cold medium B-NCS-DMSO and then gently swirl the tube to mix.
5. Use a 5-ml pipet to aliquot 1.5 ml of cells into each chilled cryovial ($1.4 \times 10^7$ cells per vial). Cap tightly.
6. Place the cryovials into a chilled freezer box and then store at −80 °C overnight.
7. Place the frozen cryovials into a liquid nitrogen tank for long-term storage.

8. One week later, remove a vial from the liquid nitrogen tank to check cell viability by starting a new suspension culture as described in Subheading 3.1.1.

### 3.2 Production of High-Titer Infected Cell Lysate

#### 3.2.1 To Grow HRV in Suspension H1-HeLa Cell Culture

1. Grow one liter of H1-HeLa cells to 500 cells/μl (total = $5x10^8$ cells).
2. Pellet cells (500×*g*, 4 °C, 5 min) in four 250-ml centrifuge bottles.
3. Wash cells into a 50-ml blue-cap tube with PBSI to a final volume of 40 ml.
4. Pellet cells (500×*g*, 4 °C, 5 min) and then decant all supernatant.
5. Wash the cells into a 500-ml Erlenmeyer flask/vent cap with PBSI to a final volume of 8.5 ml.
6. Add high-titer virus solution at MOI of 15, e.g., 1.5 ml of $5x10^9$ PFU per ml (*see* **Note 7**).
7. Rock the flask slowly (*see* **Note 8**) at RT for 1 h (hour) for virus attachment.
8. Meanwhile, warm 90 ml medium B-FBS to 35 °C.
9. Add the warm medium B-FBS to the flask and cover the cap with aluminum foil after 1-h attachment period.
10. Incubate the flask in an incubator shaker (120 rpm, 35 °C) for 8 h.

#### 3.2.2 Harvesting Virus

1. Transfer the infected cells into two 50-ml blue-cap tubes.
2. Pellet cells (500×*g*, 4 °C, 5 min).
3. Wash the pellets into a 14-ml tube with PBSI to a final volume of 10 ml.
4. Store at −80 °C until Subheading 3.2.3 or 3.2.4.

#### 3.2.3 Production of Infected Cell Lysate for Future Use as Virus Stock

1. Thaw infected cells by incubating the tubes in 35 °C water for 5–10 min (*see* **Note 9**).
2. Add 100 μl 1 M HEPES buffer, pH 7.2.
3. Vortex the tubes vigorously.
4. Freeze the tubes at −80 °C for 20 min.
5. Repeat **steps 1**, **3**, and **4** once and then **steps 1** and **3** once.
6. Pellet the cell debris in a high-speed centrifuge (10,000 rpm, 4 °C, 10 min).
7. Aliquot supernatant into 1.5-ml eppi tubes, and then store at −80 °C for future use.

*3.2.4 Production of Infected Cell Lysate for Virion Purification*

1. Add 0.5 ml 10 % NP-40 to infected cell suspension (*see* **Note 10**).
2. Break up cells by pipetting up and down 20 times with a 5-ml pipet.
3. Pellet the cell nuclei in a high-speed centrifuge (10,000 rpm, 4 °C, 10 min).
4. Transfer the clarified supernatant into a new 14-ml tube, and then store at −80 °C until purification.

### *3.3 Production of Highly Purified HRV Virions*

*3.3.1 Partial Purification with Sucrose Cushion*

1. Thaw the clarified cell lysate at 35 °C.
2. Add 400 μg RNase A into 10 ml of the clarified cell lysate from $5 \times 10^8$ cells and incubate the tube in 35 °C water for 30 min to disrupt ribosomes (*see* **Note 11**).
3. Add 1 ml 10 % *N*-lauroylsarcosine and 20 μl 2-mercaptoethanol and then mix gently (*see* **Note 12**).
4. Pour 7–8 ml lysate into an SW41 centrifuge tube (*see* **Note 13**).
5. Add a layer of 1 ml of 30 % (w/v) sucrose/buffer IV under the cell lysate in the bottom of the tube using a 1-ml disposable pipet.
6. Fill the tube to ~2 mm from the top with the rest of lysate and then PBSA2.
7. Ultracentrifuge (40,000 rpm, 16 °C) in an SW41 rotor for 2 h.
8. Decant all supernatant, and then add 50 μl PBSA2 to the pellet.
9. Cover the centrifuge tube with saran wrap and store the tube at −80 °C until sucrose gradient purification.

*3.3.2 Further Purification of Virions with Sucrose Gradient*

1. Resuspend the virus pellet with PBSA2 and transfer the virus solution into a 1.5-ml eppi tube to a final volume of 500 μl (*see* **Note 14**).
2. Vortex the eppi tube vigorously for 20 s (sec), and then microfuge ($10{,}000 \times g$, 4 °C) for 2 min to remove the insoluble debris.
3. Make a 7.5–45 % (w/w) sucrose gradient in an SW41 tube using a Gradient Master system according to the manufacturer's instruction and *see* **Note 15**.
4. Remove 0.7 ml sucrose solution from the top of the gradient to make room for the virus solution.
5. Layer the clarified virus solution on the top of the sucrose gradient, and then load the SW41 tube into an SW41 rotor.
6. Ultracentrifuge (40,000 rpm, 16 °C) for 2 h.
7. Remove the tube from the ultracentrifuge, and then visualize the virion band in the dark with a flashlight shining toward the

tube from above, and mark the position of the band with a magic marker (*see* **Note 16**).

8. Remove the sucrose above the band carefully with a P1000 pipetman, stopping 2–3 mm above the band.
9. Harvest the virion band carefully with a P1000 pipetman (typically about 1.2 ml).

### 3.3.3 Measurement of the Virion Concentration

1. Dilute the virion solution two- to tenfold with PBSA2 to make the $OD_{260nm}$ value between 0.1 and 1 for measurement. PBSA2 is used as the blank (*see* **Note 17**).
2. Measure the virion concentration by $OD_{260\ nm}$ using a traditional spectrophotometer or a NanoDrop spectrophotometer.
3. Calculation of the virion concentration:

   1 $OD_{260}$ unit = 0.133 μg virions/μl = $9.4 \times 10^9$ virions/μl.

## 4 Notes

1. The ATCC CRL-1958 cell line is a derivative of the original HRV-sensitive HeLa cells developed in Dr. Vincent Hamparian's lab in the early 1960s. The original cells were propagated as monolayer culture in Hamparian's lab. Subsequently, they were adapted to growth in suspension [29] and cured from mycoplasma infection [35] in Dr. Roland Rueckert's lab. ATCC obtained a stock from Rueckert's lab in the early 1990s and expanded it in monolayer culture to generate the CRL-1958 cell line. Therefore, ATCC CRL-1958 cells will need readaptation if they are to be grown in suspension culture.
2. Mixing DMSO and medium releases heat that kills cells. The medium/DMSO mixture needs to be chilled to 4 °C before use.
3. Avoid unnecessarily prolonged incubation of cells in the freezing medium after it has been thawed. A high concentration of DMSO is harmful to cells at RT.
4. The aluminum foil cover helps to slow down the $CO_2$ release through the filter of the cap and thus to maintain a proper pH for cell growth.
5. Healthy H1-HeLa cells double about every 22 h. Well-maintained cells can typically be passaged up to 40 times.
6. Use only cells that are still at log phase of growth for making cell stock.
7. We use non-purified high-titer infected cell lysate as the stock for infecting cells to make more viruses. HRV can be stored in a −80 °C freezer for years without losing infectivity. But HRV starts to lose infectivity within weeks at −20 °C.

8. Use just enough rotation to keep the cells in suspension.
9. Avoid unnecessarily prolonged incubation of HRV at 35 °C after the solution has been thawed.
10. Lysate prepared with NP-40 lysis should not be used directly to infect cells because NP-40 is toxic.
11. The lysate will turn turbid after this step.
12. The lysate will turn clear after this step.
13. Leave 3–4 ml of space for subsequent addition of the sucrose cushion.
14. Avoid making bubbles during the process of resuspending the virus pellet. If excess bubbles are produced, freeze the virus solution at –80 °C for 15 min to eliminate them.
15. After adding the 75 % and 45 % sucrose solution into a SW41 tube according to instruction, fill the tube to the top with 7.5 % sucrose solution. Cap the tube carefully with the "short cap" to avoid trapping of air between the cap and the sucrose solution. Wipe the sucrose solution from the side of the tube, remove all sucrose solution from the top of the cap, and then place the tube carefully into the holder before pressing the "start" key of the gradient maker. The forming conditions for 7–47 % (w/v) gradient are used here because the conditions for the 7.5–45 % (w/w) gradient are not available. The conditions for 7–47 % (w/v) gradient are as follows: time = 1 min 58 s, angle = 81.5, and speed = 16. These conditions produce good 7.5–45 % (w/w) gradients.
16. The virion band is typically located at about the position of 30 % sucrose. The virion band is visible if the total amount of virions is 40 μg or more.
17. PBSA2 does not have absorbance at 260 nm.

## References


1. Ruuskanen O, Waris M, Ramilo O (2013) New aspects on human rhinovirus infections. Pediatr Infect Dis J 32:553–555
2. Lee WM, Lemanske RF Jr, Evans MD, Vang F, Pappas T, Gangnon R, Jackson DJ, Gern JE (2012) Human rhinovirus species and season of infection determine illness severity. Am J Respir Crit Care Med 186:886–891
3. Winther B (2011) Rhinovirus infections in the upper airway. Proc Am Thorac Soc 8:79–89
4. Busse WW, Lemanske RF Jr, Gern JE (2010) Role of viral respiratory infections in asthma and asthma exacerbations. Lancet 376: 826–834
5. Turner RB, Lee WM (2009) Rhinovirus. In: Richman DD, Whitley RJ, Hayden FG (eds) Clinical virology. ASM, Washington, DC, pp 1063–1082
6. Turner RB, Couch RB (2007) Rhinoviruses. In: Knipe DM, Howley PM (eds) Fields virology. Lippincott Williams and Wilkins, Philadelphia, PA, pp 895–909
7. Savolainen C, Blomqvist S, Mulders MN, Hovi T (2002) Genetic clustering of all 102 human rhinovirus prototype strains: serotype 87 is close to human enterovirus 70. J Gen Virol 83:333–340
8. Rueckert R (1996) Picornaviridae: the viruses and their replication. In: Fields BN, Knipe DM, Howley PM et al (eds) Fields virology, 3rd edn. Lippincott-Raven, Philadelphia, PA, pp 609–654

9. Palmenberg AC, Spiro D, Kuzmickas R, Wang S, Djikeng A, Rathe JA, Fraser-Liggett CM, Liggett SB (2009) Sequencing and analyses of all known human rhinovirus genomes reveal structure and evolution. Science 324:55–59
10. Tapparel C, Junier T, Gerlach D, Cordey S, Van Belle S, Perrin L, Zdobnov EM, Kaiser L (2007) New complete genome sequences of human rhinoviruses shed light on their phylogeny and genomic features. BMC Genomics 8:224
11. Kistler AL, Webster DR, Rouskin S, Magrini V, Credle JJ, Schnurr DP, Boushey HA, Mardis ER, Li H, DeRisi JL (2007) Genome-wide diversity and selective pressure in the human rhinovirus. Virol J 4:40
12. Horsnell C, Gama RE, Hughes PJ, Stanway G (1995) Molecular relationships between 21 human rhinovirus serotypes. J Gen Virol 76(Pt 10):2549–2555
13. Ledford RM, Patel NR, Demenczuk TM, Watanyar A, Herbertz T, Collett MS, Pevear DC (2004) VP1 sequencing of all human rhinovirus serotypes: insights into genus phylogeny and susceptibility to antiviral capsid-binding compounds. J Virol 78:3663–3674
14. Price WH (1956) The isolation of a new virus associated with respiratory clinical disease in humans. Proc Natl Acad Sci USA 42:892–896
15. Pelon W, Mogabgab WJ, Phillips IA, Pierce WE (1957) A cytopathogenic agent isolated from naval recruits with mild respiratory illnesses. Proc Soc Exp Biol Med 94:262–267
16. Hamparian VV, Colonno RJ, Cooney MK, Dick EC, Gwaltney JM Jr, Hughes JH, Jordan WS Jr, Kapikian AZ, Mogabgab WJ, Monto A et al (1987) A collaborative report: rhinoviruses–extension of the numbering system from 89 to 100. Virology 159:191–192
17. Kistler A, Avila PC, Rouskin S, Wang D, Ward T, Yagi S, Schnurr D, Ganem D, Derisi JL, Boushey HA (2007) Pan-viral screening of respiratory tract infections in adults with and without asthma reveals unexpected human coronavirus and human rhinovirus diversity. J Infect Dis 196:817–825
18. Lau SK, Yip CC, Tsoi HW, Lee RA, So LY, Lau YL, Chan KH, Woo PC, Yuen KY (2007) Clinical features and complete genome characterization of a distinct human rhinovirus (HRV) genetic cluster, probably representing a previously undetected HRV species, HRV-C, associated with acute respiratory illness in children. J Clin Microbiol 45:3655–3664
19. Lee WM, Kiesner C, Pappas T, Lee I, Grindle K, Jartti T, Jakiela B, Lemanske RF Jr, Shult PA, Gern JE (2007) A diverse group of previously unrecognized human rhinoviruses are common causes of respiratory illnesses in infants. PLoS One 2:e966
20. McErlean P, Shackelton LA, Lambert SB, Nissen MD, Sloots TP, Mackay IM (2007) Characterisation of a newly identified human rhinovirus, HRV-QPM, discovered in infants with bronchiolitis. J Clin Virol 39:67–75
21. Ashraf S, Brockman-Schneider R, Bochkov YA, Pasic TR, Gern JE (2012) Biological characteristics and propagation of human rhinovirus-C in differentiated sinus epithelial cells. Virology 436:143–149
22. Hao W, Bernard K, Patel N, Ulbrandt N, Feng H, Svabek C, Wilson S, Stracener C, Wang K, Suzich J et al (2012) Infection and propagation of human rhinovirus C in human airway epithelial cells. J Virol 86:13524–13532
23. Bochkov YA, Palmenberg AC, Lee WM, Rathe JA, Amineva SP, Sun X, Pasic TR, Jarjour NN, Liggett SB, Gern JE (2011) Molecular modeling, organ culture and reverse genetics for a newly identified human rhinovirus C. Nat Med 17:627–632
24. Masters JR (2002) HeLa cells 50 years on: the good, the bad and the ugly. Nat Rev Cancer 2:315–319
25. Landry JJ, Pyl PT, Rausch T, Zichner T, Tekkedil MM, Stutz AM, Jauch A, Aiyar RS, Pau G, Delhomme N et al (2013) The genomic and transcriptomic landscape of a HeLa cell line. G3 (Bethesda) 3(8):1213–1224
26. Ketler A, Hamparian VV, Hilleman MR (1962) Characterization and classification of ECHO 28-rhinovirus-coryzavirus agents. Proc Soc Exp Biol Med 110:821–831
27. Hamparian VV, Leagus MB, Hilleman MR (1964) Additional rhinovirus serotypes. Proc Soc Exp Biol Med 116:976–984
28. Conant RM, Somerson NL, Hamparian VV (1968) Plaque formation by rhinoviruses. Proc Soc Exp Biol Med 128:51–56
29. Medappa KC, McLean C, Rueckert RR (1971) On the structure of rhinovirus 1A. Virology 44:259–270
30. Rossmann MG, Arnold E, Erickson JW, Frankenberger EA, Griffith JP, Hecht H-J, Johnson JE, Kamer G, Luo M, Mosser AG et al (1985) The structure of a human common cold virus (rhinovirus 14) and its functional relations to other picornaviruses. Nature 317:145–153
31. Sherry B, Mosser AG, Colonno RJ, Rueckert RR (1986) Use of monoclonal antibodies to identify four neutralization immunogens on a common cold picornavirus, human rhinovirus 14. J Virol 57:246–257

32. Colonno RJ, Condra JH, Mizutani S, Callahan PL, Davies ME, Murcko MA (1988) Evidence for the direct involvement of the rhinovirus canyon in receptor binding. Proc Natl Acad Sci USA 85:5449–5453
33. Greve JM, Davis G, Meyer AM, Forte CP, Yost SC, Marlor CW, Kamarck ME, McClelland A (1989) The major human rhinovirus receptor is ICAM-1. Cell 56:839–847
34. Kim SS, Smith TJ, Chapman MS, Rossmann MC, Pevear DC, Dutko FJ, Felock PJ, Diana GD, McKinlay MA (1989) Crystal structure of human rhinovirus serotype 1A (HRV1A). J Mol Biol 210:91–111
35. Lee WM, Monroe SS, Rueckert RR (1993) Role of maturation cleavage in infectivity of picornaviruses: activation of an infectosome. J Virol 67:2110–2122
36. Oliveira MA, Zhao R, Lee WM, Kremer MJ, Minor I, Rueckert RR, Diana GD, Pevear DC, Dutko FJ, McKinlay MA et al (1993) The structure of human rhinovirus 16. Structure 1:51–68
37. Hofer F, Gruenberger M, Kowalski H, Machat H, Huettinger M, Kuechler E, Blaas D (1994) Members of the low density lipoprotein receptor family mediate cell entry of a minor-group common cold virus. Proc Natl Acad Sci USA 91:1839–1842
38. Zhao R, Pevear DC, Kremer MJ, Giranda VL, Kofron JA, Kuhn RJ, Rossmann MG (1996) Human rhinovirus 3 at 3.0 A resolution. Structure 4:1205–1220
39. Hadfield AT, Lee W, Zhao R, Oliveira MA, Minor I, Rueckert RR, Rossmann MG (1997) The refined structure of human rhinovirus 16 at 2.15 A resolution: implications for the viral life cycle. Structure 5:427–441
40. Che Z, Olson NH, Leippe D, Lee WM, Mosser AG, Rueckert RR, Baker TS, Smith TJ (1998) Antibody-mediated neutralization of human rhinovirus 14 explored by means of cryoelectron microscopy and X-ray crystallography of virus-Fab complexes. J Virol 72:4610–4622
41. Verdaguer N, Blaas D, Fita I (2000) Structure of human rhinovirus serotype 2 (HRV2). J Mol Biol 300:1179–1194
42. Lee WM, Wang W (2003) Human rhinovirus type 16: mutant V1210A requires capsid-binding drug for assembly of pentamers to form virions during morphogenesis. J Virol 77:6235–6244
43. Harris JR, Racaniello VR (2005) Amino acid changes in proteins 2B and 3A mediate rhinovirus type 39 growth in mouse cells. J Virol 79:5363–5373
44. Yin FH, Lomax NB (1983) Host range mutants of human rhinovirus in which non-structural proteins are altered. J Virol 48: 410–418
45. Korpi-Steiner NL, Bates ME, Lee WM, Hall DJ, Bertics PJ (2006) Human rhinovirus induces robust IP-10 release by monocytic cells, which is independent of viral replication but linked to type I interferon receptor ligation and STAT1 activation. J Leukoc Biol 80:1364–1374
46. Chen Y, Hamati E, Lee PK, Lee WM, Wachi S, Schnurr D, Yagi S, Dolganov G, Boushey H, Avila P et al (2006) Rhinovirus induces airway epithelial gene expression through double-stranded RNA and IFN-dependent pathways. Am J Respir Cell Mol Biol 34:192–203
47. Mathur SK, Fichtinger PS, Kelly JT, Lee WM, Gern JE, Jarjour NN (2013) Interaction between allergy and innate immunity: model for eosinophil regulation of epithelial cell interferon expression. Ann Allergy Asthma Immunol 111(25–31):e21
48. Tao S, Zhu L, Lee P, Lee WM, Knox K, Chen J, Di YP, Chen Y (2012) Negative control of TLR3 signaling by TICAM1 down-regulation. Am J Respir Cell Mol Biol 46:660–667
49. Shi L, Manthei DM, Guadarrama AG, Lenertz LY, Denlinger LC (2012) Rhinovirus-induced IL-1beta release from bronchial epithelial cells is independent of functional P2X7. Am J Respir Cell Mol Biol 47:363–371
50. Zhu L, Lee PK, Lee WM, Zhao Y, Yu D, Chen Y (2009) Rhinovirus-induced major airway mucin production involves a novel TLR3-EGFR-dependent pathway. Am J Respir Cell Mol Biol 40:610–619

# Chapter 6

# Propagation of Rhinovirus-C Strains in Human Airway Epithelial Cells Differentiated at Air-Liquid Interface

**Shamaila Ashraf, Rebecca Brockman-Schneider, and James E. Gern**

## Abstract

Rhinovirus-C (RV-C) were discovered recently using molecular methods. Classical methods failed to detect them since they could not grow in standard cell culture. The complete genome sequences of several RV-C strains are now available but there is little information about their biological characteristics. HRV-C were first grown in organ culture, and more recently, we developed a system for culturing RV-C strains in differentiated epithelial cells of human airway at air-liquid interface (ALI). These cultures supported efficient replication of RV-C strains as determined by quantitative RT-PCR. This system has enabled study of the biological characteristics of RV-C strains, including quantitative research.

**Key words** Rhinovirus, Air-liquid interface, Differentiated cultures, Human airway epithelium, Quantitative RT-PCR

## 1 Introduction

Rhinoviruses (RV) are the causative agents of common colds and are the most frequent cause of acute asthma exacerbations in both children and adults [1, 2]. RV strains are phylogenetically classified into three species: A, B, and C. RV-A and RV-B have been recognized for many years, and are characterized by cross-neutralization tests into 100 serotypes. RV-C strains were more recently discovered with the use of molecular techniques (*see* also Palmenberg and Gern, Chapter 1). They have circulated unrecognized in the population due to inability to culture them in standard cell lines.

Evidence from clinical data is accumulating that RV-C are more virulent than the other species since they cause more acute asthma exacerbation [3] and RV-A and RV-C cause more severe illness in infancy than RV-B [4]. Hence it is important to study their biology. RV-C can be grown in organ culture of human sinus epithelium obtained as a by-product of human sinus surgeries [5]. Although this system provided an important tool for

David A. Jans and Reena Ghildyal (eds.), *Rhinoviruses: Methods and Protocols*, Methods in Molecular Biology, vol. 1221, DOI 10.1007/978-1-4939-1571-2_6, 

RV-C research, limited amount of tissue and variability between donor samples made it difficult to standardize for quantitative research. Therefore, we developed a cell culture system to grow RV-C strains that overcame these problems.

Human sinus or bronchial epithelial cells (HSEC/HBEC) grown at an air-liquid interface (ALI) differentiate as early as 21 days in culture to form a pseudo-stratified epithelium with cilia protruding from the apical surface, and containing goblet and mucus-producing cells (Fig. 1) (reprinted from Virology, 436, Ashraf, S. et al., Biological characteristics and propagation of human rhinovirus C in differentiated sinus epithelial cells, 143–149, Copyright 2013, with permission from Elsevier). These cultures support 1–2 logs replication of RV-C (C15 or A16) strains over 24–48 h of inoculation (Fig. 2) [6] (reprinted from Virology,

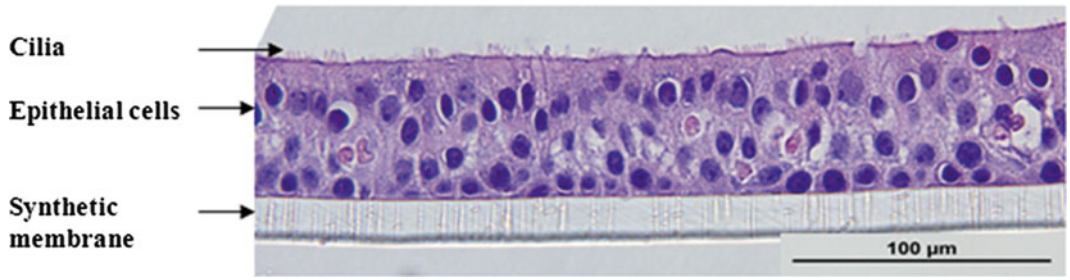


**Fig. 1** Photomicrograph of human sinus epithelium (HSE) after differentiation at ALI. A cross section of tissue was stained with hematoxylin and eosin at 600× magnification

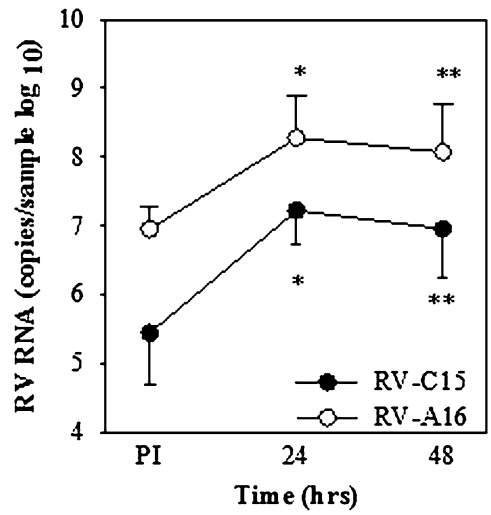


**Fig. 2** RV infection of ALI cultures. HSE ALI cultures ($n=6$) at 21 days of age were infected with RV-C15 ($2.0\times10^8$ RNA copies) or RV-A16 ($3\times10^8$ RNA copies) at 34 °C. Cell-associated virus was analyzed 4 h and again 24–48 h post-infection (PI). *$P=0.001$, **$P<0.005$ compared to viral RNA post-inoculation

436, Ashraf, S. et al., Biological characteristics and propagation of human rhinovirus C in differentiated sinus epithelial cells, 143–149, Copyright 2013, with permission from Elsevier).

HSEC/HBEC-ALI cultures have several advantages over the organ culture system. The undifferentiated cells from the tissue snippets can be expanded to form a larger pool of cells, enough for making multiple plates from the same donor. Secondly, the stocks of undifferentiated cells can be cryopreserved and used later, allowing multiple tests on different days. These cultures yield a uniform number of differentiated cells that consist entirely of epithelial cells, thus providing a more uniform substrate for viral replication. Moreover, the ALI replication system generates reproducible and reliable data since the amount of virus replication observed from a given donor with the same inoculating dose is consistent over time. Altogether, this system permits experiments involving quantitative studies of RV-C replication, pathogenic mechanisms, host-virus interactions, and testing of antiviral drugs.

## 2 Materials

### 2.1 Reagents

Penicillin/streptomycin (10,000 U pen/10 mg strep).

Human placental collagen, Type VI (5 % solution) (Sigma).

BEBM™ (bronchial epithelial cells growth medium) (Lonza).

SingleQuots™ supplements and growth factors (Lonza).

Insulin (100 U/ml).

### 2.2 Media

MEM ($Ca^{2+}$ and $Mg^{2+}$ free).

DMEM/F12 (with L-glutamine and 15 mM HEPES).

DMEM (Dulbecco's modification of Eagle's medium with 4.5 g/l glucose and L-glutamine without sodium pyruvate).

1. Complete media. Add 2.5 ml of fetal calf serum, 0.5 ml of 100× MEM nonessential amino acids, and 6 U of insulin (60 μL of 100 U/ml stock) to 47 ml of DMEM-F12 with pen/strep (5 ml per 500 ml bottle of media). Keep refrigerated at 4 °C.
2. Retinoic acid: Prepare 25 mg/ml stock solution in DMSO. Make a 1,000× dilution of the stock using PBS (with $Ca^{2+}$/$Mg^{2+}$), aliquot 0.5 ml, and freeze at −80 °C.
3. ALI medium (BEGM/DMEM): Make complete BEGM by adding SingleQuots™ to bottles of BEBM and DMEM. Mix these two solutions in a 1:1 ratio. Keep at 4 °C. Add 6 μl retinoic acid per 10 ml medium (final RA concentration = 50 nM, *see* **Note 1**) right before use.

4. Pronase/DNase enzyme solution: Add 56 mg Pronase and 4 mg DNase in a small beaker and then add 40 ml MEM ($Ca^{2+}$ and $Mg^{2+}$ free). Cover the beaker with parafilm and stir with magnetic stir bar until dissolved. Solution should be gassed with 5 % $CO_2$/95 % $O_2$ for 3 min until the solution turns bright red color. Sterilize by passing through a 0.2 μm filter and add 400 μl pen/strep. Cap tightly and keep at 4 °C till used (*see* **Note 2**).
5. Human placental collagen solution: Dissolve 10 mg of human placental collagen in 20 ml sterile water with 40 μl glacial acetic acid. Cover the beaker with parafilm and stir until collagen is dissolved. Dilute collagen solution 1:10 with sterile $H_2O$ (20 ml in 180 ml), filter sterilize (0.2 μm filter), and store at 4 °C (*see* **Note 3**).

### 2.3 Supplies

Transwell-Clear 12-well plates with inserts (12 mm diameter, 0.4 μm pore size, sterile polyester membrane).

12-Well tissue culture plates.

75 $cm^2$ Cell Bind® flasks.

Filter units (0.2 μm).

50 ml conical tubes.

Scalpels.

Forceps (sterilized).

Tissue culture dishes (100 × 20 mm).

Shaker and stir bar.

Serological pipets (sterile).

Pasteur pipets (sterile).

Hemacytometer.

Trypan blue solution.

Micropipets and tips.

Cryovials (2 ml).

Gloves.

## 3 Methods

Carry out all procedures using aseptic technique in a tissue culture hood.

### 3.1 Organ Specimen Preparation

1. Aspirate the storage media from the tube containing the tissue. Place the airway tissue specimen in 30 ml cold, sterile PBS in a 50 ml conical tube to rinse away red blood cells, mucus, and debris. Aspirate PBS with the help of a sterile Pasteur pipette. Wash the specimen three times (*see* **Note 4**).

2. Place the tissue into a sterile tissue culture dish and observe under the microscope to check the epithelium and ciliary beating. Trim away cartilage or undesired tissue using a disposable sterile scalpel and loosen the blood clots as needed (*see* **Note 5**).
3. Wash gently with PBS again.

### 3.2 Digestion with Pronase/ DNase

1. Cut the tissue specimen into small 4 × 4 mm size pieces and carefully place the pieces in a new tube with freshly prepared Pronase/DNase solution. Incubate these pieces at 4 °C from 24 to 96 h with occasional shaking to dissociate the cells (*see* **Note 6**).
2. After incubation, add fetal calf serum to a final concentration of 10 % to the tube containing the tissue specimen and shake it vigorously to dislodge cells. Let the big chunks settle down and remove the cell suspension carefully with a Pasteur pipet without disturbing the larger chunks and place in a new 50 ml tube.
3. Rinse the remaining tissue chunks with 10 ml DMEM/F12 to collect additional cells and pool them with the other cells. Centrifuge pooled cells for 10 min at 200 × *g* at 4 °C.
4. Aspirate off medium and resuspend cell pellet in 10 ml of complete media. Transfer cells to an uncoated tissue culture plate and incubate at 37 °C, 5 % $CO_2$, for 1–6 h to remove fibroblasts.
5. After incubation, carefully collect unattached cell suspension. Rinse off the plate gently with some DMEM/F12 and pool together in a 50 ml tube. Centrifuge for 10 min at 200 × *g* at 4 °C.
6. Aspirate off medium, resuspend cells in 10 ml DMEM/F12, and count the viable cells using trypan blue on a hemacytometer.
7. Centrifuge cells again, aspirate medium, and resuspend in BEGM at the desired concentration for plating or freezing (*see* **Note 7**).

### 3.3 Freezing Cells

1. Resuspend cells in BEGM at a concentration of 500,000 cells per ml (*see* **Note 8**).
2. Add 1 ml cell suspension, 0.6 ml fetal calf serum, and 0.18 ml DMSO to each cryovial, freeze them at −80 °C overnight, and transfer to a liquid nitrogen tank until needed.

### 3.4 Thawing Cells

1. Quickly thaw cells by transferring a frozen vial from −80 °C to a water bath at 37 °C. Aseptically transfer cells to a 50 ml tube. Add 10 ml of warmed DMEM/F12 medium dropwise to the cells with a Pasteur pipette while gently agitating the tube.
2. Centrifuge tube for 10 min at 200 × *g* at 4 °C.

3. Carefully remove supernatant and resuspend the cell pellet in 10 ml of warmed BEGM. Transfer cells to a T-75 $cm^2$ Cell Bind® flask and incubate flask at 37 °C incubator supplied with 5 % $CO_2$. The cells should attach and begin to grow after 24 h; aspirate and replace BEGM at this time.
4. Replace medium in the flask every 2 days as needed depending on the growth of the cells. Split or freeze the cells when they are 80 % confluent.

### 3.5 Collagen Coating of Transwell Inserts

1. Add 300 µl of 5 % human placental collagen Type VI to each insert in a 12-well plate and incubate at 37 °C, 5 % $CO_2$, for 24 h.
2. Remove collagen solution from inserts and air-dry completely in tissue culture hood for 30 min.
3. Rinse dried inserts twice with 500 µl PBS and once with 250 µl BEGM.

### 3.6 Culture of Human Airway Epithelial Cells at Air-Liquid Interface (ALI) on Collagen-Coated Transwell Inserts

1. Remove medium from 80 % confluent monolayers of human sinus or bronchial (HSE/HBE) cells from a T-75 $cm^2$ Cell Bind® flask. Wash the flask gently with 2.5 ml trypsin, aspirating it off quickly.
2. Trypsinize the cells with just enough trypsin (4 ml) to cover the cells for 3–5 min in the 37 °C incubator, checking frequently and tapping flasks firmly, just until cells are observed to float freely.
3. Transfer cells to a 50 ml conical tube containing 10 ml of DMEM/F12 and 10 % FCS to inactivate trypsin and centrifuge at 200 × *g* for 10 min.
4. Resuspend the pellet in 10 ml of DMEM/F12, remove an aliquot for counting cells, and then centrifuge the cells at 200 × *g* for 10 min (*see* **Note 9**).
5. Gently resuspend the cells in BEGM at a concentration of 750 K cells/ml.
6. Add 200 µl of 750 K cells/ml cell suspension per well for a 12-well plate insert (1.13 $cm^2$).
7. Add 1 ml BEGM to the outer wells and incubate at 37 °C, 5 % $CO_2$, for 24 h (*see* **Note 10**).
8. Aspirate medium from both outer well and insert. Add 1 ml of ALI medium to the outer well leaving cells at air-liquid interface and incubate at 37 °C (*see* **Note 11**).
9. Remove media from outer well, and remove any seepage inside the insert every other day during the first week and three times a week after that (*see* **Note 12**).
10. Cultures should start developing cilia by day 17 in culture and will exhibit increased trans-epithelial resistance (*see* **Note 13**).

### 3.7 RV-C Inoculation of Differentiated Human Airway Epithelial Cells at Air-Liquid Interface

1. Observe mature ALI cultures under the microscope for actively beating cilia. If present, remove medium from the basal compartment of the ALI cultures and wash the cells gently three times with PBS ($Ca^{+2}/Mg^{+2}$ free) to remove mucus.
2. Dilute RV-C to a desired concentration ($1 \times 10^6$ RNA copies) in BEGM with 0.01 % BSA and apply 100 µl of the inoculum to the apical surface of the ALI culture. Next, rock the plate gently on a shaker for 15 min at room temperature and then transfer the plate to an incubator (34 °C, 5 % $CO_2$) for 4 h (*see* **Note 14**).
3. Wash the cultures thrice with PBS ($Ca^{+2}/Mg^{+2}$ free) and collect samples to assess cell-associated virus in 350 µl RLT buffer (Qiagen).
4. Feed the remaining samples basally with 1 ml of ALI medium and incubate at 34 °C for 24–72 h.
5. After aspirating the media, collect the cells in 350 µl of RLT buffer for RNA extraction and qRT-PCR analysis.

### 3.8 RNA Extraction and qRT-PCR

1. Extract total RNA from the ALI cultures using the RNeasy Mini kit (Qiagen).
2. RV-RNA concentrations are determined by qRT-PCR using RV-specific primers (5; *see* also Lee et al., Chapter 3).

## 4 Notes

1. Retinoic acid is very sensitive to UV light, air, and heat, so work quickly in tissue culture hood in low light to limit its oxidation and keep aliquots on ice while working.
2. Pronase/DNase solution should be prepared fresh each time right before use.
3. Collagen-coated inserts can be stored at 4 °C.
4. Organ specimens should be freshly harvested and have viable ciliary beating. All specimens should be free from respiratory viruses and we recommend screening using a multiplex PCR for all common viruses.
5. Tissue specimens can be placed at 4 °C for up to 30 min to loosen blood clots if necessary.
6. For our purposes the optimal time for dissociation is 48 h as cell viability decreases with longer incubations. If the tissue sample is larger than normal size, the amount of Pronase/DNase solution should be increased.
7. Recommended cell concentrations: for plating 150–300 K in 10 ml per T-75 $cm^2$ flask, and for freezing, $5 \times 10^5$–$1 \times 10^6$ cells per vial.

8. Freeze $3 \times 10^5$–$1 \times 10^6$ cells, depending on the number of cells.
9. The cells obtained at P-0 and P-1 are frozen in liquid $N_2$ for future use. Cells obtained from later passages do not differentiate as well at ALI.
10. If the cells do not form a confluent monolayer after first day of seeding on the inserts, they should be kept in BEGM and allowed to grow till they become confluent and then transfer to air-liquid interface.
11. Make sure that no air bubbles are trapped underneath the inserts after addition of medium, and remove old media from the bottom of the wells every time.
12. Cell debris and mucus will collect on the apical surface as the cells grow. These can be gently washed with warmed BEGM/DMEM once per week or as needed.
13. Cultures become differentiated from 21 days onwards as observed by ciliary beating and increased trans-epithelial resistance. Cultures allowed to differentiate for 2 months permit greater RV replication as compared to those allowed to differentiate for 1 month. Cultures can be maintained for 6 months by replenishing the medium regularly and washing mucus from the apical surfaces.
14. The concentration of RV that gives the optimal replication ranges from $10^5$ to $10^6$ RNA copies/well.

## Acknowledgements

Funding for development of the ALI tissue culture system for RV-C was provided by NIH grant U19 AI070503.

### References

1. Arden KE, Faux CE, O'Neill NT et al (2010) Molecular characterization and distinguishing features of a novel human rhinovirus (HRV) C, HRVC-QCE, detected in children with fever, cough and wheeze during 2003. J Clin Virol 47:219–223
2. Nicholson KG, Kent J, Ireland DC (1993) Respiratory viruses and exacerbations of asthma in adults. Br Med J 307:982–986
3. Bizzintino J, Lee WM, Laing IA et al (2011) Association between human rhinovirus C and severity of acute asthma in children. Eur Respir J 37:1037–1042
4. Lee WM, Lemanske RF, Evans MD et al (2012) Human rhinovirus species and season of infection determine illness severity. Am J Respir Crit Care Med 186:886–891
5. Bochkov YA, Palmenberg AC, Lee WM et al (2011) Molecular modeling, organ culture and reverse genetics for a newly identified human rhinovirus C. Nat Med 17:627–632
6. Ashraf S, Brockman-Schneider R, Bochkov YA et al (2013) Biological characteristics and propagation of human rhinovirus-C in differentiated sinus epithelial cells. Virology 436: 143–149

# Chapter 7

# Infectivity Assays of Human Rhinovirus-A and -B Serotypes

**Wai-Ming Lee, Yin Chen, Wensheng Wang, and Anne Mosser**

## Abstract

Infectivity is a fundamental property of viral pathogens such as human rhinoviruses (HRVs). This chapter describes two methods for measuring the infectivity of HRV-A and -B serotypes: end point dilution ($TCID_{50}$) assay and plaque assay. End point dilution assay is a quantal, not quantitative, assay that determines the dilution of the sample at which 50 % of the aliquots have infectious virus. It can be used for all the HRV-A and -B serotypes and related clinical isolates that grow in cell culture and induce cytopathic effect (CPE), degenerative changes in cells that are visible under a microscope. Plaque assay is a quantitative assay that determines the number of infectious units of a virus in a sample. After an infectious unit of virus infects one cell, the infected cell produces progeny viruses that then infect and kill a circle of adjacent cells. This circle of dead cells detaches from the dish and thus leaves a clear hole in a cell monolayer. Plaque assay works only for HeLa-adapted HRV-A and -B serotypes that can make visible plaques on the cell monolayer. Currently the end point dilution assay and plaque assay have not been developed for the newly discovered HRV-C.

**Key words** MRC-5, HeLa cells, End point dilution, Plaque assay, Infectivity, $TCID_{50}$, PFU

## 1 Introduction

Human rhinovirus (HRV) is a large group of small RNA viruses that infect airway epithelial cells and is a major cause of respiratory illnesses [1–6]. HRV belongs to the picornavirus family and has about 150 distinct types or members. They are divided into three species: A (75 types), B (25 types), and C (about 50 types) according to serological and genome sequence variations [3, 7–13]. The 100 HRV-A and -B types were isolated and assigned as serotypes between 1956 and 1987 by traditional cultural, biochemical, and serological methods [14–16]. They are small (15–30 nm) RNA viruses that are ether resistant but acid sensitive. They grow optimally at 32–35 °C. Each serotype was defined by 20-fold or greater differences in antiserum neutralization titers during reciprocal

David A. Jans and Reena Ghildyal (eds.), *Rhinoviruses: Methods and Protocols*, Methods in Molecular Biology, vol. 1221, DOI 10.1007/978-1-4939-1571-2_7, 

cross-neutralization tests against the other 99 serotypes [8, 16]. The prototype strains of these serotypes are available at ATCC. The 50 HRV-C types were identified recently with modern PCR and sequencing techniques [3, 17–20]. Their sequences are more closely related to those of HRV-A and -B serotypes than to other GenBank sequences. HRV-C does not grow in traditional primary cell cultures and continuous cell lines. They were recently found to grow in differentiated airway epithelial cells in air-liquid interface culture or sinus organ culture (21–23; also *see* Chapter 6 in this volume). Several additional HRV-A and HRV-B types have been identified by PCR and sequencing techniques [3]. However, they have not been characterized by traditional culture methods.

HRV-A and -B serotypes can grow and induce cytopathic effect (CPE), degenerative changes in cells that are visible under a microscope, in a variety of primary cell cultures and continuous cell lines. Primary MRC-5 and WI-38 cells and the continuous H1-HeLa line are the most commonly used cells for titrating the infectivity of HRV-A and -B serotypes [5, 6, 8]. MRC-5 and WI-38 cells are widely used by clinical microbiology labs for end point dilution assay of HRV-A and -B serotypes and related field isolates from clinical samples. They are human fetal lung fibroblast diploid cells and are sensitive to the prototype strains of all 100 HRV-A and -B serotypes and many related clinical isolates. Uninfected confluent monolayers of these cells can maintain normal healthy cell morphology for up to 4 weeks. This allows the clear detection of many slow-growing HRV serotypes, strains, and clinical isolates that require a week or longer to induce observable CPE morphology. However, MRC-5 and WI-38 monolayers stain poorly with dyes such as crystal violet and thus are not used for plaque assays. H1-HeLa is an HRV-sensitive HeLa strain originally developed in the lab of Dr. Vincent Hamparian in the early 1960s. It is the standard for plaque assays and biology studies of HeLa-adapted HRV-A and -B serotypes in molecular virology labs. H1-HeLa cell monolayers are highly stainable and can support the plaque formation of HeLa-adapted HRV-A and -B serotypes [24]. However, not-yet-adapted HRV serotypes, strains, and clinical isolates grow slowly and do not form visible plaques in H1-HeLa monolayers and uninfected monolayer H1-HeLa cells start to display spontaneous CPE-like morphology 3–4 days after becoming confluent. Therefore, H1-HeLa cells are not used for the $TCID_{50}$ assay for detecting slow-growing and low-titer HRV serotypes, strains, and clinical isolates that require a week or longer to induce visible CPE.

In addition to infectivity measurement, the plaque assay is also essential for classical genetic studies of HRV and other viruses because it allows the precise isolation of virus mutants and purification of HRV strains from contaminating viruses [25, 26].

This chapter describes the detailed procedures for the end point dilution ($TCID_{50}$) assay [27, 28] and plaque assay of HRV [8, 25, 29].

## 2 Materials

### 2.1 $TCID_{50}$ Assay Using MRC-5 Cells

1. MRC-5 cells (ATCC CCL-171) (*see* **Note 1**).
2. $CO_2$ incubator.
3. −80 °C freezer.
4. Liquid nitrogen tank.
5. Sterile disposables for tissue culture:
   (a) 100-mm dishes.
   (b) 48-well plates.
   (c) 4-oz Nalgene medium bottles.
   (d) 8-oz Nalgene medium bottles.
   (e) 50-ml capped tubes.
   (f) 1.5-ml microfuge tubes.
   (g) 10-ml sterile pipettes.
   (h) 5-ml sterile pipettes.
   (i) 2-ml sterile aspirating pipettes.
   (j) Kimwipes EX-L.
   (k) 2-ml cryovials.
6. Medium A-FBS:
   To 500 ml MEM (Invitrogen 11090081), add the following ingredients:
   (a) 5 ml nonessential amino acids (Invitrogen 1114050).
   (b) 5 ml L-glutamine (Invitrogen 2503081).
   (c) 5 ml penicillin, streptomycin (Invitrogen 15140163).
   (d) 50 ml fetal bovine serum (Invitrogen 10437-028).
7. Medium A-FBS-DMSO (*see* **Note 2**):
   To 40 ml medium A-FBS, add 10 ml DMSO (dimethyl sulfoxide) (Fisher BP231-1).
8. PBSI: PBS with calcium and magnesium.
9. PBSA1 (0.1 % BSA):
   To 500 ml PBSI, add 6.7 ml 7.5 % bovine albumin fraction V.
10. PBSII: PBS without calcium and magnesium.
11. PBS-EDTA:
    To 500 ml PBSII, add 5.5 ml 0.5 M EDTA.
12. Trypsin-EDTA 1×.

### 2.2 Plaque Assay Using H1-HeLa Cell Monolayers

1. H1-HeLa cells (ATCC CRL-1958) (*see* Chapter 5 for H1-HeLa cell culture).
2. $CO_2$ incubator.

3. *See* Subheading 2.1 above for sterile disposables, PBSI and PBSA1.
4. 60-mm dishes.
5. 1,000-ml 0.20-μm filter units.
6. Distilled water.
7. 1.6 % Noble agar.
   To 100 ml distilled water add 1.6 g of noble agar. Autoclave the mixture at 121 °C for 20 min (minute) (*see* **Note 3**).
8. 10 % buffered formalin phosphate.
9. Medium A-NCS.
   To 500 ml MEM (Invitrogen 11090081), add the following ingredients:
   (a) 5 ml nonessential amino acids (Invitrogen 1114050).
   (b) 5 ml L-glutamine (Invitrogen 2503081).
   (c) 5 ml penicillin, streptomycin (Invitrogen 15140163).
   (d) 50 ml newborn calf serum (Invitrogen 16010-159).
10. 2× P6 medium:
    To make 1 L 2× P6 medium, dissolve the following ingredients in distilled water, bring volume to one liter with distilled water, and filter sterilize the mixture:
    (a) Two bags (1 L size) of MEM powder (Invitrogen 41500-034).
    (b) 4.4 g sodium bicarbonate, $NaHCO_3$ (Sigma S5761).
    (c) 16.2 g magnesium chloride hexahydrate, $MgCl_2 \cdot 6H_2O$ (Sigma M2393-500 g).
    (d) 26.6 mL 7.5 % bovine albumin fraction V (Invitrogen 15260-037).
11. 100× GOP supplement:
    To 100 ml distilled water (Invitrogen), add and dissolve the following ingredients:
    (a) 2.92 g L-glutamine (Fisher BP379-100).
    (b) 1.1 g pyruvic acid (Sigma P5280).
    (c) 2.64 g oxaloacetic acid (Sigma O7753).
12. Plaque assay stain (0.1 % crystal violet in 20 % ethanol):
    To make 5× stock: Dissolve 2.5 g crystal violet in 500 ml ethanol.
    To make a working stock: Dilute 20 ml of 5× stock to 100 ml with distilled water.

## 3 Methods

### 3.1 $TCID_{50}$ Assay Using MRC-5 Cells

#### 3.1.1 Starting an MRC-5 Cell Culture in a 100-mm Dish

1. Thaw a cryovial of cells at room temperature (RT) (*see* **Note 4**).
2. Transfer the cells into a 100-mm dish containing 10 ml of medium A-FBS.
3. Incubate cells in a $CO_2$ incubator (5 % $CO_2$, 37 °C) overnight, and then replace the medium with 10 ml of fresh medium A-FBS (*see* **Note 5**).
4. Continue to incubate cells in a $CO_2$ incubator (5 % $CO_2$, 37 °C) until they reach full confluence. This will take 3–5 days depending on the number of viable cells in the cryovial.

#### 3.1.2 Expanding and Passing MRC-5 Cell Culture

1. Detach cells from 100-mm dishes by trypsinization:
   (a) Remove medium.
   (b) Wash monolayer in each dish with 5 ml PBS-EDTA.
   (c) Add 1 ml trypsin-EDTA 1× to each monolayer.
   (d) Incubate dishes at RT for several minutes until most cells are detached (*see* **Note 6**).
2. Wash the detached cells from one 100-mm dish into a 50-ml tube containing 40 ml of medium A-FBS and mix well.
3. Pipette the cells into four 100-mm dishes, 10 ml per dish.
4. Incubate cells in a $CO_2$ incubator (5 % $CO_2$, 37 °C) until they reach full confluence.

#### 3.1.3 Cryo-Preservation of MRC-5 Cells

1. Grow cells to almost confluence in 100-mm dishes. Do not overgrow cells.
2. Detach cells from dishes by trypsinization as described in **step 1** of Subheading 3.1.2.
3. Wash the detached cells from four 100-mm dishes into a 50-ml tube with 8 ml of cold medium A-FBS (Final volume is about 12 mL).
4. Add 12 ml of cold medium A-FBS-DMSO and then swirl the tube gently to mix.
5. Use a 5-ml pipette to aliquot 1.5 ml of cells into each chilled cryovial and cap tightly.
6. Place the 16 cryovials into a chilled freezer box, and then store at −80 °C overnight.
7. Place the cryovials into a liquid nitrogen tank for long-term storage.
8. A week later, remove a vial from the liquid nitrogen tank to check cell viability by starting a new culture in a 100-mm dish as described in Subheading 3.1.1 above.

*3.1.4 Preparation of 48-well Plates of MRC-5 Cells for $TCID_{50}$ Assay*

1. Trypsinize one 100-mm dish of confluent cells as described in **step 1** of Subheading 3.1.2.
2. Wash the cells into a Nalgene medium bottle containing 75 ml medium A-FBS, and then shake the bottle gently to suspend the cells well.
3. Add 0.5 ml of cells into each well of three 48-well plates.
4. Incubate plates in a $CO_2$ incubator (5 % $CO_2$, 37 °C). The monolayers are ready for $TCID_{50}$ assay when they are 80–90 % confluent after 4–5 days.

*3.1.5 Virus Dilution, Infection, and CPE Development*

1. Make a tenfold serial dilution of virus in PBSA1 in sterile 1.5-ml eppi tube (*see* **Note 7**).
2. Remove medium from each well of the MRC-5 cell plates by aspiration.
3. Tap the plate upside down on a stack of clean Kimwipe to remove the remaining medium.
4. Add 50 μl of virus solution per well, 8 wells for each dilution.
5. Incubate plates at RT for 1 h to allow virus attachment.
6. Add 0.5 ml medium A-FBS.
7. Incubate plates in a $CO_2$ incubator (5 % $CO_2$, 35 °C).
8. Check and record the appearance of CPE (Fig. 1) in each well starting at 3 days after infection and then 5, 7, 9, 11, and 14 days (*see* **Note 8**).

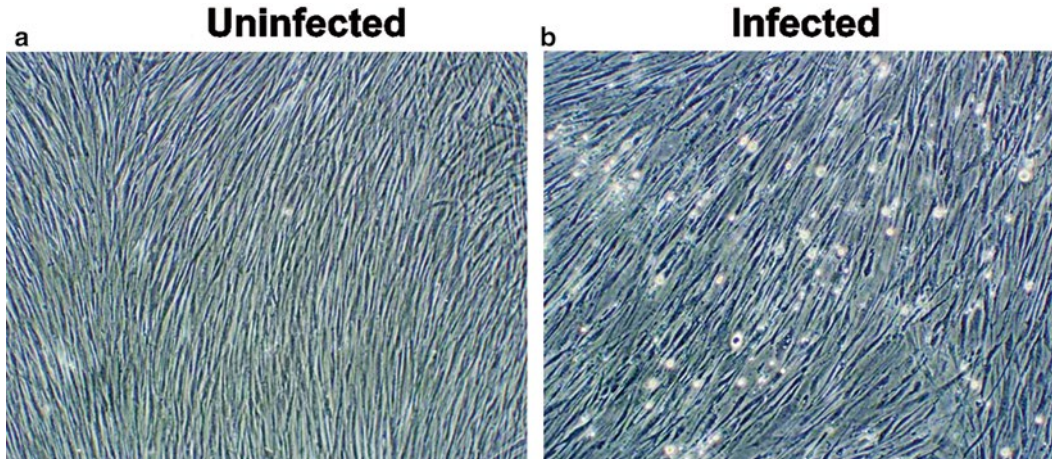


**Fig. 1** Appearance of CPE of HRV16-infected MRC-5 cells. MRC-5 cell monolayer (90 % confluent in a well of 48-well plate) was infected with ten $TCID_{50}$ of HRV16 (panel (**b**)) as described in Subheading 3.1.5. Panel (**a**) was a mock-infected control. The cells were then incubated in a $CO_2$ incubator (5 % $CO_2$, 35 °C) for 5 days

*3.1.6 Calculate Virus Titer with the Kärber End Point Method [27, 28]*

$$\text{Negative log of } TCID_{50} \text{ end point titer} = \left[\text{Negative log of highest sample concentration tested}\right] - \left[\left(\frac{\text{sum of \% infection at each dilution}}{100} - 0.5\right) \times \log \text{ of dilution}\right]$$

*Example:*

8/8 cultures infected @ 1:1 dilution.

8/8 cultures infected @ 1:10 dilution.

6/8 cultures infected @ 1:100 dilution.

2/8 cultures infected @ 1:1,000 dilution.

0/8 cultures infected @ 1:10,000 dilution.

50 µl inoculum was added to each well.

Neg. Log. $TCID_{50} = 0 - (\{[(100+100+75+25+0)/100] - 0.5\} \times 1)$.

Neg. Log. $TCID_{50} = -2.5$.

$TCID_{50}$ per 50 µl of original sample = antilog 2.5 = 320.

$TCID_{50}$ per 1 ml of original sample = $320 \times 1{,}000/50 = 6{,}400$.

### *3.2 Plaque Assay Using H1-HeLa Cell Monolayers*

*3.2.1 Make H1-HeLa Cell Monolayers in 60-mm Dishes*

1. Count cells from a suspension culture with a hemocytometer (*see* Chapter 5 for H1-HeLa cell culture).
2. Pellet enough cells ($500 \times g$, 5 min) to plate $2.4 \times 10^6$ cells per dish.
3. Resuspend cells to $8 \times 10^5$ cells per ml with medium A-NCS.
4. Add 3 ml of cell suspension (a total of $2.4 \times 10^6$ cells) per dish.
5. Swirl the dishes to distribute the cells evenly in each dish.
6. Incubate the dishes in a $CO_2$ incubator (5 % $CO_2$, 37 °C) overnight (*see* **Note 9**).

*3.2.2 Virus Dilution, Infection, and Plaque Development*

1. Check dishes microscopically to make sure that monolayers are ~90 % confluent and cells are healthy.
2. Dilute virus in PBSA1 to a final concentration of about 100 PFU/200 µl (*see* **Notes 7** and **10**) in a sterile 1.5-ml eppi tube.
3. Remove medium from cell monolayers by aspiration.
4. Wash cell monolayers once with 5 ml PBSI, and then remove PBSI by aspiration.
5. Add 200 µl of the virus dilutions to each dish by dropping the virus solution gently into the center of the monolayer.
6. Incubate dishes at RT for 1 h for virus attachment (*see* **Note 11**).
7. Prepare agar overlay:

(a) Melt a 100-ml glass bottle of 1.6 % noble agar in a microwave.

(b) Bring the noble agar to 45 °C by incubating it in a 45 °C water bath.

(c) Warm 2× P6 medium to 45 °C by incubating it in a 45 °C water bath.

(d) Mix 50 ml noble agar and 50 ml of 2× P6 medium in a Nalgene media bottle, and then incubate the mixture in a 45 °C water bath.

8. Prepare 100 ml nutrient medium overlay (1× P6/2× glucose/2x GOP supplement) in a Nalgene media bottle with the recipe below and keep at RT.

(a) 50 ml 2× P6 medium.

(b) 47 ml sterile distilled water (Invitrogen).

(c) 2 ml 100× GOP supplement.

(d) 1 ml 20 % glucose (200×).

9. Add 2.5 ml agar overlay into each dish, and then allow the agar to solidify by incubating the dishes at RT for 5–10 min (*see* **Note 12**).

10. Gently add 2.5 ml nutrient medium to the center of the plate, on top of the agar layers.

11. Incubate dishes in a $CO_2$ incubator (5 % $CO_2$, 35 °C) for 2–4 days (*see* **Note 13**).

12. Stain the monolayers:

(a) Add 2 ml 10 % buffered formalin and then incubate at RT for 15 min (*see* **Note 14**).

(b) Use a 10-ml pipette to remove the liquid.

(c) Flick off the agar into a waste container.

(d) Add 2 ml crystal violet stain gently into each dish to cover the monolayer.

(e) Use a 10-ml pipette to remove the stain after incubating at RT for 1 h.

(f) Wash off excess stain with tap water.

(g) Air-dry the stained monolayers.

13. Count the number of plaques (Fig. 2).

14. Calculate the titer of the undiluted sample by multiplying the fold of dilution and the number of plaques per dish. The titer is expressed in PFU per ml of sample.

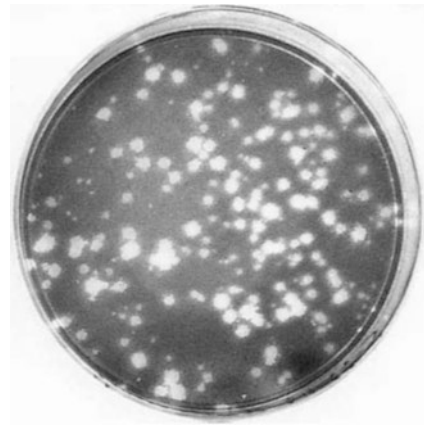

**Fig. 2** Appearance of plaques of HRV14 on a crystal violet-stained H1-HeLa cell monolayer. A H1-HeLa cell monolayer (90 % confluent in a 60-mm dish) was infected with about 100 PFU of HRV14 as described in Subheading 3.2.2. The infected monolayer was then overlaid with agar and incubated in a $CO_2$ incubator (5 % $CO_2$, 35 °C). Two days later, the monolayer was stained with *crystal violet*

## 4 Notes

1. We use WI-38 cells when MRC-5 cells are not available. The growth conditions for WI-38 cells are identical to those of MRC-5 cells. WI-38 and MRC-5 cells have similar susceptibilities to HRV.
2. Mixing DMSO and medium releases heat that kills cells. The medium/DMSO mixture needs to be chilled to 4 °C before use.
3. Over-autoclaving will degrade the noble agar and change its gelling temperature. Thus it is important to adhere to the autoclave condition of 121 °C for 20 min.
4. Avoid unnecessarily prolonged incubation of cells in the freezing medium after it has been thawed. A high concentration of DMSO is harmful to the cells at RT.
5. The DMSO from the freezing medium is toxic. It should be removed after the cells become attached to the dish.
6. Avoid over-trypsinization of the cells. Visibly monitor the monolayer continuously after the trypsin is added. As soon as most of the monolayer starts to detach, add medium A-FBS to stop trypsinization.
7. It is critical to discard pipette tips between each dilution to avoid carrying virus from the first to the subsequent dilutions. Otherwise, it may give misleadingly high infectivity results.

8. The intervals of observing and recording CPE may be adjusted according to the rate of growth and CPE development of the HRV serotype, strain, and isolate being tested. In addition, some HRV-A and -B serotypes, strains, and isolates grow poorly and can only induce CPE in patches of cells instead of the whole monolayer.
9. Avoid overgrowing the cell monolayer. Using 90 % confluent monolayers for infection gives the best plaque assay results.
10. About 100 plaques per 60-mm monolayer give the most accurate measurement. Plaques tend to fuse together when there are too many plaques in a monolayer. On the other hand, the statistical error is large when a monolayer has very few plaques. Therefore, a preliminary plaque assay of serial dilutions of virus should be performed to estimate the titer for making the dilution at about 100 PFU per 200 μl.
11. Make sure that the dishes are maintained in a horizontal position during attachment in order to develop evenly distributed plaques on monolayers.
12. Different lots of noble agar may have slightly different gelling temperatures. If the agar overlay does not solidify well after 10 min at RT or is too hard to be removed from the dish at the end of the plaque assay, use slightly more (e.g., plus 0.1 %) or less (e.g., minus 0.1 %) agar, respectively.
13. The length of plaque development depends on the plaque development rate of each serotype. HRV14 needs 2 days, HRV16 2.5 days, and HRV1A 4 days.
14. Formalin is used to kill the virus and to fix the cell monolayer before staining.

## References

1. Busse WW, Lemanske RF Jr, Gern JE (2010) Role of viral respiratory infections in asthma and asthma exacerbations. Lancet 376: 826–834
2. Ruuskanen O, Waris M, Ramilo O (2013) New aspects on human rhinovirus infections. Pediatr Infect Dis J 32:553–555
3. Lee WM, Lemanske RF Jr, Evans MD, Vang F, Pappas T, Gangnon R, Jackson DJ, Gern JE (2012) Human rhinovirus species and season of infection determine illness severity. Am J Respir Crit Care Med 186:886–891
4. Winther B (2011) Rhinovirus infections in the upper airway. Proc Am Thorac Soc 8:79–89
5. Turner RB, Lee WM (2009) Rhinovirus. In: Richman DD, Whitley RJ, Hayden FG (eds) Clinical virology. ASM, Washington, DC, pp 1063–1082
6. Turner RB, Couch RB (2007) Rhinoviruses. In: Knipe DM, Howley PM (eds) Fields virology. Lippincott Williams and Wilkins, Philadelphia, PA, pp 895–909
7. Horsnell C, Gama RE, Hughes PJ, Stanway G (1995) Molecular relationships between 21 human rhinovirus serotypes. J Gen Virol 76(Pt 10):2549–2555
8. Rueckert R (1996) Picornaviridae: the viruses and their replication. In: Fields BN, Knipe DM, Howley PM et al (eds) Fields virology, 3rd edn. Lippincott-Raven Publishers, Philadelphia, PA, pp 609–654
9. Savolainen C, Blomqvist S, Mulders MN, Hovi T (2002) Genetic clustering of all 102 human rhinovirus prototype strains: serotype 87 is close to human enterovirus 70. J Gen Virol 83:333–340

10. Ledford RM, Patel NR, Demenczuk TM, Watanyar A, Herbertz T, Collett MS, Pevear DC (2004) VP1 sequencing of all human rhinovirus serotypes: insights into genus phylogeny and susceptibility to antiviral capsid-binding compounds. J Virol 78:3663–3674
11. Kistler AL, Webster DR, Rouskin S, Magrini V, Credle JJ, Schnurr DP, Boushey HA, Mardis ER, Li H, DeRisi JL (2007) Genome-wide diversity and selective pressure in the human rhinovirus. Virol J 4:40
12. Tapparel C, Junier T, Gerlach D, Cordey S, Van Belle S, Perrin L, Zdobnov EM, Kaiser L (2007) New complete genome sequences of human rhinoviruses shed light on their phylogeny and genomic features. BMC Genomics 8:224
13. Palmenberg AC, Spiro D, Kuzmickas R, Wang S, Djikeng A, Rathe JA, Fraser-Liggett CM, Liggett SB (2009) Sequencing and analyses of all known human rhinovirus genomes reveal structure and evolution. Science 324:55–59
14. Price WH (1956) The isolation of a new virus associated with respiratory clinical disease in humans. Proc Natl Acad Sci USA 42:892–896
15. Pelon W, Mogabgab WJ, Phillips IA, Pierce WE (1957) A cytopathogenic agent isolated from naval recruits with mild respiratory illnesses. Proc Soc Exp Biol Med 94:262–267
16. Hamparian VV, Colonno RJ, Cooney MK, Dick EC, Gwaltney JM Jr, Hughes JH, Jordan WS Jr, Kapikian AZ, Mogabgab WJ, Monto A et al (1987) A collaborative report: rhinoviruses–extension of the numbering system from 89 to 100. Virology 159:191–192
17. Kistler A, Avila PC, Rouskin S, Wang D, Ward T, Yagi S, Schnurr D, Ganem D, Derisi JL, Boushey HA (2007) Pan-viral screening of respiratory tract infections in adults with and without asthma reveals unexpected human coronavirus and human rhinovirus diversity. J Infect Dis 196:817–825
18. Lau SK, Yip CC, Tsoi HW, Lee RA, So LY, Lau YL, Chan KH, Woo PC, Yuen KY (2007) Clinical features and complete genome characterization of a distinct human rhinovirus (HRV) genetic cluster, probably representing a previously undetected HRV species, HRV-C, associated with acute respiratory illness in children. J Clin Microbiol 45:3655–3664
19. Lee WM, Kiesner C, Pappas T, Lee I, Grindle K, Jartti T, Jakiela B, Lemanske RF Jr, Shult PA, Gern JE (2007) A diverse group of previously unrecognized human rhinoviruses are common causes of respiratory illnesses in infants. PLoS One 2:e966
20. McErlean P, Shackelton LA, Lambert SB, Nissen MD, Sloots TP, Mackay IM (2007) Characterisation of a newly identified human rhinovirus, HRV-QPM, discovered in infants with bronchiolitis. J Clin Virol 39:67–75
21. Ashraf S, Brockman-Schneider R, Bochkov YA, Pasic TR, Gern JE (2012) Biological characteristics and propagation of human rhinovirus-C in differentiated sinus epithelial cells. Virology 436:143–149
22. Hao W, Bernard K, Patel N, Ulbrandt N, Feng H, Svabek C, Wilson S, Stracener C, Wang K, Suzich J et al (2012) Infection and propagation of human rhinovirus C in human airway epithelial cells. J Virol 86:13524–13532
23. Bochkov YA, Palmenberg AC, Lee WM, Rathe JA, Amineva SP, Sun X, Pasic TR, Jarjour NN, Liggett SB, Gern JE (2011) Molecular modeling, organ culture and reverse genetics for a newly identified human rhinovirus C. Nat Med 17:627–632
24. Stott EJ, Tyrrell DA (1968) Some improved techniques for the study of rhinoviruses using HeLa cells. Arch Gesamte Virusforsch 23: 236–244
25. Sherry B, Rueckert R (1985) Evidence for at least two dominant neutralization antigens on human rhinovirus 14. J Virol 53:137–143
26. Sherry B, Mosser AG, Colonno RJ, Rueckert RR (1986) Use of monoclonal antibodies to identify four neutralization immunogens on a common cold picornavirus, human rhinovirus 14. J Virol 57:246–257
27. Schmidt NJ, Emmons RW (1989) General principles of laboratory. In: Schmidt NJ, Emmons RW (eds) Diagnostic procedures for viral, rickettsial, and chlamydial infections. American Public Health Association, Washington, DC, pp 1–35
28. Schmidt NJ (1989) Cell culture procedures for diagnostic virology. In: Schmidt NJ, Emmons RW (eds) Diagnostic procedures for viral, rickettsial, and chlamydial infections. American Public Health Association, Washington, DC, pp 51–100
29. Lee WM, Monroe SS, Rueckert RR (1993) Role of maturation cleavage in infectivity of picornaviruses: activation of an infectosome. J Virol 67:2110–2122

# Chapter 8

# Application of FCS in Studies of Rhinovirus Receptor Binding and Uncoating

**Shushan Harutyunyan, Arthur Sedivy, Gottfried Köhler, Heinrich Kowalski, and Dieter Blaas**

## Abstract

Fluorescence correlation spectroscopy (FCS) allows determining diffusion and relaxation properties of fluorescent molecules. It requires only extremely small amounts of sample, down to picomolar concentrations, in an effective analysis volume of a few femtoliters. In essence, FCS determines the autocorrelation of fluorescence fluctuations caused by single labeled molecules passing through the confocal volume of a microscope equipped with a suitable detector; it permits investigating interactions of (macro)molecules, even in single cells. We present an FCS protocol for exploring, under in vitro conditions, the dynamic processes that take place during the early steps of virus infection. We cover two important issues of rhinovirus research, the kinetics of directional RNA release, and virus-receptor interactions exemplified by using human rhinovirus type A2 (HRV-A2) as a model.

**Key words** Fluorescence, Autocorrelation analysis, Diffusion coefficient, Fluorescence correlation spectroscopy, HRV-A2, Uncoating, Receptor, Rhinovirus, Picornavirus

## 1 Introduction

Fluorescence correlation spectroscopy (FCS) was implemented in the early 1970s by Magde et al. [1] and has undergone a huge development since the introduction of a confocal setup by Rigler and colleagues [2]. FCS extracts information from the temporal changes of fluorescence signals emitted from a small number of molecules involved in stochastically fluctuating chemical and/or physical processes by means of time correlation. This is realized via calculating the time dependence of the similarity of two signals. FCS curves are derived by correlating fluctuations in the measured fluorescence intensity to itself, with the correlation time $\tau$, i.e., autocorrelation, or to an independently measured fluctuating signal, i.e., cross-correlation. The time-dependent decay of the correlation of fluorescence fluctuations yields quantitative information on parameters such as number of the molecules (concentration),

David A. Jans and Reena Ghildyal (eds.), *Rhinoviruses: Methods and Protocols*, Methods in Molecular Biology, vol. 1221, DOI 10.1007/978-1-4939-1571-2_8, 

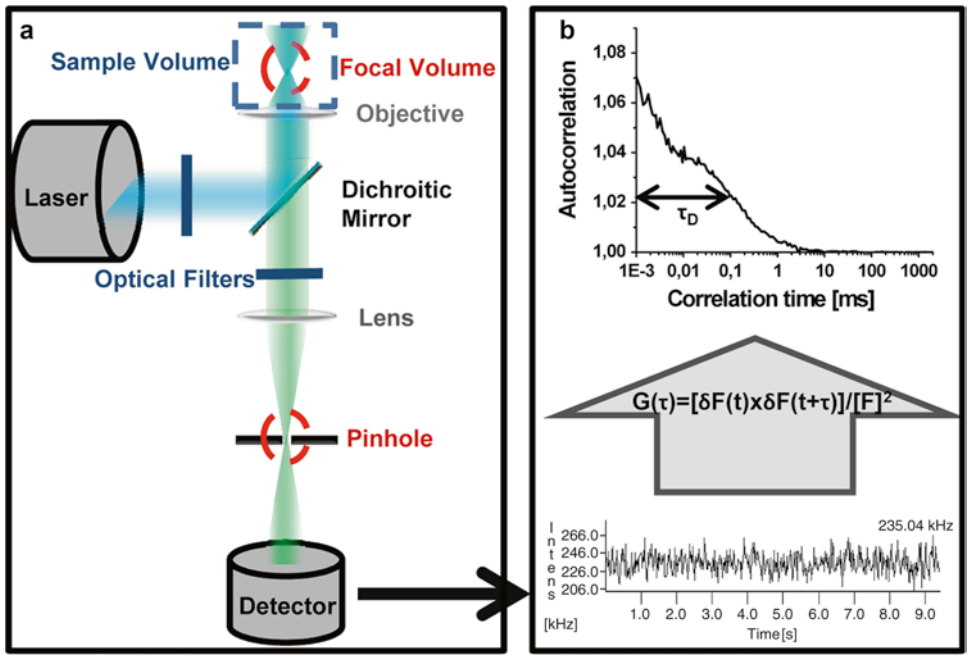


**Fig. 1** *Setup and output of FCS measurements*: (**a**) Schematic representation of an FCS setup. The *blue beam* represents excitation light coming from a laser, and the green beam fluorescence light emitted from the exited sample. (**b**) The time-dependent fluorescence intensity signal derived from the detector (*bottom*) and its subsequent analysis (*middle* and *top*). The value of the autocorrelation function *G* at correlation time $\tau$ computed via the equation is plotted against the correlation time (*top*). The *horizontal double arrow* represents the diffusion time $\tau_D$ of the molecule obtained by fitting the data to the corresponding model (*see* Fig. 2)

diffusion time (size and shape), and their changes during the course of the experiment. It thus also allows investigating the kinetics of interactions of the fluorescent species with fluorescent or non-fluorescent partners [3, 4].

Typical FCS setups use confocal microscopes with lasers as excitation sources and one or more detectors measuring the fluorescent intensity (Fig. 1a). This signal is directly processed in an electronic autocorrelator or, in more recent setups, single photons are recorded and the correlation is subsequently computed with dedicated software such as FCS ACCESS (Fig. 1b). FCS measurements require very low concentrations (from tenths of pM up to a few μM). This high sensitivity is advantageous for precious samples but has the disadvantage that the technique cannot be used for exploring low-affinity interactions.

FCS translational diffusion measurements are quite simple and well established. They allow to study the diffusive behavior of molecules in vitro and even inside the living cell, either in solution or within lipid membranes [5]. A necessary prerequisite is that the species of interest must be labeled using small fluorescent molecules such as DyLight, Alexa dyes, and fluorescein or fused to an appropriate autofluorescent molecule (e.g., GFP, YFP, mRFP).

The fluctuations in fluorescence originate from Brownian motion of the labeled analyte through a focal volume of some femtoliters that should not contain more than 100 analyte molecules. Their mean residence time within the laser-illuminated space depends on their diffusion coefficient, which, in turn, is a function of size and shape. If a small, fluorescent molecule binds a larger one it slows down (i.e., the diffusion coefficient of the complex is lower than that of its components) and emits photons for a longer time until it exits the observation volume; this results in an increase of the autocorrelation time.

Diffusion coefficient and sample concentration are obtained by fitting a theoretical model to the experimental autocorrelation curve. Several analytical expressions for theoretical autocorrelation curves are documented in the literature, such as for free diffusion of one or multiple fluorescent species through a 3D Gaussian focal volume [6]. These and other more widely used models are integrated in specialized software packages such as FCS ACCESS that accompanies the Zeiss Confocor 1 instrument. A theoretical autocorrelation curve for a single monodisperse species of fluorescent molecules diffusing in 3D space including the analytic form of the corresponding derived autocorrelation function is presented in Fig. 2.

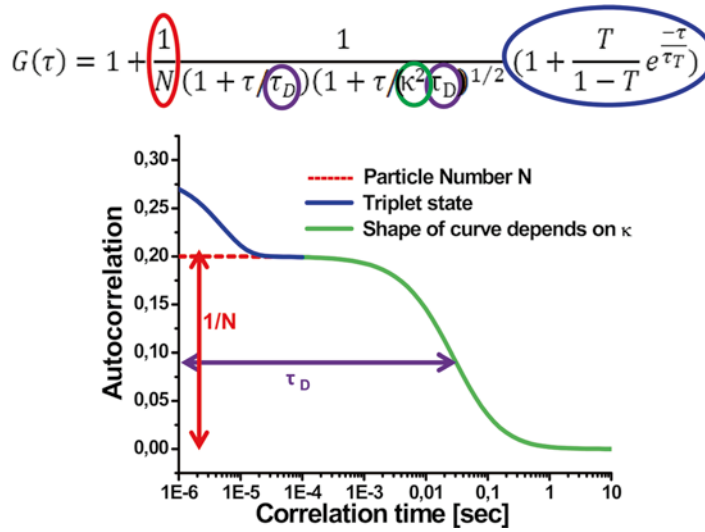


**Fig. 2** Fitting function (Eqs. (2) and (4) in Subheading 3.10, **step 1**) and the resulting theoretical autocorrelation curve: Correspondence between the parameters on *top* with parts of the curve is marked with same colors. Note that changes in the fraction of particles which are in the triplet state and the triplet lifetime will both impact on the appearance of the part of the curve representing the μs time regime (*blue*), while the part related to translational diffusion is in the range from $10^{-5}$ up to several 100 s (*green line*). The shape of the *green* part of the curve depends on the structural parameter (including the shape of the focal volume) and diffusion time $\tau_D$. Removing the part corresponding to the triplet state allows determining the number of particles in the observation volume as indicated with (1/*N*)

On infection, members of the family *Enteroviruses* first expand, lose VP4, and expose N-terminal sequences of VP1 but retain the genomic RNA, thus converting into subviral A-particles. Subsequently, the RNA exits, presumably initially as an unfolded single strand, and the A-particles are transformed into empty capsids (B-particles). In vitro, the conversion can be triggered by incubation at temperatures between 50 and 56 °C. In the following we show how FCS can be used to determine with which end (3′ or 5′) the RNA initiates egress from the HRV-2A virion. Our approach should be applicable without major modifications to a variety of other non-enveloped viruses with a single-stranded genome if uncoating can be similarly triggered in vitro via incubation at elevated temperature or changes of pH and/or ionic concentration.

Release of the viral genome is monitored as a function of time by hybridization of labeled oligonucleotides complementary to sequences of the viral RNA close to the 3′- and 5′-end, respectively. Being much smaller than the virion and the RNA, their diffusion time changes drastically following hybridization to exiting and to fully released genomic RNA present in different proportion over time after triggering uncoating [7]. Since RNA still connected to the virion and free RNA are themselves distinguishable by their diffusion coefficient, an appropriate theoretical model based on a three-component analysis (free oligonucleotide, oligonucleotide bound to exiting RNA, and oligonucleotide bound to free RNA) allows for determination of kinetics and directionality of genome egress.

We also describe how FCS can be used to quantitatively probe interactions between HRV-A2 and a soluble recombinant very-low-density lipoprotein (VLDL) receptor mimic demonstrating how affinity between a (large) virus and a (small) receptor can be monitored.

## 2 Materials

### 2.1 Reagents

1. HRV-A2 purified as described in Chapter 9 of this volume.
2. Recombinant concatemeric V33333 (a fusion of five copies of ligand-binding repeat 3 of the human VLDL receptor prepared as in ref. 8).
3. Plasmid pHRV2 for in vitro synthesis of infectious viral RNA. This is HRV-A2 cDNA under the control of a T7 RNA polymerase promoter in pBluescript II SK (+) [9].
4. Fluorescently labeled oligonucleotides complementary to the respective 3′-end and the 5′-end of HRV-A2:
   (a) 3′oligo: $dT_{25}$, FAM-labeled (complementary to nt 7,102 to ~7,200, the average size of the genomically encoded poly-A tract of HRV).

(b) 5′oligo: 5′-dAAGGGTTAAGGTTAGCCACATTCAG-3′, DyLight 488-labeled (complementary to nt 443–468 in HRV-A2 (*see* **Note 1**)).

5. Fluorescent dyes:
   (a) For FCS calibration: Rhodamine 6G.
   (b) For covalent labeling of proteins: DyLight 488 NHS ester, Cy3, Alexa (10 mg/ml in DMSO).
   (c) For non-covalent labeling of nucleic acids: YOYO-1 iodide 509 (from Life Technologies).
6. Hybridization buffer: 50 mM Tris–HCl, 75 mM KCl, 3 mM $MgCl_2$ (pH 8.3).
7. RNase buffer: Hybridization buffer containing 1 mM DTT (pH 8.3).
8. Acidification buffer: 50 mM sodium acetate (NaOAc) (pH 5.6).
9. TBSC buffer: 25 mM Tris–HCl, 150 mM NaCl, 2 mM $CaCl_2$ (pH 7.5).
10. Large-scale RNA production system—T7 (e.g., RiboMAX, Promega).
11. Enzymes and inhibitors: RNase A (10 mg/ml), RNase H (5 U/μl), RNasin (40 U/μl).

### 2.2 Equipment and Consumables

1. Nunc Lab-Tek chamber slides, eight wells, 0.2–0.4 ml, 0.8 $cm^2$.
2. Spin-X Centrifuge Tube Filter, 0.45 μm pore cellulose acetate (CA) membrane.
3. Dialysis membrane with MWCO 6–8 kDa.
4. Sephadex G100.
5. Superdex™ 75 HR 10/30, pre-packed high-resolution gel filtration column, 10 mm diameter and 30 cm height (GE Healthcare).
6. Zeiss Confocor 1 spectrofluorometer (Carl Zeiss, Germany) equipped with a Zeiss water immersion objective (C-Apochromat 63×/1.2 W Korr), an avalanche photodiode (SPCM-CD 3017), and a hardware autocorrelator (ALV 5000, AVL, Langen, Germany).
7. An argon-ion laser attenuated by optical density filters.
8. A helium–neon laser attenuated by optical density filters.
9. A dichroic mirror (580 nm) with a long-pass filter (590 nm).
10. FCS ACCESS software package.
11. Heating block.

## 3 Methods

### 3.1 Fluorescence Labeling of Virus Capsid

1. Label purified rhinovirus (5 pmol) with the amino-reactive dye DyLight 488 as described in the protocol of the manufacturer (http://www.piercenet.com/instructions/2161963.pdf).
2. Remove excess of unreacted dye by size-exclusion chromatography using a Sephadex G100 column (all steps are done at room temperature): Pour 500 μl G100 gel in hybridization buffer into the filter unit inside the 500 μl polypropylene microcentrifuge tube of a Spin-X Centrifuge Tube Filter and centrifuge at 800 rpm in a microfuge for 30 s.
3. Add another 500 μl G100 gel and centrifuge at 380×*g* in a microfuge for 1 min.
4. Centrifuge this assembly finally at (850×*g*) in a microfuge for 1 min.
5. Transfer the spin column into a new microcentrifuge tube, apply 20 μl of the sample, and centrifuge at 850×*g* in a microfuge for 1 min; again change the microcentrifuge tube.
6. Add 30 μl hybridization buffer and repeat centrifugation as in **step 4**.
7. Remove the column and save the flow-through containing the purified HRV.
8. Purity of the virus and absence of free dye may be checked by capillary electrophoresis with fluorescence detection ([10], *see* also Weiss et al., Chapter 9). For the determination of the diffusion coefficient of HRV at least 50 μl virus at 20 nM is necessary.

### 3.2 Fluorescent Labeling of Viral RNA

1. Produce viral RNA in vitro as a runoff transcript from the plasmid pHRV2 [9]. First, cleave the plasmid with Kpn*I* just behind the poly-A tail at the 3′-end of the RNA (leaving one additional guanine residue) and transcribe using the large-scale RNA production system—T7 according to the manufacturer's recommendations.
2. Extract the RNA with phenol-chloroform followed by ethanol precipitation.
3. Mix RNA (~10 nM) with YOYO-1 iodide 509 dye at a ratio of approximately 5 base pairs per dye molecule (i.e., 4 μM for the ~7,200 nt long HRV-A2 RNA) in at least 50 μl total volume with hybridization buffer and incubate at room temperature for 15 min. Since YOYO-1 iodide 509 fluoresces only after binding to nucleic acids [11], no further purification of labeled RNA is required.

### 3.3 Fluorescent Labeling of the V33333 Concatemer

1. Label V33333 receptor protein (about 2.5 μg is required for the whole experiment; *see* **Notes 2** and **3**) with DyLight Amine-Reactive Fluor 488 according to the protocol provided

by the manufacturer. Alternatively, label with Cy3 as in ref. 8. Since the protein does not contain lysines, the maximum number of dye molecules incorporated per protein molecule is one (at the N-terminus; *see* **Note 4**).

2. Remove free dye by extensive dialysis against TBSC at 4 °C using a membrane with MWCO 6–8 kDa.
3. Optionally, following **step 2** the labeled receptor can be further purified by size-exclusion chromatography through a Superdex 75 column. The labeled receptor can be stored at 4 °C for about a week without loss of activity.

### 3.4 Determination of the Diffusion Coefficient of the Separate Components

Pilot FCS experiments with individual analytes (labeled virus, labeled viral RNA, labeled recombinant receptor or oligonucleotide) need to be carried out to determine the concentration, i.e., optimal average number of fluorophores inside the observation volume giving the highest average intensity fluctuation amplitude. These "best" concentrations are then used for measuring the respective diffusion time for each component tested separately. The diffusion coefficients can then be determined (according to Subheadings 3.8–3.10). In our specific configuration of laser intensities, pinhole sizes, and buffer composition, the concentrations found optimal are given below (*see* **Note 5**). These measurements were carried out with 20 µl samples placed in Nunc Lab-Tek chamber slides.

- DyLight 488-labeled HRV-A2 (10 nM) in hybridization buffer.
- YOYO-1 iodide 509-labeled RNA (10 nM) in hybridization buffer.
- DyLight 488/FAM-labeled oligonucleotides (10 nM) in hybridization buffer; alternatively in 50 mM Tris–HCl, pH 8.3, or in RNase buffer.
- Recombinant V33333 receptor (50 nM) in TBSC buffer.

### 3.5 Identification of the Optimal Ratio of Oligonucleotide to Viral RNA

This titration experiment aims at determining the lowest concentration of the unlabeled binding partner which results in >50 % of the fluorescent component in the complex. This is done via adding increasing concentrations of in vitro-transcribed RNA to a constant concentration of free oligonucleotide (10 nM, *see* above).

1. Mix 10 µl aliquots of the labeled oligonucleotide at 20 nM with 10 µl of serial dilutions (in hybridization buffer) of in vitro-transcribed viral RNA giving final concentrations of between 0 and 1,000 nM.
2. Allow for hybridization by incubating the mixture for 10 min at 56 °C and for at least 30 s at 4 °C prior to the measurements.
3. Identify the minimum ratio of oligonucleotide to RNA giving an optimal hybridization signal as defined above. Subsequently,

use this ratio when mixing oligonucleotides with virus in RNA release kinetics measurements (Subheading 3.6).

4. To confirm that the observed change of the diffusion coefficient in the presence of viral RNA is due to hybridization, treat the sample with a mixture of RNase A (1 mg/ml final concentration) and RNase H (0.5 U/μg RNA) for 15 min in RNase buffer at 37 °C prior to the FCS measurement. Typical autocorrelation curves of free and RNA-bound oligonucleotides as well as curves derived after digestion with the RNase mixture are presented in Fig. 3 [7].

### 3.6 Determination of RNA Release Kinetics

1. Based on the optimal ratio between oligonucleotide and viral RNA established according to the previous section, mix purified (unlabeled) rhinovirus with the respective labeled oligonucleotide in hybridization buffer (in our hands final concentrations of 250 nM and 10 nM, respectively, proved best). On complete release from the capsid, the RNA concentration would thus be the same as in the experiment with in vitro-transcribed RNA.
2. Add 2 U RNasin/μl to prevent RNA degradation.
3. Initiate viral RNA release by incubating at 56 °C (*see* **Note 6**). Take aliquots (20 μl) at regular time intervals following the heat trigger, e.g., every 2–5 min as it is demonstrated in Fig. 4.
4. Alternatively, RNA release (of HRV-A2 and presumably all other minor group viruses; *see* **Note 6**) can be initiated by decreasing the pH of the sample; instead of heating, combine the mixture with a 1.5-fold volume of acidification buffer, mix, and incubate at the desired temperature. Take aliquots (10 μl) as above and re-neutralize by mixing with 10 μl 100 mM borate buffer pH 8.3 or 100 mM Tris buffer pH 8.2 (*see* **Notes 7** and **8**).
5. Transfer samples to a chamber slide and carry out FCS measurement and data analysis as described in Subheadings 3.8–3.10.
6. Calculate percentages of free oligonucleotide, oligonucleotide bound to RNA, and oligonucleotide bound to virus via partially released RNA with the FCS ACCESS software by using the three-component fit model and the diffusion coefficients previously determined for each individual component as is described in the data analysis section (Subheading 3.10, **steps 1–3**).

### 3.7 Receptor–Virus Interaction

FCS is particularly suitable for rapid determination of the association constant of a virus binding to an antibody or cognate soluble receptor including the stoichiometry of the assembled complex(es) and the kinetics of complex formation. Due to its high sensitivity, it consumes only minute amounts of material. The only limitations are the necessity of a difference of the diffusion coefficient of the components by at least 1.6 times [12] and a dissociation constant lower

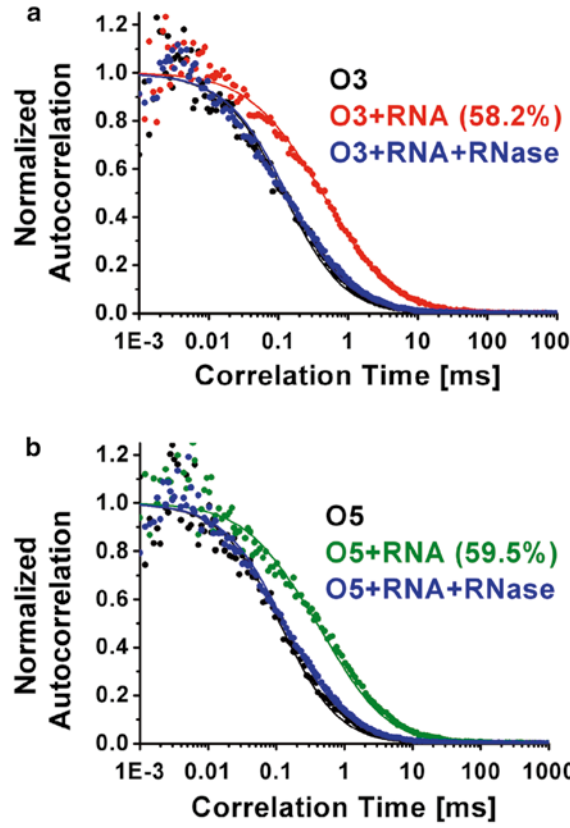


**Fig. 3** Autocorrelation curves for viral RNA and oligonucleotides obtained by fluorescence correlation spectroscopy, normalized and corrected for the triplet state: The respective oligonucleotides *black, (***a***) 3′-end specific, (***b***) 5′-end specific, were* separately hybridized to in vitro-transcribed viral RNA and FCS measurements conducted before (*red* and *green*, respectively) and after digestion with RNase A/RNase H (*blue*), respectively. *Dots*, measured data; continuous lines, one-component (*black lines*) and two-component fit (*red and green lines*; contribution of the second component calculated from the fit is given in %). Note the complete overlap of the curves corresponding to the free oligonucleotides and to the RNase-digested samples. Similar experiments using a concentration series of RNA revealed that at least a 25-fold excess (i.e., 250 nM) of heated virus or in vitro-transcribed RNA over oligonucleotide was required for a detectible hybridization. Modified from Harutyunyan et al. 2013 [7], with permission from PLOS, published under the Creative Commons Attribution License (CC-BY), http://creativecommons.org/licenses/by/3.0/

than mmolar. In FCS measurements of rhinovirus-receptor association we use Cy3- or DyLight 488-labeled recombinant receptor. However, the smaller component (be it receptor or ligand; *see* **Note 9**) can be labeled with any other dye with excitation/emission wavelengths compatible with the filter set of the particular instrument used for FCS analysis. In the following we specify the steps for titration of a constant amount of fluorescently labeled

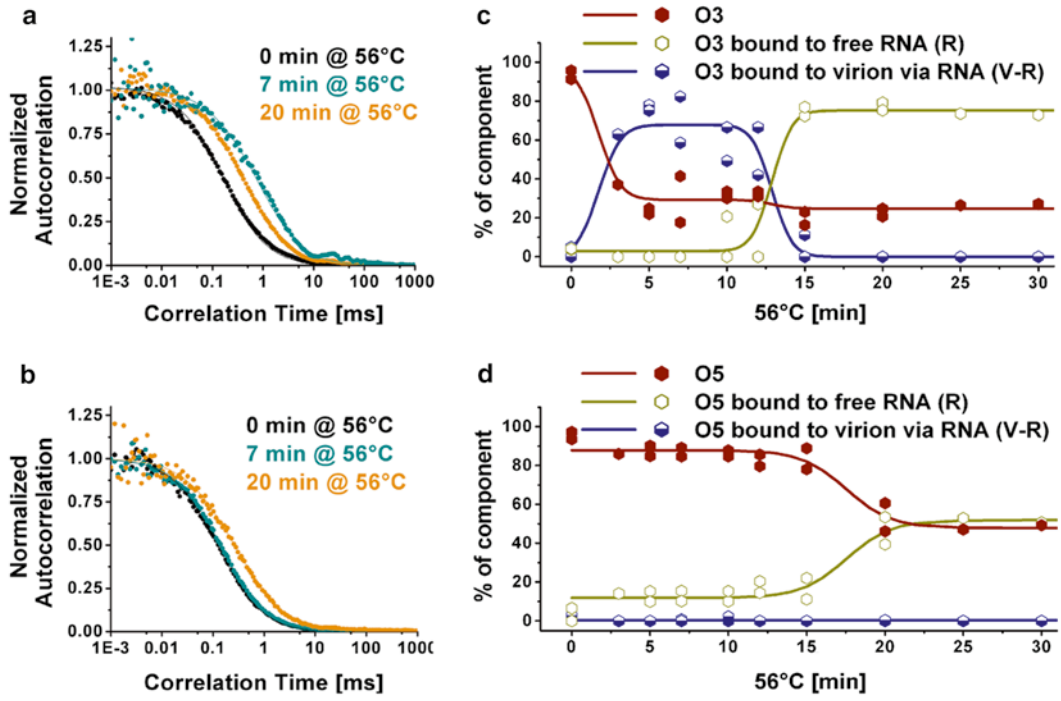


**Fig. 4** RNA sequences at the 3′- and the 5′-ends become accessible for hybridization with different kinetics: HRV2 was incubated at 56 °C for 0, 7, and 20 min. Dylight 488-labeled oligonucleotide specific for 3′ sequences (**a**) and 5′ sequences (**b**) was added and the autocorrelation function was measured. (**c**, **d**) Identical experiments were carried out but with additional time points. The percentage of free oligonucleotide (*red*), oligonucleotide hybridized to free RNA (*ochre*), and oligonucleotide hybridized to RNA connected to the virus (*blue*) was calculated for each time point by employing a three-component fitting procedure (*symbols*). For better appreciation, the respective values for each constituent (free oligo, oligo bound to RNA, and oligo bound to RNA partially extruded from the virion) were fit by a sum of Boltzmann functions (*lines*). Data points are from two independent experiments. Note that separate experiments showed the same trend over time, but there were differences in background and in the absolute values of the measurements. Reproduced from Harutyunyan et al. 2013 [7], with permission from PLOS, published under the Creative Commons Attribution License (CC-BY), http://creativecommons.org/licenses/by/3.0/

V33333 receptor with unlabeled HRV-A2 as ligand resulting in autocorrelation curves suitable for extraction of binding parameters.

1. Mix labeled V33333 at 50 nM final concentration in TBSC with graded amounts of HRV-A2 at concentrations between 2 pM and 5 μM in TBSC buffer.
2. Incubate the mixtures for 5 min at room temperature or for 30 min at 4 °C.
3. Transfer samples (25 μl) to 8-well chamber slides and carry out FCS measurement as described in Subheadings 3.8 and 3.9.
4. Calculate the translational diffusion times, percentages of the components (free receptor and virus-bound receptor), and binding parameters with the FCS ACCESS software as covered in Subheading 3.10, **steps 3** and **4**.

### 3.8 FCS Setup

1. All FCS measurements were carried out in a Confocor 1 spectrofluorometer.
2. For FITC-, FAM-, or DyLight 488-labeled HRV-A2, oligonucleotides as well as YOYO-1 iodide 509-labeled RNA use an argon-ion laser attenuated by optical density filters. Select the 488 nm line with a 450–490 nm excitation filter. Fluorescence emission of the corresponding labeled molecules/particles is directed through a dichroic mirror (510 nm) followed by a long-pass filter (515 nm) towards the detector.
3. Cy3-labeled receptor fragments are excited at 543.5 nm with a helium–neon laser attenuated by optical density filters. Fluorescence emission of the corresponding labeled molecules/particles is directed towards the detector through a dichroic mirror (580 nm) followed by a long-pass filter (590 nm).
4. Prior to each set of measurements perform at least ten calibrations of 10 s each using rhodamine 6G (or rhodamine-B, depending on the setup used) as standard with known diffusion coefficient ($D_{Rh6G} = 2.8 \times 10^{-10}$ $m^2s^{-1}$) to determine the size of the confocal volume (described further below in Subheading 3.10, **step 2**). This is mainly needed to calculate the diffusion coefficient of each sample from the measured diffusion time.
5. Adjust the focus of the microscope 150 μm above the upper side of the slide prior to all measurements to avoid optical surface effects. A scheme of a generic FCS setup and the characteristic output signal are presented in Fig. 1.

### 3.9 FCS Measurements

1. 10–50 consecutive measurements (10 s each) on at least three independently prepared samples need to be done to obtain statistically relevant values, with the respective fluorescent analytes at 10–50 nM (i.e., the concentration previously seen to give the highest intensity fluctuation, *see* Subheading 3.4) in the corresponding buffer.
2. Determine the fluorescence autocorrelation function for the respective fluorescent analytes—labeled oligonucleotides complementary to the different parts of HRV-A2 RNA, labeled virus, labeled receptor, labeled viral RNA, and labeled oligonucleotides hybridized to partially released and free genomic RNA, respectively, in the samples prepared according to the previous sections.
3. For visual comparison, normalize the autocorrelation functions to 1 at autocorrelation time zero (i.e., the corresponding autocorrelation function of one particle in the observation volume, *see* below).

### 3.10 Data Analysis

1. Autocorrelation function and calculation of diffusion times: The autocorrelation function $G(\tau)$ is used to determine fluctuation around the average fluorescence intensity:

$$G(\tau) = 1 + \langle \delta F(t) \cdot \delta F(t+\tau) \rangle / \langle F(t) \rangle^2 \quad (1)$$

where $F$ is fluorescence intensity, $\delta F$ is fluorescence intensity fluctuation from mean, $t$ is time, $\tau$ is correlation time, and angular brackets denote the time average. This equation correlates fluorescence at time $t$ with fluorescence at time $t+\tau$ [4]. The function depends on the geometric properties of the observation volume and several physical parameters such as concentration and diffusion coefficient of fluorescent species in the sample. We use the following simple equation based on a 3D Gaussian focal volume and freely diffusing molecules in all of our FCS experiments:

$$G(\tau) = 1 + g(\tau) \quad and \quad g(\tau) = \frac{1}{N} \frac{1}{\left((1+\tau)/\tau_D\right)\left((1+\tau)/\kappa^2\tau_D\right)^{1/2}} \quad (2)$$

where $N$ is the mean number of fluorescent particles in the focal volume, $g(\tau)$ is the correlation function, $\kappa = \omega_z/\omega_{xy}$ is the structural parameter (axial ratio of the focus; $\omega_z$ and $\omega_{xy}$ are axial and radial dimensions of the focal volume), and $\tau_D$ is the average diffusion time a particle needs to pass the focal volume, which is inversely related to the diffusion coefficient ($D$):

$$\tau_D = \frac{\omega_{xy}^2}{4D} \quad (3)$$

For a more detailed analysis, the autocorrelation function can be constructed using the translational and rotational diffusion of the particles as well as the fraction and time the particles stay in the triplet state and several other physical properties. Taking into account the triplet state and the photon detector afterpulsing, which are both in the μs regime, the model can be fitted using the autocorrelation function:

$$G(\tau) = 1 + g(\tau) \cdot \left(1 + \frac{T}{1-T} e^{\frac{-\tau}{\tau_T}}\right) \quad (4)$$

where $T$ is the fraction of particles in the triplet state, and $\tau_T$ is the triplet lifetime.

Calculate the diffusion times (optionally $T$ and $\tau_T$) of fluorescent species using the one- or the multicomponent fit model implemented in the software as described further below. For easier visual comparison the part of the curve at very short correlation times including the triplet state might be removed (using

Eq. (4), $T$ and $\tau_T$ obtained from fitting) and the data can be normalized to 1 at correlation time 0 (by multiplying $(G(\tau)-1)$ by the mean of the particles in the observation volume).

2. *Determination of the sample concentration.* Determine the concentration of a fluorescently labeled molecule from the autocorrelation curve obtained at an appropriate dilution by FCS. Use rhodamine 6G (Rh6G) with known diffusion coefficient ($D_{\mathrm{Rh6G}} = 2.8 \times 10^{-10}$ m$^2$ s$^{-1}$) for the calibration of the instrument and determine $\omega_{xy}$, the half short axis of the measurement volume at $x$ and $y$ dimensions, using Eq. (3).
From the measured $\omega_{xy}$ and using the known structural parameter ($\kappa$), which only depends on the instrument used, the effective volume can be derived (in our particular setup $\kappa = 5$):

$$V_{\mathrm{eff}} = \omega_{xy}^2 \cdot \pi^{3/2} \cdot \omega_z = \pi^{3/2} \cdot \kappa \cdot \omega_{xy}^3 \tag{5}$$

Finally, determine the concentration $c$, using the experimentally measured mean number of fluorescent particles and $N_{\mathrm{A}} = 6{,}022 \times 10^{23}$ mol$^{-1}$:

$$c = \frac{N}{N_{\mathrm{A}} \cdot V_{\mathrm{eff}}} \tag{6}$$

3. *Multicomponent fit models.* So far, we have considered only single-component systems. For the case of two or more distinct fluorescent particles with different diffusion coefficients but similar brightness a multicomponent fit model is required for data analysis. The corresponding autocorrelation function for multiple components has the form

$$g(t) = \frac{1}{N} \sum_{i=1}^{M} \frac{f_i}{\left((1+t)/\tau_{\mathrm{D}i}\right)\left((1+t)/\kappa^2\tau_{\mathrm{D}i}\right)^{1/2}} \tag{7}$$

where $N$ is the total number of fluorescent particles, $f_i$ the fraction of each component present at equilibrium and $\tau_{\mathrm{D}i}$ the respective diffusion coefficients, $\kappa$ the structural parameter, and $M$ the number of distinct components. In the FCS experiments described here the components range from $M = 1$ to $M = 3$.

Using Eq. (7) and employing the diffusion times previously determined for the separate components, calculate the fraction ($f_i$) of each component for the given times of incubation (*see* **Note 10**). All of this is implemented in the FCS ACCESS software. In instances of multiple components in solution and for proper and statistically significant multicomponent analysis one usually performs 5–15-min measurements. For instruments equipped with a hardware autocorrelator like the one described

here it is, however, highly recommended to perform 30–50 separate measurements of 10–20 s each for every sample and average the autocorrelation curves before starting the multi-component analysis. This allows exclusion of measurements with obvious aggregate formation (*see* **Note 11**).

4. *Average diffusion time fitting to estimate receptor-virus binding affinity*. To calculate the $K_D$ and to characterize the binding behavior (monophasic or biphasic), fit each FCS measurement of the titration to a single-component model with a corresponding mean diffusion time $\tau_D$. Theoretical models taking into account the concentrations of receptor ($c_R$) and ligand (e.g., virus, $c_V$), the diffusion times of free receptor ($\tau_R$) and of receptor-ligand complex ($\tau_{RV1}$, $\tau_{RV2}$), and the dissociation constants ($K_{D1}$, $K_{D2}$) for either mono (index 1) or biphasic (index 2) binding behavior then need to be used to fit the mean diffusion time versus the ligand concentration to the corresponding parameters:

$$\tau_D = \tau_R + (\tau_{RV1} - \tau_R)\frac{\alpha - \sqrt{\alpha^2 - 4c_V c_R}}{2c_R} \tag{8}$$

$$\tau_D = \tau_R + (\tau_{RV1} - \tau_R)\frac{\alpha - \sqrt{\alpha^2 - 4c_V c_R}}{2c_R} + \frac{(\tau_{RV2} - \tau_{RV1})\left(\beta - \sqrt{\beta^2 - 4c_V c_R}\right)}{2c_R} \tag{9}$$

$$\alpha = c_V + c_R + K_{D1} \tag{10}$$

$$\beta = c_V + c_R + K_{D2} \tag{11}$$

Perform Marquardt nonlinear least square fitting using nonlinear curve fitting software (for instance Origin, Microcal), while fixing the known parameters ($c_R$, $c_V$, $\tau_R$) generates the sought-after parameters ($K_{D1}$, $K_{D2}$, $\tau_{RV1}$, $\tau_{RV2}$) [12]. Calculate the free energy of binding $\Delta G_B$ by using the standard van't Hoff equation, which relates it to the dissociation constant $K_D$:

$$\Delta G_B = -RT \cdot \ln K_D \tag{12}$$

## 4 Notes

1. The 5′-specific oligonucleotide was selected for hybridization to the genomic RNA on the basis of complementarity to a region of low secondary structure and thus accessibility, as predicted by the Vienna RNA package version 1.8 (http://rna.tbi.univie.ac.at/cgi-bin/RNAfold.cgi).

2. The pentameric concatemer of the cysteine-rich class A ligand-binding repeat 3 (V3) of the very-low-density lipoprotein (VLDL) receptor fused to maltose-binding protein (MBP) has a high affinity to HRV-A2 exceeding that of the natural soluble VLDL receptor domain. For other viruses any other cognate soluble receptor that can be made fluorescent might be used.
3. Efficiency of labeling of V33333 with DyLight 488 is low. Therefore, modifications of the protocol of the manufacturer may be necessary to increase the yield; for instance, longer incubation time or a higher dye:receptor ratio may help.
4. The MBP moiety should be cleaved off with factor Xa prior to labeling; the cognate protease cleavage site is precisely localized between the MBP and the authentic N-terminus of the V33333 fusion protein. MBP has 36 lysine residues, which can lead to heterogeneous fluorescent labeling of the recombinant molecules carrying this fusion tag. Additionally, attachment of many hydrophobic dye molecules per receptor molecule increases the overall hydrophobicity resulting in undesired precipitation at higher concentrations. The recombinant V33333 fragment itself does not contain lysine residues; thus labeling takes place only at the N-terminus; therefore brightness is uniform. When using intact MBP-V33333 or other receptors, the number of dye molecules incorporated into one protein molecule has to be determined spectroscopically to allow proper evaluation of the derived FCS autocorrelation curves.
5. Depending on the buffer composition the sample can have different viscosities, which will influence the diffusion properties of the analyte(s). We indeed observed small but significant changes of the diffusion coefficient of oligonucleotides and viral RNA when the measurements were done in hybridization buffer versus RNase buffer. It is strongly recommended to take this into account when comparing measurements in different buffers by initial exploratory experiments such as those mentioned above.
6. This applies specifically to HRV-A2; other (rhino)viruses may require different conditions for in vitro uncoating.
7. Because of acidification and re-neutralization the sample will be finally diluted fivefold; to maintain hybridization efficiency, increase the initial concentration of the oligonucleotide to 30 nM and also add three times more virus at the beginning (Subheading 3.6, **step 1**).

**Table 1**
**Measured diffusion time and molecular brightness for DyLight 488 free in solution and after conjugation to an oligonucleotide, as well as FAM-conjugated oligonucleotide in different buffers**

| | Buffer used | Diffusion time (ms) | Molecular brightness |
|---|---|---|---|
| *DyLight488* | 50 mM NaOAc, pH 5.4 | 0.036 ± 0.002 | 25.85 ± 0.290 |
| | bb-re., pH 7.5 | 0.035 ± 0.002 | 28.41 ± 0.198 |
| | 100 mM Borate buffer, pH 8.2 | 0.035 ± 0.001 | 30.12 ± 0.153 |
| *DyLight488-oligonucleotide* | 50 mM NaOAc, pH 5.4 | 0.11 ± 0.023 | 0.74 ± 0.016 |
| | bb-re., pH 7.5 | 0.12 ± 0.006 | 8.28 ± 0.057 |
| | 100 mM Borate buffer, pH 8.2 | 0.12 ± 0.009 | 8.48 ± 0.054 |
| *FAM-oligonucleotide* | 50 mM NaOAc, pH 5.4 | 0.12 ± 0.017 | 0.63 ± 0.018 |
| | bb-re., pH 7.5 | 0.13 ± 0.009 | 8.41 ± 0.059 |
| | 100 mM Borate buffer, pH 8.2 | 0.13 ± 0.008 | 8.52 ± 0.056 |

"bb-re." sample was incubated in 50 mM NaOAc buffer (pH 5.4) for 15 min. Subsequently, it was brought to pH 7.5 by using 100 mM borate buffer (pH 8.3)

8. We observed that attachment of the fluorescent dye to an oligonucleotide diminishes its fluorescence intensity when compared to the free dye. Additionally, its fluorescence becomes more sensitive to the respective buffer composition. As can be seen in Table 1, there is a significant decrease of the measured molecular brightness of DyLight 488 and FAM (not shown) after conjugation to an oligonucleotide and fluorescence becomes almost undetectable in acidic buffer. Nevertheless, on subsequent re-neutralization fluorescence is recovered.
9. When studying interaction, in order to detect a change in diffusion coefficient, always label the smaller component.
10. For simplification we here approximate the diffusion coefficient of oligonucleotide bound to virus (via partially released RNA) by that of the virus alone in the three-component fit model. This is necessary because subviral particles with partly externalized RNA cannot be obtained as a homogenous population.
11. The occasional presence of some aggregates or dust particles in the sample characteristically causes sudden, huge jumps in the amplitude of the fluorescent intensity. We fully exclude autocorrelation curves derived from such events from further analysis to avoid corrupting our results by erroneous data. An example of such an event is presented in Fig. 5.

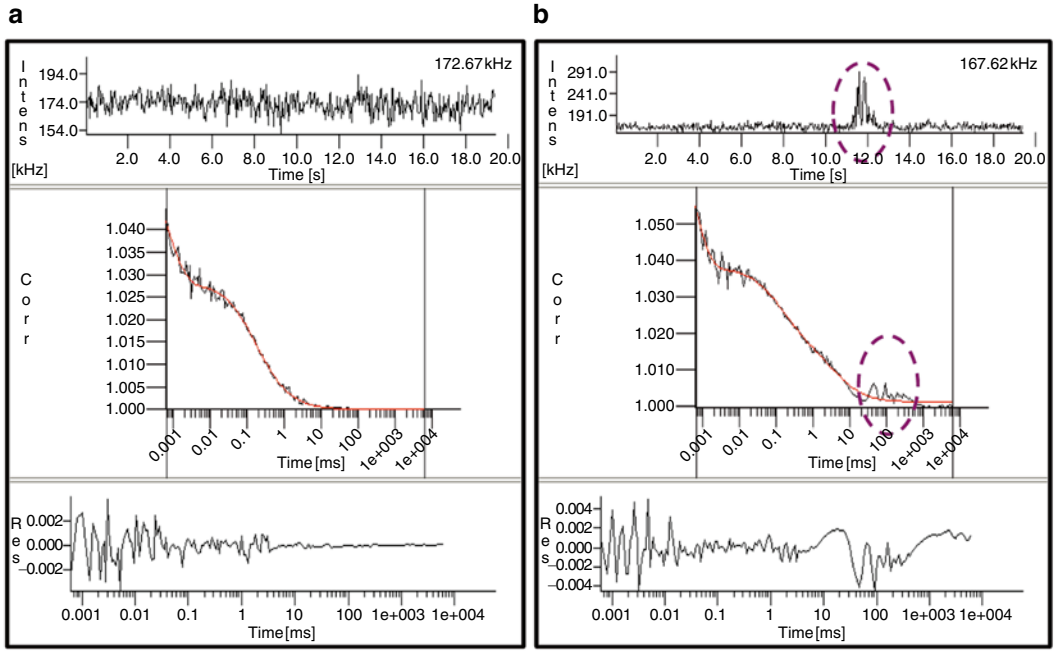


**Fig. 5** Snapshot of output from the FCS ACCESS program of a measurement like in Fig. 3a without (**a**) or with (**b**) formation of viral aggregates: *Upper panel* represents the fluctuation in fluorescence intensity over measurement time. *Middle panel* represents experimental autocorrelation curve (*black*), with fitted curve (*red*). *Bottom panel* represents the dependence between fitting margin (residual; Res) and correlation time. One-component fit model was used. Note the appearance of an aggregate at about 12 s. Such aggregates introduce irregularities in the autocorrelation curve at about 30–300 ms (jagged line enclosed by the ellipse)

## References


1. Magde D, Elson EL, Webb WW (1974) Fluorescence correlation spectroscopy. II. An experimental realization. Biopolymers 13:29–61
2. Rigler R, Widengren J (1990) Ultrasensitive detection of single molecules by fluorescence correlation spectroscopy. Bioscience 3:180–183
3. Haustein E (2007) Fluorescence correlation spectroscopy: novel variations of an established technique. Annu Rev Biophys Biomol Struct 36:151–169
4. Gosch M, Rigler R (2005) Fluorescence correlation spectroscopy of molecular motions and kinetics. Adv Drug Deliv Rev 57:169–190
5. Krieger J, Tódt K, Langowski J. "Biophysics of Macromolecules (B040): Practical Course Biophysics: Fluorescence Correlation Spectroscopy" http://www.dkfz.de/Macromol/teaching/files/fcs_practical.pdf
6. Krichevsky O, Bonnet G (2002) Fluorescence correlation spectroscopy: the technique and its applications. Rep Prog Phys 65:251–289
7. Harutyunyan S, Kumar M, Sedivy A et al (2013) Viral uncoating is directional: exit of the genomic RNA in a common cold virus starts with the poly-(A) tail at the 3′-end. PLoS Pathog 9:e1003270. doi:10.1371/journal.ppat.1003270
8. Wruss J, Rünzler D, Steiger C et al (2007) Attachment of VLDL receptors to an icosahedral virus along the 5-fold symmetry axis: Multiple binding modes evidenced by fluorescence correlation spectroscopy. Biochemistry 46:6331–6339
9. Duechler M, Skern T, Blaas D et al (1989) Human rhinovirus serotype 2: in vitro synthesis of an infectious RNA. Virology 168:159–161

10. Kremser L, Konecsni T, Blaas D et al (2004) Fluorescence labeling of human rhinovirus capsid and analysis by capillary electrophoresis. Anal Chem 76:4175–4181
11. Rye HS, Yue S, Wemmer DE et al (1992) Stable fluorescent complexes of double-stranded DNA with bis-intercalating asymmetric cyanine dyes: properties and applications. Nucleic Acids Res 20:2803–2812
12. Meseth UWT, Rigler R, Vogel H (1999) Resolution of fluorescence correlation measurements. Biophys J 76:1619–1631

# Chapter 9

# Capillary Electrophoresis, Gas-Phase Electrophoretic Mobility Molecular Analysis, and Electron Microscopy: Effective Tools for Quality Assessment and Basic Rhinovirus Research

**Victor U. Weiss, Xavier Subirats, Mohit Kumar, Shushan Harutyunyan, Irene Gösler, Heinrich Kowalski, and Dieter Blaas**

## Abstract

We describe standard methods for propagation, purification, quality control, and physicochemical characterization of human rhinoviruses, using HRV-A2 as an example. Virus is propagated in HeLa-OHIO cells grown in suspension culture and purified via sucrose density gradient centrifugation. Purity and homogeneity of the preparations are assessed with SDS-polyacrylamide gel electrophoresis (SDS-PAGE), capillary electrophoresis (CE), gas-phase electrophoretic mobility molecular analysis (GEMMA), and electron microscopy (EM). We also briefly describe usage of these methods for the characterization of subviral particles as well as for the analysis of their complexes with antibodies and soluble recombinant receptor mimics.

**Key words** Rhinovirus, Purification, Analysis, Capillary electrophoresis, Gas-phase electrophoretic mobility molecular analysis, Electron microscopy

## 1 Introduction

### *1.1 Nomenclature, Classification, and Biology of Rhinoviruses*

Human rhinoviruses belong to the genus *Enteroviruses* within the large family of *Picornaviridae* [1]. Their ss(+)RNA genome of about 7,200 nucleotides is surrounded by an icosahedral capsid, about 30 nm in diameter, and assembled from 60 copies each of the four viral proteins, VP1–VP4. So far, more than 160 HRV types have been classified using genetic divergence thresholds for type assignment [2]; they are divided into species A, B, and C [3]. HRV have also been classified according to receptor usage; twelve HRV-A (the minor group) bind members of the low-density lipoprotein receptor family, and the remaining HRV-A and -B types (the major group) recognize intercellular adhesion molecule 1 (ICAM-1) [4]. The HRV-C receptor(s) is unknown and not

David A. Jans and Reena Ghildyal (eds.), *Rhinoviruses: Methods and Protocols*, Methods in Molecular Biology, vol. 1221, DOI 10.1007/978-1-4939-1571-2_9, 

expressed in the cultured cells examined so far; only nasal mucosa tissue explants transiently sustain HRV-C replication. Production of virus on transfection of cells with full-length in vitro-transcribed viral RNA has been reported [5].

Infection starts with attachment of HRV to its cognate receptor(s) on the surface of the host cell, followed by endocytosis and uncoating of the RNA whose transfer from endosomes into the cytosol initiates production of progeny that are released by cell lysis and/or autophagy-related mechanisms.

RNA exit from the native virus particle (sedimenting at 150S) is preceded by conformational changes resulting in the formation of the A-particle, an uncoating intermediate sedimenting at 135S, which has lost the internal VP4. Upon final egress of the RNA genome, the B-particle (the empty shell sedimenting at 80S) remains [4]. Very similar, if not identical, subviral particles are produced in vitro either by incubation between 50 and 56 °C for different times or at acidic pH [6, 7]. This has allowed their detailed structural characterization [8, 9] and recently revealed the directionality of RNA release [10] (*see* also Harutyunyan et al., Chapter 8). The structural and functional characterization of such particles requires considerably pure viral preparations. We present a robust purification scheme and sensitive bioanalytical and biophysical methods to assess virus integrity and purity. As exemplified below, these methods have also proven highly effective in quantitation of virus-antibody and virus-receptor binding and in the analysis of virus uncoating.

### 1.2 Medium-Scale Growth and Purification of Human Rhinovirus

In Subheading 3.1 we present a protocol for routine preparation of virus (yielding 1–5 mg/ml; note that about 70 % of the total mass is protein and 30 % is RNA) of sufficient purity for most structural and functional studies. HRV-A2 is grown in HeLa cell suspension culture, virus progeny is released by cell disruption prior to virus-caused cell lysis, the virus is separated from cell debris by differential centrifugation, and contaminating nucleic acids and proteins are digested. This crude preparation is finally subjected to sucrose density gradient ultracentrifugation and pelleting. We have used essentially the same protocol for the production of several other serotypes although with frequently lower yield; HRV strains differ considerably with respect to growth in suspension [11] and some might give higher yields in monolayer cultures. Therefore, the suitability of suspended cells for viral propagation has to be assessed in pilot experiments before upscaling. To date all attempts at growing HRV-C in HeLa cells (and in various other cells) have failed; therefore, HRV-C cannot be produced by following the procedure below.

The purity of the virus preparation is routinely verified by SDS-PAGE separating the four capsid proteins, VP1–VP4. Dependent on the HRV type, all or at least two of these proteins can be

resolved by standard SDS-PAGE. The precursor VP0, which is cleaved on virus maturation into VP4 and VP2, may also be detected. It either stems from native empty capsids (NEC), also called natural top component [12], or from small amounts of native virus that contains several copies of VP0. The proportion of VP0 might vary considerably depending on the preparation. An example of the proteins from purified HRV-A2 separated on a 12 % SDS-polyacrylamide gel is given in Fig. 1a, upper panel. VP4 is often not seen on these gels because of its small size (~7.4 kDa in comparison to VP1, ~32.9 kDa; VP2, ~29.0 kDa; and VP3, ~26.1 kDa) and/or the associated weak staining. When virus is analyzed on a 10–20 % gradient gel, VP4 can be clearly detected by silver staining [13] (Fig. 1b). VP0 (~36.4 kDa) and VP1 are often not resolved, despite their difference in $M_r$. However, presence of VP0 in a purified virus preparation can be revealed via Western blotting with suitable antibodies raised against VP4, VP2, or VP0. For HRV-A2, the monoclonal antibody 8F5 is specific for a "sequential" epitope present in VP2 and consequently in VP0 [14] as illustrated in Fig. 1a, lower panel.

### 1.3 Analysis of Native Rhinovirus and Derived Subviral Particles by Capillary Electrophoresis with UV Detection (CE UV)

Capillary (zone) electrophoresis combined with UV detection (CE UV) is a rapid method for quantification and quality control of virus preparations [15]. It was employed not only for HRV but also for tobacco mosaic virus [16], poliovirus [17], cowpea mosaic virus [18], and influenza A virus [19]. Examples of CE, with the underlying theory, have been presented previously, including volumes of this series [20–23]. Application of CE in the analysis of biomolecular assemblies has been covered by several recent reviews, e.g., [24–26]. Therefore, we only briefly recapitulate the principles of CE. We discuss the mandatory inclusion of surfactants in the background electrolyte (BGE) and show the resolution of native and subviral particles with detergent-containing BGE. We conclude with the demonstration of how CE UV can be used for determining the stoichiometry of the interaction between a recombinant soluble receptor and HRV-A2. A protocol for CE separation of native and subviral particles is found in Subheading 3.2.

CE separates particles in the BGE according to their net charge (accelerating force) and size/shape (retarding force resulting from friction as described by Stokes's law) in an electric field of potential difference, $V$, across a capillary tube of total length $L_{total}$. The electric field strength $E$ propelling the charged particle is given by $E = V/L_{total}$. Balance between opposing forces gives rise to a constant electrophoretic velocity, $v_i$, proportional to the electric field, $E$, and the electrophoretic mobility of a molecule, $\mu_i$:

$$v_i = \mu_i \cdot E$$

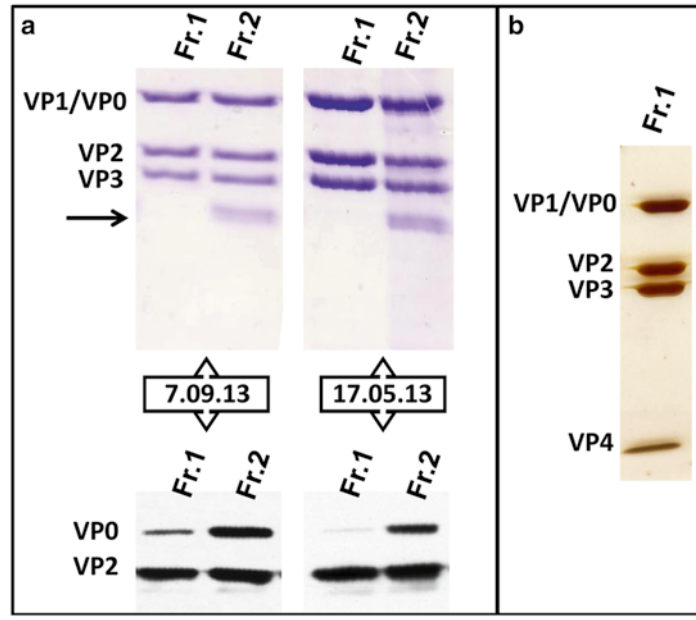


**Fig. 1** SDS-polyacrylamide gel electrophoresis and Western blot analysis of HRV-A2 capsid proteins. (**a**) *Upper panel*, Coomassie Brilliant Blue-stained reducing SDS-12 % polyacrylamide gel. *Lanes 1* and *2*, "first fraction" and "second fraction" virus from two different preparations as indicated by the dates in the *boxes* below. The *arrow* at about 20 kDa points to the subunits of denatured human ferritin stemming from the cells, as determined by mass spectroscopy analysis (unpublished results); it often contaminates "second fraction" preparations to various extents and results in a *brownish* color (*see* **Note 12**). Despite its comparably lower $M_r$ (~600 kDa for the 24 subunit molecule as compared to 8.5 MD for HRV) it co-sediments with virus because of its high density resulting from bound $Fe^{3+}$. *Lower panel*, virus samples as above separated on the same gel but transferred to a membrane followed by Western blot analysis with monoclonal antibody 8F5 and a secondary goat anti-mouse antibody conjugated to peroxidase. The individual bands corresponding to VP0 and VP2 are revealed by chemiluminescence. Notably, the VP0 content relative to VP2 differs in different preparations; furthermore, the ratio of VP0 to VP2 in "second fraction" virus is strikingly higher in each instance compared to "first fraction" virus. (**b**) Example of a "first fraction" virus separated on an SDS-10–20 % polyacrylamide gradient gel followed by silver staining according to the procedure described in ref. 13. Note that the small VP4 is clearly visible whereas it is not seen in the Coomassie Brilliant Blue-stained SDS-12 % polyacrylamide gel in (**a**)

$v_i$ can be calculated from the measured electrophoretic migration time $t_{analyte}$ (the time required for migration inside the capillary from the point of injection to the point of detection, which is the effective length of the capillary, $L_{effective}$) by

$$v_i = L_{effective} / t_{analyte}$$

It follows that the electrophoretic mobility $\mu_i$ of a substance (the steady-state velocity per unit field strength) can be expressed as

$$\mu_i = v_i / E = \left(L_{\text{effective}} \cdot L_{\text{total}}\right) / \left(t_{\text{analyte}} \cdot V\right)$$

Ionic strength and pH of the electrolyte exert a significant effect on the electrophoretic migration expressed as effective mobility $\mu_i^{\text{eff}}$, characteristic for a given analyte and a given system (e.g., *see* ref. 27). Additionally, the weakly acidic silanol groups of the capillary surface, p$K_a$ of SiOH ~2–4 [28], may become partially deprotonated dependent on the pH of the BGE. This leads to the formation of an electrical double layer at the capillary inner surface that in turn causes migration of the BGE bulk to the cathodic end of the capillary (with velocity of the electroosmotic flow, EOF, $v^{\text{EOF}} = \mu^{\text{EOF}} \cdot E$) upon application of voltage. This electroosmotic flow increases the migration of cations and reduces that of anions. The electrophoretic mobilities of the analytes calculated from migration times in the presence of an EOF are therefore apparent mobilities $\mu_i^{\text{app}}$. As EOF values vary from experiment to experiment, the migration time (or apparent mobility) cannot be used for the identification of an analyte. However, the mobility resulting from the EOF, $\mu^{\text{EOF}}$, can be determined with a neutral marker substance (e.g., DMSO, $t_{\text{EOF marker}}$), which migrates towards the cathode with the same velocity as the EOF. This allows for calculation of the highly reproducible net (i.e., effective) electrophoretic mobility, $\mu_i^{\text{eff}}$, of an analyte by the following equation:

$$\mu_i^{\text{eff}} = \mu^{\text{EOF}} - \mu_i^{\text{app}} = \left(\left(L_{\text{total}} \cdot L_{\text{effective}}\right) / \left(t_{\text{EOF marker}} \cdot V\right)\right) - \left(\left(L_{\text{total}} \cdot L_{\text{effective}}\right) / \left(t_{\text{analyte}} \cdot V\right)\right) \left[\text{m}^2 / \text{Vs}\right]$$

We routinely employ sodium borate adjusted with NaOH to pH 8.3 as BGE to analyze HRV-A2 (sub)viral particles as (1) it has minimal UV extinction in the useful detection range of 200–280 nm and (2) at this pH the acidic silanol groups of the inner wall of the fused-silica capillary are fully ionized resulting in a strong electroosmotic flow (EOF) to the cathode, while (3) at least HRV-A2 carries a net negative charge (pI of HRV-A2 is 6.8; [29]) driving it towards the anode. However, because $\mu^{\text{EOF}}$ substantially exceeds $\propto_{\text{HRV}}^{\text{eff}}$, the virus migrates with an apparent mobility, $\propto_{\text{HRV}}^{\text{app}}$, to the cathodic end of the capillary where the UV detector is placed (i.e., CE in positive polarity mode; [15]).

HRV tended to aggregate and adsorb to the capillary wall when CE UV was performed in plain sodium borate causing multiple spikes in the electropherogram. This was overcome by addition of detergents, such as SDS and Thesit®, above their critical micellar concentration (CMC) [30]. A typical electropherogram of HRV-A2, purified according to Subheading 3.1, in SDS-containing BGE

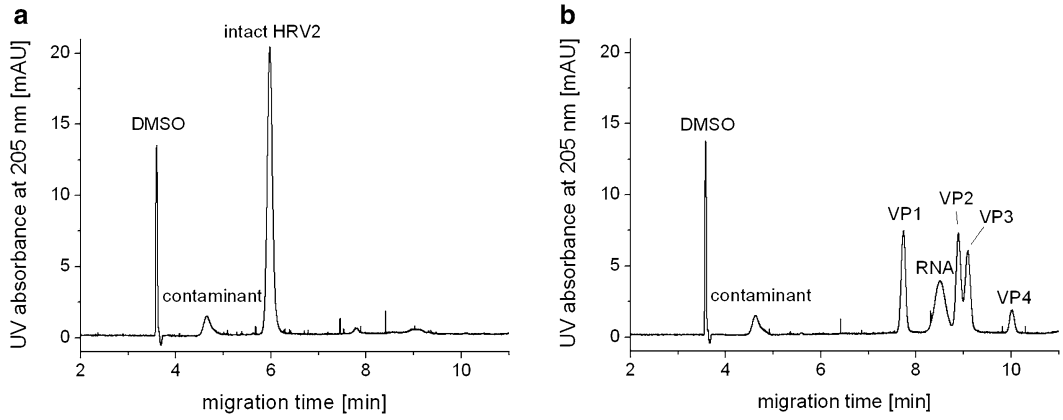


**Fig. 2** Electropherogram of an exemplary HRV-A2 preparation ("first fraction" virus) analyzed by CE UV in SDS-containing BGE prior to and after heating. (**a**) At room temperature, native HRV-A2 remains stable in 10 mM SDS resulting in a discrete narrow peak at about 6 min migration time. (**b**) Heating as described in Subheading 3.2, **step 3a** leads to complete dissociation of virions into the four viral capsid proteins VP1–4 and the viral RNA, giving rise to almost fully resolved peaks for each component. Note that the contaminant is heat stable giving a peak at about 4.6 min in both traces

is depicted in Fig. 2a. HRV-A2 gives rise to a narrow peak appearing at around 6 min. The concentration in mg/ml of native virus can be readily calculated from the respective peak area (Subheading 3.2, **step 7**). A second and smaller peak around 4.6 min corresponds to a so far unidentified component ("contaminant") present in every virus preparation at varying concentration [15]. Its lack of staining with Coomassie brilliant blue and ethidium bromide and sensitivity towards lipase (unpublished data) suggests that it is derived from cellular membranes.

While native HRV-A2, and probably other HRV, tolerates 10 mM SDS at room temperature, subviral A- and B-particles readily dissociate into their components in the presence of this detergent [31, 32]. At 56 °C, native virus also disassembles in 10 mM SDS; the resultant individual VPs are then resolved by CE, like in SDS-PAGE, but in a much shorter time and additionally offering the possibility for RNA detection. Note that the peak of the contaminant is unaltered (Fig. 2b).

HRV subviral particles, despite being disassembled in SDS, fully withstand the neutral surfactant Thesit® (a dodecyl-polyethyleneglycolether derivative) as specified in Subheading 2.2. This allowed their facile and reproducible separation by CE as specified in Subheading 2.2 while preventing aggregation. Figure 3 depicts electropherograms obtained in Thesit® containing BGE prior and after heating of HRV in sodium borate. Note that native HRV-A2 and the contaminant co-migrate in the presence of Thesit® (Fig. 3a; peak at ~3.9 min). Upon incubation of a concentrated solution of HRV-A2 at 56 °C for 10 min in the absence of detergent, the virus loses VP4 to form mostly A-particles (Fig. 3b; peak at ~4.9 min) while diluted material incubated in the same way

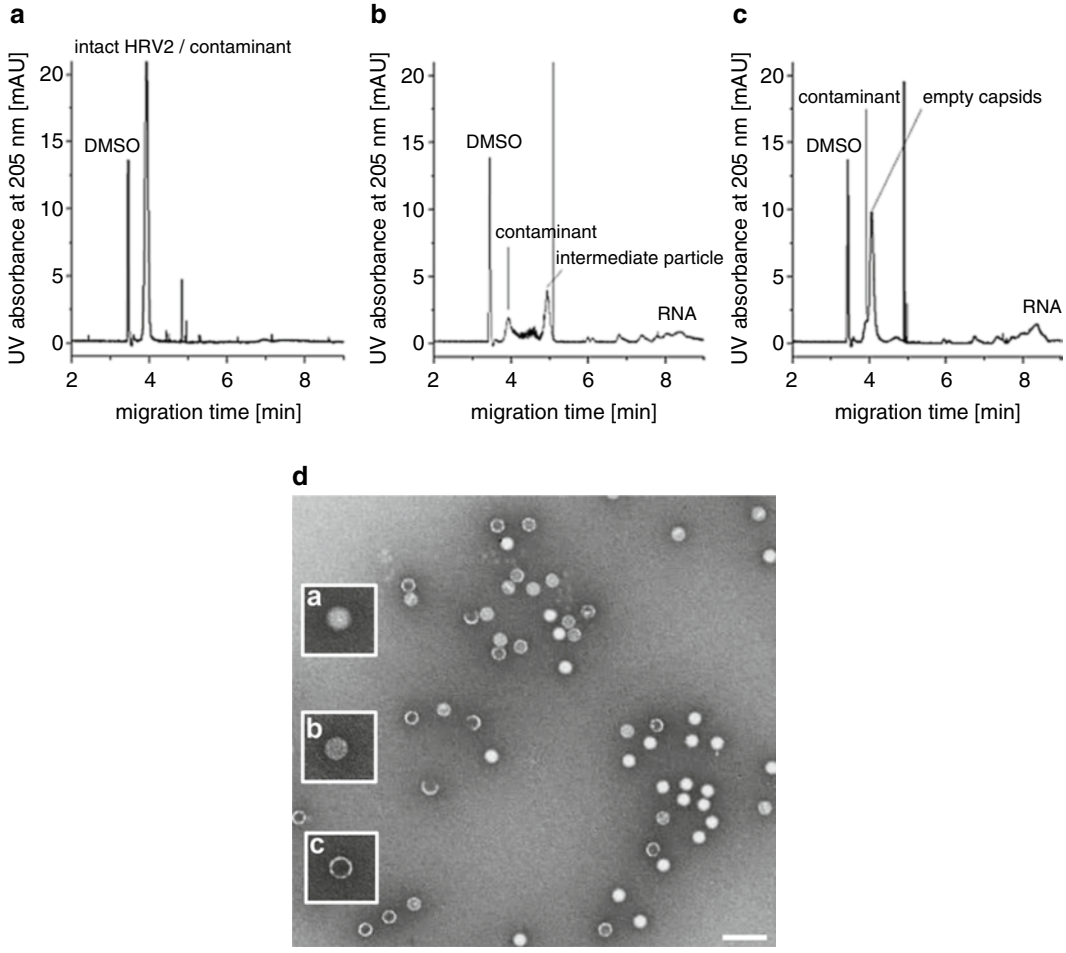


**Fig. 3** CE UV in Thesit®-containing BGE separates native virus and subviral particles. A- and B-particles were generated by heating for 10 min to 56 °C according to the procedure given in Subheading 3.2, **steps 3b** and **c**, respectively, followed by CE under the same conditions as used for native virus. Note that the contaminant co-migrates with the native virus (**a**) but is resolved from A-particles (intermediate particle, **b**) and B-particles (**c**). (**d**) Negative stain TEM image of (sub)viral particles corresponding to the individual CE traces. Native HRV-A2 was acidified as in ref. 7, stained with 2 % sodium phosphotungstate (pH 7.2) and viewed with an electron microscope at 36,000× magnification. The size bar corresponds to 100 nm. Native, A-, and B-particles are present at similar numbers under these conditions. Native virions, which are impermeable to the stain, appear as bright spheres, whereas subviral B-particles show a bright circle with a core of high density due to accumulation of stain in the (permeable) empty shell. A granular interior is typical of the (permeable) A-particle uncoating intermediate with the dye filling the space between the strands of the genomic RNA. *Insets* (**a**)–(**c**) depict prototypical particles representing the states of uncoating (i.e., beginning, intermediate, and end) at about threefold higher magnification than in the large image

is converted into free RNA and (80S) empty capsids (Fig. 3c; peak at ~4.1 min); in both instances the contaminant is unaltered.

Table 1 summarizes the detectability of viral/subviral particles in BGEs containing SDS or Thesit® [31, 32]. The effective electrophoretic mobilities of native virions and subviral particles allowing

**Table 1**
**Overview on CE UV analyses of intact HRV-A2 and derived subviral particles in BGE containing SDS or Thesit®**

| Particle | BGE with SDS | BGE with Thesit® | Particle obtained via |
|---|---|---|---|
| Intact virions | Yes | Yes | – |
| Intermediate (A) particles (including RNA) | No | Yes | (1) Heating to 56 °C of concentrated samples in sodium borate, (2) heating to 56 °C in the presence of divalent cations, (3) acidification |
| Empty capsids (B-particles (containing no RNA)) | No | Yes | Heating to 56 °C of diluted samples in sodium borate |
| Individual viral proteins and RNA | Yes | No | Heating of diluted samples to 56 °C in SDS containing BGE |

their unambiguous identification have been published [30] and were recently updated [31]; the values for viral proteins and the viral RNA are compiled in ref. 25.

As CE UV enables the separation of viral and subviral particles, factors impacting on uncoating can be easily investigated provided that the analysis is carried out in Thesit®-containing BGE. For instance, presence of $Mg^{2+}$ or $Ca^{2+}$ during uncoating triggered by heating demonstrated a stabilizing effect of these ions [32]. By the same token, binding of antibodies or soluble receptors to native or subviral particles can be investigated by CE UV with the generic protocol given in Subheading 3.2. Using SDS as additive, resolution of virus-receptor complexes differing in the number of attached recombinant soluble receptors was achieved; this study revealed a population of virions carrying between 0 and 12 receptor molecules that had been engineered as to include five copies of ligand-binding repeat three (V3) of the very-low-density lipoprotein receptor fused head to tail and carrying a maltose-binding protein at their N-terminus. Their distribution was in accordance with equilibrium binding; at saturation, a maximum of 12 molecules were indeed present per virion ([33] and Fig. 4a). This is in agreement with structural data [34, 35] indicating that one receptor molecule binds around each of the 12 fivefold vertices of the icosahedron. Furthermore, as shown in Fig. 4b, the use of Thesit® instead of SDS allowed demonstration of lower affinity binding of recombinant receptor mimics to B-particles.

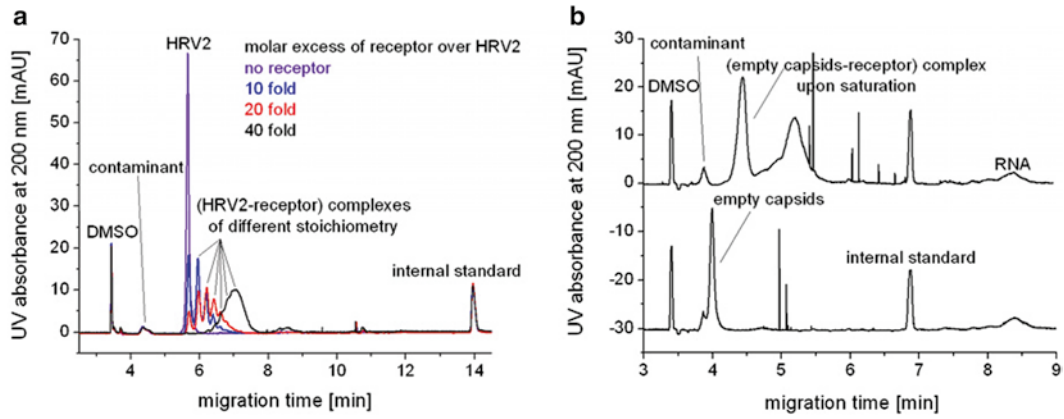


**Fig. 4** CE UV demonstrates binding of recombinant receptor fragments to native virions and empty viral capsids. (**a**) Incubation of purified HRV-A2 with graded amounts of recombinant soluble receptor in excess of virus gives rise to discrete complexes of different stoichiometry, which can be resolved in SDS-containing BGE. (**b**) B-particles (empty capsids) were prepared according to the protocol in Subheading 3.2, **step 3c**, and analyzed before (*bottom trace*) and after mixing (*top trace*) with saturating amounts of soluble recombinant receptor followed by CE UV in BGE with Thesit® to maintain integrity of the subviral particles

### *1.4 Analysis of Rhinovirus by Gas-Phase Electrophoretic Mobility Molecular Analysis (GEMMA)*

Gas-phase electrophoretic mobility molecular analysis (GEMMA; [36] also known as macro IMS (macro ion mobility spectrometry, LiquiScan-ES, nES-DMA, or ES-SMPS spectrometry)) has been established at the end of the twentieth century. It is particularly useful for the analysis of large non-covalent protein assemblies. GEMMA separates singly charged analytes in the gas phase at ambient pressure according to their electrophoretic mobility (EM) diameter, which corresponds to the particle diameter in the case of spherical analytes [37]. An aerosol containing variably charged analytes is obtained from a volatile electrolyte solution, e.g., ammonium acetate via a nano electrospray (nano ES) process operated in cone-jet mode. The resulting droplets are dried in a sheath flow of pressurized, particle-free air and $CO_2$. Concomitantly, their charge is reduced in a bipolar atmosphere (created by a $^{210}Po$ α radiation source), resulting in a population of mostly neutral, some singly charged, and a negligible amount of multiply charged analytes that are introduced into the nano differential mobility analyzer (nano DMA) unit of the instrument. Particles are transported through the nano DMA via a constant high-sheath flow of air. A tunable, orthogonal electric field is applied that leads to deviation of charged analytes from their trajectory imposed by the laminar airflow. At a given voltage, charged analytes of a specific EM diameter are deviated to an extent that allows for their detection after having passed the nano DMA. Upon arrival in the condensation particle counter (CPC) of the instrument, they nucleate the condensation of droplets in a supersaturated 1-butanol atmosphere. These condensate droplets pass through a focused laser

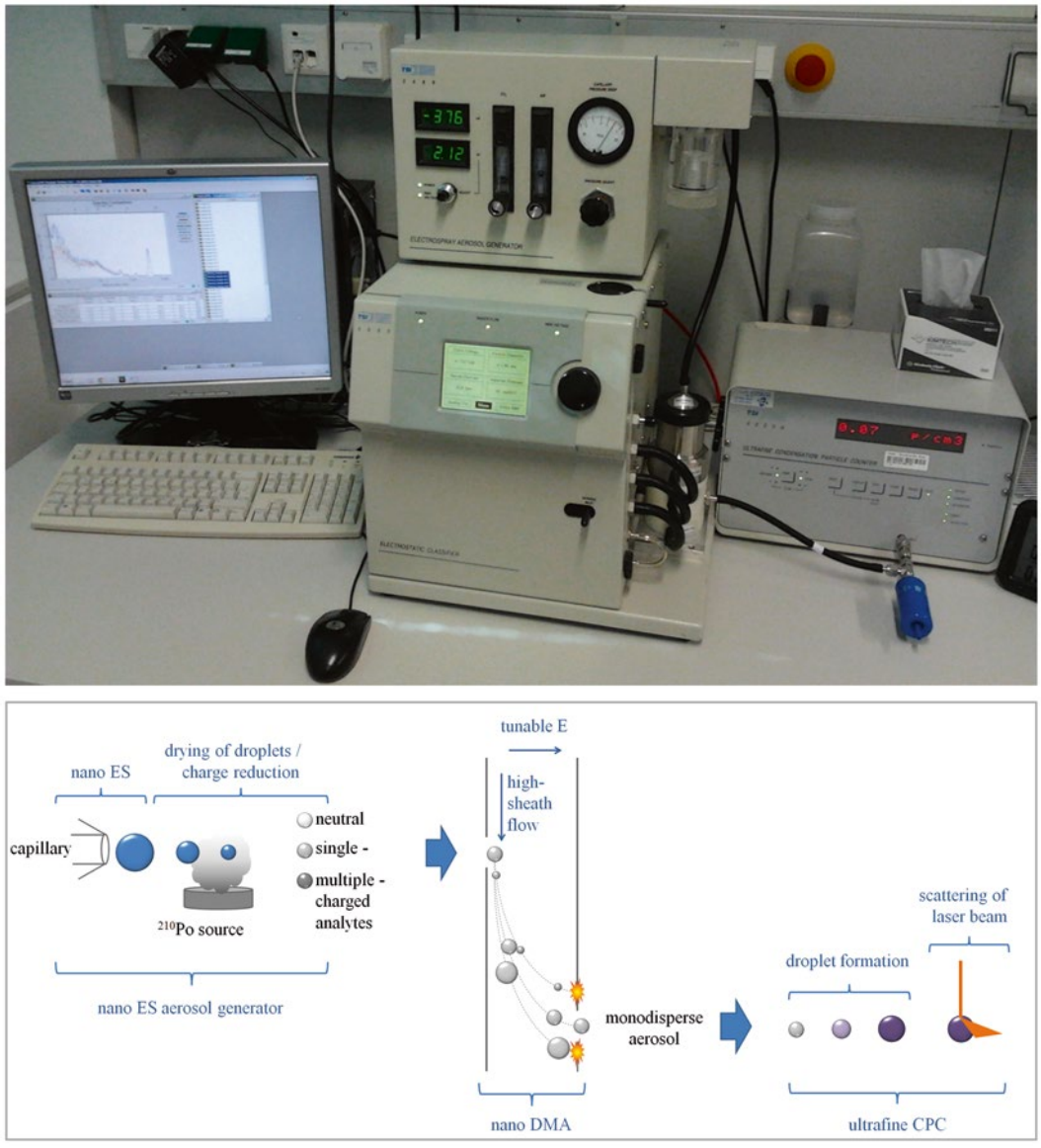


**Fig. 5** Design and scheme of a typical GEMMA system. *Upper panel*: Photograph of a GEMMA instrument (from TSI Inc). *Lower panel*: A schematic illustration of the individual components required for aerosol formation/ionisation, charge reduction, separation, and subsequent detection of particles according to their EM diameter as described in the main text

beam triggering light-scattering events, which are counted over time [38]. GEMMA is therefore suited for single-particle, particle number-based detection; the particles are resolved according to their EM diameter via voltage scanning. Figure 5 shows a photograph of a GEMMA instrument accompanied by a schematic illustration of its individual components and their role in the separation process.

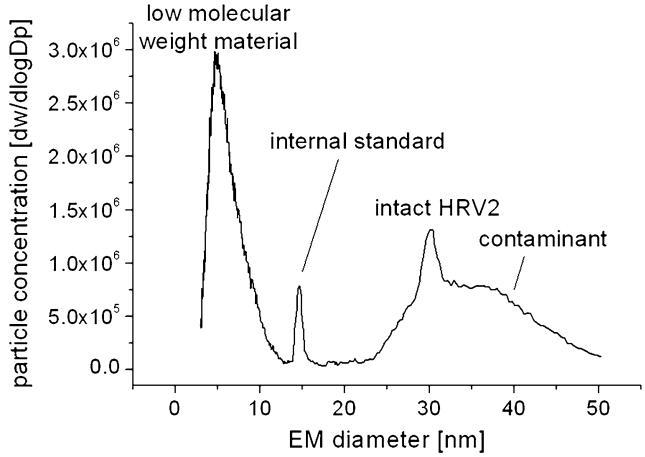


**Fig. 6** GEMMA spectrum of a HRV-A2 preparation ("first fraction"). Peaks of HRV-A2 (~8.5 MD; centered at 30 nm EMD) and the contaminant (stretching from 22 to >50 nm) are well separated from the internal standard (thyroglobulin; ~660 kDa; ~15 nm EM diameter) and smaller aggregates formed from non-volatile low $M_r$ material (between EMD 0 and 10) still present in the sample after buffer exchange to 50 mM ammonium acetate (pH 8.5)

Depending on the DMA unit, particles from the low nm EM diameter range (approx. 5 kDa MW for globular proteins) up to several 100 nm EM diameter can be analyzed [39]. Commercial GEMMA instruments can also be modified as to allow for collection of aerosol particles of selected EM diameter on a solid carrier enabling further analysis by, e.g., transmission electron microscopy [40]. Along the same lines selected analytes can be collected in buffer for assessment of biological activity. Standards with known $M_r$ allow the determination of the $M_r$ of the analyte based on the EM diameters acquired with the GEMMA instrument [41] that is increasingly employed for the analysis of viruses and viruslike particles [41–47] and other large assemblies of biomolecules, e.g., [36]. GEMMA has thus become a valuable alternative for tackling a number of questions in the field of virology.

In Subheadings 2.3 and 3.3 we give instructions for the GEMMA analysis of rhinovirus for the determination of its EM diameter (for HRV-A2 ~ 30 nm, in good accordance with X-ray analysis [41, 48]), and for assessing the binding stoichiometry of monoclonal antibodies and recombinant receptor fragments by a simplified calculation based on the increase of the respective EM diameter of the complex when compared to native virus [49]. Using essentially the same protocol, GEMMA was also exploited to obtain insight into the nature of the abovementioned contaminant that was found to exhibit an average EM diameter of approximately 35 nm, similar to rhinovirus particles but with a much broader EM diameter distribution (Fig. 6 and [31]). Paired with

its low UV absorption in CE, the contaminant is suggested to contain most likely aggregates possibly derived from cellular membranes (unpublished data).

### 1.5 Negative Stain Transmission Electron Microscopy (TEM) of Native Rhinovirus and Its Subviral Particles

Negative stain TEM is another valuable tool for the rapid assessment of the purity, homogeneity, and morphology of virus preparations. Essentially, a water-soluble heavy metal-containing salt is used to surround and penetrate the solvent-accessible space of a macromolecular assembly. Following air-drying a thin, amorphous film of the metal ions forms at these locations. Scattering of electrons by the electron-dense negative stain provides (negative) images of high contrast. Its unique power for the evaluation of the overall integrity of virions and the possible presence of contaminating material and undesired aggregates is demonstrated in Fig. 7, which shows a comparison between two independent "first fraction" preparations of HRV-A2 of different quality. The vast amount of irregularly shaped rather dull looking material is only observed in the second preparation (Fig. 7b) and likely originates from membranous material identified by CE and GEMMA [31]. We also used negative staining to visualize the structural changes occurring in rhinovirus particles upon exposure to elevated temperature and low pH, respectively, based on differential penetration of the dye into the protein shell (Fig. 3d). Although the small increase in diameter by ~4 % on transition from the native virion (Fig. 3d, inset a) to a subviral particle (Fig. 3d, inset b and c)

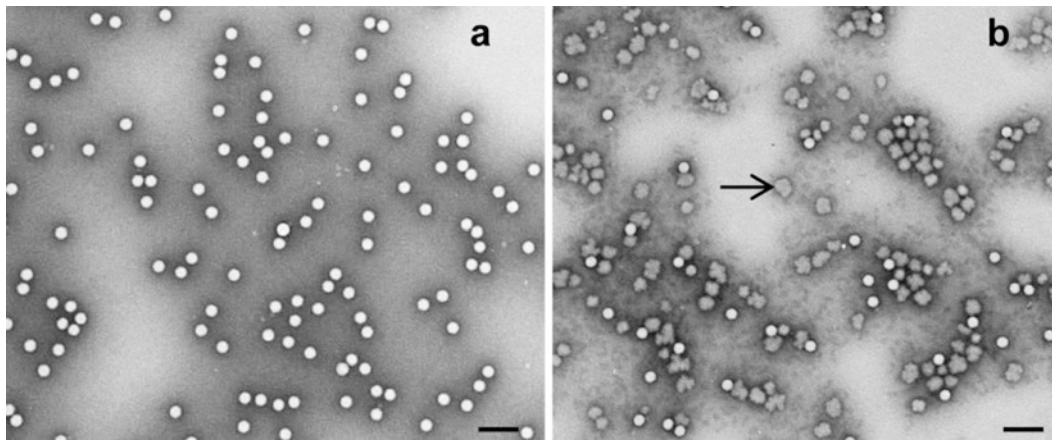


**Fig. 7** Negative stain TEM of samples from two different "first fraction" virus preparations. Preparation (**a**) is of high purity, consisting of only native, dye-impermeable bright virions. Preparation (**b**) is an example for bad quality; note the vast amount of irregularly shaped material (example indicated with arrow) of variable size comparable in dimension to virus particles. It is presumably the membranous contaminant identified by CE and GEMMA (Figs. 2, 3, and 6). The virus samples were stained with 2 % sodium phosphotungstate (pH 7.2) and the specimens viewed with an electron microscope at 36,000× magnification. The size bar corresponds to 100 nm

cannot be appreciated by visual inspection, exclusion of stain indicates native virions; penetration into the RNA-filled shell results in rather granular staining typical of the A-particle (Fig. 3d, inset b), and full penetration with intense internal stain deposition is observed in B-particles (Fig. 3d, inset c). In our hands, from the spectrum of available negative stains (listed, e.g., in ref. 50), potassium phosphotungstate turned out to be most useful. It has pH 7.2 and its ionic strength is compatible with the stability of rhinoviruses, not causing their conversion into subviral particles; it shows little tendency to form artefacts and provides crisp and detailed images. Subheadings 2.4 and 3.4 are devoted to a protocol for negative staining of native rhinoviruses and their derived subviral particles for subsequent TEM imaging.

## 2 Materials and Equipment

Use ultrapure water with resistivity of 18 MΩ cm (25 °C) or higher for preparing all buffers and solutions. Chemicals should be of electrophoresis or analytical grade. Always wear protective clothing and gloves, especially when manipulating solutions containing acrylamide and bisacrylamide, which are highly toxic. Perform all steps at room temperature unless indicated otherwise. Strictly follow all safety regulations and established waste disposal procedures for all materials and solutions. Note that work with rhinoviruses demands biosafety level 2 practices depending on the respective country.

### *2.1 Production and Purification of Human Rhinovirus from HeLa Cell Suspension Culture*

#### *2.1.1 Initiation and Maintenance of a HeLa Suspension Culture*

1. HeLa-Ohio, a strain adapted to growth in suspension culture, was originally from Flow Laboratories and is now available from the European Collection of Cell Cultures (ECACC, Salisbury, UK).
2. Complete medium for adherent cell culture: Minimal essential medium (MEM) supplemented with 10 % fetal calf serum, 100 U/ml penicillin, 100 μg/ml streptomycin, and 2 mM L-glutamine.
3. Complete medium for suspension cell culture: Minimal essential medium for suspension culture containing 7 % horse serum, 100 U/ml penicillin, 100 μg/ml streptomycin, 2 mM L-glutamine, 0.1 % (w/v) pluronic acid F68, and 1 % nonessential amino acids.
4. Phosphate-buffered saline (PBS): 8 g NaCl, 0.2 g KCl, 1.44 g $Na_2HPO_4$, 0.24 g $KH_2PO_4$. Dissolve in 1 l water (pH should be 7.4) and autoclave.
5. 0.05 % Trypsin, 0.53 mM EDTA solution in Hepes-buffered saline solution (HBSS) for cell detachment.
6. 3 l spinner flasks equipped with a Teflon-coated magnetic stirrer.

7. Polypropylene bottles with cap 500 ml (*see* **Note 1**).
8. Ultra Clear Thinwall Centrifuge Tubes 38.5 ml (*see* **Note 1**).

*2.1.2 Infection of HeLa Suspension Culture and Purification of HRV-A2*

1. Seed virus: Human rhinovirus 2 (HRV-A2) (originally from ATCC; VR482); other classical HRV-A and -B types are also available from ATCC.
2. Infection medium for suspension cell culture: Complete medium for suspension culture supplemented with 2 % horse serum and 3 mM $MgCl_2$ (*see* **Note 2**).
3. Virus preparation buffer A (VPA), 20 mM Tris–HCl (pH 7.4), 2 mM $MgCl_2$.
4. Virus preparation buffer B (VPB), 10 mM Tris–HCl (pH 7.4), 10 mM EDTA.
5. Enzymes to digest virus-associated impurities of host cell origin are prepared from dry powder dissolved in 10 mM Tris–HCl (pH 7.4) and 10 mM $MgCl_2$ at the concentrations below:
   (a) RNase A from bovine pancreas dissolved at 5 mg/ml.
   (b) DNase I grade II from bovine pancreas dissolved at 5 mg/ml.
   (c) Trypsin from porcine pancreas dissolved at 10 mg/ml.
6. *N*-laurylsarcosine.
7. 55 ml each of a 7.5 and 45 % sucrose solution (w/w) prepared in VPA at room temperature for pouring a continuous density gradient using an adequate gradient mixer.
8. A sonicator bath.

### 2.2 Capillary Electrophoresis

1. We use an Agilent (Waldbronn, Germany) 3D CE instrument equipped with a fused silica capillary from Polymicro (Phoenix, AZ, USA), 50 μm inner diameter, 375 μm outer diameter; total length of the capillary between 59 and 61 cm, effective length was 8.5 cm shorter. Any comparable instrument with similar capabilities can be used with similar results. Electrophoresis was at 20 °C with 25 kV (resulting in a field strength of ~42 kV/m). Detection is at 200 nm, 205 nm (*see* **Note 3**), and 260 nm (*see* **Note 4**) at the cathodic end of the capillary (positive polarity mode).
2. We use Agilent ChemStation Plus software package for data acquisition, storage, and analysis.
3. BGE, 100 mM sodium borate (pH 8.3) supplemented with SDS (BGE-SDS), or Thesit® (BGE-Thesit) at 10 mM. Filter through a surfactant-free cellulose acetate membrane syringe filter (0.2 μm pore size; *see* **Note 5**).

4. Sample buffer, either 100 mM sodium borate (pH 8.3) supplemented with 10 mM SDS or plain 100 mM sodium borate (pH 8.3) as detailed in Table 1. Also sodium borate at 50 mM is suitable as sample buffer. Buffers are filtered as stated for BGEs.
5. Sodium hydroxide, 1 M, for conditioning of fresh capillaries as well as rinsing of capillaries after each run.
6. DMSO stock solution 1:200 (v/v) in water (for determination of the EOF).
7. Benzoic acid may be added to the samples at ~0.02 mg/ml final concentration as internal standard from a more concentrated stock solution (*see* **Note 6**).
8. 50 mM sodium acetate (pH 5.0).
9. Polypropylene vials with a 0.3 ml cone-shaped interior cup for the diluted samples.
10. Polypropylene vials (1 ml).
11. Snap cap polyurethane.
12. A standard water bath or thermo mixer.

### 2.3 Gas-Phase Electrophoretic Mobility Molecular Analysis

1. We use the GEMMA instrument from TSI Inc (Shoreview, MN, USA). It consists of a nano ES aerosol generator (model 3480), including a $^{210}$Po charge reduction device, an electrostatic classifier unit (series 3080) with a nano DMA employed in the high-flow mode, and an ultrafine CPC (model 3025 A). Other GEMMA instruments with similar capabilities should be able to be used with similar effectiveness.
2. Fused silica cone tip capillaries for the electrospray process are 25 cm long with either 25 or 40 μm inner diameter from TSI Inc. As the surface-to-volume ratio of 25 μm inner diameter capillaries is higher than for 40 μm capillaries, we opted for the latter as this reduces analyte adsorption to the fused silica surface and thus increases the signal.
3. Ammonium acetate 50 mM, pH 8.5. Filter as described in Subheading 2.2, **step 3**. The pH of ammonium acetate can be somewhat decreased as can be the buffer molarity as long as the current recorded in the nano ES source of the GEMMA remains below about –500 nA (*see* **Note 7**).
4. Centrifugal filter tubes, 10 kDa MWCO (PES membrane).
5. Thyroglobulin may be used as a standard (660 kDa; EM diameter 15 nm) and added to the sample from a stock solution in ammonium acetate to a final concentration of approximately 10 nM (*see* **Note 8**).

### 2.4 Negative Stain Transmission Electron Microscopy

1. 400 mesh copper grids coated with a continuous carbon layer in house.
2. Sharp thin tweezers.
3. Whatman 3 MM filter paper.
4. Petri dish or grid box.
5. Stopwatch.
6. 2 % (w/v) sodium or potassium phosphotungstate; adjust to pH ~7.2 with NaOH.
7. Baltek 500 Bal-Tec SCD Sputter Coater for glow discharging the carbon grids.
8. FEI Morgagni 268D electron microscope equipped with an 11 megapixel CCD camera (Morada from Olympus-SIS). Any other similar electron microscope may be used with comparable effectiveness.
9. Digital image acquisition is done via the iTEM software compatible with the FEI Morgagni user interface.

## 3 Methods

### 3.1 Purification of Rhinovirus (e.g., HRV-A2) from Infected Cells in Suspension Culture

#### 3.1.1 Preparation of Seed Virus

1. Seed HeLa-Ohio cells in sixteen 162 $cm^2$ T-flasks, each containing 50 ml complete medium for adherent cell culture and grow in a tissue culture incubator in 5 % $CO_2$ atmosphere at 37 °C.
2. When about 90 % confluent, aspirate medium and wash cells with PBS at room temperature; remove as much buffer as possible but take care that the cells do not dry out.
3. Detach adherent cells by incubation with 3 ml trypsin-EDTA per flask in the tissue culture incubator until most of the cells are floating (~5 min; avoid longer times to prevent cell death).
4. Resuspend the trypsinized HeLa cells in 4 l complete medium for suspension culture (*see* **Note 9**), distribute into two 3 l spinner flasks, transfer in the tissue culture incubator set at 37 °C, and stir at 25 rpm.
5. After 4 days, transfer the cell suspension into 500 ml centrifuge tubes and spin at 825 × *g* and room temperature.
6. Resuspend the cell pellet in 4 l infection medium for suspension culture.
7. Challenge the cells with a previously prepared HRV-A2 seed virus at a multiplicity of infection (MOI) of 1.
8. Distribute into two 3 l spinner flasks and continue incubation in a tissue culture incubator at 34 °C for 16.5 h.
9. Collect cells (*see* **Note 10**) as above (**step 5**) but at 3,600 × *g*.

10. Resuspend pellet in 40 ml cold (4 °C) PBS and disrupt cells in a homogenizer (40 strokes with tight-fitting piston).
11. For maximum homogenization, subject suspension to three cycles of freezing and thawing and 3 min sonication in a sonicator bath to disperse viral aggregates.
12. Remove larger aggregates by centrifugation for 30 min at 26,900 × *g* and 4 °C.
13. Save the supernatant (seed virus), aliquot, and store at –80 °C.
14. Use one aliquot to determine the $TCID_{50}$/ml [51]. The infectious virus concentration routinely obtained is about $10^9$ $TCID_{50}$/ml totaling ~$4 \times 10^{10}$ $TCID_{50}$. Note that the ratio between physical particles (determined, e.g., by capillary electrophoresis or transmission electron microscopy, *see* Subheadings 3.2 and 3.4) and infectious particles (plaque-forming units, PFU) is particularly high for HRV, with values reported in the literature ranging from 24–240 up to 2,000 for HRV-A2 [52, 53], ~6,500 for HRV-B14 [53], and ~300–4,400 for HRV-16 [54].

*3.1.2 Medium-Scale Virus Growth and Purification*

1. Grow, collect, and infect HeLa cells as above but using 12 l medium and six 3 l spinner flasks.
2. Resuspend infected cell pellet in cold (4 °C) VPB (replacing PBS used in **step 10** of the seed virus preparation) and homogenize (*ibid*. Subheading 3.1.1, **step 10**).
3. For removal of cellular debris, centrifuge at 47,800 × *g* and 4 °C.
4. Subject the saved supernatant to ultracentrifugation in a Beckman Ti45 rotor (or equivalent) at 125,000 × *g* for 2 h at 4 °C.
5. Resuspend the virus pellets (from four tubes) in a total of 4 ml VPA.
6. Add RNase A (0.25 mg total) and DNase I (0.25 mg total) from stocks and incubate the crude virus preparation at room temperature for 10 min.
7. Add trypsin to a final concentration of 0.05 % (w/v) and continue incubation for 5 min at 37 °C.
8. Add *N*-laurylsarcosine to a final concentration of 1 % (w/v), mix briefly on a vortex, and leave sample overnight at 4 °C.
9. Pellet insoluble material by centrifugation in a microcentrifuge at 18,400 × *g* for 15 min at 4 °C.
10. Load equal volumes of supernatant onto 7.5–45 % (w/w) sucrose density gradients preformed in six Beckman Ultraclear or equivalent tubes kept at 4 °C and centrifuge for 3.5 h in an SW32 rotor (or equivalent) at 76,800 × *g* and 4 °C without engaging the centrifugal brake.

11. Carefully remove tubes and place upright in an appropriate rack. An opaque band roughly in the middle of the gradient can be discerned visually ("first fraction" virus), normally accompanied by a diffuser, brownish band just above ("second fraction" virus).
12. Collect the material present in each band separately by puncture with a needle attached to a 5 ml syringe. This typically results in two ~5 ml virus-containing fractions per gradient.
13. Separately combine the fractions 38.5 ml Ultra Clear Thinwall corresponding to each band and dilute with VPA to fill one 38.5 ml Ultra Clear Thinwall centrifuge tube each.
14. Pellet virus overnight in a suitable swing-out rotor at 76,800 × *g* and 4 °C.
15. Discard supernatant and resuspend the pelleted virus in 100–200 µl of cold (4 °C) 50 mM sodium borate, pH 7.4 (*see* **Note 11**).
16. Freeze 50 µl aliquots at –80 °C for long-term storage. If necessary, store in smaller aliquots to avoid repeated freeze/thawing cycles which may lead to virus inactivation. Purified virus is normally at ~$10^{11}$ $TCID_{50}$/ml, with a total virus concentration of between 1 and 5 mg/ml. The second fraction has usually about ten times lower infectivity.
17. Analyze 1 µl of the HRV preparation alongside with protein size markers by denaturing and reducing (Tris–HCl based) discontinuous SDS-PAGE on a 15 % mini-gel (0.75 mm thick) followed by Coomassie Brilliant Blue R-250 staining (*see* **Note 12**).

### 3.2 Capillary Electrophoresis with UV Detection of Native and Subviral HRV Particles

1. For concentration determination, dilute purified HRV 1:20 (v/v) in BGE-SDS; for other experiments use a final concentration of about 0.3 mg/ml in sample buffer (*see* Subheading 2.2, **step 4**).
2. DMSO (about 1: 4,000 (v/v) final dilution) and (optionally) benzoic acid as EOF marker and internal standard might be included (*see* **Note 13**). Addition of two standards allows for correction of slightly shifting EOF values by alignment of the electropherograms [55].
3. Starting from a typical virus preparation produce subviral particles and fully dissociated virus as follows:
   (a) Heat virus diluted in BGE-SDS (*see* **step 1**) for 10–15 min at 56 °C (in a water bath or a thermomixer) for complete dissociation of virions into the individual protein subunits (VP1–VP4) and the genomic RNA.
   (b) Heat concentrated virus prepared as in Subheading 3.1.2, **step 15**, to 56 °C for 10 min to obtain, almost exclusively, intermediate A-particles [31] (*see* **Note 14**). Heating is followed by sample dilution as in **step 1**.

(c) Heat virus diluted about ten times in BGE to 56 °C for 10 min to obtain, almost exclusively, B-particles. Dilute sample further as in **step 1** if necessary.

(d) Adjust the pH to ≤5.6 by mixing concentrated virus with sodium acetate 50 mM (pH 5.0), incubate for 15 min at ambient temperature, and re-neutralize by addition of 100 mM sodium borate (pH 8.3) to produce mainly A-particles [31] (*see* **Note 15**). Then dilute sample as in **step 1** if necessary.

4. Add benzoic acid and DMSO to the subviral particle-containing sample(s) as above (**step 2**; *see* **Note 16**).
5. Transfer about 10 μl of diluted (and cleared) sample to a vial with a cone-shaped interior cup, close with a snap cap, and place in the CE tray.
6. Inject samples into the capillary at around 250–450 mbar s (depending on the intended peak height and the sample concentration).
7. Calculate virus concentration (mg/ml) by correction of the virus peak area for migration time and taking into account the sample dilution before relating the value to a reference electropherogram of known virus concentration (*see* **Note 17**).
8. Flush the capillary with sodium hydroxide followed by water (postconditioning) and with the respective BGE (preconditioning) between runs for 2 min each.

### *3.3 Gas-Phase Electrophoretic Mobility Molecular Analysis of Rhinovirus*

#### *3.3.1 Removal of Non-volatile Buffer Components for GEMMA Analysis (See **Note 18**)*

1. Dilute purified HRV-A2 with 50 mM ammonium acetate buffer (pH 8.5) to about 0.25 mg/ml and a final volume of 30 μl.
2. Transfer 500 μl ammonium acetate buffer in a 10 kDa MW cutoff centrifugal filter tube (*see* **Note 19**). Weigh, add the diluted virus, and weigh again. Calculate the difference in weight for **step 8**.
3. Centrifuge at 9,300 × *g* until most of the buffer has passed the membrane (6.5–7 min; the filter should not run dry).
4. Discard the eluate and replenish the retentate with 500 μl ammonium acetate.
5. Repeat centrifugation as in **step 3**.
6. Pour 50 μl ammonium acetate buffer onto the filter, mix gently, and collect the concentrated, buffer-exchanged virus-containing sample.
7. Wash membrane twice with 50 μl ammonium acetate by pipetting the buffer solution up and down several times. Collect each washing solution and pool with sample from **step 6**.
8. The pooled samples (now in ammonium acetate) are weighed and adjusted to ~25 μg/ml based on the original weight of the

diluted virus (**step 2**) via addition of ammonium acetate, assuming a buffer density of 1 mg/μl. Store at 4 °C until use (*see* **Note 7**).

#### 3.3.2 GEMMA Settings

1. After buffer exchange, dilute HRV-A2 in the same ammonium acetate buffer to a final concentration of about 2.0 nM (*see* **Note 20**).
2. Use the following settings for GEMMA analysis of the diluted HRV-A2 sample:
   (a) 0.1 lpm (liters per minute) sheath flow of CO2 (Messer, 99.5 %) and 1.0 lpm sheath flow of particle-free compressed air for the nano ES process (*see* **Note 21**).
   (b) 4.4 psid (pounds per square inch differential, approximately 30 kPa) pressure difference across the capillary for introduction of samples into the capillary.
   (c) Operate the nano ES source at ~2–3 kV positive polarity, resulting in currents of 300–400 nA (the actual value depends on the buffer/electrolyte used in the analysis) to achieve a stable spray in the cone jet mode.
   (d) Set the sheath flow of the nano DMA to 15 lpm particle-free air for analysis of analytes in the range of 3–50 nm EM diameter (which includes HRV, *see* Subheading 1.4).
3. Carry out individual measurements for ~110 s corresponding to the analyzed EM diameter range, followed by ~20 s reset time.
4. Compute a median GEMMA spectrum from 5 to 10 individual scans to eliminate non-reproducible spikes.

### 3.4 Negative Staining Transmission Electron Microscopy of HRV and Its Subviral Particles

#### 3.4.1 Negative Staining of Virus Specimens

1. Place a copper grid (400 mesh) with the carbon-coated side facing up onto a cleaned microscope slide and glow discharge in a Baltek 500 Bal-Tec SCD Sputter Coater for ~30 s at 20 mA (*see* **Note 22**).
2. Place 4 μl drops of virus-containing sample, three or more 20 μl drops of water, and two 20 μl drops of staining solution on a piece of parafilm; keep at distance to avoid mixing.
3. Clamp the grid with tweezers outside the glow-discharged area.
4. Contact grid with the sample for ~60 s. Longer times might be necessary with more diluted samples to allow for sufficient adsorption of the protein on the carbon surface.
5. Blot off the surplus of sample from the grid onto a Whatman filter paper.
6. Wash away residual unbound sample by touching a drop of water. Blot off with filter paper.
7. Repeat with at least two more drops of water on the parafilm.

8. Touch the first drop of negative stain with the grid and wait for 20 s. Remove excess stain by draining with filter paper.
9. Touch the second drop of negative stain for 1 min and blot off surplus stain with filter paper.
10. Finally air-dry and secure in a grid box or Petri dish in a vacuum chamber until viewing in a transmission electron microscope.

### *3.4.2 Transmission Electron Microscopy of Negative-Stained Rhinovirus Specimens*

The following are instructions covering the essential operational steps for image acquisition of negative-stained rhinovirus specimens with an FEI Morgagni 268D electron microscope operating at 80 kV. Some adaptation will be required for other types of TEM.

1. Remove Petri dish containing stained carbon grids from the vacuum chamber and fix the grid tightly in a standard microscope holder for the EM.
2. Fill liquid nitrogen tank with ~850 ml of liquid $N_2$ to cool and stabilize the microscope.
3. Switch on the microscope internal user interface.
4. Check if the vacuum and high-tension status of the microscope are stable and running. Immediately report any problems that prevent normal operation to the lab/facility manager.
5. Remove the projection chamber window cover and switch on the high-tension console on the microscope.
6. Switch on the filament heating in high-tension window. The beam should slowly become visible in the projection chamber (*see* **Note 23**).
7. Wait until the electron beam intensity reaches the saturation limit.
8. Set spot size of the electron beam to 3.
9. Manually set the condenser aperture to 300 μm aperture.
10. With no specimen in the microscope, go from low-magnification (or shadow-magnification) mode to higher magnification mode (e.g. 1.4 k × magnification), bring the beam to crossover and center it on the phosphorescent screen with Beam shift X and Beam shift Y knobs.
11. Spread beam with the "Intensity" knob to the size of the small circle displayed in the center of the phosphorescent screen and if necessary, re-center by adjusting the condenser aperture with X and Y screws on the microscope column.
12. Go back to low or shadow mode.
13. Insert holder with the stained grid into the microscope stage. Once vacuum is produced after activating the pump allow the holder to go into the microscope column. The objective aperture has to be out.

14. Screen the whole grid to identify grid squares where carbon film is visible.
15. Mark the coordinates of at least three grid squares of interest per grid in stage tab of the user interface without saving the optical settings.
16. Go to a higher working magnification (880× and above) and insert the objective aperture (typically 50 μm). If the beam disappears, or if the image is seen in inverted contrast, center the objective aperture:
    (a) Make sure that the camera is not inserted (*see* **Note 24**).
    (b) Focus the sample at working magnification and switch on the diffraction mode.
    (c) Using the X and Y objective screws on the microscope column center the objective aperture (outer circle) around the beam spot. It is not necessary to center it exactly. Do this quickly in order to prevent damage to the specimen by the high-intensity electron beam.
    (d) Go back to the phosphorescent screen by switching off the diffraction mode. Spread beam across the whole screen with the "Intensity" knob if necessary.
17. If changing magnification: Center the electron beam with X and Y beam shifts and adjust the beam spread with "Intensity" knob.
18. Start digital image acquisition using the iTEM software.
19. Save images on an internal server or an external hard drive.
20. Remove sample holder and replace the grid with a new sample grid. Insert sample holder into the TEM and repeat the procedure starting from **step 14**.

## 4 Notes

1. Bottles and tubes to be used must be suitable to the make and model of the centrifuge or ultracentrifuge used.
2. Omission of $Mg^{2+}$ in the infection medium reduces the final yield of HRV to about 10 %.
3. In our experience there was no significant difference when measuring virus at 200 or 205 nm; nevertheless, the same wavelength should be used in comparative measurements.
4. Native virus and A-particles are also detected at 260 nm indicating the presence of RNA.
5. Buffers are stored at 4 °C prior to usage. Since this leads to detergent separation from the aqueous buffer phase, allow BGE stocks to equilibrate to room temperature and mix the solutions thoroughly before drawing aliquots. This, however, leads

to excessive foaming during vortexing. Therefore, BGE preparations are usually made the day prior to CE analysis to allow collapse of the foam during overnight storage. BGE homogenization on the day of analysis is then done by just gently shaking the flask. In order to further reduce spikes recorded during electrophoresis, centrifuge the BGE prior to application.

6. Benzoic acid (BA) has rather low solubility. Therefore, use concentrations of around 1 mg/ml for preparation of a stock solution. Initially run BA alone and the samples without adding BA in parallel to check whether its peak overlaps with an essential peak in the electropherogram of the samples.
7. Ammonium acetate serves as electrolyte solution to electrospray HRV-A2 after buffer exchange; its pH is of importance: HRV-A2 is stable at neutral or slightly basic pH; however, we observed that storage in ammonium acetate of pH 7.4 (which we also used for GEMMA) leads to some uncoating. This is probably due to its low buffering capacity at this pH; on uptake of $CO_2$, the pH might drop, even upon overnight storage. Therefore, we usually employ ammonium acetate of pH 8.5 as electrolyte solution.
8. Inclusion of an internal standard, such as thyroglobulin, allows for semiquantitative evaluation of the recorded spectra.
9. Cell sheets detached from the flasks need to be dispersed into single cells by carefully aspirating with a pipette and ejecting them repeatedly. This is best done in a small volume. The concentrated suspension is then mixed with suspension medium that is low in $Ca^{2+}$, thus reducing the formation of clusters. Horse serum is used because it also contains less $Ca^{2+}$ than fetal calf serum and is cheaper. It is highly recommended to test several batches in advance in a small-scale pilot infection experiment of suspended HeLa cell culture in order to pick a lot that gives the highest virus yield.
10. At this time post-infection most virus progeny still reside inside the cells and can be efficiently released by freeze-thawing in a small volume of buffer. Processing the cells after virus-induced lysis has occurred slightly increases the yield. However this requires handling much larger volumes containing substantial amounts of serum proteins that need to be removed.
11. Sodium borate buffer lacks UV absorbance and is compatible with amino-specific labeling reagents.
12. Virus obtained from the lower band ("first fraction" virus) is typically of high purity according to SDS-PAGE and CE UV; virus retrieved from the upper band ("second fraction" virus) is less pure, presumably due to co-sedimenting ferritin that gives rise to a brownish color and a series of closely spaced bands in the SDS-PAGE at about 20 kDa (compare lanes 1 and 2 in

Fig. 1a). The origin of the apparently different sedimentation of the virus in the first and second fractions is unclear. The specific infectivity of the second fraction is lower with respect to the first fraction. For most structure-function experiments we thus use "first fraction" virus and "second fraction" virus for pilot experiments with lesser demand on sample purity such as ELISA.

13. DMSO (1:200 (v/v) in water) is further diluted 1:20 (v/v) upon addition to the samples to achieve a final dilution of 1:4,000 (v/v); to adjust for peak height (the marker peak should not considerably exceed the peak height of the analyte) an even higher overall DMSO dilution can be employed. Benzoic acid is usually employed at about 0.02 mg/ml; again, this can be varied to appropriately adjust the relative peak height to the analyte peak.
14. In the presence of divalent cations the ratio between A- and B-particles is increased [32].
15. The appropriate volume ratio must be determined beforehand by mixing larger amounts of plain buffers and checking the resultant pH (≤6.5 or ~7.5) with a pH electrode prior to the virus uncoating experiments.
16. All samples to be analyzed by CE except when testing freshly purified virus preparations should have concentrations of ~0.3 mg/ml as already stated in **step 1** of Subheading 3.2, via appropriately diluting prior to or after the treatments, such as heating or acidification. Before CE analysis, it is beneficial to remove aggregates by centrifugation (30 s in an Eppendorf centrifuge at full speed) to prevent occurrence of spikes in the electropherogram; in particular, A-particles tend to aggregate because of their hydrophobic nature.
17. $\mu^{EOF}$ values vary slightly between experiments and, therefore, also the analyte migration time. Hence, a particular substance passes through the detection window at different velocities from one experiment to the next. The lower the velocity, the longer the passage time and consequently, the larger the peak area (and vice versa). Quantitative applications of CE therefore require introduction of a correction factor accounting for the above variability of migration time to allow for an accurate comparison between the peak area of a particular sample and a standard preparation run separately. This is done using the following formula:

$$\text{corrected peak area}_{\text{sample}} = \text{measured peak area}_{\text{sample}} \cdot (t_{\text{standard}}/t_{\text{sample}})$$

$$c_{\text{sample}} = (\text{corrected peak area}_{\text{sample}}/\text{peak area}_{\text{standard}}) \cdot (\text{dilution}_{\text{standard}}/\text{dilution}_{\text{sample}}) \cdot c_{\text{standard}}$$

The concentration of the virus (mg/ml) as obtained from the peak area recorded at 200 or 205 nm, calculated by using the above equation and a virus sample of known concentration,

can be converted to the number of virions/ml using $M_r$ ~8.5 MD. The concentration of a pure virus sample can also be calculated using the following relationship: 1 mg /ml virions = $7.7 \cdot A_{260}$ [56].

18. Non-volatile sample components (e.g., salts, sugars, and surfactants) might form aggregates on evaporation of the solvent droplets; they then behave like larger particles in terms of their EM diameter. For this reason, volatile electrolyte solutions (such as ammonium acetate) must be employed as GEMMA sample buffers. Unsuitable solutions (e.g., sodium borate present in purified HRV-A2) must be exchanged against a volatile buffer.
19. Buffer exchange via size-exclusion chromatography on Sephadex is not advisable; we found low-molecular-weight oligosaccharides apparently released from the dextran polymer beads.
20. Depending on the bore size of the capillary the virus concentration should be between 0.5 and 2.0 nM.
21. Sheath flow of $CO_2$ and air controls the sizing range for a given GEMMA setup; increasing the sheath flow leads to sharper analyte peaks [40] but reduces the EMD size range that can be analyzed.
22. We use grids immediately after glow discharge, which renders them hydrophilic allowing for efficient binding and even distribution of the virions.
23. If the electron beam does not become visible in the projection chamber, then check (1) for proper heating of the filament; (2) if the camera is turned on, (3) the projection chamber cover has been removed, (4) the beam blanker is off, or (5) the small projection screen is blocking the beam. Another possible reason is improper centering of the electron beam on the specimen at high magnification. Go to low or shadow mode and check if the beam needs to be re-centered.
24. It is essential to make sure that the camera is moved out while adjusting the objective aperture. Omitting this step can lead to damage of the camera's scintillator and eventually also permanently ruin its CCD sensor due to the high intensity of the electron beam in diffraction mode.

## Acknowledgements

The work described in this chapter was made possible via various grants and the DK "Structure and Interaction of Macromolecules" funded by the Austrian Science Fund (FWF). We thank Guenter Resch (Campus Science Support Facilities) for help with the electron microscope and Günter Allmaier (Techn. Univ. Vienna) for making available the GEMMA instrument.

## References


1. Knowles NJ, Hovi T, Hyypiä T et al (2012) Picornaviridae. In: King AMQ, Adams MJ, Carstens EB, Lefkowitz EJ (eds) Virus taxonomy: classification and nomenclature of viruses: ninth report of the international committee on taxonomy of viruses. Elsevier Academic, San Diego, pp 855–880
2. McIntyre CL, Knowles NJ, Simmonds P (2013) Proposals for the classification of human rhinovirus species A, B and C into genotypically assigned types. J Gen Virol 94:1791–1806
3. Palmenberg AC, Rathe JA, Liggett SB (2010) Analysis of the complete genome sequences of human rhinovirus. J Allergy Clin Immunol 125:1190–1199
4. Fuchs R, Blaas D (2012) Productive entry pathways of human rhinoviruses. Adv Virol 2012:826301
5. Bochkov YA, Palmenberg AC, Lee WM et al (2011) Molecular modeling, organ culture and reverse genetics for a newly identified human rhinovirus C. Nat Med 17:627–632
6. McGregor S, Mayer HD (1968) Biophysical studies on rhinovirus and poliovirus. I. Morphology of viral ribonucleoprotein. J Virol 2:149–154
7. Korant BD, Lonberg-Holm K, Noble J et al (1972) Naturally occurring and artificially produced components of three rhinoviruses. Virology 48:71–86
8. Garriga D, Pickl-Herk A, Luque D et al (2012) Insights into minor group rhinovirus uncoating: the X-ray structure of the HRV2 empty capsid. PLoS Pathog 8:e1002473
9. Pickl-Herk A, Luque D, Vives-Adrián L et al (2013) Uncoating of common cold virus is preceded by RNA switching as determined by X-ray and cryo-EM analyses of the subviral A-particle structure. Proc Natl Acad Sci U S A 110:20063–20068
10. Harutyunyan S, Kumar M, Sedivy A et al (2013) Viral uncoating is directional: exit of the genomic RNA in a common cold virus starts with the poly-(A) tail at the 3′-end. PLoS Pathog 9:e1003270
11. Thomas DC, Conant RM, Hamparian VV (1970) Rhinovirus replication in suspension cultures of HeLa cells. Proc Soc Exp Biol Med 133:62–65
12. Korant BD, Lonberg-Holm K, Yin FH et al (1975) Fractionation of biologically active and inactive populations of human rhinovirus type 2. Virology 63:384–394
13. Gromova I, Celis EJ (2006) Protein detection in gels by silver staining: a procedure compatible with mass-spectrometry. In: Celis JE, Carter N, Hunter T, Simons K, Small JV, Shotton D (eds) Cell biology: a laboratory handbook, vol 4, 3rd edn. Elsevier, Academic, Amsterdam, pp 219–223
14. Skern T, Neubauer C, Frasel L et al (1987) A neutralizing epitope on human rhinovirus type 2 includes amino acid residues between 153 and 164 of virus capsid protein VP2. J Gen Virol 68:315–523
15. Okun VM, Ronacher B, Blaas D et al (1999) Analysis of common cold virus (human rhinovirus serotype 2) by capillary zone electrophoresis: the problem of peak identification. Anal Chem 71:2028–2032
16. Grossman PD, Soane DS (1990) Orientation effects on the electrophoretic mobility of rod-shaped molecules in free solution. Anal Chem 62:1592–1596
17. Oita I, Halewyck H, Pieters S et al (2009) Improving the capillary electrophoretic analysis of poliovirus using a Plackett-Burman design. J Pharm Biomed Anal 50:655–663
18. Liang S, Schneider RJ (2009) Capillary zone electrophoresis of cowpea mosaic virus and peak identification. Electrophoresis 30:1572–1578
19. Horka M, Kubicek O, Kubesova A et al (2011) Rapid separation and identification of the subtypes of swine and equine influenza A viruses by electromigration techniques with UV and fluorometric detection. Analyst 136:3010–3015
20. Altria KD (1996) Fundamentals of capillary electrophoresis theory. Methods Mol Biol 52: 3–13
21. Schmitt-Kopplin P, Fekete A (2008) The CE way of thinking: “all is relative!”. Methods Mol Biol 384:611–629
22. Simonet BM, Rios A, Valcárcel M (2008) Capillary electrophoresis separation of microorganisms. Methods Mol Biol 384:569–590
23. Okun VM, Ronacher B, Blaas D et al (2000) Affinity capillary electrophoresis for the assessment of complex formation between viruses and monoclonal antibodies. Anal Chem 72: 4634–4639
24. Desai MJ, Armstrong DW (2003) Separation, identification, and characterization of microorganisms by capillary electrophoresis. Microbiol Mol Biol Rev 67:38–51
25. Kremser L, Bilek G, Blaas D et al (2007) Capillary electrophoresis of viruses, subviral particles and virus complexes. J Sep Sci 30: 1704–1713
26. Subirats X, Blaas D, Kenndler E (2011) Recent developments in capillary and chip electrophoresis of bioparticles: viruses, organelles, and cells. Electrophoresis 32:1579–1590

27. Jouyban A, Kenndler E (2006) Theoretical and empirical approaches to express the mobility of small ions in capillary electrophoresis. Electrophoresis 27:992–1005
28. Parks GA (1965) The isoelectric points of solid oxides, solid hydroxides, and aqueous hydroxo complex systems. Chem Rev 65:177–198
29. Schnabel U, Groiss F, Blaas D et al (1996) Determination of the pI of human rhinovirus serotype 2 by capillary isoelectric focusing. Anal Chem 68:4300–4303
30. Kremser L, Petsch M, Blaas D et al (2006) Influence of detergent additives on mobility of native and subviral rhinovirus particles in capillary electrophoresis. Electrophoresis 27:1112–1121
31. Weiss VU, Subirats X, Pickl-Herk A et al (2012) Characterization of rhinovirus subviral A particles via capillary electrophoresis, electron microscopy and gas-phase electrophoretic mobility molecular analysis: Part I. Electrophoresis 33:1833–1841
32. Subirats X, Weiss VU, Goesler I et al (2013) Characterization of rhinovirus subviral A particles via capillary electrophoresis, electron microscopy and gas phase electrophoretic mobility molecular analysis: part II. Electrophoresis 34: 1600–1609
33. Konecsni T, Kremser L, Snyers L et al (2004) Twelve receptor molecules attach per viral particle of human rhinovirus serotype 2 via multiple modules. FEBS Lett 568:99–104
34. Querol-Audi J, Konecsni T, Pous J et al (2009) Minor group human rhinovirus-receptor interactions: geometry of multimodular attachment and basis of recognition. FEBS Lett 583: 235–240
35. Verdaguer N, Fita I, Reithmayer M et al (2004) X-ray structure of a minor group human rhinovirus bound to a fragment of its cellular receptor protein. Nat Struct Mol Biol 11:429–434
36. Kaufman SL, Skogen JW, Dorman FD et al (1996) Macromolecule analysis based on electrophoretic mobility in air: globular proteins. Anal Chem 68:1895–1904
37. Kapellios EA, Karamanou S, Sardis MF et al (2011) Using nanoelectrospray ion mobility spectrometry (GEMMA) to determine the size and relative molecular mass of proteins and protein assemblies: a comparison with MALLS and QELS. Anal Bioanal Chem 399:2421–2433
38. Koropchak JA, Sadain S, Yang X et al (1999) Nanoparticle detection technology for chemical analysis. Anal Chem 71:386A–394A
39. Intra P, Tippayawong N (2008) An overview of differential mobility analyzers for size classification of nanometer-sized aerosol particles. SJST 30:243–256
40. Kallinger P, Weiss VU, Lehner A et al (2013) Analysis and handling of bio-nanoparticles and environmental nanoparticles using electrostatic aerosol mobility. Particuology 11:14–19
41. Bacher G, Szymanski WW, Kaufman SL et al (2001) Charge-reduced nano electrospray ionization combined with differential mobility analysis of peptides, proteins, glycoproteins, noncovalent protein complexes and viruses. J Mass Spectrom 36:1038–1052
42. Thomas JJ, Bothner B, Traina J et al (2004) Electrospray ion mobility spectrometry of intact viruses. Spectroscopy 18:31–36
43. Kaddis CS, Lomeli SH, Yin S et al (2007) Sizing large proteins and protein complexes by electrospray ionization mass spectrometry and ion mobility. J Am Soc Mass Spectrom 18:1206–1216
44. Allmaier G, Laschober C, Szymanski WW (2008) Nano ES GEMMA and PDMA, new tools for the analysis of nanobioparticles-protein complexes, lipoparticles, and viruses. J Am Soc Mass Spectrom 19:1062–1068
45. Pease LF, Tsai DH, Brorson KA et al (2011) Physical characterization of icosahedral virus ultra structure, stability, and integrity using electrospray differential mobility analysis. Anal Chem 83:1753–1759
46. Pease LF 3rd (2012) Physical analysis of virus particles using electrospray differential mobility analysis. Trends Biotechnol 30: 216–224
47. Guha S, Li M, Tarlov MJ et al (2012) Electrospray-differential mobility analysis of bionanoparticles. Trends Biotechnol 30: 291–300
48. Verdaguer N, Blaas D, Fita I (2000) Structure of human rhinovirus serotype 2 (HRV2). J Mol Biol 300:1179–1194
49. Laschober C, Wruss J, Blaas D et al (2008) Gas-phase electrophoretic molecular mobility analysis of size and stoichiometry of complexes of a common cold virus with antibody and soluble receptor molecules. Anal Chem 80: 2261–2264
50. Harris JR (2007) Negative staining of thinly spread biological samples. Methods Mol Biol 369:107–142
51. Reed LJ, Muench H (1938) A simple method of estimating fifty percent endpoints. Am J Hyg 27:493–497
52. Abraham G, Colonno RJ (1984) Many rhinovirus serotypes share the same cellular receptor. J Virol 51:340–345
53. Butterworth BE, Grunert RR, Korant BD et al (1976) Replication of rhinoviruses. Arch Virol 51:169–189

54. Sachs LA, Schnurr D, Yagi S et al (2011) Quantitative real-time PCR for rhinovirus, and its use in determining the relationship between TCID50 and the number of viral particles. J Virol Methods 171:212–218
55. Reijenga JC, Martens JH, Giuliani A et al (2002) Pherogram normalization in capillary electrophoresis and micellar electrokinetic chromatography analyses in cases of sample matrix-induced migration time shifts. J Chromatogr B Analyt Technol Biomed Life Sci 770:45–51
56. Rueckert RR (1976) On the structure and morphogenesis of picornaviruses. In: Fraenkel-Conrat H, Wagner RR (eds) Comprehensive virology, vol 6. Plenum, New York, NY, pp 131–213

# Chapter 10

# Proteases of Human Rhinovirus: Role in Infection

**Lora M. Jensen, Erin J. Walker, David A. Jans, and Reena Ghildyal**

## Abstract

Human rhinoviruses (HRV) are the major etiological agents of the common cold and asthma exacerbations, with significant worldwide health and economic impact. Although large-scale population vaccination has proved successful in limiting or even eradicating many viruses, the more than 100 distinct serotypes mean that conventional vaccination is not a feasible strategy to combat HRV. An alternative strategy is to target conserved viral proteins such as the HRV proteases, $2A^{pro}$ and $3C^{pro}$, the focus of this review. Necessary for host cell shutoff, virus replication, and pathogenesis, $2A^{pro}$ and $3C^{pro}$ are clearly viable drug targets, and indeed, $3C^{pro}$ has been successfully targeted for treating the common cold in experimental infection. $2A^{pro}$ and $3C^{pro}$ are crucial for virus replication due to their role in polyprotein processing as well as cleavage of key cellular proteins to inhibit cellular transcription and translation. Intriguingly, the action of the HRV proteases also disrupts nucleocytoplasmic trafficking, contributing to HRV cytopathic effects. Improved understanding of the protease-cell interactions should enable new therapeutic approaches to be identified for drug development.

**Key words** Human rhinovirus, 3C protease, 2A protease, Disruption of nuclear transport, Subcellular localization, Inhibition of cap-dependent translation

## 1 Introduction

Human rhinoviruses (HRV) are the major etiological agents of the common cold, with significant worldwide health and economic impact, from both the initial infection with HRV and secondary infections [1, 2]. Although HRV infection is self-limiting and causes mild symptoms, in elderly patients or those with underlying respiratory illness, such as asthma, infection may result in severe complications [3–6]. HRV infections cause up to 80 % of all virus-induced asthma exacerbations [7, 8], which are associated with up to 16 deaths per week in Australia (http://aihw.gov.au/deaths-from-asthma/) and 25 per week in the USA (http://aihw.gov.au/deaths-from-asthma/). Although vaccination has been a highly successful strategy to limit and indeed to eradicate viruses, vaccination for HRV does not appear to be feasible as there are over 100 distinct serotypes [9] (*see* chapter by Palmenberg and Gern in this volume)

David A. Jans and Reena Ghildyal (eds.), *Rhinoviruses: Methods and Protocols*, Methods in Molecular Biology, vol. 1221, DOI 10.1007/978-1-4939-1571-2_10, 

and cross-reactions between only small groups of serotypes have been reported [10, 11]. A more viable strategy for limiting disease severity is to target well-conserved viral proteins or their interactions with host proteins.

HRV belongs to the *Picornaviridae* family and has a single-strand, positive-sense RNA genome [12]. It is classified within the enterovirus genus typified by poliovirus [13]; indeed, initial advances in the understanding of HRV biology derive from its close relationship to poliovirus [14], culminating in sequence analysis of HRV from laboratory strains and field isolates [2, 15, 16] and recently, with the description of HRV-C [17]. HRV are commonly grouped by receptor usage or on the basis of genomic sequence homology; these groupings are described in detail in the chapter by Palmenberg and Gern in this volume.

The HRV genomic RNA includes open reading frames for 12 proteins flanked by a 5′ Vpg (encoded within the genome) and a 3′ poly-A tail; structural proteins are encoded in the 5′ region of the genome, while the nonstructural proteins are encoded in the 3′ region [2, 13, 18]. Following virus attachment and genome release into the host cell cytoplasm, the viral RNA is translated into a single polyprotein that undergoes proteolytic self-cleavage by the viral proteases 2A and 3C ($2A^{pro}$ and $3C^{pro}$, respectively; *see* Fig. 1) [2, 19]

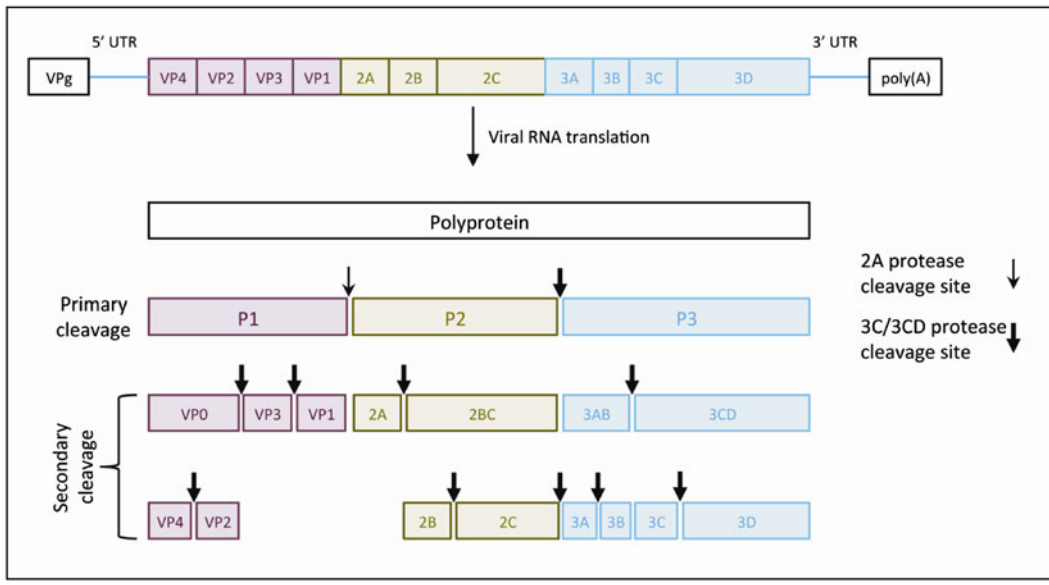


**Fig. 1** Overview of HRV genome organization and polyprotein processing. The HRV genome is organized as a single positive-strand RNA, which is translated as a single polyprotein; the polyprotein consists of structural proteins (P1, shown in *red*) and nonstructural proteins (P2 and P3, shown in *green* and *blue*). As the nascent polyprotein is produced, the primary cleavage points produce the P1, P2, and P3 fragments, which are then cleaved via secondary cleavages into individual viral proteins. The specific protease responsible for each cleavage is shown by thin and thick arrows ($2A^{pro}$ and $3C^{pro}$, respectively)

as the polyprotein is being synthesized, generating functional structural and nonstructural proteins for continued viral RNA replication [20] and assembly of progeny virions. $2A^{pro}$ initiates polyprotein cleavage by releasing the nonstructural proteins from the capsid/structural proteins [21, 22], while $3C^{pro}$ releases the other viral components. Initial cleavage by $2A^{pro}$ ensures the release of the precursor capsid protein P1 from the polyprotein. P1 is then cleaved into its component parts VP0, VP3, and VP1 by $3C^{pro}$ (Fig. 1; 23–25). $2A^{pro}$ catalyzes its own release from the polyprotein, but does not appear to act on cellular substrates as part of the larger protein [22]. In contrast, $3C^{pro}$ can function as its precursor, $3C^{pro}D$, before it is cleaved from 3D [19]. Specific and timely cleavage of the polyprotein into its functional components is essential for virus replication and assembly, making the proteases viable targets for drug development. Indeed, major effort has been focused on the development of specific inhibitors of $3C^{pro}$ that are effective across HRV serotypes (e.g., 20, 26, 27). Several publications have described the families of $3C^{pro}$ inhibitors that have been developed using structure-based design and will not be discussed in detail here. The most efficacious inhibitor to date is Rupintrivir (formerly AG7088), an irreversible HRV $3C^{pro}$ inhibitor that showed strong promise in the laboratory against all HRV serotypes and clinical isolates [18, 27] due to its interaction with a highly conserved amino acid sequence in $3C^{pro}$ [20]. While Rupintrivir showed efficacy in subsequent clinical trials, presenting a reduced viral load and illness severity in experimental infection [28], it did not significantly decrease viral load or illness severity in natural infection due primarily to a requirement for the drug to be taken either prior to or immediately after infection, and further trials were terminated [29].

Demonstration of the link between HRV infection and asthma exacerbation has resulted in increased interest in drug development targeting HRV, while the availability of a reverse genetic system for HRV, new immunochemical tools to study $2A^{pro}$ and $3C^{pro}$, and development of new imaging technologies have resulted in a greater understanding of HRV biology. In this chapter, we discuss current understanding of the role of HRV proteases in infection. Given that picornavirus proteases are conserved across families, they present a viable target for drug development, but a practical approach may also be to target interactions of proteases with cellular factors rather than the proteases directly.

## 2 Protease Structure and Activity

HRV14 [13] and HRV2 [2] were the first two HRV serotypes to be completely sequenced. Comparison of the protease sequences from these two serotypes with mammalian and bacterial proteases

revealed that the $2A^{pro}$ and $3C^{pro}$ sequences, while largely dissimilar to other proteases, retain some sequence homology with small and large bacterial trypsin-like proteases, respectively. The results from genetic [14, 15], mutagenic [14, 30, 31], and modeling [32, 33] studies on different serotypes concur that the catalytic site structure of $2A^{pro}$ and $3C^{pro}$, despite containing a cysteine (Cys) nucleophile, is most similar to that of small bacterial or large trypsin-like serine (Ser) proteases, respectively [15]. The classification of the Cys nucleophile-containing $2A^{pro}$ and $3C^{pro}$ as trypsin-like Ser proteases is unconventional, as natural trypsin-like proteases are normally classified based on the nucleophile (the central amino acid) in the catalytic site which is either Ser, Cys, aspartic acid (Asp), or zinc (Zn) [34]. Furthermore, while there is very low homology between HRV $2A^{pro}$ or $3C^{pro}$ and trypsin-like Ser cellular proteases, the two HRV proteases have high homology with one another, suggesting that $2A^{pro}$ and $3C^{pro}$ diverged from a common ancestor [15]. As can be seen in Fig. 2, $2A^{pro}$ and $3C^{pro}$ from HRV2 and HRV16 show high amino acid homology, yet there are critical differences in some amino acid residues.

Studies examining the substrate requirements of HRV14 $3C^{pro}$ expressed in *Escherichia coli* indicate that the protease requires an authentic glutamine/glycine (Gln/Gly) highly scissile bond to be

```
HRV2_2A       1 VHVGNLIYRNLHLFNSEMHESILVSYSSDLIIYRTNTVGDDYIPSCDCTQATYYCKHKNR
HRV16_2A      7 VHVGNLIYRNLHLFNSDIHDSILVSYSSDLIIYRTSTQGDGYIPTCNCTEATYYCKHKNR
                ****************  * *************** * ** *** * ** **********

HRV2_2A      61 YFPITVTSHDWYEIQESEYYPKHIQYNLLIGEGPCEPGDCGGKLLCKHGVIGIVTAGGDN
HRV16_2A     67 YYPINVTPHDWYEIQESEYYPKHIQYNLLIGEGPCEPGDCGGKLLCKHGVIGIITAGGEG
                * ** ** ****************************************** ****

HRV2_2A     121 HVAFIDLRHFHCAEEQ
HRV16_2A    127 HVAFIDLRHFHCAEEQ
                ****************
```

```
HRV2_3C       1 GPEEEFGMSLIKHNSCVITTENGKFTGLGVYDRFVVVPTHADPGKEIQVDGITTKVIDSY
HRV16_3C      1 GPEEEFGMSIIKNNTCVVTTTNGKFTGLGIYDRILILPTHADPGSEIQVNGIHTKVLDSY
                ********* ** * ** ** ******** ***    ******* **** ** *** ***

HRV2_3C      61 DLYNKNGIKLEITVLKLDRNEKFRDIRRYIPNNEDDYPNCNLALLANQPEPTIINVGDVV
HRV16_3C     61 DLFNKEGVKLEITVLKLDRNEKFRDIRKYIPESEDDYPECNLALVANQTEPTIIKVGDVV
                ** ** * ******************* ***  ***** ***** *** ***** *****

HRV2_3C     121 SYGNILLSGNQTARMLKYSYPTKSGYCGGVLYKIGQVLGIHVGGNGRDGFSAMLLRSYFT
HRV16_3C    121 SYGNILLSGTQTARMLKYNYPTKSGYCGGVLYKIGQILGIHVGGNGRDGFSSMLLRSYFT
                ********* ******** **************** ************* ********

HRV2_3C     181 DVQ
HRV16_3C    181 EQQ
                  *
```

**Fig. 2** Amino acid sequence alignment of HRV2 and HRV16 for $2A^{pro}$ and $3C^{pro}$. *Asterisks* indicate conservation of amino acid between HRV2 and HRV16

present in substrate peptides and, in vitro, it is unable to cleave mutagenically substituted cleavage sites in a synthetic protein. Interestingly, even though the presence of the natural Gln/Gly bond is necessary for $3C^{pro}$ activity in vitro, the presence of the Gln/Gly bond does not necessarily confer $3C^{pro}$ cleavage (i.e., they are not mutually inclusive) [30, 35]. For example, experimental production of an authentic peptide with a Gln/Gly bond, corresponding to an internal coding region of the $3C^{pro}$ sequence, is not recognized as a cleavage site by $3C^{pro}$ in vitro, in vivo, or during infection [35] suggesting that there is a secondary characteristic of either the $3C^{pro}$ or the peptide which is critical for recognition and cleavage. Recognition, in vivo, almost certainly occurs based on the primary sequence, as well as the secondary and tertiary structure, of the polyprotein [19, 36, 37].

Substitutions in the $3C^{pro}$ amino acid sequence at histidine-40 (His-40), glutamic acid-71 (Glu-71), or Cys-146 result in proteolytically inactive $3C^{pro}$ mutants [37]. Although the amino acid sites on the polyprotein necessary for $3C^{pro}$ cleavage are well documented, the role of the secondary and tertiary structure of the polyprotein necessary for $3C^{pro}$ recognition remains uncertain. This is partly due to the limited amino acid homology of cleavage site flanking sequences between different serotypes [19, 37] (e.g., HRV2 and HRV16, *see* Fig. 3), and that the crystal structure of the polyprotein has not been examined for all known HRV serotypes. Examination of the secondary and tertiary structure of the proteases from different serotypes will, undoubtedly, provide many insights into the role of amino acid sequence/physical structure on HRV during infection.

Similar results have been obtained for HRV $2A^{pro}$. The cleavage sites of numerous serotypes are heterogeneous; amino acids on the P′ side of the cleavage site are highly conserved between many serotypes and the $2A^{pro}$ appears to favor a P1 site of valine (Val) or alanine (Ala). Preferred amino acids for $2A^{pro}$ activity also occur at P2 (threonine or asparagine) and P3 (threonine or lysine) and the P4 residue is aliphatic in all examined cases. The HRV14 $2A^{pro}$ is the exception, requiring tyrosine (Tyr) and Ser at P1–P2, respectively. Mutagenesis of the P1 residues resulted in reduced cleavage by HRV2 $2A^{pro}$ in few cases, though the majority of residue substitutions did not significantly affect the cleavage ability of HRV2 $2A^{pro}$. However, when the P1′ residue was changed from Gly, $2A^{pro}$ could no longer cleave at this position for any of the serotypes examined. Interestingly, $2A^{pro}$ does not appear to have particular specificity for its own cleavage site [38]. Since $2A^{pro}$ is known to bind to its own cleavage site in *cis*, and other polyprotein cleavage sites in *trans*, these conformations have been suggested to be responsible for the permissive binding capacity of $2A^{pro}$ at its own cleavage site, with stricter conditions for binding other sites in *trans* [38, 39].

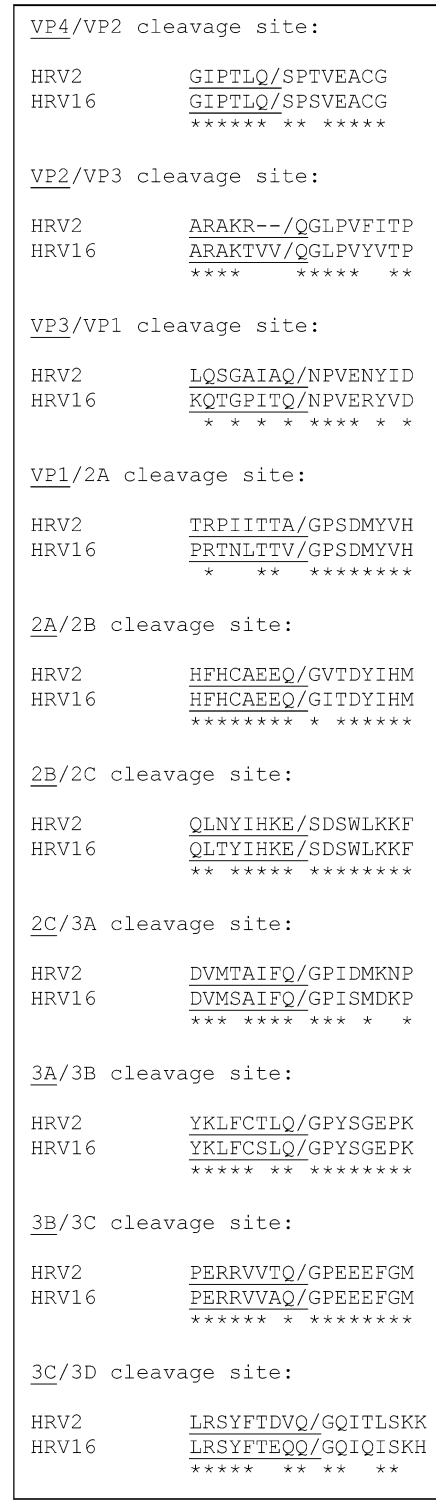


**Fig. 3** Amino acid sequence alignment of HRV2 and HRV16 polyprotein cleavage sites. *Asterisks* indicate conservation of amino acid between HRV2 and HRV16. Underlined residues correspond to the underlined viral protein, as indicated in each sub-heading; the amino acid at the junction of underlined and non-underlined amino acid sequences indicates the cleavage site between the two viral proteins. For reference, eight amino acid residues have been given for either side of the cleavage site for HRV2 and HRV16

## 3 Proteases and the Host Cell

Apart from their essential role in polyprotein processing, proteases also target several host proteins for cleavage (Table 1), either to mobilize cellular components for viral use or to inhibit specific antiviral pathways. As both $2A^{pro}$ and $3C^{pro}$ have been implicated in cleavage of cytoplasmic and nuclear proteins, altering cellular functions, assessment of their subcellular localization in HRV-infected cells can be a measure of the accessibility of the reported target proteins to $2A^{pro}$ and $3C^{pro}$ activity.

**Table 1**
**Host cell proteins targeted by HRV proteases**

| Host protein | Cellular localization | Cellular effect | Viral protease | Reference |
|---|---|---|---|---|
| PABP (poly-A-binding protein) | Cytoplasmic | Host translation shutoff | $2A^{pro}$ and $3C^{pro}$ | Chase and Semler [55], |
| eIF4G (eukaryotic translation initiation factor 4G) | Cytoplasmic | Host translation shutoff | $2A^{pro}$ | Etchison and Fout [56], Berstein [80], and Lloyd et al. [57] |
| MAP4 (microtubule-associated protein 4) | Cytoplasmic | Disruption of host microtubule network | $3C^{pro}$ | Joachims et al. [47] |
| OCT1 (octamer-binding transcription factor) | Nuclear | Disruption of host transcription | $3C^{pro}$ | Amineva et al. [40] |
| PCBP2 (poly(rC)-binding protein 2) | Nuclear and Cytoplasmic | Enhance viral translation/RNA replication | $3C^{pro}$ and $3C^{pro}D$ | Andino et al. [63], Andino et al. [64], Parsley et al. [65], and Gamarnik and Andino [66] |
| Nup153 (nucleoporin 153) | Nuclear membrane | Disruption of nucleocytoplasmic transport | $2A^{pro}$ and/or $3C^{pro}$ | Watters and Palmenberg [71] and Walker et al. [75] |
| Nup98 (nucleoporin 98) | Nuclear membrane | Disruption of nucleocytoplasmic transport | $2A^{pro}$ | Watters and Palmenberg [71] and Walker et al. [75] |
| Nup214 (nucleoporin 214) | Nuclear membrane | Disruption of nucleocytoplasmic transport | $2A^{pro}$ and/or $3C^{pro}$ | Watters and Palmenberg [71] and Ghildyal et al. [76] |
| Nup62 (nucleoporin 62) | Nuclear membrane | Disruption of nucleocytoplasmic transport | $2A^{pro}$ | Park et al. [81] |

### 3.1 Subcellular Localization of 3C$^{pro}$

During the initial stages of infection, 3C$^{pro}$-containing viral proteins begin accumulating in the nucleus, with these viral proteins gradually becoming cytoplasmic 4 h post-infection. As well as being located in the nucleus with access to RNA synthesis machinery, it has been shown that 3C$^{pro}$ co-localizes with the nucleolar chaperone protein nucleophosmin B23 [40], critical in ribosomal subunit assembly [41, 42]. Soon after synthesis, 3C$^{pro}$-containing proteins are located in punctate regions in the nucleoli. By 8 h, 3C$^{pro}$ is ubiquitous in the cell. Furthermore, although mature 3C$^{pro}$ is small enough to diffuse across the nuclear membrane, large 3C$^{pro}$ precursors are able to enter the nuclei of the cell via an as yet undefined mechanism [40]. 3C$^{pro}$ and 3C$^{pro}$D are thus ideally localized to act on nuclear as well as cytoplasmic components.

### 3.2 Subcellular Localization of 2A$^{pro}$

Localization of 2A$^{pro}$ in HRV-infected cells appears to be cell-type dependent. In human bronchial epithelial cells, 2A$^{pro}$ is localized in the cytoplasm, and also as strong, distinctly perinuclear circles. In HRV-infected HeLa cells, 2A$^{pro}$ is cytoplasmic but not nearly as distinct on the periphery of the nucleus [43]. Thus, 2A$^{pro}$, by virtue of its localization, has access to cytoplasmic substrates, but may not have access to components within the nuclei.

### 3.3 Effect on Cellular Response to HRV Infection

3C$^{pro}$ of some HRV serotypes is able to directly cleave melanoma differentiation-associated protein 5 (MDA-5) [44] and retinoic acid-inducible gene 1 RIG-I [45], cytoplasmic sensors of viral nucleic acids [46]. HRV14 3C$^{pro}$ also cleaves the cytoskeletal protein, microtubule-associated protein 4 (MAP-4), which results in depolymerization of the cellular microtubule network [47].

Picornavirus 3C$^{pro}$ directly and indirectly acts on cellular DNA-dependent RNA polymerases (polymerase I, pol II, and pol III) [48] via cleavage of polymerase-associated factors, or regulators, including but not limited to TATA-box-binding protein (TBP) (in poliovirus at least) [49], octamer-binding protein (OCT-1) [40], histone H3, and DNA polymerase III (shown for encephalomyocarditis virus-infected [50] and poliovirus-infected [51] cells, respectively, and likely to be analogous in HRV infection). As well as effects on cellular components in individual cells, HRV 3C$^{pro}$ has also been shown to increase production of interleukin-8 (IL-8) and granulocyte macrophage colony-stimulating factor (GM-CSF) in an HRV16 3C$^{pro}$-transfected cell culture system, by inducing transcription from IL-8 and GM-CSF promoters of a luciferase reporter in an activator protein 1 (AP-1) and nuclear factor kappa-light-chain enhancer of activated B cell (NF-κB)-dependent manner [52]. Interestingly, if intercellular adhesion molecule 1 (ICAM-1) is bound to anti-ICAM-1 in HRV16-infected human respiratory epithelial cell line (BEAS-2B), there is an inhibition of IL-8 production [53]. However, a reduction in IL-8 with ICAM-1/anti-ICAM-1 binding is not seen in *primary* human bronchial epithelial cells

during HRV16 infection, even though there is a reduction in RANTES (regulated on activation, normal T cell expressed and secreted) production [54]. In these studies, the authors suggest that $3C^{pro}$ alone is sufficient for induction of IL-8 during HRV infection. While the precise mechanism of this complex cytokine induction, or the role of protease activity therein, is unknown, it is likely, as suggested above, that attachment via ICAM-1 plays a role in the initiation of cytokine/chemokine induction during infection. Alternatively, as only the $3C^{pro}$ was transfected in these in vitro systems, at an amount which may be higher than during natural infection, it may be a complex interaction between attachment, transcription of viral RNA, or synthesis of other viral proteins which induce the promoters to produce IL-8 and GM-CSF.

### 3.4 Subversion of Cap-Dependent Translation

During the initial stages of infection, HRV induces structural and functional modifications in the host cell translation machinery, subverting host cell ribosomes so that only viral RNA will be translated. In contrast to cap-dependent cellular translation, viral RNA translation is mediated via the cap-independent internal ribosome entry site (IRES) in the 5′ noncoding region (NCR) of the RNA [55]. In order to convert ribosomal cap-dependent to cap-independent translation, HRV $2A^{pro}$ cleaves the eIF4G component of the eukaryotic initiation factor 4F (eIF4F) complex [56, 57]. This complex comprises three multisubunit complexes: eIF4E, eIF4A, and eIF4G which mediate cap binding by the complex [58] and mRNA processing for ribosomal binding [59, 60] and act as a scaffold for the eIF4E complex [61, 62], respectively. The switch from viral translation to replication of the viral genome is also achieved via redirection of host cell machinery through strategic protease activity (*see* below).

### 3.5 Switching from Translation to Replication

There is limited literature on HRV in this regard; most of our understanding comes from studies on poliovirus, which is presumed to be typical for picornaviruses in general. The $3C^{pro}$ and $3C^{pro}D$ cleave full-length poly(rC)-binding protein 2 (PCBP2) proteins, which interact with loops in the 5′ NCR, forming a complex with $3C^{pro}D$ to initiate negative-strand RNA synthesis [63–66]. PCBP2 is composed of three heterogeneous nuclear ribonucleoprotein (hnRNP) K homologous domains with a linker region [67]. The cleavage of this linker region by $3C^{pro}$ disrupts PCBP2 bound to 5′ NCR loops and halts cap-*in*dependent translation. The truncated version, however, is still able to bind to one 5′ NCR loop and maintain viral RNA synthesis [67]. In order to benefit the virus, there may be more host cell proteins that are cleaved to complement, or back up, PCBP2 cleavage in the change from viral RNA translation to replication, though these remain poorly defined [55].

HRV14 $3C^{pro}$ cleaves poly (A)-binding protein (PABP) in three places, and hence is believed to inhibit cap-dependent translation

indirectly [55]. In eukaryotic cells, PABP binds to the poly (A) tract, has a flexible linker in the protein interaction domain at the C-terminus (PABC), and has three recognition motifs for RNA [68]; these recognition motifs assist in the circularization of the mRNA to facilitate multiple rounds of translation [69]. Since viral RNA translation occurs in a 5′–3′ manner, and viral replication occurs from 3′ to 5′, there is a high probability that the ribosome will collide with the polymerase unless there is a distinct switch between translation and replication. Cleavage of PCBP2 and PABP either affords a synergistic effect or functions to ensure that the virus is able to switch between translation of viral proteins and replication of the viral genome [55].

### 3.6 Disruption of Nuclear Transport

Cleavage of distinct nucleoporin proteins (Nups) that are the building blocks comprising the cellular nuclear pore complexes (NPCs) results in disruption of signal-dependent nucleocytoplasmic transport and signaling in HRV-infected cells. This cleavage has been attributed to HRV $2A^{pro}$, which shows different cleavage rates depending on whether $2A^{pro}$ is from HRV-A, HRV-B, or HRV-C. Additionally, HRV $2A^{pro}$ cleaves multiple sites in several Phe/Gly-containing Nups (FG Nups), which comprise the central channel of NPCs, resulting in nuclear-cytoplasmic transport disruptions [70, 71]. Large molecules require the FG Nups to help facilitate active transport across the nucleus via interactions with the host cell importin (Imp) superfamily of transporters, while small molecules of <50 kDa are able to transit the NPC by passive diffusion. Cleavage of Nups in infected cells generally leads to an efflux of nuclear proteins, such as Sam 68, La, PTB, SRp20, and nucleolin, to the cytoplasm [71–73].

The specificities for $2A^{pro}$ derived from different subgroups vary greatly for Nup62, Nup98, and Nup153, as well as for eIF4G (HRV-A > HRV-C >> HRV-B) [71]. This may be the reason why HRV-B viruses are often associated with less virulent forms of HRV illness than HRV-A and HRV-C [74].

In a similar fashion to HRV $2A^{pro}$, HRV $3C^{pro}$ has been shown to cleave Nup153 in vitro [75], as well as Nup358 and Nup214 either directly or indirectly [76]. In HRV-infected cells, the order of cleavage is postulated to be Nup98, Nup153 followed by Nup62 (with cleavage of Nup98 and Nup62 believed to be mainly mediated via $2A^{pro}$). Interestingly, these Nups are all FG Nups involved in shuttling molecules across the NPC, whereas $3C^{pro}$ does not appear to cleave non-FG Nups, such as Nup93 and Nup133, which are involved in NPC structure rather than transport through the NPC; this correlates with the observation that the gross structure of the NPC remains largely intact during HRV infection. The effect of Nup cleavage by $3C^{pro}$ on the permeability of the nuclear membrane is considerable, resulting in the diffusion into the nucleus of large normally cytoplasmic molecules that lack nuclear targeting sequences [76].

## 4 Conclusions

As outlined above, the HRV proteases $2A^{pro}$ and $3C^{pro}$ are critical for HRV infection and replication. Their ability to initiate host cell shutoff by cleaving eIF4G ($2A^{pro}$) to switch the cell to cap-independent translation [56, 57] and cleaving PABP ($3C^{pro}$) to indirectly inhibit cap-dependent translation [55] are example of their critical role in virus replication. Further, immune system modulation via cytokine induction [52, 77], resulting in the "cold" symptoms and exacerbation of underlying airway illness, may relate directly to the role of proteases in HRV infection.

Although HRV infection is usually self-limiting and causes mild symptoms [3, 4], it is responsible for significant worldwide health and economic impact [1, 2]. In particular, the many HRV serotypes mean that vaccination is currently not an option [9]; a prophylactic that limits disease by targeting well-conserved viral proteins or interactions with host cells appears to be a more feasible option. Anti-HRV drug discovery research has focused on inhibitors to prevent virus attachment to target cells, but since HRVs use at least two different cellular receptors, ICAM-1 [78] and LDL (low-density lipoprotein) receptor [79], targeting receptor binding would require patients to take prophylactics blocking both cellular receptors and antiviral treatment after laboratory testing to determine the causative subtype. A better option appears to be targetting viral proteins which are highly conserved between the serotypes; the HRV proteases represent a highly practical opportunity in this context. The encouraging results obtained in experimental infection trials with the anti-$3C^{pro}$ drug Rupintrivir are consistent with this idea, and encourage optimism in anti-protease drug development for the future.

## Acknowledgements

This research was supported by National Health and Medical Research Council (Australia) project (APP545844 and APP1027312) grants and SPRF1 fellowship (to DAJ; APP1002486).

### References

1. Gwaltney JM (1975) Yale J Biol Med 48:17–45
2. Skern T, Sommergruber W, Blaas D, Gruendler P, Fraundorfer F, Pieler C, Fogy I, Keuchler E (1985) Nucleic Acid Res 13:2111–2126
3. Arruda E, PitkÃranta A, Witek TJ, Doyle CA, Hayden FG (1997) J Clin Microbiol 35: 2864–2868
4. Pitkaranta A, Hayden FG (1998) Ann Med 30: 529–537
5. Nicholson KG, Kent J, Hammersley V, Cancio E (1997) Br Med J 315:1060–1064
6. Message SD, Laza-Stanca V, Mallia P, Parker HL, Zhu J, Kebadze T, Contoli M, Sanderson G, Kon OM, Papi A, Jeffery PK, Stanciu LA, Johnston SL (2008) Proc Natl Acad Sci 105: 13562–13567
7. Nicholson KG, Kent J, Ireland DC (1993) BMJ 307:982–986

8. Johnston SL, Pattemore PK, Sanderson G, Smith S, Lampe F, Josephs L, Symington P, O'Toole S, Myint SH, Tyrrell DAJ, Holgate ST (1995) Br Med J 310:1225–1229
9. Fox JP (1976) Am J Epidemiol 103:345–354
10. Cooney MK, Kenny GE (1970) J Immunol 105:531–533
11. Cooney MK, Fox JP, Kenny GE (1982) Infect Immun 37:642–647
12. Rueckert RR (1996) In: Fields BN, Knipe DM, Howley PM (eds) Fields virology, 3rd edn, Lippincott-Raven, Philadelphia, PA, p 609–654
13. Stanway G, Hughes PJ, Mountford RC, Minor PD, Almond JW (1984) Nucleic Acid Res 12: 7859–7875
14. Knott JA, Orr DC, Montgomery DS, Sullivan CA, Weston A (1989) Eur J Biochem 182: 547–555
15. Bazan JF, Fletterick RJ (1988) Proc Natl Acad Sci U S A 85:7872–7876
16. Savolainen C, Mulders MN, Hovi T (2002) Virus Res 85:41–46
17. Lau SK, Yip CC, Tsoi HW, Lee RA, So LY, Lau YL, Chan KH, Woo PC, Yuen KY (2007) J Clin Microbiol 45:3655–3664
18. Binford SL, Maldonado F, Brothers MA, Weady PT, Zalman LS, Meador JW 3rd, Matthews DA, Patick AK (2005) Antimicrob Agents Chemother 49:619–626
19. Cordingley MG, Callahan PL, Sardana VV, Garsky VM, Colonno RJ (1990) J Biol Chem 265:9062–9065
20. Matthews DA, Dragovich PS, Webber SE, Fuhrman SA, Patick AK, Zalman LS, Henrickson TF, Love RA, Prins TJ, Marakovits JT, Zhou R, Tikhe J, Ford CE, Meador JW, Ferre RA, Brown EL, Binford SL, Brothers MA, DeLisle DM, Worland ST (1999) Proc Natl Acad Sci U S A 96:11000–11007
21. Toyoda H, Nicklin MJH, Murray MG, Anderson CW, Dunn JJ, Studier FW, Wimmer E (1986) Cell 45:761–770
22. Sommergruber W, Zorn M, Blaas D, Fessl F, Volkmann P, Maurer-Fogy I, Pallai P, Merluzzi V, Matteo M, Skern T, Kuechler E (1989) Virology 169:68–77
23. Kräusslich HG, Wimmer E (1988) Annu Rev Biochem 57:701–754
24. Kay J, Dunn BM (1990) Biochim Biophys Acta 1048:1–18
25. Lawson MA, Semler BL (1990) Curr Top Microbiol Immunol 161:49–87
26. Dragovich PS, Zhou R, Skalitzky DJ, Fuhrman SA, Patick AK, Ford CE, Meador Iii JW, Worland ST (1999) Bioorg Med Chem 7: 589–598
27. Patick AK, Binford SL, Brothers MA, Jackson RL, Ford CE, Diem MD, Maldonado F, Dragovich PS, Zhou R, Prins TJ, Fuhrman SA, Meador JW, Zalman LS, Matthews DA, Worland ST (1999) Antimicrob Agents Chemother 43:2444–2450
28. Hayden FG, Turner RB, Gwaltney JM, Chi-Burris K, Gersten M, Hsyu P, Patick AK, Smith GJ, Zalman LS (2003) Antimicrob Agents Chemother 47:3907–3916
29. Patick AK, Brothers MA, Maldonado F, Binford S, Maldonado O, Fuhrman S, Petersen A, Smith GJ 3rd, Zalman LS, Burns-Naas LA, Tran JQ (2005) Antimicrob Agents Chemother 49:2267–2275
30. Orr DC, Long AC, Kay J, Dunn BM, Cameron JM (1989) J Gen Virol 70:2931–2942
31. Cheah KC, Leong LE, Porter AG (1990) J Biol Chem 265:7180–7187
32. Petersen JF, Cherney MM, Liebig HD, Skern T, Kuechler E, James MN (1999) EMBO J 18: 5463–5475
33. Seipelt J, Guarne A, Bergmann E, James M, Sommergruber W, Fita I, Skern T (1999) Virus Res 62:159–168
34. Neurath H (1984) Science 224:350–357
35. Cordingley MG, Register RB, Callahan PL, Garsky VM, Colonno RJ (1989) J Virol 63:5037–5045
36. Ypma-Wong MF, Dewalt PG, Johnson VH, Lamb JG, Semler BL (1988) Virology 166: 265–270
37. Leong LE, Walker PA, Porter AG (1993) J Biol Chem 268:25735–25739
38. Skern T, Sommergruber W, Auer H, Volkmann P, Zorn M, Liebig HD, Fessl F, Blaas D, Kuechler E (1991) Virology 181:46–54
39. Hellen CU, Lee CK, Wimmer E (1992) J Virol 66:3330–3338
40. Amineva SP, Aminev AG, Palmenberg AC, Gern JE (2004) J Gen Virol 85:2969–2979
41. Sipos K, Olson MOJ (1991) Biochem Biophys Res Commun 177:673–678
42. Szebeni A, Olson MOJ (1999) Protein Sci 8: 905–912
43. Amineva SP, Aminev AG, Gern JE, Palmenberg AC (2011) J Gen Virol 92:2549–2557
44. Barral PM, Morrison JM, Drahos J, Gupta P, Sarkar D, Fisher PB, Racaniello VR (2007) J Virol 81:3677–3684
45. Barral PM, Sarkar D, Fisher PB, Racaniello VR (2009) Virology 391:171–176

46. Barral PM, Sarkar D, Su Z-Z, Barber GN, DeSalle R, Racaniello VR, Fisher PB (2009) Pharmacol Therapeut 124:219–234
47. Joachims M, Harris KS, Etchison D (1995) Virology 211:451–461
48. Lin J-Y, Chen T-C, Weng K-F, Chang S-C, Chen L-L, Shih S-R (2009) J Biomed Sci 16:103
49. Clark ME, Lieberman PM, Berk AJ, Dasgupta A (1993) Mol Cell Biol 13:1232–1237
50. Falk MM, Grigera PR, Bergmann IE, Zibert A, Multhaup G, Beck E (1990) J Virol 64: 748–756
51. Clark ME, HÃmmerle T, Wimmer E, Dasgupta A (1991) EMBO J 10:2941–2947
52. Funkhouser AW, Kang J, Tan A, Li J, Zhou L, Abe MK, Solway J, Hershenson MB (2004) Pediatr Res 55:13–18
53. Kim J, Sanders SP, Siekierski ES, Casolaro V, Proud D (2000) J Immunol 165:3384–3392
54. Schroth MK, Grimm E, Frindt P, Galagan DM, Konno SI, Love R, Gern JE (1999) Am J Respir Cell Mol Biol 20:1220–1228
55. Chase AJ, Semler BL (2012) Future Virol 7: 179–191
56. Etchison D, Fout S (1985) J Virol 54: 634–638
57. Lloyd RE, Grubman MJ, Ehrenfeld E (1988) J Virol 62:4216–4223
58. Sonenberg N, Morgan MA, Merrick WC, Shatkin AJ (1978) Proc Natl Acad Sci 75: 4843–4847
59. Ray BK, Lawson TG, Kramer JC, Cladaras MH, Grifo JA, Abramson RD, Merrick WC, Thach RE (1985) J Biol Chem 260:7651–7658
60. Rozen F, Edery I, Meerovitch K, Dever TE, Merrick WC, Sonenberg N (1990) Mol Cell Biol 10:1134–1144
61. Lamphear BJ, Yan R, Yang F, Waters D, Liebig HD, Klump H, Kuechler E, Skern T, Rhoads RE (1993) J Biol Chem 268:19200–19203
62. Lamphear BJ, Kirchweger R, Skern T, Rhoads RE (1995) J Biol Chem 270:21975–21983
63. Andino R, Rieckhof GE, Baltimore D (1990) Cell 63:369–380
64. Andino R, Rieckhof GE, Achacoso PL, Baltimore D (1993) EMBO J 12:3587–3598
65. Parsley TB, Towner JS, Blyn LB, Ehrenfeld E, Semler BL (1997) RNA 3:1124–1134
66. Gamarnik AV, Andino R (1998) Genes Dev 12:2293–2304
67. Perera R, Daijogo S, Walter BL, Nguyen JHC, Semler BL (2007) J Virol 81:8919–8932
68. Kozlov G, Trempe J-F, Khaleghpour K, Kahvejian A, Ekiel I, Gehring K (2001) Proc Natl Acad Sci 98:4409–4413
69. Jacobson A, Favreau M (1983) Nucleic Acids Res 11:6353–6368
70. Park N, Katikaneni P, Skern T, Gustin KE (2008) J Virol 82:1647–1655
71. Watters K, Palmenberg AC (2011) J Virol 85: 10874–10883
72. Gustin KE, Sarnow P (2002) J Virol 76: 8787–8796
73. Fitzgerald KD, Chase AJ, Cathcart AL, Tran GP, Semler BL (2013) J Virol 87:2390–2400
74. Bizzintino J, Lee WM, Laing IA, Vang F, Pappas T, Zhang G, Martin AC, Khoo SK, Cox DW, Geelhoed GC, McMinn PC, Goldblatt J, Gern JE, Le SouÃf PN (2011) Eur Res J 37: 1037–1042
75. Walker EJ, Younessi P, Fulcher AJ, McCuaig R, Thomas BJ, Bardin PG, Jans DA, Ghildyal R (2013) PLoS One 8:e71316
76. Ghildyal R, Jordan B, Li D, Dagher H, Bardin PG, Gern JE, Jans DA (2009) J Virol 83: 7349–7352
77. Singh M, Lee S-H, Porter P, Xu C, Ohno A, Atmar RL, Greenberg SB, Bandi V, Gern J, Amineva S, Aminev A, Skern T, Smithwick P, Perusich S, Barrow N, Roberts L, Corry DB, Kheradmand F (2010) J Allergy Clin Immunol 125:1369e2–1378e2
78. Greve JM, Davis G, Meyer AM, Forte CP, Yost SC, Marlor CW, Kamarck ME, McClelland A (1989) Cell 56:839–847
79. Hofer F, Gruenberger M, Kowalski H, Machat H, Huettinger M, Kuechler E, Blaas D (1994) Proc Natl Acad Sci U S A 91:1839–1842
80. Bernstein HD, Sonenberg N Baltimore D (1985) *Poliovirus mutant that does not selectively inhibit host cell protein synthesis.* Molecular and Cellular Biology. 5(11):2913–2923
81. Park N, Skern T, Gustin KE (2010) *Specific Cleavage of the Nuclear Pore Complex Protein Nup62 by a Viral Protease.* Journal of Biological Chemistry 285(37): 28796–28805

# Chapter 11

# A Protocol to Express and Isolate HRV16 3C Protease for Use in Protease Assays

**Lora M. Jensen, Erin J. Walker, and Reena Ghildyal**

## Abstract

Human rhinovirus (HRV) proteases are highly conserved across serotypes and have very similar target specificity. However, there are some serotype-specific differences in their action. It is therefore necessary when performing in vitro protease assays to ensure that the recombinant proteases are specific to the serotype of the HRV under study. We describe a simple method for isolating HRV16 3C protease from a bacterial expression system, including transformation of bacterial cells with a commercially available cDNA plasmid which can be adapted to use for 3C proteases from any other HRV serotypes. The extracted, active 3C protease can then be used for in vitro protease assays.

**Key words** HRV16 3C protease, In vitro protease activity assays, Recombinant protein purification

## 1 Introduction

Human rhinoviruses (HRVs) are small, positive-stranded RNA viruses responsible for respiratory infections worldwide [1]. As well as being the etiological agent responsible for the "common cold," infection with HRVs also results in the majority of asthma exacerbations [2, 3]. Unfortunately there are currently no vaccines against HRV as there are more than 100 serotypes, each of which has different characteristics. The differences between HRV serotypes extend beyond cross-reactivity to their viral components. Of all the proteins in HRVs, the most active in driving the host cell towards cap-independent translation and viral replication are the viral proteases 2A and 3C ($2A^{pro}$ and $3C^{pro}$, respectively). These proteases are responsible for host cell machinery disruption via cleavage of multiple host cell proteins (e.g., eIF4G, PABP) [4, 5]; disruption of cell nuclear-cytoplasmic transport by cleaving nuclear pore proteins (e.g., Nup 62, Nup153) [6, 7]; and potentially modulating the immune response [8]. The study of $2A^{pro}$ and $3C^{pro}$ is challenging as their characteristics vary between serotypes [5]. It is therefore preferable when studying HRV proteases to isolate and

David A. Jans and Reena Ghildyal (eds.), *Rhinoviruses: Methods and Protocols*, Methods in Molecular Biology, vol. 1221, DOI 10.1007/978-1-4939-1571-2_11, 

manipulate the protease of the same serotype used in other experiments. Here we provide a method for isolation of HRV16 $3C^{pro}$ from a commercial expression plasmid. This method relies on the use of a bacterial expression system to produce the $3C^{pro}$ of interest. After expression and induction, the bacteria are centrifuged and the resultant pellet is lysed and cleaned to collect the HRV $3C^{pro}$. This protease can then be used in a protease assay to cleave proteins, and results can be observed via Western blotting methods. A similar method could be used for isolation and expression of the $3C^{pro}$ of any HRV serotype, or for expression of $2A^{pro}$.

## 2 Materials

### 2.1 Generating HRV16 3C Expression Clone and Inducing 3C Expression

1. BL21(DE3) competent cells or similar cells for protein expression.
2. HRV16 3C cDNA expression plasmid (*see* **Note 1**).
3. Autoclaved Luria Broth: 85 mM NaCl, 1 % peptone (tryptone), 0.5 % yeast extract.
4. Luria agar plates: 85 mM NaCl, 2 % bacterial agar, 1 % peptone (tryptone), 0.5 % yeast extract with an appropriate antibiotic added.
5. 1 M isopropyl-beta-D-thiogalactopyranoside (IPTG).
6. Sterile 17 × 100 mm culture tubes.
7. Water bath at 42 °C.
8. Shaking incubator at 37 °C.

### 2.2 Isolating HRV16 3C

1. Pellet of *E. coli* IPTG-induced cells.
2. Native lysis buffer: 50 mM $NaH_2PO_4$, 300 mM NaCl, 10 mM imidazole (pH 8.0).
3. Lysozyme (10 mg/mL).

### 2.3 Collecting Ohio-Hela Cell Lysate

1. 0.05 % Trypsin/0.02% EDTA: Dissolve 1 g of EDTA (Na salt, MW 372.25) in 100 mL of 1× PBS. Autoclave. Dissolve 2.5 g of trypsin in 100 mL of 1× PBS. Sterile filter. Aliquot into 1 mL aliquots and freeze.
2. 10× PBS: 26.82 mM KCl, 1.36 M NaCl, 101.48 mM $Na_2HPO_4$, 17.63 mM $KH_2PO_4$.
3. Complete media: 10 % FBS, DMEM, and 1× PSN.
4. RIPA buffer: 150 mM NaCl, 1 % Triton X 100, 0.1 % SDS, 0.5 % sodium deoxycholate (*see* **Note 2**), 50 mM Tris (pH 8).
5. 0.2 % Trypan blue.
6. Confluent flask/dish of Ohio-Hela cells.
7. Hemocytometer and cover slip.

### 2.4 Setting Up Protease Reactions

1. HRV14 10x cleavage buffer: 1.5 M NaCl, 0.5 M Tris–HCl (pH 7.5).
2. Nuclease-free water.
3. Ohio-Hela lysate.
4. Collected HRV16 3C protease.
5. Laemmli buffer: 3 mM bromophenol blue, 30 % glycerol (v/v), 346 mM sodium dodecyl sulfate (SDS), 0.35 M Tris (pH 6.8), 603 mM dithiothreitol (DTT).

## 3 Methods

All reactions are set up on ice and must be kept as cold as possible, unless otherwise specified.

### 3.1 Generating HRV16 3C Expression Clone

1. Precool culture tube on ice. Remove competent cells from −70 °C freezer and place on ice for a few minutes, until the cells are just thawed. Use 100 μL of cells per transformation.
2. Add 25–50 ng of plasmid DNA to the thawed competent cells. Quickly flick the tube to disperse the DNA. Place the tubes on ice for 10 min.
3. Heat shock the cells in the water bath at 42 °C for 90 s, and then immediately place on ice again for 2 min.
4. Add 900 μL of cold LB media to each tube and incubate at 37 °C for 60 min in a shaking incubator at 220 rpm.
5. After 1 h, plate 100 μL of transformed cells onto antibiotic plates and incubate for ~16 h at 37 °C.

### 3.2 Inducing Expression of 3C Protease

1. Aliquot 5 mL of LB media into a culture tube, adding the appropriate antibiotic, and inoculate the LB with one colony from the transformation plate.
2. Incubate for 16 h at 37 °C, with shaking at 220 rpm.
3. The following day, use 0.5 mL of the 5 mL culture to inoculate 50 mL of LB with antibiotic (*see* **Note 3**).
4. Shake the culture at 37 °C until the $OD_{600}$ reaches 0.3–0.5.
5. Induce expression of 3C protease with a final concentration of 1 mM IPTG and incubate with shaking at 220 rpm for 5 h at 37 °C.
6. Collect the bacterial cells in 6 mL aliquots by centrifugation (12,000 × *g* for 10 min), discard the supernatant, and freeze cells at −20 °C until required.

### 3.3 Recovering HRV16 3C (Adapted from Qiagen QIAexpressionist Protocol 14)

1. Resuspend the *E. coli* pellet in 600 μL of "native lysis buffer" (*see* **Note 4**). Make sure that the cells are properly resuspended before continuing with the lysis (*see* **Note 5**).
2. Add lysozyme to 1 mg/mL (60 μL in 600 μL), and gently pipette up and down. Incubate cells on ice for 30 min.
3. After 30 min, gently vortex the cells, being careful to avoid frothing.
4. Centrifuge the lysate for 10 min at 12,000–15,000 × *g* at 4 °C to remove cellular debris.
5. Transfer the supernatant containing HRV16 3C to a fresh tube without disturbing the cell pellet; keep the 3C on ice. The supernatant should contain clean, active HRV16 3C.

### 3.4 Collecting Ohio-Hela Cell Lysate

1. Bring HRV14 3C 10x cleavage buffer from –20 °C to room temperature to thaw.
2. Wash cell monolayer with warm PBS followed by trypsinization with trypsin/EDTA at 37 °C.
3. Once trypsinized, count cells: pipette 900 μL of complete media into a 1.5 mL Eppendorf tube. Add 100 μL of cell suspension in tryspin/EDTA to the 900 μL of complete media. Take 20 μL of this cell suspension and dilute 1:2 with 20 μL of 0.2 % trypan blue. Gently mix. Using a hemocytometer, add 10 μL to either side and count the cells as advised by the manufacturer. Calculate the number of cells you have per mL to determine the volume of RIPA buffer required (use 1 mL per $1 \times 10^7$ cells).
4. Centrifuge the cells at 500 × *g*, 4 °C, for 5 min. Remove supernatant, being careful not to dislodge the pellet. Resuspend the cells in 1 mL cold PBS.
5. Centrifuge again at 500 × *g*, 4 °C, for 5 min. Carefully remove the supernatant until the pellet is dry. Discard supernatant.
6. Add required volume of RIPA buffer to the pellet, being sure to resuspend pellet well.
7. Lyse the cells gently at 4 °C for 30 min, either with constant rotation or manually by inverting the tube twice every 5 min. While the cells are lysing, begin setting up protease reactions.
8. After 30 min of lysis, centrifuge the cells at 12,000 × *g*, 4 °C, for 5 min. Carefully collect supernatant for use in the protease reaction.

### 3.5 Setting Up Protease Reactions

1. To prepare 50 μL protease reactions, use nuclease-free water, HRV14 3C 10× cleavage buffer, Ohio-Hela cell lysate, and the HRV16 3C protease. Add nuclease-free water to one PCR tube first. Add the Ohio-Hela lysate, and HRV14 3C cleavage buffer next. Add the HRV16 3C last. Continue for all reactions. *See* Table 1 for reaction volumes.

**Table 1**
**Protease assay reaction volumes**

| Reaction | OHela lysate (μL) | HRV14 cleavage buffer (μL) | HRV16 3C (μL) | Nuclease-free water (μL) |
|---|---|---|---|---|
| Lysate only (0 h)[a] | 20 | 5 | 0 | 25 |
| Lysate only (16 h)[a] | 20 | 5 | 0 | 25 |
| 10 μL 3C | 20 | 5 | 10 | 15 |
| 15 μL 3C | 20 | 5 | 15 | 10 |
| 25 μL 3C | 20 | 5 | 25 | 0 |

[a]0- and 16-h controls show changes in lysate, such as endogenous degradation of proteins within the given time frame. Neither control contains any 3C

2. As well as HRV16 3C reactions, controls for lysate-only changes are required. Stop the 0-h control as soon as all reagents are mixed together by adding 10 μL of 5× Laemelli buffer to the sample and storing at −20 °C immediately.
3. Incubate the remaining reactions at 30 °C for 16 h. Stop the reactions by adding 5× Laemelli buffer and heating the samples at 90 °C for 5 min. Freeze at −20 °C until ready to analyze.
4. Proteins can be loaded on an acrylamide gel and transferred for Western blotting for visualization and staining. Figure 1 demonstrates typical results observed using this protocol. The anti-His blot shows increasing amounts of 3C protease corresponding to the reactions in Table 1, the anti-PABP (poly-A-binding protein) blot shows a decrease in PABP indicating 3C protease activity [9] while the tubulin blot shows equal loading in all lanes.

## 4 Notes

1. We use an expression plasmid with a recombinant His tag, to easily identify the 3C protease.
2. Sodium deoxycholate must be protected from light and we have found that it dissolves better at 5 % than 10 %.
3. The culture volumes can be scaled up to produce larger volumes of 3C protease as required.
4. The volume of lysis buffer can be adjusted depending on the volume of induced culture used to produce a pellet. We use 100 μL per mL of bacterial culture.
5. Addition of the lysis buffer can make the pellet very sticky and difficult to resuspend. If this is the case, a small volume of water (~50–100 μL) can be added to help loosen the pellet, before addition of the lysis buffer.

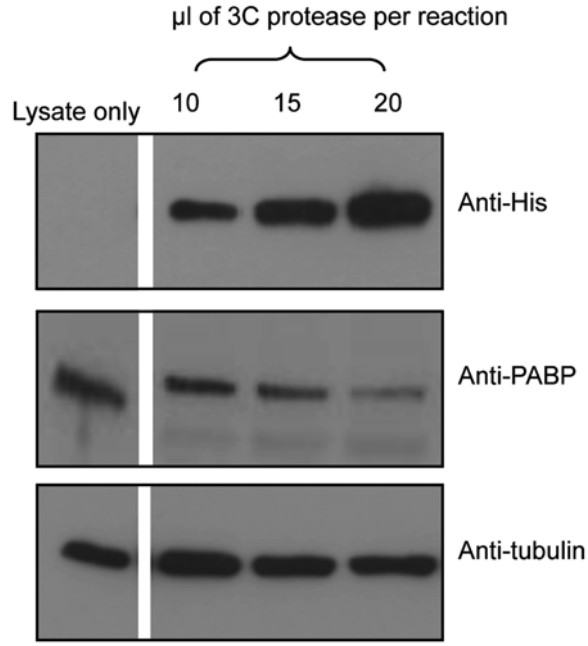


**Fig. 1** Typical Western blot results for the protease assay. Ohio-HeLa cell lysate was collected in RIPA buffer without inhibitors. Identical volumes of cell lysate were incubated for 16 h with different volumes of HRV16 3C protease, as indicated. Lysates were subjected to SDS-PAGE on 12.5 % gels and Western analysis using the indicated primary antibodies/horseradish peroxidase-conjugated secondary antibodies and enhanced chemiluminescence

## References

1. Racaniello VR (2001) Picornaviridae: the viruses and their replication. In: Knipe DM, Howley PM (eds) Fields virology. Lippincott/Raven, Philadelphia, PA, p 685–722
2. Lee WM et al (2007) A diverse group of previously unrecognized human rhinoviruses are common causes of respiratory illnesses in infants. PLoS One 2:e966
3. Nicholson KG, Kent J, Ireland DC (1993) Respiratory viruses and exacerbations of asthma in adults. BMJ 307:982–986
4. Chase AJ, Semler BL (2012) Viral subversion of host functions for picornavirus translation and RNA replication Future. Virol 7:179–191
5. Watters K, Palmenberg AC (2011) Differential processing of nuclear pore complex proteins by rhinovirus 2A proteases from different species and serotypes. J Virol 85:10874–10883
6. Ghildyal R et al (2009) Rhinovirus 3C protease can localize in the nucleus and alter active and passive nucleocytoplasmic transport. J Virol 83: 7349–7352
7. Gustin KE, Sarnow P (2002) Inhibition of nuclear import and alteration of nuclear pore complex composition by rhinovirus. J Virol 76: 8787–8796
8. Funkhouser AW et al (2004) Rhinovirus 16 3C protease induces interleukin-8 and granulocyte-macrophage colony-stimulating factor expression in human bronchial epithelial cells. Pediatr Res 55:13–18
9. Bushell M et al (2001) Disruption of the interaction of mammalian protein synthesis eukaryotic initiation factor 4B with the poly(A)-binding protein by caspase- and viral protease-mediated cleavages. J Biol Chem 276:23922–23928

# Chapter 12

# Reverse Genetics System for Studying Human Rhinovirus Infections

**Wai-Ming Lee, Wensheng Wang, Yury A. Bochkov, and Iris Lee**

## Abstract

Human rhinovirus (HRV) contains a 7.2 kb messenger-sense RNA genome which is the template for reproducing progeny viruses after it enters the cytoplasm of a host cell. Reverse genetics refers to the regeneration of progeny viruses from an artificial cDNA copy of the RNA genome of an RNA virus. It has been a powerful molecular genetic tool for studying HRV and other RNA viruses because the artificial DNA stage makes it practical to introduce specific mutations into the viral RNA genome. This chapter uses HRV-16 as the model virus to illustrate the strategy and methods for constructing and cloning the artificial cDNA copy of a full-length HRV genome, identifying the infectious cDNA clone isolates, and selecting the most vigorous cDNA clone isolate to serve as the standard parental clone for future molecular genetic study of the virus.

**Key words** RNA virus, Full-length infectious cDNA clone, In vitro transcription, Transfection

## 1 Introduction

HRV is a small single-stranded RNA virus. Its naked positive-sense RNA genome is infectious; that is, it can initiate a complete viral reproduction cycle that produces infectious progeny viruses when it is transfected into a permissive cell [1–3].

After its invention in the early 1970s, recombinant DNA technology/genetic engineering quickly became a powerful tool for studying DNA viruses. Unfortunately, genetic engineering technique is not easily applied to RNA molecules. In hopes of being able to use genetic engineering as a routine technique for studying RNA viruses, researchers explored new ways to regenerate RNA viruses from the cDNA copies of their genomes. In 1978, Taniguchi and co-workers reported the regeneration of RNA bacteriophage Qbeta from a plasmid that carried the full-length cDNA copy of the viral RNA genome [4]. However, regeneration

David A. Jans and Reena Ghildyal (eds.), *Rhinoviruses: Methods and Protocols*, Methods in Molecular Biology, vol. 1221, DOI 10.1007/978-1-4939-1571-2_12, 

of RNA virus directly from a cloned cDNA copy of its genome is very inefficient and only works for some RNA viruses. For example, 1 μg of plasmid DNA carrying the cDNA copy of the poliovirus 1 genome produced only seven infectious units of progeny virus and the same amount of HRV14 plasmid generated no virus when they were transfected into HeLa cells [2, 5]. These problems were soon overcome by the use of in vitro T7 RNA transcripts derived from the cloned cDNA copy of a viral RNA genome. In 1984, Paul Ahlquist and co-workers reported the regeneration of the bromo mosaic virus by transfecting the T7 RNA transcripts of the cDNA clone of its genome into host cells [6]. T7 RNA transcripts have been shown to be as efficient as the viral RNA genome in regenerating progeny virus and the method works for every positive, single-stranded RNA virus. For example, 1 μg of T7 RNA transcripts from the cDNA clones of poliovirus 1 and HRV14 produced 1.5 and 2 million infectious units of virus, respectively [2].

Making an infectious full-length cDNA clone of the large linear single-stranded RNA genome of HRV is a complex project that requires the use of multiple methods. Here, we use the HRV-16 laboratory strain as the model virus to illustrate the overall strategy and methods for cloning the cDNA copy of a full-length HRV genome (viral RNA extraction, cDNA synthesis, PCR amplification of the HRV genome, cloning of the PCR fragments, assembly of the PCR fragments into a full-length cDNA clone), identifying the infectious cDNA clones (making in vitro RNA transcripts, transfecting the RNA transcripts into HeLa cells, and testing viral infectivity), and selecting one of the infectious clones to serve as the standard parental clone for future molecular genetic work (determining the growth kinetics of their progeny viruses and the infectivity of their RNA transcripts).

## 2 Materials

### 2.1 Construction of the Full-Length cDNA Clone

1. Cloning vector: pMJ3 plasmid DNA (*see* **Note 1**).
2. Equipment:
   (a) Incubator shaker.
   (b) 37 °C incubator for bacterial plates.
   (c) Eppendorf thermomixer.
   (d) PCR machine.
3. PCR primers: They are typically ordered from Eurofins-MWG-Operon or Sigma-Proligo. The basic "desalt" grade is sufficient for PCR.

4. Restriction enzymes: They are typically ordered from New England Biolab (NEB), and come with 10× reaction buffer and BSA.
5. Sterile disposables for molecular cloning.
   (a) 1.5-ml DNA LoBind (LB) eppi tube (Eppendorf 022431021).
   (b) 0.5-ml DNA LoBind (LB) eppi tube (Eppendorf 022431005).
   (c) 20–200-μl barrier pipette tips.
   (d) 100–1,000-μl barrier pipette tips.
   (e) 0.2-ml thin-wall polypropylene eight-tube strips for PCR.
   (f) Domed eight-cap strips for 0.2-ml PCR tubes.
   (g) 50-ml Falcon blue-cap tubes.
   (h) 14-ml polypropylene tubes.
   (i) 5-ml polystyrene tubes.
6. Reagents for viral RNA extraction:
   (a) Phenol—UltraPure.
   (b) Chloroform.
   (c) 2-Propanol.
   (d) Ethanol—Absolute.
   (e) Glycoblue, 15 μg/μl (Invitrogen AM9515).
   (f) DNase/RNase-free distilled water.
   (g) Distilled water.
7. 5× Nucleic acid (NA) extraction buffer:
   To 220 ml distilled water, add the following ingredients:
   (a) 125 ml 2 M Tris, pH 7.5.
   (b) 150 ml 5 M NaCl.
   (c) 5 ml 0.5 M EDTA.
8. Buffered phenol:
   To prepare buffered phenol, follow the steps below.
   (a) Add 300 ml distilled water into 500 g phenol crystals in a brown bottle.
   (b) Incubate the bottle in a 65 °C water bath until all phenol crystals become liquid.
   (c) Aliquot 30 ml liquid phenol (lower layer) and 5 ml water into a 50-ml blue-cap tube.
   (d) Store the phenol at 4 °C (water-saturated phenol is stable at 4 °C for years).

(e) To buffer phenol from acidic to neutral pH:
- Remove the upper water layer from one phenol tube.
- Add 15 ml 2× NA extraction buffer and mix well.
- Centrifuge (2,000 × *g*, 10 min) to separate the phenol and aqueous phases.
- Remove the upper aqueous phase.

9. Phenol/chloroform:
To 20 ml buffered phenol, add 20 ml chloroform, mix well, spin at 2,000 × *g* for 10 min, and then remove the upper aqueous phase.
10. Reagents for cDNA synthesis and PCR (particulars of specific reagents we use are given; other suppliers may be used but protocol may require optimization):
(a) AMV-RTase, 10 U/μl and 5× reaction buffer (Promega M510F).
(b) Random hexa-primers (Promega C1181).
(c) RNasin, 40 U/μl (Promega N2615).
(d) 10 mM dNTP (Promega U151B).
(e) Platinum PCR SuperMix HF (Invitrogen 12532-016).
11. Cloning reagents:
(a) CIP, calf intestinal alkaline phosphatase (NEB M0290L).
(b) T4 kinase with reaction buffer (NEB ML0201L).
(c) PCR-terminator enzyme kit with reaction buffer (Lucigen 40037-2).
(d) T4 DNA ligase with reaction buffer (NEB M0202L).
(e) 10 mM ATP (Invitrogen 18330-019).
12. Reagents for DNA fragment isolation and analysis:
(a) 10× TBE.
(b) Low-melting-point (LMP) agarose.
(c) Agarose.
(d) 10× BlueJuice (or other similar) gel loading buffer (Invitrogen 10816-015).
(e) 1 kb DNA ladder.
(f) Geneclean kit (MP Biomedicals 111001400).
13. TE buffer:
To 494 ml distilled water, add the following ingredients, and then filter-sterilize:
(a) 5 ml 1 M Tris–HCl buffer, pH 8.0.
(b) 1 ml 0.5 M EDTA.

14. Ammonium acetate solution, 7.5 M.
15. Ampicillin stock (100 mg/ml, 1,000×) solution (*see* **Note 2**):
    Dissolve 1 g ampicillin sodium salt in 10 ml sterilized water.
16. 2× YT bacterial liquid medium for suspension culture:
    In 1,000 ml distilled water, dissolve the following ingredients, autoclave, cool to 70 °C, and then add 1 ml ampicillin stock:
    (a) 10 g Bacto yeast extract.
    (b) 16 g Bacto tryptone.
    (c) 5 g NaCl.
17. 2× YT bacterial solid medium for plating:
    In 1,000 ml distilled water, dissolve the following ingredients, autoclave, cool to 70 °C, add 1 ml ampicillin stock, and then aliquot 25 ml into each petri dish (Falcon #1001).
    (a) 10 g Bacto yeast extract.
    (b) 16 g Bacto tryptone.
    (c) 5 g NaCl.
    (d) 20 g Bacto agar.
18. Other supplies for the cloning work:
    (a) *E. coli* DH5 alpha competent cells (*see* **Note 3**).
    (b) SOC medium.
    (c) Colony Fast-Screen (Restriction Screen) kit (Epicentre #FS0472H).
    (d) Qiaprep Spin Miniprep kit (Qiagen #27106).

### 2.2 Identification of Infectious Full-Length cDNA Clones

1. H1-HeLa cells (*see* Chapter 5).
2. MRC-5 cells (*see* Chapter 7).
3. Incubator shaker.
4. $CO_2$ incubator.
5. High-speed centrifuge (e.g., Sorvall RC6).
6. −80 °C freezer.
7. Sterile disposables for cell culture works:
   (a) 60-mm dishes.
   (b) 48-well plate.
   (c) 5-ml sterile pipettes.
   (d) 10-ml sterile pipettes.
   (e) Cell lifter.
   (f) 1,000-ml 0.20 μm filter unit.

8. Medium A-NCS
   To 500 ml MEM (Invitrogen 11090081), add the following ingredients:
   (a) 5 ml nonessential amino acids (Invitrogen 1114050).
   (b) 5 ml L-glutamine (Invitrogen 2503081).
   (c) 5 ml penicillin, streptomycin (Invitrogen 15140163).
   (d) 50 ml newborn calf serum (Invitrogen 16010-159).
9. Medium A-FBS:
   To 500 ml MEM (Invitrogen 11090081), add the following ingredients:
   (a) 5 ml nonessential amino acids (Invitrogen 1114050).
   (b) 5 ml L-glutamine (Invitrogen 2503081).
   (c) 5 ml penicillin, streptomycin (Invitrogen 15140163).
   (d) 50 ml fetal bovine serum (Invitrogen 10437-028).
10. Reagents for in vitro transcription:
   (a) T7 RNA polymerase, 50 U/μl, comes with 5× reaction buffer and 0.1 M DTT.
   (b) RNasin, 40 U/μl.
   (c) 10 mM dNTP.
11. Reagents for transfection:
   (a) Lipofectamine 2000 transfection reagent.
   (b) OptiMEM reduced-serum medium.
12. PBSI: PBS with calcium and magnesium.
13. PBSA1 (0.1 % BSA):
   To 500 ml PBSI, add 6.7 ml 7.5 % bovine albumin fraction V.
14. 1 M HEPES buffer, pH 7.2–7.5.

### 2.3 Identification of the Most Vigorous Infectious cDNA Clone Isolate for Future Molecular Genetic Work

1. HBS (1×):
   To make 1 l HBS, dissolve the following ingredients in 900 ml distilled water. Then adjust pH to 7.2 with 1 N NaOH, bring the final volume to 1,000 ml with distilled water, and sterilize the buffer with a 0.20 μm filter unit.
   (a) 5 g HEPES.
   (b) 8 g Sodium chloride.
   (c) 0.37 g Potassium chloride.
   (d) 0.1 g Sodium phosphate dibasic, $Na_2HPO_4$.
   (e) 1 g Dextrose.
   (f) 0.15 g Calcium chloride dihydrate, $CaCl_2{\cdot}2H_2O$.
2. DEAE-dextran.

## 3 Methods

### 3.1 Construction of the Full-Length cDNA Clone

#### 3.1.1 Determination of the Complete Sequence of Your Target HRV Serotype/Strain for PCR Primer Design

The genome sequences of the prototypes and lab strains of all 100 HRV-A and -B serotypes and 17 HRV-C types have been published [2, 8–19]. These sequences are available at GenBank. For example, the GenBank accession number of the genome sequence of HRV-16 lab strain is L24917. If your target HRV has not yet been sequenced, you should be able to determine the sequence promptly using a randomly primed PCR method and high-throughput sequencing [20].

Once the complete genome sequence is known, PCR primers can be made to amplify the viral cDNA for cloning. The PCR fragments can be cloned and then cut and pasted together to form the full-length clone with standard protocol and commercially available reagents.

#### 3.1.2 The Plan of the Construction of Full-Length cDNA Clone of HRV-16

1. Overall strategy:
   The cDNA of the HRV-16 genome is cloned as three overlapping fragments (A [5′], B [middle], and C [3′] as described below). The three fragments are then assembled into the full-length clone (Fig. 1).

   The efficiency of PCR amplification of the 5′ and 3′ ends of the viral genome is limited by the sequence of the primers that locate at the genome's termini. These two primers need to match the exact 5′ and 3′ terminal sequences, which may make suboptimal PCR primers. Therefore, smaller amplicons (about 1.5 Kbps) are designed for the 5′ (A) and 3′ (C) end fragments. Fortunately, better PCR primers can be made for more efficient amplification of the middle fragment because the locations of these primers are flexible. Therefore, a longer amplicon (about 5 kbps) is designed for the middle (B) fragment.

   (a) Fragment A (1,498 bp): Base 1–1,487, including the NdeI unique site for full-length cDNA assembly.

   (b) Fragment B (4,582 bp): Base 1,407–5,977, including the NdeI and BlpI sites (*see* **Note 4**) for full-length cDNA assembly.

   (c) Fragment C (1,281 bp): Base 5,888–7,117 and poly $A_{40}$ tail, including the BlpI sites for full-length cDNA assembly.

2. PCR primer design:

   (a) Fragment A primers (F1 and R1):
   Primer F1 (TTAAAACTGGATCTGGGTTGT) is composed of the first 21 bases of the HRV-16 genome.

   Primer R1 (ATATA**GAGCTC**AAACTCCAATTGTT ATGTCTAAC) includes the reverse complement sequence of base# 1,465–1,487, an artificial SacI site (**GAGCTC**)

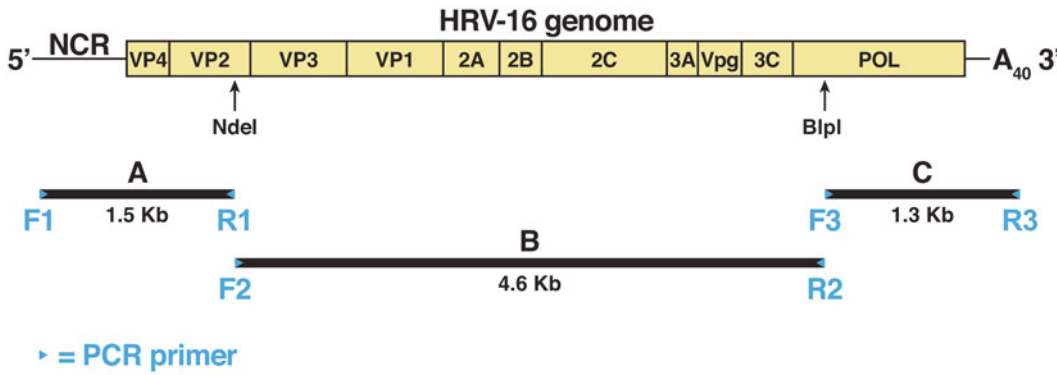


PCR primer sequences:
F1: TTAAAACTGGATCTGGGTTGT
R1: ATATAGAGCTCAAACTCCAATTGTTATGTCTAAC

F2: CAATAACTCAGCAACTCTTATAGTAC
R2: ATATAGAGCTCGTTGTGGATCTATATCTAGTGTTG

F3: GTAACACAGAGTGCAGTTTG
R3: ATATAGAGCTC$(T)_{40}$ATAAAACTAACAAACTATTC

**Fig. 1** Strategy for cloning the full-length cDNA of the HRV-16 genome. The genome structure of HRV-16 is shown on the top. The NdeI and BlpI restriction enzyme sites were used for cloning. Viral RNA was extracted from infected cell lysate and converted into cDNA. Three pairs of PCR primers (F1/R1, F2/R2, and F3/R3) were used to generate three overlapping PCR fragments (*A*, *B*, and *C*). Each PCR fragment was cloned and the plasmid isolates containing the correct sequences were identified by restriction analysis and sequencing. Then the fragments *A*, *B*, and *C* were assembled into a full-length clone with NdeI and BlpI restriction sites

for cloning, and terminal ATATA for effective SacI digestion of the PCR fragment.

(b) Fragment B primers (F2 and R2):
Primer F2 (CAATAACTCAGCAACTCTTATAGTAC) is composed of base# 1,407–1,432.

Primer R2 (ATATA**GAGCTC**GTTGTGGATCTATA TCTAGTGTTG) includes the reverse complement sequence of base# 5,954–5,977, an artificial SacI site (**GAGCTC**) for cloning, and terminal ATATA for effective SacI digestion of the PCR fragment.

(c) Fragment C primers:
Primer F3 (GTAACACAGAGTGCAGTTTG) is composed of base# 5,888–5,907.

Primer R3 (ATATA**GAGCTC**TTTTTTTTTTTTTTT TTTTTTTTTTTTTTTTTTTTTTTTTTTATAAAACTA ACAAACTATTC) includes the reverse complement sequence of the last 20 bases of HRV-16 genome and a poly A tail of 40 bases. It also carries an artificial SacI site

(**GAGCTC**) for cloning and subsequent linearization of the full-length cDNA for in vitro transcription, and terminal ATATA for effective SacI digestion of the PCR fragment.

3. PCR amplification and cloning of DNA fragments A, B, and C: The three DNA fragments are amplified using the same PCR conditions, but with different elongation times (2 min for A, 5 min for B, and 1.5 min for C) according to their sizes.

   The PCR products of all three fragments are kinase-treated, digested with SacI, and then ligated with StuI-SacI double-digested and CIP-treated pMJ3 DNA. The ligation mixture is transformed into competent *E. coli*. Colonies are screened for the presence of the correct insert by restriction analysis and also by sequencing in the case of fragment A. Four good colonies for each fragment are isolated. Four independent plasmid isolates are needed for each fragment because some of the cDNA fragments may have lethal or disabling mutations that are created by the error-prone viral RNA polymerase and PCR DNA polymerase, and the cloning process.

   The clones for each PCR fragment:

   (a) Clone A (4,673 bp) contains fragment A with the complete 5′ HRV-16 sequence fused correctly with the T7 promoter.

   (b) Clone B (7,757 bp) contains fragment B.

   (c) Clone C (4,456 bp) contains fragment C with a poly A tail of 40 bases.

4. Assembly of the three fragments into a full-length clone:
   For each clone, equal amounts of plasmid DNA of the four good isolates are pooled. For clone A, DNA is digested with NdeI and SacI and followed by CIP treatment; for clone B, DNA is digested with NdeI and BlpI; and for clone C, DNA is digested with BlpI and SacI.

   The desired restriction (R) fragments are purified using the LMP agarose gel method. They are:

   (a) R fragment A: 4,615 bp containing pMJ3 vector and viral bases 1–1,436.

   (b) R fragment B: 4,511 bp containing viral bases 1,435–5,948.

   (c) R fragment C: 1,217 bp containing viral bases 5,946–7,117, poly $A_{40}$ and the SacI site.

To assemble the full-length clone, the three R fragments are ligated at a molecular ratio of 1:1:1 and the ligation mixture is transformed into competent *E. coli*. Colonies are screened for the presence of full-length insert by restriction analysis. Twenty independent good colonies should be isolated for the first round of

infectivity screening. Five infectious clone isolates will be selected for further characterization. The infectivity of their in vitro transcripts and growth kinetics of their progeny virus are determined for selecting the most vigorous cDNA clone isolate to become the standard parental clone for future molecular genetic work.

### 3.1.3 Extraction of Viral RNA

1. Add the following material into a 1.5-ml LB eppi tube:
   (a) 320 μl of infected cell lysate of HRV-16 lab strain.
   (b) 80 μl 5× NA extraction buffer.
   (c) 2 μl glycoblue (15 μg/μl) (*see* **Note 5**).
   (d) 300 μl buffered phenol.
2. Vortex vigorously in an Eppendorf thermomixer for 2–3 min.
3. Microfuge for 5 min at room temperature (RT).
4. Transfer the upper aqueous layer into a 1.5-ml LB eppi tube containing 200 μl phenol/chloroform.
5. Repeat **steps 2** and **3**.
6. Transfer the upper aqueous layer into a 1.5-ml LB eppi tube containing 350 μl isopropanol.
7. Mix well and then incubate at RT for >1 h for RNA to precipitate.
8. Microfuge (10 min, RT) to pellet the RNA precipitant (*see* **Note 6**).
9. Remove supernatant and add 0.6 ml 75 % ethanol.
10. Vortex vigorously for 15 s and then microfuge for 2 min at RT.
11. Remove all supernatant.
12. Repeat **steps 9–11** and then air-dry the RNA pellet.
13. Dissolve each RNA pellet in 40 μl DNase/RNase-free water.

### 3.1.4 cDNA Synthesis

1. Add the following material to a 0.2-ml PCR tube:
   (a) 12.25 μl DNase/RNase-free distilled water.
   (b) 10 μl 5× AMV-RTase buffer.
   (c) 5 μl 10 mM dNTP.
   (d) 1.25 μl random primers.
   (e) 0.75 μl RNasin.
   (f) 20 μl RNA.
   (g) 0.75 μl AMV-RTase.
2. Run the following reverse transcription program in a PCR machine:
   (a) 25 °C for 5 min.
   (b) 42 °C for 10 min.

(c) 50 °C for 20 min.

(d) 85 °C for 5 min.

3. Transfer the reaction mixture to a 0.5-ml LB eppi tube and store at –20 °C.

### 3.1.5 PCR Amplification of PCR Fragments A, B, and C

1. Add the following material into a 0.2-ml PCR tube:
   (a) 90 µl Platinum PCR SuperMix HF.
   (b) 2 µl 25 µM Forward primer.
   (c) 2 µl 25 µM Reverse primer.
   (d) 10 µl cDNA.
2. Run the following PCR program:
   (a) 94 °C for 2 min.
   (b) 94 °C for 20 s.
   (c) 52 °C for 30 s.
   (d) 68 °C for 4 min (1 min for 1 kb fragment).
   (e) Repeat **steps (b)** to **(d)** 27 times.
   (f) 68 °C for 10 min.
   (g) 4 °C forever.
3. Transfer the reaction mixture to 0.5-ml LB eppi tube and store at –20 °C.

### 3.1.6 Preparation of PCR DNA Fragments for Cloning

#### Remove Proteins and Nucleotides from the PCR Fragment

1. Add the following reagents to each PCR product (~100 µl) in a 1.5-ml LB eppi tube:
   (a) 110 µl TE.
   (b) 130 µl 6 M ammonium acetate.
   (c) 2 µl Glycoblue (15 µg/µl).
   (d) 100 µl phenol/chloroform.
2. Vortex for 10 s and then microfuge at RT for 3 min.
3. Transfer the upper aqueous phase into a 1.5-ml LB eppi tube containing 900 µl 100 % EtOH.
4. Mix well and then incubate at RT for >1 h.
5. Microfuge (10 min, RT) to pellet DNA.
6. Remove supernatant and add 0.6 ml 75 % ethanol.
7. Vortex vigorously for 10 s and then microfuge for 2 min at RT.
8. Remove all supernatant.
9. Repeat **steps 6–8** and then air-dry the RNA pellet.
10. Dissolve the DNA pellet in 20 µl DNase/RNase-free water.

Kinase Treatment and End-Repair the PCR DNA Fragments (*See* **Note 7**)

1. Add the following material to 20 µl of PCR DNA fragment:
   (a) 6 µl 5× PCR-terminator buffer.
   (b) 3 µl dd-water.
   (c) 1 µl PCR-terminator enzyme (Lucigen 40037-2).
2. Mix gently and incubate the mixture at RT (25 °C) for 15 min (*see* **Note 8**).
3. Add the following material to each reaction mixture:
   (a) 180 µl TE.
   (b) 130 µl 6 M ammonium acetate.
   (c) 1 µl Glycoblue (15 µg/µl).
   (d) 100 µl phenol/chloroform.
4. Perform extraction, ethanol precipitation, microcentrifugation, washing, and air-drying as described in **steps 2–9** of Subheading Remove Proteins and Nucleotides from the PCR Fragment above.
5. Dissolve the DNA pellet in 20 µl DNase/RNase-free water.

*3.1.7 Restriction Digestion and Gel Purification of the PCR DNA Fragments*

1. Complete digestion of each PCR DNA fragment with SacI restriction enzyme.
2. Prepare a 1 % LMP agarose gel in 1× TBE buffer in a UV-transmissible gel box (*see* **Note 9**).
3. Add 10 µl 10× loading dye to 100 µl PCR product and then load the mixture into a well of the gel (*see* **Note 10**).
4. Run and then stain the gel with EtBr in the UV-transmissible gel box (*see* **Note 11**).
5. Visualize the DNA bands with a long-wave UV lamp (*see* **Note 12**).
6. Excise the agarose fragment containing the desired band with a razor blade and spatula into a 1.5-ml LB eppi tube.
7. Purify the PCR DNA fragment from agarose with Geneclean kit according to the manufacturer's instruction.
8. Elute the DNA fragment with 20 µl DNase/RNase-free water.

*3.1.8 Ligation of the PCR DNA Fragments with StuI-SacI-Digested and CIP-Treated pMJ3 DNA*

1. Prepare the following ligation mixture for each PCR DNA fragment:
   (a) 14.4 µl water.
   (b) 3 µl 10× ligase buffer.
   (c) 10 µl purified PCR fragment.
   (d) 0.1 µl linearized/CIP-treated pMJ3 vector DNA (~50 ng) (*see* **Note 13**).
   (e) 2.5 µl T4 DNA ligase.
2. Mix gently and incubate at 16 °C in a PCR machine overnight.

*3.1.9 Transformation of the Ligation Mixture into Competent E. coli*

1. Thaw a tube of competent *E. coli* in ice water.
2. Chill four labeled 5-ml Falcon tubes in ice water for 2 min.
3. Add 40 μl competent *E. coli* gently to the bottom of each chilled Falcon tube.
4. Add 5 μl ligation mixture (*see* **Note 14**) to the competent cells and swirl the pipette tip gently to mix.
5. Incubate the Falcon tubes in ice water for 30 min.
6. Heat shock the transformation mixtures at 41 °C for 50 s.
7. Incubate the transformation tubes in ice water for 2 min.
8. Add 0.4 ml 37 °C SOC to each transformation tube.
9. Incubate the transformation tubes in a 37 °C shaker (100 rpm) for 1 h.
10. Plate the transformation mixture on a 2× YT agar plate containing 100 μg/ml ampicillin.
11. Incubate plates in a 37 °C bacterial incubator overnight.

*3.1.10 Screen for the Clones Containing the Correct HRV Inserts*

1. Pick 6–12 colonies for each PCR fragment.
2. Inoculate each colony into 0.5 ml 2× YT/ampicillin medium in a well of a 48-well plate.
3. Incubate plates in a 37 °C shaker (100 rpm) overnight.
4. Transfer 200 μl culture from each well into a 1.5-ml LB eppi tube.
5. Microfuge the tubes at low speed to pellet the bacteria and then remove the supernatant.
6. Perform Fast Restriction Screen (Epicentre) of the plasmids according to the instructions.
7. For each PCR fragment, identify six colonies containing the correct insert by restriction analysis.

*3.1.11 Preparation of Plasmid DNA for the Assembly of Full-Length cDNA Clone*

1. Grow a 6 ml culture of each clone in a 14-ml tube.
2. Purify plasmid DNA with a Qiagen spin column according to the instructions.
3. Verify the presence of cloning restriction sites in each isolate by restriction analysis:
   (a) Clone A: NdeI and SacI.
   (b) Clone B: NdeI and BlpI.
   (c) Clone C: BlpI and SacI.
4. Identify four good isolates for each clone by restriction pattern analysis and additional analysis for Clones A and C as described below.
   (a) Clone A: correct fusion of the T7 promoter and 5′ end of HRV-16 cDNA by sequencing the junction.

(b) Clone C: poly A tail of 40 bases by restriction analysis (*see* **Note 15**).

5. For each clone, equal amounts of plasmid DNA of the four good isolates are pooled.
6. Double restriction digestion of plasmid DNA in NEB buffer 4:
   (a) Clone A: NdeI and SacI.
   (b) Clone B: NdeI and BlpI.
   (c) Clone C: BlpI and SacI.
7. Treat digested DNA of Clone A with 50 U CIP at 37 °C overnight.
8. Purify the desired restriction (R) fragments using the LMP agarose gel method:
   (a) R fragment A: 4,615 bp containing pMJ3 vector and viral bases 1–1,436.
   (b) R fragment B: 4,511 bp containing viral bases 1,435–5,948.
   (c) R fragment C: 1,217 bp containing viral bases 5,946–7,117, polyA$_{40}$.

#### 3.1.12 Construction of Full-Length cDNA Clone

1. Ligate the three R fragments (at a molecular ratio of 1:1:1) as described in Subheading 3.1.7 above.
2. Transform the ligation mixture into competent *E. coli* as described in Subheading 3.1.8 above.
3. Screen the colonies for the presence of the full-length insert by restriction analysis.
4. Select 20 independent full-length isolates for infectivity screening (*see* **Note 16**).
5. Grow a 12 ml culture of each isolate (in two 14-ml tubes).
6. Isolate plasmid DNA with a Qiagen miniprep spin column according to the instructions and elute DNA with 200 μl water.
7. To each DNA sample, add 200 μl of 2× NA extraction buffer and 300 μl of phenol/chloroform.
8. Perform extraction, ethanol precipitation, microcentrifugation, washing, and air-drying as described in **steps 2–9** of Subheading Remove Proteins and Nucleotides from the PCR Fragment above.
9. Dissolve plasmid DNA of each isolate in 50 μl DNase/RNase-free water and then measure the DNA concentration by spectrophotometer at $OD_{260\ nm}$.

### 3.2 Identification of Infectious Full-Length cDNA Clones

Some of the full-length cDNA clones may be noninfectious because they have lethal mutations that were created by the error-prone viral RNA polymerase and PCR DNA polymerase, and the cloning process.

*3.2.1 Generation of In Vitro Transcripts of Full-Length HRV-16 cDNA*

1. Completely linearize 3 μg of plasmid DNA for each full-length isolate with SacI by incubating the following digestion mixture at 37 °C for 4 h:
   (a) 12.8 μl DNase/RNase-free water.
   (b) 5 μl 10× NEB buffer.
   (c) 0.2 μl 100 μg/ml BSA.
   (d) 30 μl of DNA (0.1 μg/μl).
   (e) 2 μl Sac I (20 U/μl).
2. Run 2 μl of each digest in a 0.8 % agarose gel to verify the completion of digestion.
3. Store the digested DNA at −20 °C until in vitro transcription.
4. Prepare the following in vitro transcription mixture:
   (a) 13.5 μl water.
   (b) 10 μl 5× T7/T3 buffer.
   (c) 2.5 μl 10 mM NTP.
   (d) 5 μl 0.1 M DTT.
   (e) 17 μl DNA digest (~1 μg DNA).
   (f) 1 μl RNasin (40 U/μl).
   (g) 1 μl T7 RNA pol (50 U/μl, Invitrogen 18033019).
5. Incubate the mixture at 37 °C for 45 min.
6. Remove 2 μl of the transcription mixture for agarose gel analysis and store the rest at −80 °C until transfection.
7. Run 2 and 4 μl RNA transcripts along with 1 μg of virion RNA in a 0.8 % agarose/1× TBE gel to check the quality and quantity of the transcripts. The above reaction condition typically yields 0.1 μg of full-length transcript per μl (Fig. 2).

*3.2.2 Transfection of In Vitro Transcripts into H1-HeLa Cell Monolayers (See **Note 17**)*

1. Prepare 80–90 % confluent HeLa cell monolayers in 60-mm dishes as described in Subheading 3.2.1 of Chapter 7.
2. Prepare transfection mixtures at RT:
   (a) Add 250 μl OptiMEM into the bottom of a 5-ml Falcon tube.
   (b) Add 10 μl Lipofectamine 2000 directly into the OptiMEM, and then tap the tube gently to mix.
   (c) Incubate the Lipofectamine/OptiMEM mixture at RT for 5 min.
   (d) Add 250 μl OptiMEM into the bottom of another 5-ml Falcon tube.
   (e) Add 20 μl transcripts (typically about 2 μg) directly into OptiMEM, and then tap the tube gently to mix.

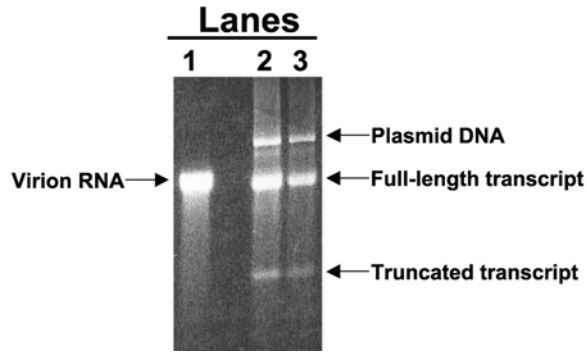


**Fig. 2** T7 in vitro transcripts of HRV16 full-length cDNA. T7 in vitro transcripts were made as described in Subheading 3.2.1. Virion RNA was extracted from purified virions as described in Subheading 3.1.3. The concentration of virion RNA was measured with $OD_{260\ nm}$ (1 OD = 40 μg/ml). The RNAs were electrophoresed in a 0.8 % agarose/1× TBE gel and the gel was stained with EtBr. *Lane 1*: 1 μg virion RNA, *lane 2*: 4 μl T7 transcripts, and *lane 3*: 2 μl T7 transcripts

(f) Use a P1000 pipetman to transfer all 270 μl of the transcript/OptiMEM directly into the Lipofectamine/OptiMEM, and then tap the tube gently to mix well.

(g) Incubate the resulting transfection mixture at RT for about 20 min.

3. Prepare the HeLa cell monolayer for transfection at about 15 min after **step 2f**:
   (a) Remove the growth medium.
   (b) Wash each monolayer with 4 ml OptiMEM, and then completely remove the media.
   (c) Add 1 ml OptiMEM to each monolayer.
4. Pour the transfection mixture from the 5-ml tube onto the monolayer.
5. Swirl each dish gently 2–3 times to disperse the transfection mixture.
6. Wash the remaining transfection mixture from the Falcon tube into the monolayer with 1 ml OptiMEM.
7. Swirl each dish gently 2–3 times again to disperse the transfection mixture.
8. Incubate the dishes at 35 °C for 3 h.
9. Replace transfection medium with 4 ml medium A-FBS.
10. Continue to incubate the dishes at 35 °C for another 20 h.

### *3.2.3 Preparation of Cell Lysate of the Transfected HeLa Cells*

1. Freeze the dishes at −80 °C for >10 min to lyse the cells.
2. Thaw the frozen cells at RT and then add 40 μl 1 M HEPES solution.

3. Scrape each monolayer with a cell lifter and then pipette the cell/medium mixture into a 14-ml Falcon tube.
4. Freeze (−80 °C)-thaw cell/medium mixture one more time and then vortex vigorously for 10 s.
5. Remove cell debris by spinning in a high-speed centrifuge (10,000 rpm, 4 °C) for 10 min.
6. Transfer the clarified supernatant into a 5-ml Falcon tube and then store at −80 °C until the infectivity assay.

*3.2.4 Identification of Infectious Clones (See **Note 18**)*

1. Prepare one 48-well plate of 90 % confluent MRC-5 cells as described in Subheading 3.1.4 of Chapter 7.
2. Remove media from each well of MRC-5 cells by aspiration.
3. Add 10 μl of cell lysate into a well, two wells for each isolate.
4. Incubate plates for 1 h at RT to allow virus attachment.
5. Add 0.5 ml medium A-FBS.
6. Incubate the plates at 35 °C.
7. Check and record the appearance of cytopathic effect (CPE) in each well: first check at 3 days after infection and then at days 5 and 7.
8. Pick five isolates that induce the quickest CPE appearance for further characterization.

### *3.3 Identification of the Most Vigorous Infectious cDNA Clone Isolate for Future Molecular Genetic Work*

Some of the infectious full-length cDNA clones may produce transcripts with suboptimal infectivity or progeny viruses with suboptimal growth rates due to a disabling mutation already existing in the original viral genomic RNA or created during the PCR and cloning process. To identify the best infectious cDNA clone isolate for future molecular genetic work, five candidates are screened by measuring the growth kinetics of their progeny viruses and the infectivity of their in vitro transcripts in H1-HeLa cells (*see* **Note 19**).

*3.3.1 Production of High-Titer Stock of the Infectious Isolates for Growth Kinetics Measurement*

1. Prepare 90 % confluent HeLa cell monolayers in 100-mm dishes (two dishes for each isolate) by seeding $6 \times 10^6$ cells (in 8 ml medium A-NCS) per dish, and then incubating at 37 °C for 12 h.
2. Remove medium and then wash monolayer once with PBSI.
3. Add 1 ml of virus stock from a transfection dish.
4. Incubate at RT for 1 h to allow virus attachment.
5. Add 4 ml medium A-FBS per dish and then incubate the dishes at 35 °C.
6. Check cell monolayers at 24, 36, 48, 60, and 72 h after infection. Transfer the dish to a −80 °C freezer when >90 % of the cells display CPE. If no CPE appears, transfer the dish to −80 °C at 72 h after infection.

7. Thaw the dishes at RT (~10 min).
8. Add 50 μl 1 M HEPES buffer pH 7.2.
9. Scrape cells with a cell lifter and pipette the cell lysate from two dishes into a 14-ml Falcon tube for each isolate.
10. Perform two more freeze (−80 °C, 20 min)-thaw (35 °C, 10 min) cycles to further break up the cells.
11. Pellet cell debris in a high-speed centrifuge (10,000 rpm, 4 °C) for 10 min.
12. Aliquot supernatants into 1.5-ml eppi tubes and then store in a −80 °C freezer.
13. If >90 % of cells in a dish display CPE within 24 h, the cell lysate of this dish will likely have a high enough titer (about $5 \times 10^8$ PFU per ml) for growth kinetics measurement.

    If it needs >24 h to develop severe CPE, pass the virus one more time by repeating **steps 1–12**.
14. Titer the virus stock using plaque assay as described in Subheading 3.2.2 of Chapter 7. Also pay attention to the plaque sizes. Typically, faster growers have larger plaques.

### 3.3.2 Measurement of Viral Growth Kinetics

1. Set up an HRV suspension culture by infecting $1 \times 10^8$ HeLa cells with $2 \times 10^9$ PFU of virus as described in Subheading 3.2.1 of Chapter 5. Then culture the infected cells in 20 ml of medium B-FBS at 35 °C.
2. Remove 0.5 ml cells from a culture at 2, 3, 4, 5, 6, 7, 8, and 10 h after infection (*see* **Note 20**). The 0.5 ml sample is added into a 1.5-ml eppi tube containing 5 μl 1 M HEPES buffer, pH 7.2.
3. Break up the infected cells by three freeze (−80 °C, 20 min)-thaw (35 °C, 10 min) cycles.
4. Pellet the cell debris in a microfuge (10,000 rpm, 4 °C) for 10 min.
5. Transfer the supernatant into 1.5-ml eppi tubes and then store at −80 °C for plaque assay.
6. Titer by plaque assay. Pick the clone with the highest titer.

### 3.3.3 Determination of the Infectivity of In Vitro Transcripts

1. Prepare 90 % confluent HeLa cell monolayers in 60-mm dishes as described in Subheading 3.2.1 of Chapter 7.
2. Prepare transfection solution D with the following recipe:
   (a) 1 ml HBS.
   (b) 200 μg DEAE-dextran.
   (c) 2 μl RNasin (80 U).
3. Prepare the transfection mixture by mixing 1, 0.1, or 0.01 ng of transcripts into 0.2 ml transfection solution D and then incubate the mixture at RT for 5 min.

4. Wash each monolayer once with 4 ml HBS and then completely remove the HBS.
5. Add 0.2 ml transfection mixture to each dish.
6. Incubate the dishes at RT for 1 h.
7. Remove the transfection mixture from each dish and then wash the dish once with 4 ml PBS (*see* **Note 21**).
8. Add agar and liquid overlay as described in the plaque assay protocol in **steps 8–11** of Subheading 3.2.2 of Chapter 7.
9. Incubate the dishes at 35 °C for 3 days for plaque development as described in **steps 12** and **13** of Subheading 3.2.2 of Chapter 7.
10. Count plaques and calculate infectivity per μg of transcript.

### *3.4 Complete Sequencing of the Chosen Infectious cDNA Clone*

The cDNA clone that is selected to be the parent for future molecular genetic work should be completely sequenced to establish its identity. More importantly, the exact sequence is needed for the planning of future cloning and mutagenesis work.

## 4 Notes

1. Vector pMJ3 was constructed by Mike Janda at UW-Madison specifically for the construction of the infectious full-length cDNA clones of positive-stranded RNA viruses [2]. It has a modified T7 promoter with a unique blunt StuI site at its 3′ end (TAATACGACTCACTATAGGCCT) for the fusion of the 5′ end of the viral cDNA to the last functional base of the T7 promoter. With this design, the T7 in vitro RNA transcripts of the cDNA clones only have two non-viral bases (GG) at their 5′ end. These two Gs have minimal, if any, inhibitory effect on the infectivity of the transcripts [2, 7]. pMJ3 has an ampicillin-resistant gene and is available on request.
2. Ampicillin is very sensitive to heat and light. If you have problems with its degradation, you can use carbenicillin (Sigma C3416) instead. Carbenicillin is a more stable analog of ampicillin. We use it at a concentration of 50 μg/ml.
3. We also have had good results with *E. coli* JM109 competent cells and XL1-Blue Supercompetent cells.
4. A second BlpI restriction site is located in fragment A. But BlpI digestion of fragment A is not needed for the assembly of the full-length clone.
5. Glycoblue has two functions. It helps to precipitate the RNA or DNA as a carrier. Its blue color also helps to visualize the RNA or DNA pellets to avoid discarding the pellets by mistake. However, we have found that reverse transcriptase activity is

inhibited by high concentration of glycoblue, so use glycoblue according to the recipe.

6. The RNA precipitant will appear as a small light blue pellet.
7. Invitrogen's Platinum PCR SuperMix HF uses Taq polymerase. Taq polymerase does not have proofreading function (3′ exonuclease activity). Therefore, the majority of the PCR product has a single-base A extension at the 3′ terminus of the DNA fragment. This single-base A blocks the blunt-end ligation of the PCR fragment and the vector. Lucigen's PCR-terminator enzyme kit has exonuclease activity that removes these single A base and also kinase activity that adds 5′ phosphates to the DNA fragments for ligation. If polymerases with the proofreading function, such as Vent or Pfu, are used for PCR, the PCR fragments will have blunt ends. These PCR fragments need only kinase treatment for ligation.
8. Avoid over-incubation, which will cause deletion of essential viral bases from the ends of the PCR fragments by the exonuclease activity of the PCR-terminator kit.
9. LMP agarose gel takes longer to solidify than regular agarose gel.
10. We use a 1 Kb DNA ladder in a control lane to estimate the size of the PCR fragments.
11. The LMP agarose gel is extremely fragile. Handle it very carefully. Keep the gel in the dark during EtBr staining.
12. Make sure that only long-wave UV is used because short-wave UV induces DNA damage, particularly in the presence of EtBr.
13. A control ligation without PCR DNA fragments is used to gauge how many colonies might have an empty vector.
14. Some components of the transformation mixture have an inhibitory effect on transformation of *E. coli* cells. Avoid using too much ligation mixture in the transformation reaction.
15. A poly A tail with a minimum of 40 As is required for optimal infectivity of the viral RNA transcripts [2]. However, some of the Clone C isolates may have much shorter poly A tails (<30 As) due to polymerase error during PCR. Therefore, the isolates with longer poly A tails will be identified for the construction of the full-length cDNA clone.

    To roughly determine the length of the poly A tail, plasmid DNA of Clone C is digested with restriction enzymes that cut very close to the poly A tail regions to generate a short poly A tail fragment (<300 bps). The digest is then analyzed with a 1.5–2 % agarose gel.
16. Some of the full-length isolates will produce non-infectious transcripts because they have lethal mutations in the cDNA. Some of the viral genomes used for RNA extraction may

already have lethal mutations since the viral RNA polymerase has a high error rate. The lethal mutations could also be introduced into the cDNA during PCR and cloning.

17. H1-HeLa cells are used for the transfection of viral RNA from HeLa-adapted HRV-A and HRV-B serotypes, and HRV-C viruses. For HRV-A and -B clinical isolates that have not been adapted to HeLa cells, MRC-5 or WI-38 cells should be used for transfection. The HeLa transfection procedure is applicable to MRC-5 and WI-38 cells.
18. Genomic RNA from HRV-C replicates and produces progeny viruses when it is transfected into HeLa cells [8, 21]. However, its progeny viruses cannot infect HeLa, MRC-5, or WI-38 cells which do not have the receptor for HRV-C. Therefore, the infectivity of HRV-C progeny viruses should be tested in differentiated airway epithelial cells in air-liquid interface culture or sinus organ culture as described previously [8, 21, 22].
19. For HRV-A and -B clinical isolates that have not been adapted to HeLa cells, their progeny viruses should be amplified and tested for growth kinetics in MRC-5 or WI-38 cells. For HRV-C, their progeny viruses should be amplified and tested for growth kinetics in differentiated airway epithelial cells in air-liquid interface culture or sinus organ culture [8, 21, 22]. Methods for determining the infectivity of in vitro transcripts of HRV-A and -B clinical isolates and HRV-C are not available.
20. Inject some $CO_2$ from a $CO_2$ tank into the flask every time after sampling. This will help to maintain a proper pH in the medium for viral growth.
21. DEAE-dextran inhibits the growth of HRV. The excess DEAE-dextran needs to be thoroughly washed away after transfection [2].

## References


1. Turner RB, Lee WM (2009) Rhinovirus. In: Richman DD, Whitley RJ, Hayden FG (eds) Clinical virology. ASM, Washington, DC, pp 1063–1082
2. Lee WM, Monroe SS, Rueckert RR (1993) Role of maturation cleavage in infectivity of picornaviruses: activation of an infectosome. J Virol 67:2110–2122
3. Rueckert R (1996) Picornaviridae: the viruses and their replication. In: Fields BN, Knipe DM, Howley PM et al (eds) Fields virology, 3rd edn. Lippincott-Raven Publishers, Philadelphia, PA, pp 609–654
4. Taniguchi T, Palmieri M, Weissmann C (1978) QB DNA-containing hybrid plasmids giving rise to QB phage formation in the bacterial host. Nature 274:223–228
5. Racaniello VR, Baltimore D (1981) Molecular cloning of poliovirus cDNA and determination of the complete nucleotide sequence of the viral genome. Proc Natl Acad Sci USA 78:4887–4891
6. Ahlquist P, French R, Janda M, Loesch-Fries LS (1984) Multicomponent RNA plant virus infection derived from cloned viral cDNA. Proc Natl Acad Sci USA 81:7066–7070

7. Janda M, French R, Ahlquist P (1987) High efficiency T7 polymerase synthesis of infectious RNA from cloned brome mosaic virus cdna and effects of 5' extensions on transcript infectivity. Virology 158:259–262
8. Bochkov YA, Palmenberg AC, Lee WM, Rathe JA, Amineva SP, Sun X, Pasic TR, Jarjour NN, Liggett SB, Gern JE (2011) Molecular modeling, organ culture and reverse genetics for a newly identified human rhinovirus C. Nat Med 17:627–632
9. Huang T, Wang W, Bessaud M, Ren P, Sheng J, Yan H, Zhang J, Lin X, Wang Y, Delpeyroux F et al (2009) Evidence of recombination and genetic diversity in human rhinoviruses in children with acute respiratory infection. PLoS One 4:e6355
10. Palmenberg AC, Spiro D, Kuzmickas R, Wang S, Djikeng A, Rathe JA, Fraser-Liggett CM, Liggett SB (2009) Sequencing and analyses of all known human rhinovirus genomes reveal structure and evolution. Science 324:55–59
11. McErlean P, Shackelton LA, Lambert SB, Nissen MD, Sloots TP, Mackay IM (2007) Characterisation of a newly identified human rhinovirus, HRV-QPM, discovered in infants with bronchiolitis. J Clin Virol 39:67–75
12. Tapparel C, Junier T, Gerlach D, Cordey S, Van Belle S, Perrin L, Zdobnov EM, Kaiser L (2007) New complete genome sequences of human rhinoviruses shed light on their phylogeny and genomic features. BMC Genomics 8:224
13. Harris JR, Racaniello VR (2005) Amino acid changes in proteins 2B and 3A mediate rhinovirus type 39 growth in mouse cells. J Virol 79:5363–5373
14. Kistler AL, Webster DR, Rouskin S, Magrini V, Credle JJ, Schnurr DP, Boushey HA, Mardis ER, Li H, DeRisi JL (2007) Genome-wide diversity and selective pressure in the human rhinovirus. Virol J 4:40
15. Lau SK, Yip CC, Tsoi HW, Lee RA, So LY, Lau YL, Chan KH, Woo PC, Yuen KY (2007) Clinical features and complete genome characterization of a distinct human rhinovirus (HRV) genetic cluster, probably representing a previously undetected HRV species, HRV-C, associated with acute respiratory illness in children. J Clin Microbiol 45:3655–3664
16. Lee WM, Wang W, Rueckert RR (1995) Complete sequence of the RNA genome of human rhinovirus 16, a clinically useful common cold virus belonging to the ICAM-1 receptor group. Virus Genes 9:177–181
17. Hughes PJ, North C, Jellis CH, Minor PD, Stanway G (1988) The nucleotide sequence of human rhinovirus 1B: molecular relationships within the rhinovirus genus. J Gen Virol 69(Pt 1):49–58
18. Skern T, Sommergruber W, Blaas D, Gruendler P, Fraundorfer F, Pieler C, Fogy I, Kuechler E (1985) Human rhinovirus 2: complete nucleotide sequence and proteolytic processing signals in the capsid protein region. Nucleic Acids Res 13:2111–2126
19. Stanway G, Hughes PJ, Mountford RC, Minor PD, Almond JW (1984) The complete nucleotide sequence of a common cold virus: human rhinovirus 14. Nucleic Acids Res 12:7859–7875
20. Djikeng A, Halpin R, Kuzmickas R, Depasse J, Feldblyum J, Sengamalay N, Afonso C, Zhang X, Anderson NG, Ghedin E et al (2008) Viral genome sequencing by random priming methods. BMC Genomics 9:5
21. Hao W, Bernard K, Patel N, Ulbrandt N, Feng H, Svabek C, Wilson S, Stracener C, Wang K, Suzich J et al (2012) Infection and propagation of human rhinovirus C in human airway epithelial cells. J Virol 86:13524–13532
22. Ashraf S, Brockman-Schneider R, Bochkov YA, Pasic TR, Gern JE (2012) Biological characteristics and propagation of human rhinovirus-C in differentiated sinus epithelial cells. Virology 436:143–149

# Chapter 13

# Reverse Genetic Engineering of the Human Rhinovirus Serotype 16 Genome to Introduce an Antibody-Detectable Tag

**Erin J. Walker, Lora M. Jensen, and Reena Ghildyal**

## Abstract

The ability to accurately detect viral proteins during infection is essential for virology research, and the lack of specific antibodies can make this detection difficult. Reverse genetic engineering of virus genomes to alter the wild-type genome is a powerful technique to introduce a detectable tag onto a viral protein. Here we outline a method to incorporate an influenza hemagglutinin epitope tag onto the 2A protease of HRV16. The method uses site-directed mutagenesis PCR to introduce the sequence for the HA antigen onto either the C or N termini of 2A protease while keeping the relevant internal cleavage sites intact. The new viral product is then cloned into a wild-type HRV16 plasmid and transfected into Ohio Hela cells to produce recombinant virus.

**Key words** Human rhinovirus, Reverse genetic engineering

## 1 Introduction

Human rhinoviruses (HRVs) are small, positive-strand RNA viruses belonging to the Picornavirus family. They cause a significant proportion of viral upper respiratory tract infections as well as the majority of asthma exacerbations [1, 2], making HRV a virus of medical importance. Improving our understanding of the activity of viral components within the host cell is therefore important to the future development of treatment options for high-risk patients.

Disruption of host cell function is mediated by 2A and 3C proteases, which act to prevent host cell transcription and translation while still allowing the host cellular machinery to replicate viral RNA and manufacture viral proteins [3, 4]. Despite decades of research into the specific functions of 2A and 3C proteases, there are a number of key aspects of HRV infection that are unknown; for example, the lack of high-specificity antibodies to HRV 2A protease means the cellular localization of this component during

David A. Jans and Reena Ghildyal (eds.), *Rhinoviruses: Methods and Protocols*, Methods in Molecular Biology, vol. 1221, DOI 10.1007/978-1-4939-1571-2_13, 

an infection course is currently unknown. Thus, the ability to study the cellular localization and individual effects of each protease within the context of live virus has been somewhat hampered by a lack of detection options for the 2A and 3C proteases.

Here we used reverse genetic engineering methods to introduce an influenza hemagglutinin epitope (HA) tag onto the 2A protease of HRV16, enabling accurate detection of the 2A protease with a commercially available anti-HA antibody. This method uses site-directed mutagenesis PCR to introduce the desired tag onto either the C- or N-terminus of 2A protease while keeping the required protease cleavage sites intact. The tag-modified PCR product is then cloned into a full-length HRV16 cDNA plasmid, followed by in vitro transcription of the cDNA clone into viral RNA. The viral RNA can then be easily transfected into host cells to produce live virus particles. We demonstrate typical western blot results showing detection of the HA tag and activity of the recombinant virus, which is comparable to results observed using the wild-type HRV16 virus. While we provide specific details to incorporate an HA tag into the HRV16 genome, this protocol can be adapted to incorporate an antibody-detectable tag of choice into any virus of interest.

## 2 Materials

### 2.1 Site-Directed Mutagenesis PCR, PCR Cleanup, and Restriction Digests

1. cDNA clone of HRV16, pR16.11 (*see* Chapter 12).
2. PCR primers to introduce HA tag; *see* Table 1 (*see* **Note 1**). As well as site-directed mutagenesis primers, external primers are required to amplify a large section of the HRV16 genome and are also shown in Table 1. These primers need to be located external to restriction enzyme digest sites to provide sites for ligation of the mutated sequence. *See* Fig. 1 for details.
3. Taq DNA polymerase, $MgCl_2$, dNTPS (25 mM each), and PCR buffer.
4. Wizard SV gel and PCR cleanup system (or other comparable cleanup systems).
5. Restriction enzymes BstXI and Bsu15I/ClaI and compatible buffers.
6. Spectrophotometer (we use the Nanodrop).

### 2.2 Agarose Gel Electrophoresis

1. Tris-acetate-EDTA (TAE) buffer (50×): 2 M Tris base, 1 M acetic acid, 50 mM EDTA (pH 8.0). Dilute 1:50 with nuclease-free water to make a 1× solution.
2. Agarose for DNA separation.
3. Gel-red for DNA visualization.
4. DNA size marker.

**Table 1**
**List of primers used for PCR-based site-directed mutagenesis**

| Primer name | Primer sequence (5′–3′) |
|---|---|
| N-terminal HA tag_F | ctgttgggcctagtgacatgTACCCATACGATGTT CCAGATTACGCTtatgtgcatgttggtaat |
| N-terminal HA tag_R | attaccaacatgcacataAGCGTAATCTGGAACAT CGTATGGGTAcatgtcactaggcccaacag |
| C-terminal HA tag_F | tagatcttagacactttcacTACCCATACGATGTT CCAGATTACGCTtgtgctgaagaacaagga |
| C-terminal HA tag_R | tccttgttcttcagcacaAGCGTAATCTGGAACA TCGTATGGGTAgtgaaagtgtctaagatcta |
| HRV16_2A forward | GCATCTGTATTTTGGCAGCA |
| HRV16_2A reverse | TCTTTGCTTCACTGGCATACA |

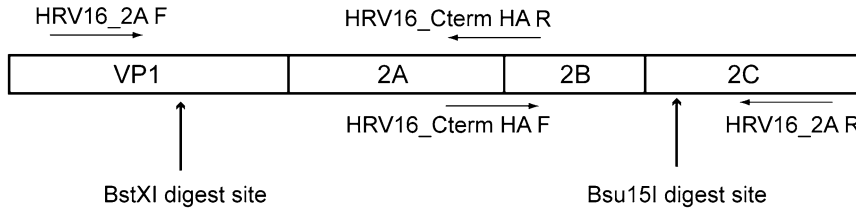


**Fig. 1 Example of the primer design required to introduce an HA tag onto the C-terminus of HRV16 2A protease.** Firstly, locate two restriction enzyme digest sites that are external to where the new tag sequence needs to be inserted (BstXI and Bsu15I, in VP1 and 2C, respectively). These restriction sites will be used to clone in the new DNA fragment. Then design PCR primers that allow amplification of the region of interest, including the restriction sites (primers HRV16_2A F and R). Finally, design primers that include the new sequence of interest as well as ~18–20 bp of 5′ and 3′ flanking sequence from the original genome (HRV16_Cterm HA F and R)

5. 1 % TAE-agarose: Dissolve 1 g of agarose in 100 mL of 1× TAE buffer by gentle heating in a microwave. Allow molten TAE-agarose to cool to ~50 °C. Add 5 μL of gel-red to molten agarose and pour into casting tray with comb. Allow to set for 20 min.

### *2.3 Cloning and Bacterial Transformation*

1. Double-digested PCR product and vector.
2. Plasmid miniprep kit.
3. T4 DNA ligase and buffer.
4. DH10B *E. coli* electrocompetent cells.
5. Biorad Gene Pulser II Electroporation system.
6. Electroporation cuvettes.
7. Autoclaved Luria Broth: 85 mM NaCl, 1 % peptone (tryptone), 0.5 % yeast extract.

8. Luria agar plates: 85 mM NaCl, 2 % bacterial agar, 1 % peptone (tryptone), 0.5 % yeast extract with 100 μg/mL ampicillin added.

### 2.4 In Vitro Transcription Reaction

1. Plasmid DNA.
2. SacI restriction enzyme.
3. T7 polymerase, T7 polymerase buffer, and DTT.
4. Recombinant RNasin ribonuclease inhibitor.
5. 100 mM NTP mix.

### 2.5 Cell and Virus Culture and Transfections

1. Ohio Hela cells.
2. High-glucose Dulbecco's modified Eagle medium (DMEM) with antibiotics (penicillin-streptomycin-neomycin) and both with/without 10 % vol/vol heat-inactivated fetal bovine serum.
3. Lipofectamine 2000.

## 3 Methods

All reactions are set up on ice unless otherwise specified.

### 3.1 Generate PCR Product and Restriction-Digested Fragment and Vector for Cloning

1. To generate PCR fragments containing the required tag, perform two PCR reactions as shown in Table 2. For each PCR reaction, ensure that the correct forward and reverse primers are used. For example, to generate mutation fragments for the N terminal HA tag, pair the HRV16_2A forward and N-terminal HA tag reverse primers to create fragment 1, and the HRV16_2A reverse and N-terminal HA tag forward primers to create fragment 2. The template for this reaction is a full-length HRV16 clone, pR16.11 (ATCC VRMC-8) [5].
2. Confirm that each fragment is the correct size by electrophoresis of 5 μL of PCR product on 1 % TAE agarose (100 V for ~45–60 min). Using the primers listed above, fragments 1 and 2 for the N-terminal HA tag should be 402 bp and 1,012 bp, respectively, while fragments 1 and 2 for the C-terminal HA tag should be 798 bp and 616 bp, respectively.
3. Column purify each PCR fragment using the Wizard PCR cleanup kit as described by the manufacturer. Quantitate the purified PCR product by spectrophotometric analysis.
4. To generate the full-length PCR product containing the HA tag, perform the PCR reaction as shown in Table 3.
5. Confirm that the final product is of the correct size by electrophoresis of 5 μL on 1 % TAE-agarose gel. For both the N- and C-terminal HA tags, the full-length PCR product should be 1,387 bp.

**Table 2**
**PCR reaction setup for first-round site-directed mutagenesis**

| Reagent | Volume (μL) | Final concentration |
|---|---|---|
| 5× Mango Taq buffer | 10 | 1× |
| MgCl2 (50 mM) | 1.4 | 1.4 |
| dNTPs (2 mM each) | 5.0 | 0.2 mM each |
| Forward primer (10 μM) | 5.0 | 1 μM |
| Reverse primer (10 μM) | 5.0 | 1 μM |
| Nanopure water | To 50 μL | – |
| Taq polymerase (5 U/μL) | 0.5 | 0.01 U |
| Plasmid DNA (25–50 ng) | Variable | 25–50 ng |
| Total | 50 μL | |

*Cycling conditions*:
[94 °C 3′]×1
[94 °C 20″, 60 °C 20″, 72 °C 30″]×34
[72 °C 3′]×1
[Hold at 4 °C]

**Table 3**
**PCR reaction setup for second-round site-directed mutagenesis**

| Reagent | Volume (μL) | Final concentration |
|---|---|---|
| 5× Mango Taq buffer | 10 | 1× |
| $MgCl_2$ (50 mM) | 1.4 | 1.4 |
| dNTPs (2 mM each) | 5.0 | 0.2 mM each |
| HRV16 2A forward primer (10 μM) | 5.0 | 1 μM |
| HRV16 2A reverse primer (10 μM) | 5.0 | 1 μM |
| Nanopure water | To 50 μL | – |
| Taq polymerase (5 U/μL) | 0.5 | 0.01 U |
| PCR fragment 1 | Variable | 25–50 ng |
| PCR fragment 2 | Variable | 25–50 ng |
| Total | 50 μL | |

*Cycling conditions*:
[94 °C 3′]×1
[94 °C 1′, 38 °C 1′, 72 °C 2′]×1
[94 °C 30″, 40 °C 30″, 72 °C 2′]×4
[94 °C 15″, 50 °C 30″, 72 °C 2’]×25
[72 °C 3′]×1
[Hold at 4 °C]

6. Column purify the full-length PCR product using the Wizard PCR cleanup kit as described by the manufacturer. Elute in 60 μL of elution buffer.
7. Set up the first restriction digest using BstXI for both the full-length PCR product and cloning vector (e.g., pR16.11) (*see* **Note 2**). Retain a small amount of the cleaned full-length PCR product and undigested vector for later electrophoresis to confirm that complete digestion has been achieved. Incubate the reaction at 37 °C for 4 h.
8. Column purify digested PCR product and vector to enable second digest in different buffer. Elute in 60 μL of elution buffer.
9. Set up the second restriction digest using Bsu15I for both the PCR product and cloning vector. Retain a small amount of the cleaned full-length PCR product for later electrophoresis to confirm that complete digestion has been achieved. Incubate the reaction at 37 °C for 4 h.
10. Confirm that complete digestion has been performed for each restriction enzyme by electrophoresis of 5 μL of full-length, BstXI-digested, and BstXI + Bsu15I-digested PCR product as well as undigested vector DNA, BstXI-digested vector, and BstXI + Bsu15I-digested vector on 1 % TAE-agarose. Digestion of the PCR product with BstXI should yield a product of 1,244 bp and subsequent digestion with Bsu15I should yield a product of 1,046 bp. This is the double-digested PCR product required for ligation. Digestion of pR16.11 with BstXI should yield a linear vector of ~9.4 kb and subsequent digestion with Bsu15I should yield a double-digested vector of ~8.4 kb.
11. Once complete digestion has been confirmed, gel purify the double-digested PCR product and double-digested vector by electrophoresing the remaining product on separate 1 % TAE-agarose gels, without any marker (*see* **Note 3**). Excise the double-digested PCR product and vector DNA from the agarose gel using a clean scalpel and process according to the Wizard gel purification protocol. Elute in 50 μL of elution buffer. Quantitate the amount of PCR product recovered using a spectrophotometer.

### 3.2 Ligation Reaction and Bacterial Transformation

1. Prepare a 10 μL ligation reaction, using 1 μL of 10× T4 DNA ligase reaction buffer and 1 μL of T4 DNA ligase. The amount of vector and insert required will depend on the concentration of each fragment recovered from the agarose gel. Use the following formula to determine how much of each to use (*see* **Note 4**):

$$\frac{\text{ng of vector} \times \text{kb size of insert}}{\text{kb size of vector}} \times \text{molar ratio of} \frac{\text{insert}}{\text{vector}} = \text{ng of insert}$$

Incubate reaction overnight at 16 °C.

2. The following day, add 1–2 μL of ligation reaction to 50 μL of just-thawed DH10B cells, flick gently but quickly to mix, and incubate on ice for 10 min (*see* **Note 5**). Cells and tubes must remain ice cold at all times.
3. Add cell-DNA mix to precooled electroporation cuvette. Electroporate using the following settings: voltage 2.5 kV, capacitance 25 μF, and resistance 200 Ω.
4. Quickly add 1 mL of LB to the cuvette to remove the bacteria and place in a culture tube. Incubate at 37 °C for 1 h, with shaking (210 rpm).
5. After 1 h, remove the bacteria and centrifuge at 3,300 rpm (~1,000 × *g*) for 3 min to pellet the cells. Remove 800 μL of media and resuspend the pellet in the remaining 200 μL. Plate the cell suspension on an agar plate with ampicillin and incubate overnight at 37 °C.
6. The following day, pick 4–6 colonies from each plate and incubate at 37 °C for 16 h in 5 mL of LB with ampicillin (100 μg/mL), with shaking.
7. Isolate the plasmid DNA using the plasmid miniprep kit, following the manufacturer's instructions.
8. Confirm the DNA sequence of the clones by sequencing, using the HRV16_2A forward and reverse primers as sequencing primers.

### 3.3 In Vitro Transcription Reaction to Generate Viral RNA

1. Linearize the plasmid DNA with SacI. The restriction enzyme digestion is performed in a 50 μL volume and includes 4 μL of enzyme (10 U/μL), 5 μL of reaction buffer, and 10 μg of plasmid. Incubate the reaction at 37 °C for 4–6 h.
2. Confirm complete linearization by electrophoresis of 5 μL of the digest reaction on 1 % agarose, using intact plasmid DNA as a control.
3. Set up the in vitro transcription reaction as shown in Table 4. Incubate the reaction at 37 °C for 45 min and then place on ice to stop the reaction.
4. Confirm that the majority of RNA transcripts are of full length by electrophoresis on 0.8 % TAE agarose gel. Aliquot and store at −80 °C until required.

### 3.4 RNA Transfection to Generate Recombinant Virus

1. The day before transfection, seed approximately $3 \times 10^5$ Ohio Hela cells into 35 mm dishes so that they are ~80 % confluent the following day.
2. Prepare the lipofectamine 2000 reagent as recommended by the manufacturer for a 6-well plate, substituting 5 μL of the in vitro-transcribed RNA for DNA.

**Table 4**
**In vitro transcription reaction setup to generate viral RNA**

| Reagent | Volume (μL) | Final concentration |
|---|---|---|
| 5× T7 buffer | 50 | 1× |
| Promega RNasin (40 U/μL) | 5 | 0.8 U/μL |
| NTP (5 mM each) | 25 | 0.5 mM |
| DTT (0.1 M) | 25 | 10 mM |
| T7 polymerase (50 U/μL) | 5 | 1 U/μL |
| Digested plasmid DNA (0.2 μg/μL) | 25 | 5 μg |
| Nuclease-free water | 115 | |
| Total | 250 | |

3. Add the RNA-lipofectamine mix to the cells and incubate at 37 °C for 24–48 h, until significant CPE (cytopathic effect) is observed, approximately 24–48 h. Freeze the dishes at −80 °C to lyse the cells and release the viral particles.
4. Thaw the dishes, collect the supernatant, vortex well, and centrifuge at 4,000 rpm (~1,500 × *g*) for 15 min to clarify the virus and remove cellular debris. Aliquot the virus in 250 μL aliquots and store at −80 °C.
5. Use one aliquot to infect a sub-confluent T75 flask of Ohio Hela cells, to generate enough live virus to perform subsequent experiments; remove the old media, wash the cells with warm 1× PBS, replace the media, and add the virus directly to the flask. Gently rock to disperse the virus. Incubate at 37 °C with 5 % $CO_2$ for 24–48 h, until significant CPE is observed. Freeze the flask as described in **step 3**, and repeat **step 4** to clarify the virus.
6. Titrate the virus to determine the virus titre using a TCID50 assay [6].
7. An infection time course can then be performed to collect infected whole-cell protein lysates, as previously described [7]. Figure 2 shows typical results for the recombinant C-terminal HA-tagged 2A HRV16. The anti-HA antibody demonstrates the presence of 2A at the correct size, appearing at 6 h p.i.; anti-VP2 antibodies demonstrate that infection with HRV was achieved; anti-eIF4G antibodies show that the HA-tagged 2A is still active, as cleavage products are visible at 3, 6, and 9 h p.i.; and anti-tubulin antibodies are included as a loading control.

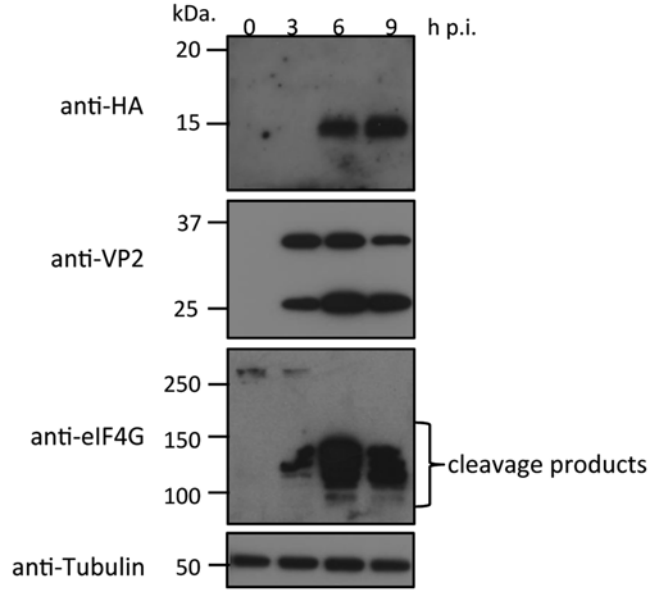


**Fig. 2 Typical Western blot results for an infection time course with HRV16 C-terminal HA-tagged 2A protease.** Ohio-HeLa cells were infected with HRV16 C-terminal HA tag (MOI of 1) and cells lysed using RIPA buffer containing protease and phosphatase inhibitors at the time points shown. Cell lysates were subjected to SDS-PAGE on 12.5 % gels and Western analysis using the indicated primary antibodies/horseradish peroxidase-conjugated secondary antibodies and enhanced chemiluminescence (Perkin Elmer). The specificity of the antibodies and approximate size are indicated on the *left*. Cleavage products of eIF4G are indicated on the *right*. *pi* post-infection

## 4 Notes

1. This sequence should extend 18–25 bp either side of the new sequence that is to be added into the original genome. In Table 1 the HA tag is shown in uppercase and the original HRV16 genome sequence is in lower case.
2. We have found that efficient restriction digestion is best achieved by using BstXI first, followed by Bsu15I (ClaI).
3. The double-digested vector DNA can be treated with calf intestinal alkaline phosphatase (CIAP) to remove 5′ phosphate groups prior to gel purification, if desired. This prevents religation of the linearized vector; however due to the double digest, in practice we have found very few clones without the intended sequence.
4. We use a molar ratio of 3:1 insert:vector, and where possible use 100–200 ng of vector DNA.

5. Increasing the volume of ligation reaction in the transformation does not guarantee more colonies, and tests in our lab indicate that adding too much of the ligation reaction can inhibit the transformation.

## Acknowledgements

We thank Dr Wai-Ming Lee for the kind gift of anti-VP2 antibodies and the pR16.11 HRV16 plasmid.

### References

1. Johnston SL et al (1995) Community study of role of viral infections in exacerbations of asthma in 9–11 year old children. BMJ 310(6989):1225–1229
2. Kaur B et al (1998) Prevalence of asthma symptoms, diagnosis, and treatment in 12–14 year old children across Great Britain (international study of asthma and allergies in childhood, ISAAC UK). BMJ 316(7125):118–124
3. Younessi P, Jans DA, Ghildyal R (2012) Modulation of host cell nucleocytoplasmic trafficking during picornavirus infection. Infect Disord Drug Targets 12(1):59–67
4. Racaniello VR (2001) Picornaviridae: the viruses and their replication. In: Knipe DM, Howley PM (eds) Fields virology. Lippincott/Raven, Philadelphia, PA, pp 685–722
5. Lee WM, Wang W (2003) Human rhinovirus type 16: mutant V1210A requires capsid-binding drug for assembly of pentamers to form virions during morphogenesis. J Virol 77(11):6235–6244
6. Reed LJ, Muench H (1938) A simple method of estimation fifty percent endpoints. Am J Hyg 27(5):493–497
7. Walker EJ et al (2013) Rhinovirus 3C protease facilitates specific nucleoporin cleavage and mislocalisation of nuclear proteins in infected host cells. PLoS One 8(8):e71316

# Chapter 14

# Mouse Models of Rhinovirus Infection and Airways Disease

**Nathan W. Bartlett, Aran Singanayagam, and Sebastian L. Johnston**

## Abstract

Mouse models are invaluable tools for gaining insight into host immunity during virus infection. Until recently, no practical mouse model for rhinovirus infection was available. Development of infection models was complicated by the existence of distinct groups of viruses that utilize different host cell surface proteins for binding and entry. Here, we describe mouse infection models, including virus purification and measurement of host immune responses, for representative viruses from two of these groups: (1) infection of unmodified Balb/c mice with minor group rhinovirus serotype 1B (RV-1B) and (2) infection of transgenic Balb/c mice with major group rhinovirus serotype 16 (RV-16).

**Key words** Purification, Major group, Minor group, Serotype, Hela cells, In vivo infection

## 1 Introduction

Rhinoviruses are members of the *Picornaviridae* family and are the most common cause of viral infection in man. They are involved in the pathogenesis of numerous respiratory diseases that range in severity from the common cold to life-threatening exacerbations of asthma and chronic obstructive pulmonary disease (COPD). Combined the medical, social, and financial impact of rhinovirus infections is massive [1]. Despite the huge burden of disease associated with rhinovirus infections there are currently no vaccines or anti-rhinoviral treatments available. Prior to 2008 the lack of a practical small animal model of rhinovirus infection represented a major roadblock to investigating host immune mechanisms involved in rhinovirus immune pathogenesis. One of the main issues confronting mouse model development was virus host cell receptor usage. The majority of rhinoviruses can be classified into two groups based on receptor binding: major group viruses such as RV-16 that utilize intercellular cell adhesion molecule 1 (ICAM-1) and minor group

David A. Jans and Reena Ghildyal (eds.), *Rhinoviruses: Methods and Protocols*, Methods in Molecular Biology, vol. 1221, DOI 10.1007/978-1-4939-1571-2_14, 

viruses such as RV-1B that bind to low-density lipoprotein receptor (LDLR). Development of mouse models was guided by previous in vitro studies investigating rhinovirus mouse and human cell tropism. Major group rhinoviruses were unable to bind to mouse ICAM-1 and infect murine epithelial cells. To render mouse cells permissive for major group rhinovirus infection expression of a chimeric mouse ICAM-1 molecule which contained the terminal immunoglobulin domain of human ICAM-1 was required. This was in contrast to minor group viruses that were able to bind both human and mouse LDLR and infect cells from both species [2]. Given the differential permissiveness of mouse cells for major and minor group rhinoviruses we concluded that normal Balb/c mice should become infected by minor group viruses. Achieving infection with major group viruses would require transgenic mice expressing chimeric human-mouse ICAM-1.

Another critical issue associated with these models was virus purification. We developed a new method for rhinovirus purification which was rapid (could be completed within a day, compared to previous protocols involving ultracentrifugation over several days) and not technically complicated. We now had a protocol to produce consistent high-titre rhinovirus (we could produce minor group RV1B and major group RV16) that could be used in repeat experiments to generate reproducible data [3]. These models are now employed by several labs and have contributed to multiple publications which have provided novel insight into immune mechanisms during rhinovirus infection [4–8].

## 2 Materials

### 2.1 Cells and Reagents Required for Rhinovirus Growth and Titration

Prepare all reagents at room temperature in microbiological safety cabinet. Store medium at 4 °C.

1. Rhinovirus serotype 1B (RV-1B), obtained from American Type Tissue Culture Collection (ATCC VR-1366). Rhinovirus serotype 16 (RV-16), obtained from ATCC (VR-283).
2. H1 Hela cells (obtained from ATCC CRL-1958).
3. Hela cell growth medium: Add 10 mL HEPES buffer 1 M, 50 mL fetal bovine serum, and 5 mL sodium bicarbonate 7.5 % solution to 500 mL Dulbecco's modified Eagle medium (DMEM).
4. Hela cell infection medium: Add 10 mL Hepes buffer 1 M, 10 mL fetal bovine serum, and 5 mL sodium bicarbonate 7.5 % solution to 500 mL DMEM.
5. Trypsin E diluted fivefold in phosphate-buffered saline (PBS).
6. Sterile cell scrapers.
7. 37 °C water bath.
8. Benchtop shaker.

### 2.2 Reagents and Components for Rhinovirus Purification

1. Polyethylene Glycol 6000.
2. 5 M Sodium chloride solution—weigh 146.1 g of sodium chloride and add to 450 mL double-distilled water ($ddH_2O$). Dissolve with stirrer. Add $ddH_2O$ until final volume of 500 mL. Filter sterilize. Store at room temperature.
3. Amicon ultracentrifugal device 100,000 NMCO (Millipore, USA).
4. Tube roller.
5. Benchtop centrifuge.

### 2.3 qPCR (Taqman) Screening hu/muICAM-1 Transgenic Mice

1. Ear biopsy from mice from Balb/c x hu/muICAM-1 mating.
2. Genomic DNA extraction kit (Qiagen cat no. 69506).
3. qPCR primers and probes (for hu/muICAM-1 transgene and control).
4. qPCR master mix (Qiagen cat no. 20435).
5. Taqman machine.

### 2.4 Intranasal Infection and Assessment of Immune Responses

1. Isoflurane.
2. Pentobarbitone.
3. BAL buffer—weigh 0.14 g lidocaine and add to 40 mL phosphate-buffered saline (PBS) with 400 μL of 0.5 M EDTA solution.
4. ACK lysis buffer—weigh 8.29 g ammonium chloride (0.15 M) and 1.0 g potassium bicarbonate (10 mM). Add to 800 mL $ddH_2O$. Add 200 μL 0.5 M EDTA solution. Check pH and ensure 7.2–7.4 (add 1 M NaOH solution or 1 M HCl dropwise to alter pH accordingly). Top up volume to 1 L. Filter sterilize.
5. Medium—add 50 mL fetal bovine serum to 500 mL RPMI-1640 medium with 10 mL Hepes and 5 mL 7.5 % sodium bicarbonate solution.
6. REASTAIN Quick diff kit.
7. Cytospin funnels, slide holders, and centrifuge.

## 3 Methods

### 3.1 Hela Cell Culture for Rhinovirus Infection, Growth, and Purification

Carry out all methodological steps at room temperature, unless otherwise stated (*see* **Note 1**).

1. *Virus stocks*: Passage rhinovirus 1B or 16 in confluent Ohio HeLa cells to produce working virus stocks via master, sub-master, and seed stock using standard virological techniques. Collect infected cell lysate into culture medium, divide into 3 mL aliquots, and store at −80 °C. Seed stock aliquots will be used to produce more working stock when this runs out (*see* **Note 2**).

2. *Inoculum*: This will be used to amplify sufficient quantity of virus from working stock to enable infection of 25 × 175 $cm^2$ flasks required for production of purified virus for mouse infections (Subheading 3.1, **step 4**). Grow Hela H1 cells in Hela cell growth medium at 37 °C with 5 % $CO_2$ in 2 × 175 $cm^2$ flasks. When 90 % confluent, wash cells with 10 mL Hela cell infection medium and add 25 mL diluted virus working stock (3 mL virus aliquot diluted with 22 mL infection medium to give 25 mL inoculum per flask). Rock flasks at room temperature for 1 h and then incubate at 37 °C with 5 % $CO_2$ until 100 % cytopathic effect (CPE) observed by light microscopy (approximately 24 h).
3. Harvest cells by dislodging (bang flask with hand) into culture medium and transfer infected cell-media suspension (approximately 50 mL for two flasks combined) to 50 mL Falcon tube. Lyse cells and release virus by freeze/thawing twice (freeze in –80 °C freezer or on dry ice and then thaw quickly in 37 °C water bath).
4. Centrifuge thawed lysate in 50 mL Falcon tube at 2,000 × *g* for 15 min to pellet cell debris. Collect and filter clarified virus-containing supernatant through 0.2 μm syringe filter and add to Hela cell infection medium to produce volume (500 mL) of inoculum required to infect 25 × 175 $cm^2$ flasks (20 mL inoculum per flask).
5. *Purified virus* for mouse infection: Use H1 Hela cells (ATCC CRL-1958) in 25 × 175 $cm^2$ flasks to produce concentrated purified virus for in vivo mouse infection. When cells are 90 % confluent, replace the growth medium with 20 mL per flask infection medium containing diluted virus inoculum.
6. Rock flask at room temperature for 1 h and then incubate at 37 °C with 5 % $CO_2$ until CPE is observed throughout which should be approximately 24 h (*see* **Note 3**).
7. Collect cells by banging to dislodge into culture medium, transferring to 10 × 50 mL Falcon tubes, and centrifuge to pellet. During cell collection, a sterile cell scraper may be required to dislodge cells that remain adherent. Discard culture supernatant, resuspend pellets (10) in 5 mL PBS each, and combine into single 50 mL Falcon tube (50 mL total). Pellet by centrifugation. Repeat washes by resuspending in 50 mL PBS and pelleting by centrifugation. Centrifuge at 388 × *g* for 10 min after each wash and resuspend in final volume of 36 mL PBS.

### 3.2 RV Purification and Assessment of Infectious Titre and Quality

1. Freeze-thaw twice to lyse cells and then centrifuge to pellet cell debris at 2,000 × *g*.
2. Filter clarified virus-containing supernatant through a 0.2 μm syringe filter (*see* **Note 4**).
3. To precipitate virus add 2.8 g Polyethylene Glycol (PEG) 6000 and 4 mL of 5 M NaCl, mix on a roller for 5 min to dissolve PEG, followed by incubation on ice for 1 h with gentle mixing by hand inversion every 20 min.

4. Recover the precipitated virus by centrifugation at 2,500 × *g* for 1 h, dissolve virus pellet in 15 mL of PBS (*see* **Note 5**), mix on a roller for 5 min, and then centrifuge at 4,000 rpm for 15 min to remove insoluble debris.
5. Filter the virus using a 0.2 μm syringe filter into an Amicon ultracentrifugal device (Millipore, USA).
6. Concentrate filtered supernatant (containing virus) to approx 0.5 mL in Amicon Ultra (100,000 NMCO) centrifugal filtration device, centrifuging at 2,000 × *g*. Add 10 mL of PBS, pipette (P1000) thoroughly to mix concentrated virus in filtration device (but careful not to damage filter with pipette tip), and repeat concentration (*see* **Note 6**). Harvest concentrated virus and wash out centrifugal device with additional 2 × 1 mL of PBS—combine washes with 0.5 mL concentrated virus to give 2.5 mL total. Aliquot into 2 × 250 μL and 4 × 500 μL or as required and store at −80 °C. Also prepare two small-volume aliquots for testing virus titre in vitro and in vivo (*see* **Note 7**).
7. Measure virus infectious titre using Ohio HeLa cells. Serially dilute purified RV-1B stock tenfold to give dilution factors $10^{-1}$–$10^{-8}$ and add 50 μL of each dilution added to eight replicate wells of HeLa cells in 96-well plate.

Use UV-inactivated virus as a control for the inoculum (expose concentrated virus to 1,200 μJ/cm² ultraviolet light for 30 min).

Incubate plate at 37 °C with 5 % $CO_2$ for 4 days. Determine highest dilution where CPE is still visible using a light microscope by counting CPE-positive wells.

Determine tissue culture infective dose 50 % ($TCID_{50}$)/mL value by scoring the sum of positive wells followed by use of the Spearman Karber formula ($M = xk + d\ [0.5 - (1/n)\ (r)]$, wherein xk = dose of highest dilution, $r$ = sum of positive responses, $d$ = spacing between dilutions, and $n$ = wells per dilution).

### 3.3 PCR Screening to Identify hu/muICAM-1 Heterozygous Mice

1. Extract genomic DNA according to the manufacturer's instructions eluting into 200 μL.
2. Screen genomic DNA for pHu/MuICAM-1-specific sequence by PCR using primers NS 25 (GGG CAG TCA CAG CTA AAA CCT) and NS2 26 (TCC AGG GAG CAA AAC AAC TTC T) (*see* **Note 8**).
3. Use Taqman RT-PCR using standard cycle conditions.

### 3.4 Intranasal Infection of Mice and Assessment of Characteristic Immune Responses

1. Purchase 6–8-week-old female BALB/c or C57BL/6 mice. House in individually ventilated cages in specific pathogen-free conditions. For infection with RV-16 identify hu/muICAM-1 heterozygous mice as described in Subheading 3.3.
2. For intranasal RV dosing, lightly anesthetize mouse with vaporized isoflurane (Merial, UK), administered via an induction chamber. Monitor mice. As soon as respiratory rate slows to one breath per second, remove mouse from

chamber and administer 50 μL of purified virus via a pipette directly to the nostrils (*see* **Note 9**).

3. Cull mice at time point of interest with terminal anesthesia, by intraperitoneal injection of 200 μL pentobarbitone solution.
4. Bronchoalveolar lavage (BAL): Expose trachea by dissection and insert plastic cannula (outside diameter = 1.27 mm, Becton Dickinson, UK). Lavage with 1.5 mL of BAL buffer. Centrifuge recovered fluid at 10,000 × *g* for 1 min using benchtop centrifuge. Remove supernatant, snap freeze in liquid nitrogen, and store at −80 °C for measurement of secreted proteins and cytokines by ELISA. Numerous cytokines, chemokines, interferons, mucin proteins, and other soluble factors can be detected in BAL supernatant during rhinovirus infection.
5. Resuspend cell pellet in 200 μL of ACK lysis buffer to lyse red blood cells. Leave for 10 s and neutralize by diluting with 1.0 mL of medium. Centrifuge at 10,000 × *g* for 1 min and discard supernatant. To obtain BAL cell suspension resuspend cell pellet in 1 mL of medium.
6. Cytospin assay to identify BAL cell populations: Add 100 μL of BAL cell suspension to a cytospin funnel and spin down onto Shandon cytoslide at 500 rpm for 5 min using the Cytospin3 system (Shandon, USA). Air-dry slides for 4 h and stain with REASTAIN quick-diff kit. Differentially count 300 cells per slide to determine percentage of each cell type. At day 1 post-infection the predominant inflammatory cells are neutrophils (Fig. 1a). By day 7 neutrophil numbers have decreased as lymphocytes are observed (Fig. 1b).

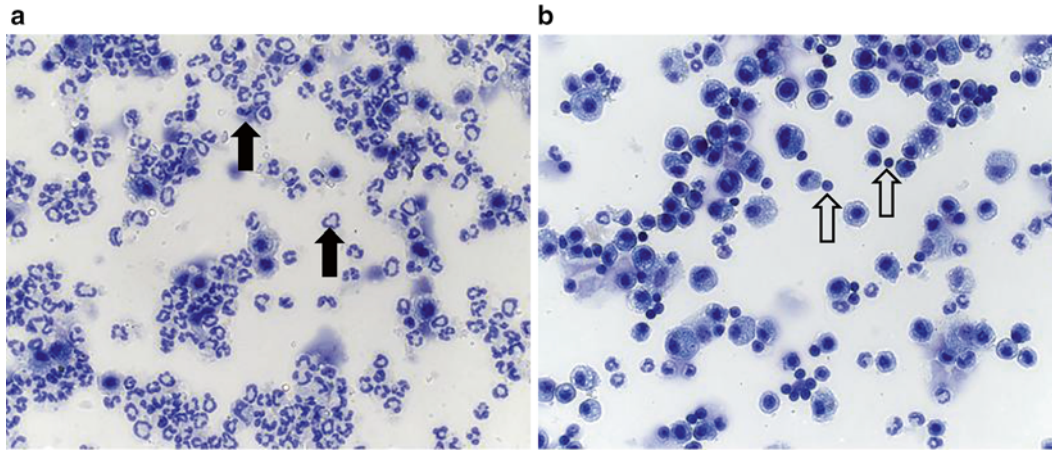


**Fig. 1** Measurement of inflammatory cells in BAL during rhinovirus infection. Balb/c mice were infected intranasally with $5 \times 10^6$ $TCID_{50}$. BAL was collected and inflammatory cells were identified using cytospin assay. (**a**) One day post-infection the majority of cells are neutrophils (*black arrow*). (**b**) By day 7 neutrophil numbers have reduced significantly and lymphocytes (*open arrow*) are observed

7. Lung tissue for RNA extraction: Harvest the right apical lobe and store in 500 μL RNAlater at −80 °C. Extract RNA using RNeasy kit (Qiagen cat no. 74106) and reverse transcribe to cDNA using Omniscript RT kit (Qiagen 205113). Assess expression of genes of interest by Taqman quantitative PCR.

## 4 Notes

1. To avoid bacterial contamination of Hela cells, ensure that the outside surface of all reagent bottles is cleaned thoroughly with 70 % ethanol prior to placing in microbiological safety cabinet. Ensure that a sterile non-touch technique is used throughout and, in particular, avoid the tips of pipettes touching the rim of flasks and containers.
2. It is important to carefully store viruses and document passage number. Hierarchical passaging will ensure that working stocks are always derived from virus of the same passage number.
3. When infecting $25 \times 175$ cm$^2$ flasks with RV1B, monitor cells regularly to ensure that they are maximally infected (majority are rounded up) but most are still adhered to the flask so that there is minimal lysis. This is important because virus is purified from cell pellets. Culture media is discarded, so if cell lyses and virus is released infectivity will be lost.
4. When filtering supernatant via syringe filter, ensure that syringe is withdrawn slightly before changing filter. This will prevent leakage and loss of virus.
5. During purification, after the virus precipitation step, the precipitate should be dissolved in 15 mL PBS. At this point the precipitate can be difficult to get into solution. To achieve this, first add a small volume of PBS (around 2 mL) and use a 1 mL pipette tip to break up the precipitate by agitating. Pipette the precipitate/PBS mix up several times until it dissolves. Add 5 mL of PBS and repeat process. When precipitate is fully solubilized, make up volume to 15 mL with PBS.
6. During purification, when filtering virus via Amicon ultracentrifugal device, ensure that after each centrifugation the remaining concentrated virus volume is mixed with a 1 mL pipette, to prevent blockage of the filter. Concentration down to 0.5 mL volume may take considerable time and require transfer of virus to another ultracentrifugal device, if filter gets blocked.
7. Prior to undertaking large experiments, always test virus in vivo by infecting a small number of mice with purified RV and UV-inactivated RV. Check BAL neutrophil numbers at 24 h post-infection to assess level of inflammatory response produced and also to ensure that no bacterial contamination is

present in preparation (mice dosed with UV-inactivated RV1B should have <5 % neutrophils at 24 h post-infection).

8. The conventional PCR assay cannot distinguish between heterozygotes and homozygous positive hu/mu ICAM-1 transgenic mice. To control for transgene dosage only heterozygotes are used. This is ensured by mating heterozygote males with Balb/c females. 50 % of the offspring are transgene heterozygous.
9. Mice must be correctly anesthetized because the virus will be immediately inhaled without any apparent response by the mouse. If mouse is over-anesthetized then dosing may trigger respiratory distress preventing effective delivery to the lungs. This is usually indicated by the inoculum "bubbling" out of the nose.

## References

1. Bartlett N, Johnston S (2008) Rhinoviruses. In: Mahy B, Regenmortel M (eds) Encyclopedia of virology. Elsevier, Oxford, pp 467–475
2. Tuthill TJ, Papadopoulos NG, Jourdan P, Challinor LJ, Sharp NA, Plumpton C, Shah K, Barnard S, Dash L, Burnet J et al (2003) Mouse respiratory epithelial cells support efficient replication of human rhinovirus. J Gen Virol 84: 2829–2836
3. Bartlett NW, Walton RP, Edwards MR, Aniscenko J, Caramori G, Zhu J, Glanville N, Choy KJ, Jourdan P, Burnet J et al (2008) Mouse models of rhinovirus-induced disease and exacerbation of allergic airway inflammation. Nat Med 14:199–204
4. Slater L, Bartlett NW, Haas JJ, Zhu J, Message SD, Walton RP, Sykes A, Dahdaleh S, Clarke DL, Belvisi MG et al (2010) Co-ordinated role of TLR3, RIG-I and MDA5 in the innate response to rhinovirus in bronchial epithelium. PLoS Pathog 6:e1001178
5. Bartlett NW, Slater L, Glanville N, Haas JJ, Caramori G, Casolari P, Clarke DL, Message SD, Aniscenko J, Kebadze T et al (2012) Defining critical roles for NF-kappaB p65 and type I interferon in innate immunity to rhinovirus. EMBO Mol Med 4:1244–1260
6. Collison A, Hatchwell L, Verrills N, Wark PA, de Siqueira AP, Tooze M, Carpenter H, Don AS, Morris JC, Zimmermann N et al (2013) The E3 ubiquitin ligase midline 1 promotes allergen and rhinovirus-induced asthma by inhibiting protein phosphatase 2A activity. Nat Med 19:232–237
7. Glanville N, Message SD, Walton RP, Pearson RM, Parker HL, Laza-Stanca V, Mallia P, Kebadze T, Contoli M, Kon OM et al (2013) GammadeltaT cells suppress inflammation and disease during rhinovirus-induced asthma exacerbations. Mucosal Immunol 6:1091–1100
8. Traub S, Nikonova A, Carruthers A, Dunmore R, Vousden KA, Gogsadze L, Hao W, Zhu Q, Bernard K, Zhu J et al (2013) An anti-human icam-1 antibody inhibits rhinovirus-induced exacerbations of lung inflammation. PLoS Pathog 9:e1003520

# Index


## A

Air–liquid interface .....5, 50, 64, 68, 70
  differentiated cultures ..... 5, 50, 64, 65, 70, 72, 169
  HeLa cells..... 50, 53, 56, 58, 72, 73, 102, 116, 117, 136, 144, 150, 153, 165, 166, 169, 174, 177–179, 182, 184, 185, 187
  human airway epithelium .....63–70
  MRC-5.....72, 73, 75, 76, 79, 153, 165, 169
  suspension culture.....50, 52, 55–58, 77, 102, 113, 114, 116, 166
Autocorrelation analysis ..... 83–85, 90–98

## C

Capillary electrophoresis.....13, 19, 20, 88, 101–125
Cell culture ..... 4, 12, 26, 40, 50, 56, 64, 72, 73, 75, 77, 113, 114, 116, 123, 136, 153, 183–184

## D

Diffusion coefficient..... 85, 86, 88–90, 93–95, 97, 98
Drug/s .....65
  development .....131, 139
  groups .....3, 4
  intercalating .....4
  reactivity .....4, 5
  sensitivity.....4
  virus-drug complexes .....4

## E

Electron microscopy .....101–125
Electrophoresis ..... 172, 174, 176, 177
Electrophoretic mobility.....5, 101–125

## F

Fluorescence correlation spectroscopy (FCS) .....68, 83–99

## G

Gas phase .....101–125

## I

Infectivity assays
  end-point dilution .....72, 77
  PFU.....50, 51, 56, 77–78, 80, 117, 166
  plaque assay .....4, 72–74, 77–80, 166, 167
  TCID50 .....72, 75–77, 117, 118, 178
In vitro transcription .....154, 157, 163, 172, 174, 177, 178

## P

Picornavirus.....1–3, 6, 26, 49, 71, 131, 136, 137, 171
Polymerase chain reaction (PCR)
  nucleic acid isolation.....17, 18
  quantitative RT-PCR .....26, 36
  reverse transcription (RT)-PCR..... 12, 14–22, 40–43
Positive strand RNA.....11, 171
  5'UTR ..... 9, 40, 44
  VP4/VP2 ..... 2, 40, 44
Proteases.....11, 129–139
  2A protease..... 9, 171–173, 179
  3C protease.....171, 172
  HRV16 3C protease .....143–148
  in vitro protease activity assays.....143–148
  subcellular localization.....135, 136

## R

Receptor .....2–7, 50, 52, 83–98, 101–103, 108, 109, 111, 130, 139, 169, 181, 182
Reverse genetics.....149–169
  full-length infectious cDNA clone ..... 150, 153–154, 162–165
  reverse genetic engineering.....171–180
Rhinovirus classification
  genotypes..... 2, 6, 7, 39–47
  HRV-A2.....86, 88, 92, 93, 97, 102, 103, 105–108, 112–125
  HRV type ..... 39, 101, 102
  major group ..... 101, 181, 182
  minor group.....4, 90, 101, 181, 182


David A. Jans and Reena Ghildyal (eds.), *Rhinoviruses: Methods and Protocols*, Methods in Molecular Biology, vol. 1221, DOI 10.1007/978-1-4939-1571-2, © Springer Science+Business Media New York 2015

Rhinovirus classification (*cont.*)
molecular analysis ..... 119–120
serotype ..... 11, 12, 26, 27, 33, 39, 49, 50, 52, 63, 81, 102, 129, 131–133, 136, 139, 143, 144, 155, 169, 171–180, 182
species ..... 1–8, 11, 26, 39, 41, 63, 71, 84, 85, 94, 182
Rhinovirus culture ..... 49–59
high-titer virus stock ..... 52
Rhinovirus detection
molecular typing ..... 29, 31–33
multiplex PCR ..... 11–23
nested-PCR ..... 11–23
virus taxonomy ..... 1–8
Rhinovirus–host cell interaction
disruption of nuclear transport ..... 138
inhibition of cap-dependent translation ..... 137
Rhinovirus immunology ..... 2
Rhinovirus purification ..... 49–59, 182–185
Rhinovirus uncoating ..... 83–99
RNA virus ..... 26, 49, 71, 143, 149, 150, 167, 177

## T

Transfection ..... 102, 154, 163–167, 169, 174, 177–179

## V

Viral load ..... 26, 131